

FAST PYROLYSIS OF CORN RESIDUES FOR ENERGY PRODUCTION

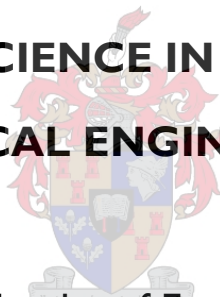
by

Stephen Danje

Thesis presented in partial fulfilment
of the requirements for the Degree

Of

**MASTER OF SCIENCE IN ENGINEERING
(CHEMICAL ENGINEERING)**



In the Faculty of Engineering
at Stellenbosch University

Supervisor

Prof. JH. Knoetze

Co-Supervisor

Prof. JF. Görgens

December 2011

DECLARATION

By submitting this thesis electronically, I declare that the entirety of the work contained therein is my own, original work, that I am the sole author thereof (save to the extent explicitly otherwise stated), that reproduction and publication thereof by Stellenbosch University will not infringe any third party rights and that I have not previously in its entirety or in part submitted it for obtaining any qualification.

.....

13...../....09...../.....2011.....

Signature (Stephen Danje)

Date

Copyright © 2011 Stellenbosch University

All rights reserved

ABSTRACT

Increasing oil prices along with the climate change threat have forced governments, society and the energy sector to consider alternative fuels. Biofuel presents itself as a suitable replacement and has received much attention over recent years. Thermochemical conversion processes such as pyrolysis is a topic of interest for conversion of cheap agricultural wastes into clean energy and valuable products. Fast pyrolysis of biomass is one of the promising technologies for converting biomass into liquid fuels and regarded as a promising feedstock to replace petroleum fuels. Corn residues, corn cob and corn stover, are some of the largest agricultural waste types in South Africa amounting to 8 900 thousand metric tonnes annually (1.7% of world corn production) (Nation Master, 2005).

This study looked at the pyrolysis kinetics, the characterisation and quality of by-products from fast pyrolysis of the corn residues and the upgrading of bio-oil. The first objective was to characterise the physical and chemical properties of corn residues in order to determine the suitability of these feedstocks for pyrolytic purposes. Secondly, a study was carried out to obtain the reaction kinetic information and to characterise the behaviour of corn residues during thermal decomposition. The knowledge of biomass pyrolysis kinetics is of importance in the design and optimisation of pyrolytic reactors. Fast pyrolysis experiments were carried out in 2 different reactors: a Lurgi twin screw reactor and a bubbling fluidised bed reactor. The product yields and quality were compared for different types of reactors and biomasses. Finally, a preliminary study on the upgrading of bio-oil to remove the excess water and organics in order to improve the quality of this liquid fuel was performed.

Corn residues biomass are potential thermochemical feedstocks, with the following properties (carbon 50.2 wt. %, hydrogen 5.9 wt. % and Higher heating value 19.14 MJ/kg) for corn cob and (carbon 48.9 wt. %, hydrogen 6.01 wt. % and Higher heating value 18.06 MJ/kg) for corn stover. Corn cobs and corn stover contained very low amounts of nitrogen (0.41-0.57 wt. %) and sulphur (0.03-0.05 wt. %) compared with coal (nitrogen 0.8-1.9 wt. % and sulphur 0.7-1.2 wt. %), making them emit less sulphur oxides than when burning fossil fuels. The corn residues showed three distinct stages in the thermal decomposition process, with peak temperature of pyrolysis shifting to a higher value as the heating rate increased. The activation energies (E) for corn residues, obtained by the application of an iso-conversional method from thermogravimetric tests were in the range of 220 to 270 kJ/mol.

The products obtained from fast pyrolysis of corn residues were bio-oil, biochar, water and gas. Higher bio-oil yields were produced from fast pyrolysis of corn residues in a bubbling fluidised bed reactor (47.8 to 51.2 wt. %, dry ash-free) than in a Lurgi twin screw reactor (35.5 to 37 wt. %, dry ash-free). Corn cobs produced higher bio-oil yields than corn stover in both types of reactors. At the optimised operating temperature of 500-530 °C, higher biochar yields were obtained from corn stover than corn cobs in both types of reactors. There were no major differences in the chemical and physical properties of bio-oil produced from the two types of reactors. The biochar properties showed some variation in heating values, carbon content and ash content for the different biomasses. The fast pyrolysis of corn residues produced energy products, bio-oil (Higher heating value = 18.7-25.3 MJ/kg) and biochar (Higher heating value = 19.8-29.3 MJ/kg) comparable with coal (Higher heating value = 16.2-25.9 MJ/kg). The bio-oils produced had some undesirable properties for its application such as acidic (pH 3.8 to 4.3) and high water content (21.3 to 30.5 wt. %). The bio-oil upgrading method (evaporation) increased the heating value and viscosity by removal of light hydrocarbons and water. The corn residues biochar produced had a BET Brynauer-Emmet-Teller (BET) surface area of 96.7 to 158.8 m²/g making it suitable for upgrading for the manufacture of adsorbents. The gas products from fast pyrolysis were analysed by gas chromatography (GC) as CO₂, CO, H₂, CH₄, C₂H₄, C₂H₆, C₃H₈ and C₅⁺ hydrocarbons. The gases had CO₂ and CO of more than 80% (v/v) and low heating values (8.82-8.86 MJ/kg).

OPSOMMING

Die styging in olie pryse asook dreigende klimaatsveranderinge het daartoe gelei dat regerings, die samelewing asook die energie sektor alternatiewe energiebronne oorweeg. Bio-brandstof as alternatiewe energiebron het in die afgelope paar jaar redelik aftrek gekry. Termochemiese omskakelingsprosesse soos pirolise word oorweeg vir die omskakeling van goedkoop landbou afval na groen energie en waardevolle produkte. Snel piroliese van biomassa is een van die mees belowende tegnologiese vir die omskakeling van biomassa na vloeibare brandstof en word tans gereken as 'n belowende kandidaat om petroleum brandstof te vervang. Mielieafval, stronke en strooi vorm 'n reuse deel van die Suid Afrikaanse landbou afval. Ongeveer 8900 duisend metriek ton afval word jaarliks geproduseer wat optel na ongeveer 1.7% van die wêreld se mielie produksie uitmaak (Nation Master, 2005).

Hierdie studie het gekyk na die kinetika van piroliese, die karakterisering en kwaliteit van byprodukte van snel piroliese afkomstig van mielie-afval asook die opgradering van bio-brandstof. Die eerste mikpunt was om die fisiese en chemiese karakteristieke van mielie-afval te bepaal om sodoende die geskiktheid van hierdie afval vir die gebruik tydens piroliese te bepaal. Tweedens is 'n kinetiese studie onderneem om reaksie parameters te bepaal asook die gedrag tydens termiese ontbinding waar te neem. Kennis van die piroliese kinetika van biomassa is van belang juis tydens die ontwerp en optimering van piroliese reaktore. Snel piroliese eksperimente is uitgevoer met behulp van twee verskillende reaktore: 'n Lurgi twee skroef reaktor en 'n borrelende gefluidiseerde-bed reaktor. Die produk opbrengs en kwaliteit is vergelyk. Eindelik is 'n voorlopige studie oor die opgradering van bio-olie uitgevoer deur te kyk na die verwydering van oortollige water en organiese materiaal om die kwaliteit van hierdie vloeibare brandstof te verbeter.

Biomassa afkomstig van mielie-afval is 'n potensiële termochemiese voerbron met die volgende kenmerke: mielie stronke- (C - 50.21 massa %, H - 5.9 massa %, HHV - 19.14 MJ/kg); mielie strooi - (C - 48.9 massa %, H - 6.01 massa %, HHV - 18.06 MJ/kg). Beide van hierdie materiale bevat lae hoeveelhede N (0.41-0.57 massa %) and S (0.03-0.05 massa %) in vergelyking met steenkool N (0.8-1.9 massa %) and S (0.7-1.2 massa %). Dit beteken dat hierdie bronne van biomassa laer konsentrasies van swaer oksiedes vrystel in vergelyking met fossielbrandstowwe. Drie kenmerkende stadia is waargeneem tydens die termiese afbraak van mielie-afval, met die temperatuur piek van piroliese wat skuif na 'n hoer

temperatuur soos die verhittingswaarde toeneem. Die waargenome aktiveringsenergie (E) van mielie-afval bereken met behulp van die iso-omskakelings metode van TGA toetse was in die bestek: 220 tot 270 kJ/mol.

Die produkte verkry deur Snel Piroliese van mielie-afval was bio-olie, bio-kool en gas. 'n Hoër opbrengs van bio-olie is behaal tydens Snel Piroliese van mielie-afval in die borrelende gefluidiseerde-bed reaktor (47.8 na 51.2 massa %, droog as-vry) in vergelyking met die Lurgi twee skroef reaktor (35.5 na 37 massa %, droog as-vry). Mielie stronke sorg vir 'n hoër opbrengs van bio-olie as mielie strooi in beide reaktore. By die optimum bedryfskondisies is daar in beide reaktor 'n hoër bio-kool opbrengs verkry van mielie stingels teenoor mielie stronke. Geen aansienlike verskille is gevind in die chemiese en fisiese kenmerke van van die bio-olie wat geproduseer is in die twee reaktore nie. Daar is wel variasie getoon in die bio-kool kenmerke van die verskillende Snel Piroliese prosesse. Snel piroliese van mielie-afval lewer energie produkte, bio-olie (HVW = 18.7-25.3MJ/kg) en bio-kool (HVW = 19.8-29.3 MJ/kg) vergelykbaar met steenkool (HVW = 16.2-25.9 MJ/kg). Die bio-olies geproduseer het sommige ongewenste kenmerke getoon byvoorbeeld suurheid (pH 3.8-4.3) asook hoë water inhoud (21.3 – 30.5 massa %). Die metode (indamping) wat gebruik is vir die opgradering van bio-olie het gelei tot die verbetering van die verhittingswaarde asook die toename in viskositeit deur die verwydering van ligte koolwaterstowwe en water. Die mielie-afval bio-kool toon 'n BET (Brunauer-Emmet-Teller) oppervlakte area van 96.7-158.8 m²/g wat dit toepaslik maak as grondstof vir absorbante. The gas geproduseer tydens Snel Piroliese is geanaliseer met behulp van gas chromatografie (GC) as CO₂, CO, H₂, CH₄, C₂H₄, C₂H₆, C₃H₈ and C₅⁺ koolwaterstowwe. Die vlak van CO₂ en CO het 80% (v/v) oorskry en met lae verhittingswaardes (8.82-8.86 MJ/kg).

ACKNOWLEDGEMENTS

I gratefully acknowledge and thank my supervisors Professor Hansie Knoetze and Professor Johann Görgens, Department of Process Engineering, University of Stellenbosch for helpful guidance, advice and encouragement throughout this work. I am also very grateful to Dr Marion Carrier, Bio-fuels Researcher in the Department of Chemical Engineering for advice and guidance in making this research possible. Their enthusiasm and expertise inspired my work and their guidance, suggestions and patience are greatly appreciated.

Also, I would like to thank Dr Stahl (Karlsruhe Institute of Technology, Germany) and the supporting staffs of Institute of **T**echnical **C**hemistry-**C**hemical and **P**hysical Processing (**ITC-CPV, KIT-Germany**) for their patience, cooperation and friendly attitude and all other forms of assistance during the exchange program. I would like to thank my project sponsor SASOL for funding this project. Thanks also to my family members and my friends for their encouragements and supports. I thank God for guiding me throughout the project.

Table of contents

DECLARATION	i
ABSTRACT	ii
OPSOMMING	iv
ACKNOWLEDGEMENTS	vi
LIST OF FIGURES	xii
LIST OF TABLES	xiii
ABBREVIATIONS AND NOMENCLATURE	xv
Chapter 1: Introduction	1
1.1 Biofuel program in South Africa	3
1.2 Objectives of this study	4
1.3 Structure of Report	6
Chapter 2: Literature study	7
2.1 Major components of plant biomass	7
2.1.1 Macromolecular substances	8
2.1.2 Low-molecular weight substances	9
2.2 Biomass raw materials used in this study	10
2.2.1 Corn stover.....	10
2.2.2 Corn cob	10
2.3 Thermogravimetric analysis (TGA)	11
2.3.1 Kinetic analysis	11
2.4 Thermochemical processes	14
2.4.1 Combustion.....	15
2.4.2 Gasification.....	15
2.4.3 Liquefaction	15
2.4.4 Hydrogenation	16
2.4.5 Pyrolysis processes	16
2.5 Fast Pyrolysis	19
2.5.1 Process description.....	19
2.5.2 Reactor parameters	20
2.6 Literature review on corn residues fast pyrolysis	25
2.7 Industrial plants	26
2.8 Bio-oil from Fast Pyrolysis	28

2.8.1 Product description.....	28
2.8.2 Chemical nature of bio-oil	29
2.8.3 Properties of bio-oil	30
2.8.4 Storage properties of bio-oil.....	34
2.9 Methods for chemical characterisation	34
2.9.1 Composition by solvent fractionation	35
2.9.2 Volatile compounds by solid-phase micro-extraction	35
2.9.3 Volatile carboxylic acids and alcohols.....	35
2.9.4 Extractives	36
2.9.5 Carbonyl groups determination.....	36
2.9.6 Molecular mass determination.....	36
2.9.7 Elemental analysis	36
2.9.8 Sugars	37
2.9.9 Organic acids.....	37
2.9.10 Poly aromatic Hydrocarbons (PAH).....	37
2.9.11 Phenols	38
2.9.12 Total acid Number (TAN)	38
2.9.13 Esters.....	38
2.10 Methods for physical characterisation	39
2.10.1 Water content	39
2.10.2 Solids and its components.....	39
2.10.3 Homogeneity.....	39
2.10.4 Stability	40
2.10.5 Flash point	40
2.10.6 Viscosity and pour point	40
2.10.7 Heating values	41
2.10.8 Density	41
2.11 Bio-oil applications.....	42
2.11.1 Combustion and electricity production.....	42
2.11.2 Synthesis gas production.....	44
2.11.3 Boilers	45
2.11.4 Steam reforming.....	46
2.11.5 Chemicals extracted from bio-oils.....	46
2.11.6 Emulsification.....	47

2.12 Bio-oil downstream processes	48
2.12.1 Physical techniques	48
2.12.2 Chemical techniques	50
2.12.3 Physico-chemical techniques	53
2.13 Summary of literature	55
Chapter 3: Methodology and Materials	58
3.1 Materials	58
3.2 Procedures	60
3.2.1 Sampling	60
3.2.2 Thermogravimetric analysis (TGA)	60
3.2.3 Biomass kinetics analysis	61
3.2.4 Fast pyrolysis processes	61
3.2.5 Process operating conditions	67
3.3 Physical and chemical characterisations of biomass	68
3.3.1 Proximate analysis	68
3.3.2 Heating value	69
3.3.3 Elemental analysis	70
3.3.4 Density	71
3.3.5 Inorganic composition	71
3.3.6 Lignocellulosic composition	72
3.3.7 Particle size distribution	74
3.4 Characterisation of bio-oil	74
3.4.1 Density of bio-oil	74
3.4.2 Ash	75
3.4.3 Moisture content	75
3.4.4 Heating value	75
3.4.5 pH	76
3.4.6 Elemental analysis	76
3.4.7 Viscosity	77
3.4.8 Dehydration of bio-oil liquids	77
3.5 Characterisation of biochar	77
3.5.1 Elemental analysis	77
3.5.2 Heating value	78
3.5.3 Ash content	78

3.5.4 Surface area and total pore volume.....	78
3.5.5 Particle size distribution.....	80
3.6 Gas analysis.....	80
3.6.1 Corn residues non condensable gas product	80
3.6.2 Pyrolysis vapour analysis	81
Chapter 4: Characterisation of biomass feedstocks.....	82
4.1 Results and Discussion.....	82
4.1.1 Lignocellulosic compositional analysis.....	82
4.1.2 Proximate and ultimate analyses:.....	85
4.1.3 Heating values	87
4.1.4 Particle density and shape	90
4.1.5 Biomass inorganic composition.....	91
4.1.6 Char inorganic composition.....	93
Chapter 5: Thermal behaviour of corn residues.....	96
5.1 Results and Discussion.....	96
5.1.1 Analysis of thermo-analytical curves.....	96
5.1.2 Effect of heating rate on devolatilisation.....	104
5.1.3 Proximate analysis.....	105
5.1.4 Kinetic study using an isoconversional method.....	108
5.1.5 Quality of fit	110
Chapter 6: Fast pyrolysis products characterisation.....	116
6.1 Results and Discussion.....	116
6.1.1 Biomass physical and chemical properties.....	116
6.1.2 Particle size distribution	117
6.1.3 Mode of heat transfer	119
6.1.4 Products yields	119
6.1.5 Characterisation of bio-oil	126
6.1.5.1 Properties of bio-oil	126
6.1.5.2 Ultimate and proximate analyses	128
6.1.5.3 Heating values.....	130
6.1.5.4 Chemical analysis of pyrolysis gas	130
6.1.5.5 Viscosity and solids content of bio-oil	132
6.1.5.6 Dehydration of bio-oil.....	134
6.1.6 Characterisation of biochar	135

6.1.6.1 Ultimate and proximate analyses	136
6.1.6.2 Heating value	139
6.1.6.3 Surface area	140
6.1.6.4 Particle size distribution	142
6.1.6.5 Slurry viscosity	144
6.1.7 Characterisation of gas.....	146
6.1.7.1 Non-condensable gas composition	146
6.1.7.2 Non-condensable gas adiabatic flame temperatures.....	148
6.1.8 Product energy distribution.....	151
Chapter 7: Conclusions and recommendations.....	152
References.....	157
Appendices.....	177

LIST OF FIGURES

Figure 1: The mind map of the study.....	5
Figure 2: General components in plant biomass.....	7
Figure 3: Pyrolysis product yields from wood at various temperatures	21
Figure 4: Uses of FP products Redrawn from	43
Figure 5: Lurgi Twin screw reactor process flow diagram.....	62
Figure 6: Bubbling fluidised bed reactor process flow diagram	65
Figure 7: TGA mass and temperature profiles.....	69
Figure 8: Scheme of the on-line process gas analysis	81
Figure 9: CC TG/DTG curve temperature illustration graph	97
Figure 10: TG curve for CC.....	99
Figure 11: DTG curve for CC	100
Figure 12: TG curve for CS	101
Figure 13: DTG curve for CS	102
Figure 14: The trend of proximate analysis.....	107
Figure 15: Friedman's plots for CC	111
Figure 16: Friedman's plots for CS.....	112
Figure 17: Apparent activation energy dependence on conversion for CC.....	114
Figure 18: Apparent activation energy dependence on conversion for CS.....	115
Figure 19: Particle size distribution of biomass feedstock in a LTSR	118
Figure 20: Particle size distribution of biomass feedstock in a BFBR.....	118
Figure 21: Viscosity vs Shear rate for CC bio-oils.....	133
Figure 22: Viscosity vs Shear rate for CS bio-oils.....	134
Figure 23: Viscosity variation for CS slurries	144
Figure 24: Viscosity variation for CC slurries.....	145
Figure 25: The non-condensable gas compositions of corn residues	147
Figure 26: Corn stover non-condensable gas flame temperatures	150
Figure 27: Corn cobs non-condensable gas flame temperatures.....	150

LIST OF TABLES

Table 1: Typical lignocellulose contents of some plant materials.	8
Table 2: Typical mineral components of targeted Corn cobs (CC) and Corn stover (CS)	9
Table 3: Dry matter distribution in corn residues (CR).....	10
Table 4: Product yields from various biomass conversion techniques	17
Table 5: Pyrolysis reactions at different temperatures	23
Table 6: Literature review on FP of CC and CS.....	26
Table 7: Fast pyrolysis research institutes.....	28
Table 8: The representative chemical composition of liquid from FP	29
Table 9: Comparison of physical and chemical properties of bio-oil with heavy fuel oil.....	31
Table 10: Comparison of energy density by volume and by weight.....	34
Table 11: Properties of crude and upgraded oils	53
Table 12: Comparison of raw bio-oil and upgrading bio-oil after reactive distillation.	55
Table 13: Proposed bio-oil upgrading strategy.....	57
Table 14: Fast pyrolysis experimental conditions	67
Table 15: Lignocellulosic composition of corn cob (CC) and corn stover (CS) (wt. % df)	82
Table 16: Physical and chemical properties of CR	84
Table 17: South African coal properties.....	88
Table 18: Heating values correlations.....	89
Table 19: Biomass elemental composition	92
Table 20: Ash inorganic composition	93
Table 21: Devolatilisation % of total inorganic elements at 550 ^o C	95
Table 22: Temperature devolatilisation parameters for CC and CS at different heating rates	97
Table 23: Proximate analysis obtained from TGA and analytical method	108
Table 24: Kinetic parameters of the biomass thermal decomposition	110
Table 25: Quality of fit percentages (%) of kinetic model predictions for CR	113
Table 26: Physical and chemical properties of corn residues (CR)	117

<i>Table 27: Product distribution yields obtained at 500-530 °C using a bubbling fluidised bed reactor (BFBR) and Lurgi twin screw reactor (LTSR) on CS, CC and CRM.</i>	<i>121</i>
<i>Table 28: Product yields from previous studies on Fast Pyrolysis of biomass.</i>	<i>125</i>
<i>Table 29: Physical and chemical properties of bio-oils from Fast pyrolysis of Corn residues</i>	<i>127</i>
<i>Table 30: Gas components identified from FP of CR at 500 °C</i>	<i>131</i>
<i>Table 31: Solids content (wt. %) of CR bio-oils</i>	<i>133</i>
<i>Table 32: Properties of upgraded bio-oil from FP of CR.</i>	<i>135</i>
<i>Table 33: Characterisation of biochar from FP of CR</i>	<i>138</i>
<i>Table 34: Comparison of properties of coal, CR biomasses and CR biochars.....</i>	<i>142</i>
<i>Table 35: Particle size distribution of biochar from BFBR (μm)</i>	<i>143</i>
<i>Table 36: Particle size distribution of biochar slurries from LTSR (μm).....</i>	<i>143</i>
<i>Table 37: GC non-condensable gas analysis.....</i>	<i>146</i>
<i>Table 38: Energy recoveries of products from CR</i>	<i>151</i>

ABBREVIATIONS AND NOMENCLATURE

AC	Ash Content
AC _O	Biomass ash content
AC _{CHAR}	Biochar ash content
AKTS	Advanced Thermal Analysis Software
ASTM	American society of testing and materials
BET	Brunauer-Emmet-Teller
BFBR	Bubbling fluidised bed reactor
Biochar	Pyrolysis char (Includes ash)
CC	Corn cobs
CHNS-O	Carbon, Hydrogen, Nitrogen, Sulphur and Oxygen
COD	Carbon Oxygen Demand
CR	Corn residues
CRM	Corn residue mixture [70% Stover and 30% Cobs]
CS	Corn stover
daf	Dry and ash-free
df	dry free
DIN	Deutschland Institute of standardisation
DTG	Derivative thermogravimetry
EIS	Ether-Insolubles
EQ	Fuel/Air Equivalence Ratio
ES	Ether-soluble
ESP	Electrostatic precipitators
FC	Fixed Carbon
H/C	Hydrogen carbon molar ratio
KIT	Karlsruhe Institute of Technology
Liquids Yields	All Liquids products from pyrolysis [water + Bio-oil]

LR	Long run (Fast pyrolysis)
LTSR	Lurgi twin screw reactor
MC	Moisture content
M_{CHAR}	Mass of biochar produced
M_{L}	Mass of liquid product
M_{O}	Biomass initial mass
n.a	Not applicable
n.d	Not determined
O/C	Oxygen carbon molar ratio
ODW	Oven Dried Weight sample
PDU	Process Demonstration Unit
ppm	Parts per million
SD	Standard Deviation
SU or US	Stellenbosch University
TGA	Thermogravimetric analysis
TOC	Total Oxygen Demand
VM	Volatile Matter
WC	Water content
WC_{L}	Water content in liquid product
Wt. %	Weight percentage
XRF	X-Ray Fluorescence
Yields (wt. %)	Weight option of respective product expressed as percentage of original weight (of biomass) before pyrolysis
Y_{LIQUID} (wt. %)	Yield of liquid
Y_{GAS} (wt. %)	Yield of gas
Y_{BIOCHAR} (wt. %)	Yield of biochar
WS	Water Soluble
WIS	Water Insolubles

Abbreviation	Name	Units
Q	Volumetric flow rate	m ³ /hr
T	Temperature	° C [or K]
E	Activation Energy	KJ/mol
A	Pre-exponential factor	-
μ	Viscosity	Pa.s
F	Feed rate	kg/hr
HHV	Higher heating value	MJ/kg
LHV	Lower heating value	MJ/kg
ρ	Density	kg/m ³
α	Conversion	-
Y	Yield	-
t	Time	hr
P	Pressure	kPa
L	Lignin content	Wt. %
C _E	Holocellulose	Wt. %
E _X	Extractives content	Wt. %
T _w	Maximum peak temperature (water loss)	° C
T _a	Maximum peak temperature (Hemicelluloses)	° C
T _b	Maximum peak temperature (Cellulose)	° C
H	Heating rate	° C/min [K/min]
a	Weight of biomass in the range	Wt. %
b	Cumulative weight of biomass	Wt. %
(HHV)*	Calculated higher heating value	MJ/kg
m/z	Molecular mass	-
φ	Fuel/Air Equivalence Ratio	-

Chapter I: Introduction

The world depended on biologically produced energy to supply its needs for heat until this past century (Asif and Muneer, 2007). Biomass is still used in large quantities for heating and cooking in most developing countries (Dermibas, 2001a). Today, fossil fuels make up most of the energy consumption supplying more than 80% of the world's energy demand (www.solcomhouse.com). Due to the increasing levels of gaseous emissions in the atmosphere, there is a need for urgent considerations of biomass feedstocks as a significant energy resource (Matthews, 2008).

Biomass is the third most common and important energy source consumed in the world after coal and oil (Bapat *et al.*, 1997; Hall and Rosillo-Calle, 1991; Liang and Kozinski, 2000). Both fossil fuels and biomass are products of the solar resource. The ability to re-grow harvested biomass feedstock and recapture the carbon dioxide emitted to the atmosphere through the photosynthesis process allows the possibility of excess carbon balance of less than that of fossil fuels (Johnson, 2009). It provides a clean environment and renewable energy that could dramatically improve the economy and energy security for South Africa. Biomass has become a very vital energy source, due to the world's fast depleting fossil fuels, increase in energy demand, the high costs of fossil fuels as well as the environmental concern about emission levels of CO₂, SO₂ and NO_x. It is unique in providing the only renewable source of fixed carbon, which is essential for biofuel production. Developing countries have a great interest in biomass conversion, since their economies are largely based on agriculture and forestry (Vamvuka *et al.*, 2003).

Renewable biomass resources include wood, energy crops, agricultural and forestry residues, algae and municipal solid waste (Dermibas, 2001b). Most energy conversion work has been done on woody biomass (Mohan *et al.*, 2006). These different biomasses may vary in their physical and chemical properties due to their diverse origin and species (Chen *et al.*, 2003). Agricultural waste is the main biomass in South Africa and there are large quantities of various crops. At present, the South African agricultural sector generates the most biomass from the corn production planted on an area of 3.3 million hectares out of the total 14.7 million hectares of arable land (Salter, s.a). Corn is the largest produced food crop in South Africa largely used for conversion into secondary products (corn flakes, corn flour

and glucose) (Salter, s.a). According to the 2005 Agriculture Statistics, the world corn production reached 524 173 thousand metric tonnes, of which 1.7% is produced by South Africa (approximately 8900 thousand metric tonnes of corn) (Nation Master, 2005). The large quantities of corn residues makes them a good potential feedstock for bio-fuels producing a tonne of residue per tonne of corn produced (Myers and Underwood, 1992; Leask and Daynard, 1973). The use of the biomass as an energy source will depend on the thermochemical technologies which are able to convert them into higher energy products (Sensoz *et al.*, 2006).

Large scale implementation of biomass as energy source may require thermochemical technologies such as pyrolysis for production and conversion. Pyrolysis is defined as the thermo-chemical decomposition of organic materials in the absence of oxygen or other reactants (Dermibas, 2009). It is also the first stage of biomass thermo-chemical conversion, which converts biomass resources into bio-oils, biochar, water and gases, of which the relative yields depend on pyrolysis conditions (Sensoz *et al.*, 2006a). The different types of pyrolysis results in different product ratios (Onay and Kockar, 2003). Gasification (Marrero *et al.*, 2004) (sometimes coupled with pyrolysis) maximises gas production while vacuum pyrolysis gives a more even spread of products, with biochar and bio-oil as the main products (Rabe, 2005). Slow pyrolysis and torrefaction give biochar as the main product (Bergman and Kiel 2005).

Pyrolysis process was used for charcoal and coke production in the ancient Egyptian times. In the 1980s, researchers discovered that by fast heating, followed by quenching of the vapours the liquid yields could be significantly increased (Mohan *et al.*, 2006). More recently, pyrolysis was used for maximising the liquid production although biochar and gas are also produced as by-products (Kawser *et al.*, 2004). Amongst the thermo-chemical processes, fast pyrolysis has become an alternative because of the ease of operation. In this study, fast pyrolysis was chosen for bio-oil maximisation. The product yields and properties of final products of fast pyrolysis are highly dependent on biomass type, moisture content of biomass, chemical and structural composition of the biomass, temperature, heating rates, reactors, particles size, residence time and others (Dermibas, 2009). To achieve an advanced pyrolysis process for improving product yields and quality from pyrolysis of selected corn residues, in-depth studies on the fast pyrolysis are needed.

The liquid product, bio-oil, approximates biomass in elemental composition (Mohan *et al.*, 2006). Bio-oil is composed of a very complex mixture of oxygenated hydrocarbons, reflecting the oxygen contents of the original biomass feedstock (Mohan *et al.*, 2006). Bio-oils and biochar are generally preferred products because of their high energy content, their low nitrogen and sulphur contents and their opportunity to be converted into useful chemicals. It is also useful as a fuel, which may be added to Coal to Liquid (CTL) oil refinery feedstocks or upgraded to produce transport fuels (Henrich, 2007).

The solid product, char, can be used as a fuel, either directly as briquettes or as biochar-oil slurry since it has high energy content. It can also be used as feedstocks to prepare adsorbents or as biochar soil supplement. The gas generated has a high content of hydrocarbons and sufficiently high calorific value to be used for process heat and feedstock drying in a pyrolysis plant (Karaosmanoglu *et al.*, 1999).

1.1 Biofuel program in South Africa

Non-renewable fossil fuels, such as crude oil, coal and natural gas are the main sources of energy worldwide. However, such fuels emit among others, carbon dioxide (CO₂), which gives rise to the greenhouse effect in the atmosphere, contributing to global warming and international long-term climate change. As a result, there are continuous international efforts and initiatives to protect the environment, notably, commitment under the Kyoto Protocol (1997) to reduce greenhouse gas emission to an average of 5% below the levels in 1990. The European Union (EU) among other regional blocks has a set target to gradually increase the use of biofuel in the transport sector to 10% by 2020 (EurActive, 2008). The main advantages of using biofuel are its renewability and less sulphur oxides gas emissions. It also does not contribute to a net rise in the level of CO₂ in the atmosphere, and consequently to the greenhouse effect (Sensoz *et al.*, 2006a). In 1998, it was estimated that South Africa produced 1.4% of the global CO₂ emissions (Salter, s.a). The implementation of biofuels in South Africa is in line with the government policy of ensuring sustainable development of the energy sector as well as promoting a cleaner environment. The government under the ministry of Minerals and Energy has embarked on the growth of renewable energy as a fuel source after oil, gas, hydro-electricity and coal (www.nationmaster.com). This industrial biofuels strategy sets bold targets, including the aim for 4.5% of road transport fuels in South Africa to be replaced with bio-fuels by 2013. South Africa is blessed with natural resources, particularly coal and uranium, which are the

main sources of energy. However, these are depleting energy resources and increasing demand has made it necessary for the government to embark on alternative renewable energy sources.

1.2 Objectives of this study

In this study, corn cobs (CC) and corn stover (CS) were chosen as the biomass source for energy products production from fast pyrolysis. Fast pyrolysis was conducted in a bubbling fluidised bed reactor and Lurgi twin screw reactor. The influence of the chemical and physical properties of the biomass, particle size and different types of fast pyrolysis reactors on the pyrolysis yields and products quality was investigated. The chemical and physical characteristics of bio-oil and biochar products were also studied in order to determine their feasibility of being a potential source of renewable fuel and chemical feedstock. The outline of this study is given in the mind map (Figure 1).

Objectives of Research:

The main purpose of this study was to evaluate the potential of converting South African corn residues by fast pyrolysis to energy products. In order to achieve this, the following objectives are defined:

1. To determine and compare the lignocellulosic composition, chemical and physical properties, and thermal behaviour of corn stover and corn cobs with the aim of predicting their pyrolytic behaviour and finding their suitability as feedstocks for fast pyrolysis.
2. To determine and compare the product distribution of fast pyrolysis of corn residues in a Lurgi twin screw reactor and bubbling fluidised bed reactor and study the effect of feedstocks properties.
3. To characterise physical and chemical properties of liquid products, biochar and gases obtained from corn residues fast pyrolysis reactors and determine the effect of biomass properties and types of reactors (Lurgi twin screw reactor and Bubbling fluidised bed reactor).
4. To dehydrate the bio-oils from corn residues produced in a bubbling fluidised bed reactor and study the physical properties of dehydrated bio-oils.

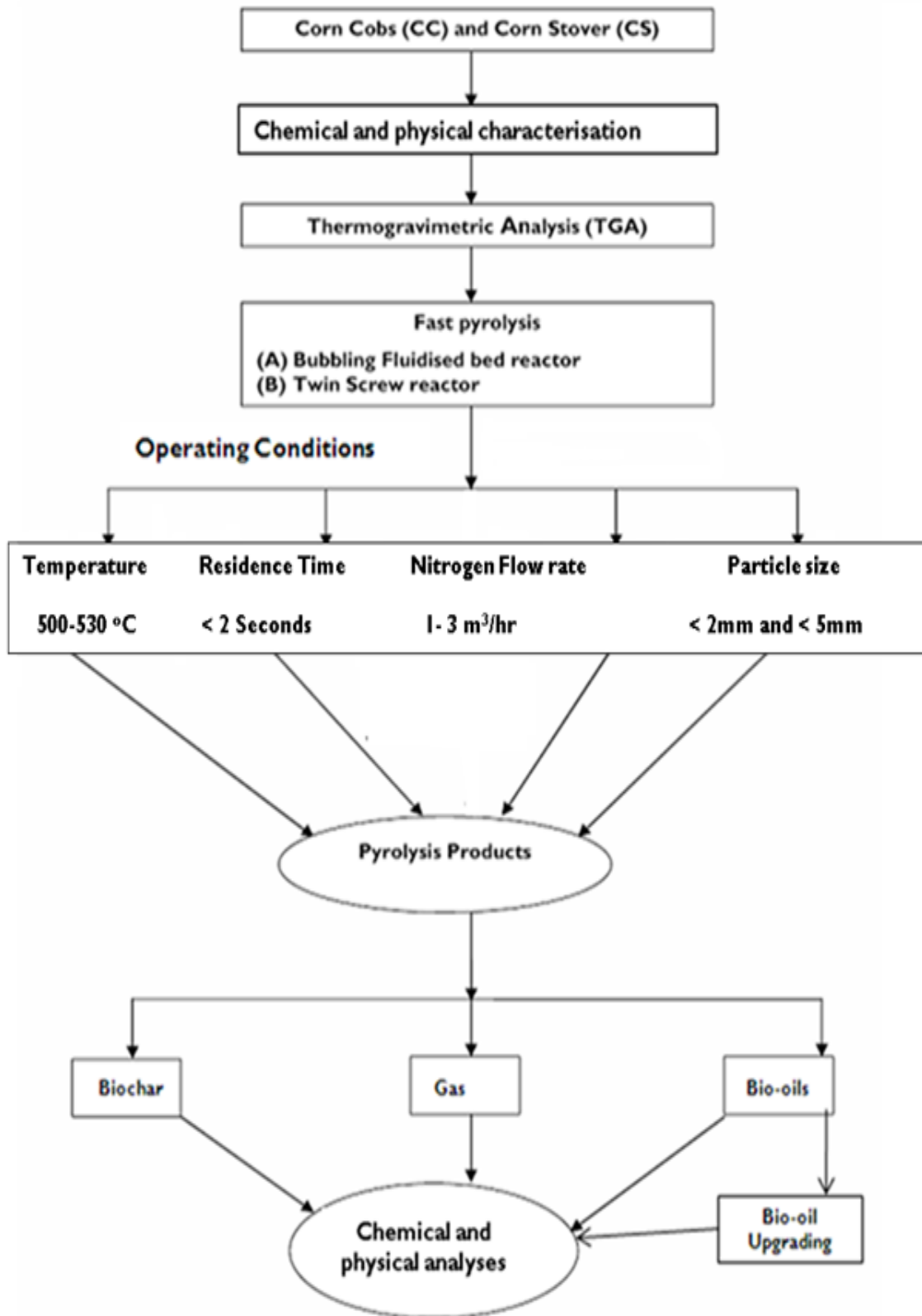


Figure 1: The mind map of the study

1.3 Structure of Report

This thesis is organised in the following manner: Following the brief introduction and discussion of the biofuels industry in South Africa in Chapter 1, the literature review of pyrolysis of biomass is presented in Chapter 2. Chapter 3 details the experimental procedure and characterisation techniques of pyrolysis products (bio-oil, biochar and gas). Chapter 4 deals with the results and discussion on the biomass physical and chemical properties and Chapter 5 reports the results and discussion on thermogravimetric analysis of the biomass. The results and discussion of the products yields and characterisation of fast pyrolysis products are presented in chapter 6. Conclusions and recommendations of the study are summarised in Chapter 7 and future research directions in fast pyrolysis technology and some thoughts on experimental procedures are also included.

Chapter 2: Literature study

Biomass originates from any living matter on earth. Plants utilise solar energy by means of photosynthesis to produce biomass (McKendry, 2002; Perez *et al.*, 2002). Biomass feedstocks can be divided into three categories: wastes (biomass residues, mostly from agricultural and municipal solid waste), forest residues (saw dust, wood and bark residues) and crops (short rotation crops, sugar cane bagasse crop, oil seed crops, grasses and cereal crops) (Dermibas, 2001a; Goyal *et al.*, 2006). Biomass is composed of components which vary in type and species, described in the following section.

2.1 Major components of plant biomass

The chemical components of biomass are very different from that of the fossil matter (Mohan *et al.*, 2006). The presence of high oxygen content in plant biomass means the pyrolytic chemistry differs largely from those of other fossil feeds (Czernik and Bridgwater, 2004). Plant biomass is essentially a composite material constructed from oxygen-containing organic polymers. Figure 2 shows the major structural chemical components of plant biomass which will be discussed in this section.

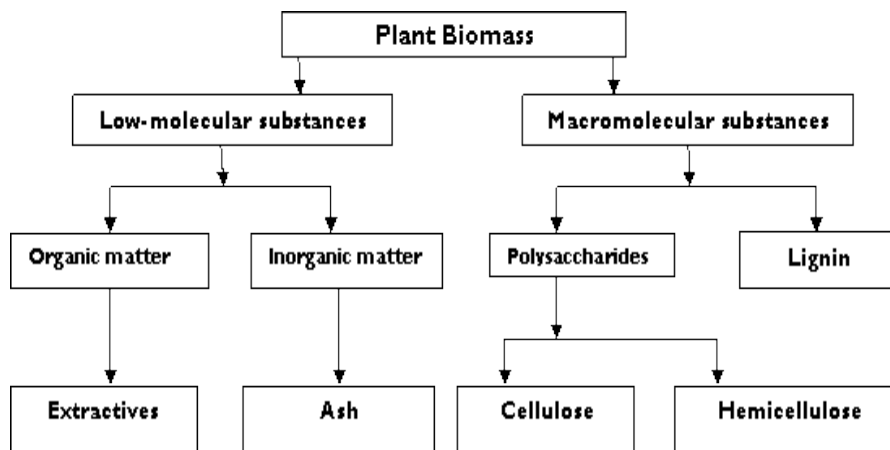


Figure 2: General components in plant biomass (Redrawn from (Mohan *et al.*, 2006))

The major biomass components (lignocellulosic composition) consist of cellulose (a glucosan polymer), hemicelluloses (which are also called polyoses), lignin, and in lower proportions inorganic materials and extractives (Mohan *et al.*, 2006). The weight percent of cellulose, hemicelluloses, and lignin vary in different biomass materials (Graboski and Bain, 1981; Mohan *et al.*, 2006). The typical lignocellulosic contents of some plant materials are given in

Table 1. The main goal of this study is to convert corn cob (CC) and corn stover (CS) whose lignocellulosic composition differ in terms of hemicelluloses and cellulose amounts. These differences should lead to different product yields and quality.

Table 1: Typical lignocellulose contents of some plant materials.

Lignocellulose content (wt. % daf)			
Plant Material	Hemicelluloses	Cellulose	Lignin
Orchard grass (Van Soest <i>et al.</i> , 1964)	40.0	32.0	4.7
Rice straw (Solo <i>et al.</i> , 1965)	27.2	34.0	14.2
Corn stover (Banchorndhevakul, 2002)	40.8	32.4	25
Corn cob (Garrote <i>et al.</i> , 2003)	40.5	34.3	18.8
Bamboo (Han, 1998)	26-43	15-26	21-31
Birch wood (Solo <i>et al.</i> , 1965)	25.7	40.0	15.7

2.1.1 Macromolecular substances

Cellulose

Cellulose is a linear polymer chain of 1, 4-D-glucopyranose units (Mohan *et al.*, 2006). These units are linked in the alpha-configuration, and the molecules have a molecular weight of around (10^6 Da or more). Cellulose is insoluble and due to the intramolecular and intermolecular hydrogen bonds has crystals making it completely insoluble in aqueous solutions and soluble in solvents such as *N*-methylmorpholine-*N*-oxide (NMNO), CdO/ethylenediamine (cadoxen) and dimethylacetamide (Sheppard, 1930; Turner *et al.*, 2004; Swatloski *et al.*, 2002). Cellulose in most biomass is the largest lignocellulosic component followed by hemicelluloses, lignin and ash (Goyal *et al.*, 2006).

Hemicelluloses

A second major biomass lignocellulosic component is hemicelluloses, which are composed of polysaccharides found mostly in cell walls consisting of branched structures (Toubul, 2008). It is a mixture of polysaccharides, composed almost entirely of sugars such as glucose, mannose, xylose and arabinose, methylglucuronic and galacturonic acids (Goyal *et al.*, 2006). These molecules have an average molecular weight of 30,000 Da (Mohan *et al.*, 2006).

Lignin

The third major lignocellulosic component of biomass is lignin. Lignins are branched, substituted, mononuclear aromatic polymers in the cell walls of certain biomass species. It is

regarded as a high molecular mass group of amorphous cross-linked resin and chemically related compounds. The main building blocks of lignin are believed to be a three-carbon chain attached to rings of six carbon atoms, called phenyl-propanes (McKendry, 2002; McCathy *et al.*, 2000). It is the main binder for the agglomeration of fibrous cellulosic components while also providing protection against the rapid fungal and microbial attacks of cellulosic fibres (Mohan *et al.*, 2006).

2.1.2 Low-molecular weight substances

Inorganic minerals

Inorganic materials in biomass contain varying mineral content that ends up in the pyrolytic liquid and solid products as ash. The most common inorganic elements in biomass are calcium (Ca), potassium (K), magnesium (Mg) and silica (Si), while concentrations of other elements such as phosphorous (P) and sodium (Na) are minor (Boman *et al.*, 2004). Table 2 shows some typical values of the mineral components in different targeted biomasses.

Table 2: Typical mineral components of targeted Corn cobs (CC) and Corn stover (CS) (Mullen *et al.*, 2009)

Element	CC (g/kg)	CC (wt. %)	CS (g/kg)	CS (wt. %)
Si	5.33	0.53	27.9	2.79
Al	0.18	0.018	5.09	0.51
Fe	0.08	0.008	2.35	0.24
Ca	0.23	0.023	3.25	0.33
Mg	0.55	0.055	2.34	0.23
Na	0.10	0.01	0.23	0.023
K	10.38	1.04	4.44	0.44
Ti	0.003	0.0003	0.37	0.04
Mn	0.01	0.001	0.98	0.1
P	1.11	0.11	2.15	0.22
Ba	0.11	0.011	0.02	0.002
Sr	0.002	0.0002	0.005	0.0005
S	0.14	0.014	0.05	0.005

Extractives

Another biomass component is comprised of organic extractives. These can be extracted from biomass with polar solvents (such as alcohol, water or methylene chloride) or nonpolar solvents (such as hexane or toluene). The extractive compounds include waxes, fats, alkaloids, proteins, phenolics, sugars, pectins, mucilages, resins, gums, terpenes, essential oils, glycosides, saponins, and starches (Mohan *et al.*, 2006). These components in

biomass function as energy reserves, intermediates in metabolism, and as protection against insect attack and microbial destruction. Extractives contribute to properties such as smell, colour, flammability, decay resistance, density and taste (Miller, 1999).

2.2 Biomass raw materials used in this study

For this study, only corn cob (CC) and corn stover (CS) are studied which constitute one of the most important agricultural wastes in South Africa.

2.2.1 Corn stover

Corn stover (CS) residues constitute half of the weight of the total corn plant, comprising of stalk, leaf, tassel and husk (Myers and Underwood, 1992). Table 3 indicates the dry matter distribution in corn residues. CS consists of the leaves, husk and stalks of maize plants left in a field after harvest. Stover makes up about half of the yield of corn residue, and it is a common agricultural product in areas where large amounts of corn are produced. CS can also contain other grasses, weeds and the non-grain part of harvested corn. It is very bulky and can absorb moisture if exposed to the atmosphere (Troxler, s.a.).

2.2.2 Corn cob

Corn cob (CC) consists of the residue left from removing the maize grains from the cobs during harvesting. Cobs make up about 20 wt. % of the yield of the corn residue shown in Table 3. CC can also contain other leaves and the grain part of harvested corn and has higher water content than the CS after harvesting. The separation of the stalks, husks and leaves, from the CC is achieved by passing a stream of air through the corn plant residue with the lighter stalks, husks and leaves being discharged to the ground with the cobs being collected in a wagon box on the apparatus (Coulter *et al.*, 2008). CC's are becoming an important feedstock for ethanol and gasification plants. They have more consistent density and ash content than CS (Edwards *et al.*, 2008).

Table 3: Dry matter distribution in corn residues (CR) (Myers and Underwood, 1992).

Corn Residue	wt. % of residue df basis
Stalk	50
Leaf	20
Cob	20
Husk	10

2.3 Thermogravimetric analysis (TGA)

Biomass thermal decomposition analysis is a key step in pyrolysis conversion and describes the process where volatile components consisting of gases are released as the biomass fuel is heated (Biagini *et al.*, 2008). It involves heating a sampled biomass at specific heating rates and studying its change in mass as a function of temperature and time (Brown, 2001). The release of the volatiles is due to the breaking down of the lignocellulosic biomass, being cellulose, lignin and hemicelluloses components (Yang *et al.*, 2007; Varhegyi *et al.*, 1997; Biagini *et al.*, 2008; Di Blasi, 2008). Several researchers (Lapuerta *et al.*, 2004; Garcia-Perez *et al.*, 2001; Aiman and Stubington, 1993; Darmstadt *et al.*, 2001; Cai and Alimujiang, 2009; Mengeloglu and Kabakci, 2008) investigated the thermogravimetric kinetics of different biomass feedstocks. The thermogravimetric analysis of corn residues have been studied by few researchers (Kumar *et al.*, 2008; Zabaniotou *et al.*, 2007; Cao *et al.*, 2004; Cai and Chen, 2008; Yu *et al.*, 2008; Tsai *et al.*, 2001).

Other important parameters such as heating rate, peak temperatures, proximate analysis and the nature and physical properties of biomass that determine the quality and yield of pyrolysis products are also determined (Kumar *et al.*, 2008; Zabaniotou *et al.*, 2007). TGA studies are important for obtaining information on biomass feedstocks thermal conversion and to acquire knowledge about the stability and chemical structure of the materials. The information and knowledge on biomass pyrolysis kinetics are vital for proper design of a fast pyrolysis reactor which plays an important role in large scale pyrolysis process. Biomass thermal conversion process in an inert atmosphere can be described as the sum of the decomposition of its main components, i.e. cellulose, hemicelluloses and lignin (Gronli, 1996; Gronli *et al.*, 2002; Varhegyi *et al.*, 1997). Although TGA provides general information on the overall reaction kinetics of biomass, rather than individual reactions, it could be used as a tool for providing comparative kinetic data for various reaction parameters such as temperature and heating rate.

2.3.1 Kinetic analysis

The kinetic analysis of biomass thermal decomposition is usually based on the rate equation (Biagini *et al.*, 2008):

$$\frac{d\alpha}{dt} = A \exp\left[-\frac{E}{RT}\right] f(\alpha) \quad \text{Equation 1}$$

In equation 1 α is the reacted fraction of the sample or conversion, A and E are the Arrhenius parameter pre-exponential factor and activation energy respectively, and $f(\alpha)$ is the reaction model. T (K) is the temperature and R (Gas constant, J/Kmol.K). These three kinetic parameters (A , E and $f(\alpha)$) are needed to provide a mathematical description of the biomass decomposition process and can be used to reproduce the original kinetic data and predict the process kinetics outside the experimental temperature region (Vyazovkin, 2006). There are two main approaches for the mathematical determination of these three parameters, namely model-fitting and model-free or iso-conversional method (Biagini *et al.*, 2008).

2.3.1.1 Model-fitting approach

The model-fitting approach is based on the initial assumption of a function for $f(\alpha)$ from a selection of available and well known models (Biagini *et al.*, 2008; Vyazovkin, 2006) and the fitting of the chosen model to experimental data in order to obtain the Arrhenius parameters. The application of the model-fitting approach is to manipulate the differential or integral form of the rate equation until a straight line plot can be obtained. The reaction model that gives the straightest line is selected and E and A are then obtained from the values of slope and intercept. Examples of this method are those by Coats *and* Redfern (1965), Freeman *and* Carrol (1958) and Duvvuri *et al.* (1975). According to Caballero *and* Conesa (2005) and Varhegyi *et al.* (1997), the limitation of this kind of analysis is that the data are very often over manipulated leading to a masking of errors in the TG data. In more recent times, owing in part to positive developments in cheaply available desktop computing power, model-fitting approaches have tended towards the use of non-linear least-squares analysis. Non-linear regression analysis involves searching for values of the kinetic parameters that minimises the squared sum of the differences between the experimental and calculated values of TG (Thermogravimetry) or DTG (Derivative thermogravimetry) data (Varhegyi *et al.*, 1989; Varhegyi, 2007; Luangkiattikhun *et al.*, 2008; Caballero *et al.*, 1997). Using DTG data for example, non-linear regression can be done by minimising the sum;

$$s = \sum \left[\left(\frac{d\alpha}{dt} \right)_{exp} - \left(\frac{d\alpha}{dt} \right)_{calc} \right]^2 \quad \text{Equation 2}$$

Where $\left(\frac{d\alpha}{dt}\right)_{exp}$ and $\left(\frac{d\alpha}{dt}\right)_{calc}$ stand for the experimental and calculated DTG curves respectively.

The decomposition of biomass is too complex to be realistically described using the single component model in equation (1), so a multi-component model is frequently assumed in model-fitting analysis. The material studied is assumed to be composed of pseudo components, which refer to a group of reactive species that exhibit similar reactivity e.g. cellulose, hemicelluloses, lignin and extractives (Varhegyi, 2007). In this case equation (1) becomes;

$$\left(\frac{d\alpha}{dt}\right) = \sum y_i A_i \exp\left[-\frac{E_i}{RT}\right] f(\alpha_i) \quad \text{Equation 3}$$

Where y_i is the contribution of pseudo component i to the total mass loss.

The common criticism of the classical and non-linear regression model-fitting approaches is that the values of the Arrhenius parameters obtained are often ambiguous. The ambiguity lies in the basis of the approach which is the adoption of a reaction models (α). The parameters thus calculated are inevitably tied to the specific reaction model assumed. The situation frequently arises where different reaction models are able to satisfactorily fit the data whereas the corresponding values of E and A are decisively different (Vyazovkin, 2006; Ramajo-Escalera *et al.*, 2006).

2.3.1.2 Iso-conversional approach

The iso-conversional method does not require the choosing of a reaction model and is thus 'model-free'. It allows the estimation of activation energy (E) as a function of conversion(α), without assuming any particular form of the reaction model, $f(\alpha)$. The main principle behind this method is that the reaction rate for a constant extent of conversion varies only with the temperature (Vyazovkin, 2006). The iso-conversional method employs data from multiple heating rates as this is the only practical way to obtain data on the variation of the reaction rate at a particular extent of conversion. Vyazovkin (2006) found that the use of multiple heating rates is generally capable of producing kinetic parameters that can serve the practical purpose of predicting kinetic data outside the experimental temperature range. The most common application of the iso-conversional analysis was developed by Friedman (1964). The temperature dependence is universally described by the Arrhenius equation in

equation (1). This method involves computing the logarithms of both sides of equation (1) to obtain:

$$\ln\left(\frac{d\alpha}{dt}\right) = \ln[Af(\alpha)] - \frac{E}{RT} \quad \text{Equation 4}$$

A plot of $\ln\left(\frac{d\alpha}{dt}\right)$ against $1/T$ known as Friedman's plot at the same degree of conversion from data taken at various heating rates will result in a series of lines, each with slope equal to $-E_{\alpha}/R$, corresponding to each value of conversion, α . Thus the variation of E with α is obtained. Friedman's method is useful for studying the multi-step nature of biomass devolatilisation and the corresponding dependence of activation energy, E on conversion, α . As part of this study the available biomass feedstocks will be studied by TGA analysis before any FP experiments are done.

2.4 Thermochemical processes

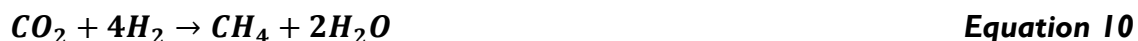
Energy products from agricultural wastes can be produced through two main processes, namely bio-chemical and thermochemical processes (McKendry, 2002; Goyal *et al.*, 2006). In this study, only thermochemical processes have been presented. Thermochemical conversion processes of biomass have two fundamental approaches (Goyal *et al.*, 2006). The first approach is gasification, torrefaction, hydrogenation and combustion of biomass (Hayes, 2008). The second basic approach is to directly convert the biomass by high temperature pyrolysis, high pressure liquefaction, low temperature pyrolysis and supercritical extraction (Onay and Kockar, 2003). These approaches directly convert the biomass into higher energy rich liquids, solids and gaseous products (Dermibas, 2001; Goyal *et al.*, 2006). The choice of conversion process selected depends on the type and amount of biomass, the physical state required of the product, i.e., final product use requirements, economics of the process, environmental conditions, and the overall project objectives (Faaij, 2006). Pyrolysis as a conversion technology is developing and receiving special attention as it can directly convert biomass feedstocks into solid, liquid and gaseous products by thermal degradation in the absence of oxygen (Piskorz, 2002; Meir and Faix, 1999). Pyrolysis process offers efficient utilisation of agricultural residues, especially in countries with a large agricultural industry. In this thesis, the focus is on low temperature pyrolysis while other conventional processes will only be discussed in brief.

2.4.1 Combustion

This technology burns any kind of solid biomass or waste in air to produce heat energy in boilers, burners, turbines and internal combustion engines (Sims *et al.*, 2004; Herold, 2007). This is the easiest and oldest way of producing heat energy from biomass wastes (Klass, 1998). In a combustion process, some biomass (depending on the type combustion equipment) requires some pre-treatment like drying, chopping, grinding, etc., which are associated with higher operating costs and financial expenditure (Mckendry, 2002).

2.4.2 Gasification

Gasification is a thermo-chemical process in which the biomass feedstock is heated in an oxidising atmospheres (oxygen, steam, carbon dioxide or a mixture of these), at high temperature in the range 800-900 °C (Hisham *and* Eid, 2008). The gasification process produces gaseous products mainly consisting of methane (CH₄), hydrogen (H₂), carbon monoxide (CO) and carbon dioxide (CO₂). These products can be used for power and heat generation or for gaseous and hydrocarbon liquid fuel production in a Fischer-Tropsch process (Klass, 1998). For gasification, the level of oxygen is limited to less than 30 (v/v) % O₂ (Sims *et al.*, 2004). The reactions involved in gasification are the following (Demirbas, 2001a; McKendry, 2002; White *and* Plasket, 1981; Othmer, 1980):



Equation 10 is the Sabatier reaction

2.4.3 Liquefaction

In a liquefaction process, liquid is produced from biomass by thermo-chemical conversion at low temperature (250-330 °C) and high pressure (5-20 MPa). In some cases sodium carbonate catalyst is used to enhance the rate of reaction in the presence of high hydrogen partial pressure (Appel *et al.*, 1980) and a solvent. The most commonly used solvent in liquefaction studies is water (Moffatt *and* Overend, 1985; Naber *et al.*, 1997; Goudriaan *and*

Peferoen, 1990). He *et al.* (2000) also reported that the addition of CO as a process gas was more effective than H₂ producing higher bio-oil yield and increased the conversion rates. The liquefaction process is expensive and also the product is in a tarry phase, which is not easy to handle (Demirbas, 2001a). The biomass components are decomposed into small molecules in aqueous medium or using an organic solvent. The fuel from liquefaction has a lower oxygen content which makes it more compatible to conventional fuels, stable on storage and requires less upgrading to produce liquid hydrocarbon fuel (Morf, 2001) than from pyrolysis. Oxygen is removed from the biomass, mainly as (CO₂) and result in a bio-crude product with oxygen content of bio-oil as low as 10-18 wt. % (Demirbas, 2000).

2.4.4 Hydrogenation

Hydrogenation is a process for producing CH₄ by hydro-gasification. Syngas (a mixture of H₂ and CO) is produced in the first stage. The carbon monoxide formed is then reacted with hydrogen to form methane (Othmer, 1980).

2.4.5 Pyrolysis processes

Pyrolysis is a thermo-chemical decomposition technique in which biomass feedstock is transformed into bio-oil (liquid fuel), biochar (solid fuel) and non-condensable gas (gaseous fuel) that can be used as improved fuels or intermediate energy carriers (Sims *et al.*, 2004; Girardet *et al.*, 2005). The product spectrum from pyrolysis is dependent on the process temperature, pressure and residence time of the pyrolysis vapours (Bridgwater *et al.*, 1999a; Bridgwater and Peacocke, 2000; Czernik and Bridgwater, 2004; Yaman, 2004). Essentially the method consists of heating the biomass in an nitrogen (N₂) atmosphere up to a certain desired temperature free of oxygen (O₂) or with less O₂ than required for combustion (Mohan *et al.*, 2006). Decomposition of biomass involves complex interaction of mass and heat transfers with chemical reactions, resulting in the evaporation of water and vapours, and production of some non-condensable gases (Gronli, 2000). The solid matrix (biochar) consists mainly of carbon, but includes most of the minerals present in the biomass. A large part of the produced vapours can be condensed to a brown liquid bio-oil, leaving the non-condensable gases as a combustible fuel for immediate use. The different types of pyrolysis will be discussed in the next section with a particular attention on fast pyrolysis (FP). In this study, only the following types of pyrolysis conversion are discussed in brief: **Torrefaction** (mild pyrolysis treatment for energy densification and storage of biomass) (Boerrigter *et al.*, 2006), **Slow pyrolysis** (or conventional pyrolysis; is focused on biochar production)

(Karaosmanoglu *et al.*, 1999; Mohan *et al.*, 2006), **Vacuum Pyrolysis** (produces high quality liquids and biochar) and **Fast Pyrolysis** (high liquids yields are obtained) (Bridgwater and Peacocke, 2000; Oasmaa *et al.*, 2003). The reaction conditions and the product distribution of pyrolysis and gasification processes are shown in Table 4.

Table 4: Product yields from various biomass conversion techniques (Bridgwater, 2003; Bergmann and Kiel, 2005)

Process	Comments	Solid	Liquid	Gas
Fast pyrolysis	500 °C, short residence	12	75	13
Slow/Vacuum	450-500°C, long residence	35	30	35
Gasification	>800 °C, long residence	10	5	85
Torrefaction	200-300 °C, long residence time	70	-	30

In gasification solid biomass feedstocks or wastes are heated up in the presence of oxidising agents in specified amounts. The final gaseous outputs can be used for power and heat generation or, with cleaning of these gases followed by catalytic Fischer-Tropsch synthesis, gaseous fuel or liquid fuel can be produced. Gasification process maximises the production of gases to up to 85% at higher temperatures than those for fast and slow pyrolysis process (Bridgwater, 2003). High temperature pyrolysis (temperature of 900-1000 °C) can achieve the same gas yields as gasification (Zanzi *et al.*, 1996). In this study, the production of a large amount of bio-oil for fuels production is required. Therefore, Fast Pyrolysis of crop wastes was selected which results in up to 75 wt. % liquids yields to maximise liquids production.

2.4.5.1 Torrefaction

The main objective of torrefaction is to upgrade biomass under low temperature and long residence time (1 hour) (Bergmann and Kiel, 2005). It is conducted in an inert atmosphere similar to conventional pyrolysis; however the temperature is lower and ranges between 200-300°C and pressure near atmospheric (Uslu, 2008). Torrefied solid fuel can replace coal and provides extra advantages; it can be used in combustion, pyrolysis and gasification for production of heat and power, and Fischer-Tropsch liquids hydrocarbons (Uslu, 2008; Hopkins and James, 2008). The product of the process is a solid, biochar like substance. The properties of torrefied biomass are:

- A lower moisture content, higher heating value and increased energy density of the biomass.
- More brittle than untorrefied biomass.

- Hydrophobic nature: Torrefied biomass does not gain moisture in storage, and is therefore more stable and resistant to fungal attack (CGPL, 2006).
- Energy density: A more energy density product is formed. The weight is reduced to approximately 70%. Pach *et al.* (2002) and Uslu *et al.* (2008) found that 80-90% of the original biomass energy content is retained after the torrefaction process. Torrefied biomass has potential in various industries like raw material for pellet production; reducer for smelters in the steel industry, manufacturing of charcoal or activated carbon, gasification, and co-firing for boiler applications. The different types of lignocellulosic feedstocks can be handled in a torrefaction process (Bergmann *and* Kiel, 2005).

2.4.5.2 Slow pyrolysis

Slow pyrolysis also known as conventional pyrolysis or carbonisation, has been around for thousands of years where it was mostly used for charcoal production. In this process biomass feedstock is slowly heated to approximately 450-500 °C (Bridgwater, 2003) in an inert atmosphere with varying vapour residence time of 5-30 min (Bridgwater, 1994, 2001). The residence time is controlled by slowly feeding N₂ gas through the reactor. The longer residence time causes the vapours to continue reacting and allows secondary reactions of vapours, which reduce the organic liquid yield (Bridgwater *et al.*, 1999a). As shown in Table 4, slow pyrolysis produces approximately 35 wt. % of biochar, 30 wt. % of liquid and 35 wt. % of gas. The main product is usually biochar. This latter may be used as solid fuel or to produce adsorbents.

2.4.5.3 Vacuum pyrolysis

Vacuum pyrolysis is a much newer technology than conventional slow pyrolysis. The main difference between vacuum pyrolysis and slow pyrolysis is that it is done under vacuum instead of using an inert gas to replace air. This limits secondary reactions, which results in higher bio-oil yields, and lower gas yields. The vacuum removes condensable gases from the reaction zone, and prevents further re-condensation and secondary reactions. This process is usually conducted at 10-20 kPa, where conventional pyrolysis is carried out at atmospheric conditions. The temperature range is similar to conventional pyrolysis, and typically lies somewhere between 450 and 500 °C (Bridgwater, 2003). Because of the lower pressure biomass fragments tend to evaporate more easily. This removes them from the reaction zone, and results in a significantly reduced residence time (Typically 0.2 seconds)

(Scott *and* Piskorz, 1982). Therefore, the bio-oil obtained is of lower insolubles and viscosity than from conventional pyrolysis. Pyrolysis of wood biomass under vacuum conditions was first performed in 1914 by Klason (Pakdel *and* Roy, 1988) and the objectives of his work were to find the cause of exothermic reactions and to identify the primary and secondary pyrolysis products. Pakdel *and* Roy (1988) and others from the University of Laval in Canada have extensively researched the specific bio-oil production by vacuum pyrolysis.

2.5 Fast Pyrolysis

2.5.1 Process description

The moderate temperature of approximately 500 °C (Czernik *and* Bridgwater, 2004; Bridgwater, 2003) and short vapour residence time of 1-2 seconds (Yaman, 2004) in FP are optimum for producing bio-oil liquids. FP occurs quickly, therefore, not only chemical reaction kinetics but also mass and heat transfer processes, as well as phase changes, play significant roles. The important issue is to bring the reacting biomass feedstock particles to the optimum process temperature and reduce their exposure to intermediate (lower) temperatures that favour production of biochar. This objective can be achieved by using small particles (≤ 2 mm) (Bridgwater, 2003). In FP, the conversion of biomasses generates mostly vapours and aerosols and small amounts of biochar. After quenching, cooling and condensation of the vapours and aerosols, a dark brown bio-oil liquid is formed. Fast pyrolysis is related to the conventional pyrolysis processes for producing biochar and bio-oil, but it is an advanced process, with optimised controlled process operating parameters to give high bio-oil liquid yields. The important features of a FP process for producing liquids are (Bridgwater *et al.*, 1999a):

- Very high heating rates and heat transfer rates at the biomass particle reaction interface usually require a finely ground biomass feed of typically less than 3 mm as biomass generally has a low thermal conductivity.
- Carefully controlled pyrolysis reaction for temperature around 500°C and vapour phase temperature of 400-450 °C.
- Short vapour residence times of typically less than 2 seconds.
- Rapid cooling of the pyrolysis vapours to give the bio-oil product.

The pyrolysis reactor conditions have influence on product yields and the pyrolysis products quality hence the parameters (heating rate, reaction temperature, particle size, and vapour residence time) were discussed in the next section.

2.5.2 Reactor parameters

Fast pyrolysis of biomass has been extensively reviewed (Goyal *et al.*, 2006; Kersten *et al.*, 2005). These reviews typically discussed the parameters important for reactor design, the challenges involved, some comparisons of different feedstocks, and evaluated the product quality. Pyrolysis experiments have been performed on wood, bark, sewage residues, cereal residues, sugar cane bagasse, nuts and seeds, grasses, algae and forestry residues (Mohan *et al.*, 2006). The following parameters and data are important in the FP process.

2.5.2.1 Heating rate

The increase in heating rate increases the bio-oil yield (Basak *and* Putun, 2006). Sukiran *et al.* (2009) on palm fruit branches studies and many other researchers on different feedstocks and types of FP reactors also found out the same variation of heating rate to bio-oil yields. In fast heating rates of the biomass, solid particle pass charring zone at lower temperature more quickly to reduce the biochar production, and improved the bio-oil production. The low heating rates simulate slow pyrolysis which produces mainly biochar and fast heating rates simulate FP with the highest liquid yield. Cetin *et al.* (2005) reported that the biochar gasification reactivity increased with an increase in the heating rate employed in biochar preparation. This could be attributed to the higher BET total surface areas in biochars produced at higher heating rates.

2.5.2.2 Reaction temperature

For most types of biomass, the liquid yields in FP are optimised between 450-500 °C (Bridgwater, 2003). The influence of temperature on the product yields is illustrated in Figure 3 for data from FP of wood. From Figure 3, at very low temperatures the biochar formation is high. This is because the heating rate is lower, and therefore slow pyrolysis is simulated. If the temperature is increased beyond 500 °C the incondensable gas production becomes favoured, and the liquid yield decreases. This is because the conditions are moving towards gasification conditions. Similar findings were reported by Bridgwater *et al.* (1999a).

The detailed pyrolysis reactions of biomass lignocellulosic components and products formed at different pyrolysis temperatures are described in Table 5. Cellulose is the main component of most biomass and the thermal decomposition mostly studied and best understood (Van de Velden *et al.*, 2010). The three primary reactions of cellulose are (Van de Velden *et al.*, 2010): (i) the fragmentation to hydroxyacetaldehyde, acids and alcohols; (ii) depolymerisation dominates at temperatures between 300 and 450°C which produce anhydrous sugarslike levoglucosan and oligosaccharides in tarry phase; and (iii) At low temperatures (< 300°C) dehydration is dominant which favours biochar, water and gas production (Table 5). Decomposition of cellulose to carbonyl compounds, acids and alcohols occur at around 500 °C (Table 5). At higher temperatures, depolymerisation and fragmentation are dominant. Further increases in temperature (> 500 °C), or very long vapour residence times, will cause secondary reactions to occur between vapour and solid phase to form gas (Bridgwater *et al.*, 1999).

Hemicelluloses the second major biomass component, are decomposed in a similar way to cellulose: by dehydration at low temperatures (< 180 °C) and depolymerisation at higher temperatures (Shafizedah, 1982). Alen *et al.* (1996) reported that hemicellulose produces anhydride fragments, biochar, gas and water, while depolymersisation produces furans, volatile organics and levoglucosenone. Lignin is the most thermally stable lignocellulosic component (Demirbas, 2000). At temperatures below 500 °C dehydration dominates, while at higher temperatures lignin monomers are formed (Van de Velden *et al.*, 2010).

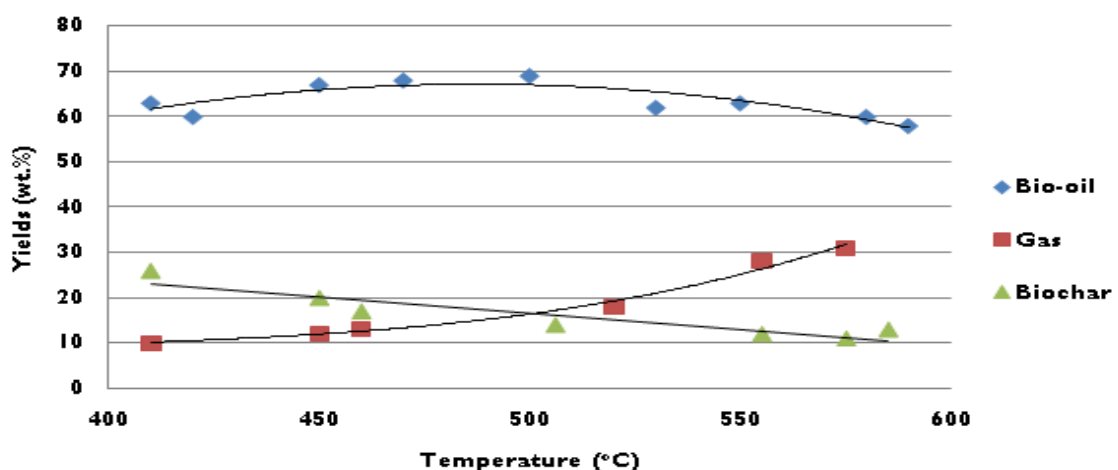


Figure 3: Pyrolysis product yields from wood at various temperatures (Redrawn from (Toft, 1996)).

Condensation reactions also occur at lower temperatures ($< 400\text{ }^{\circ}\text{C}$) with the subsequent formation of lower molecular weight liquids which can also react. However, inorganic species such as K, Na, Fe and Al can have a major impact on these reactions by changing the physical and chemical structure of cellulose (Yang *et al.*, 2006). Due to a variety of reactions that take place during pyrolysis the reaction may be either endothermic or exothermic. For small particles with immediate removal of vapours the pyrolysis reaction is considered endothermic, whereas pyrolysis reactions in larger particles and longer vapour residence times are likely to be exothermic (Ahuja *et al.*, 1999).

The temperature also affects the gas yields and the gas composition produced from fast pyrolysis. Li *et al.* (2004) found that at high temperatures above $500\text{ }^{\circ}\text{C}$ in fast pyrolysis produced a hydrogen-rich gas and higher gas yield. Carbon dioxide is one of the main gaseous degradation products (Prins *et al.*, 2006; Bridgema *et al.*, 2008), its concentration is very high in early stages of FP due to relatively low conversion temperature of mainly hemicellulose (Roel *et al.*, 2010) (Table 5). Table 5 shows the types of reactions, temperatures and products produced from a FP processes.

Table 5: Pyrolysis reactions at different temperatures (Van de Velden *et al.*, 2010; Li *et al.*, 2004; Uzun *et al.*, 2007)

Temperature °C	Reaction	Products		
		Liquids	Solids	Gas
< 300 °C	<ul style="list-style-type: none"> • Free radical Initiation • Elimination of water • Depolymerisation 	Carbonyl compounds	Biochar	H ₂ O CO CO ₂
300-450 °C	<ul style="list-style-type: none"> • Breaking of glycosydic linkages of polysaccharide • Depolymerisation 	Mixture of Levoglucosan, furans, Aromatics, Anhydrides and oligosaccharides in tarry phase	Biochar	CO ₂ , CO, CH ₄ , H ₂ , C ₂ H ₄ , C ₂ H ₆ , H ₂ O
450-500 °C	<ul style="list-style-type: none"> • Dehydration ,rearrangement and fission of sugar units. 	Carbonyl compounds such as acetaldehyde, vanillins, acids, alcohols, glyoxal and acrolein	Biochar	C ₂ H ₄ , C ₂ H ₆ , CO ₂ , H ₂
>500 °C	<ul style="list-style-type: none"> • A mixture of all the above reactions 	A mixture of all the above products		H ₂
Condensation From < 400 °C	<ul style="list-style-type: none"> • Unsaturated products condense and cleave to biochar 		A highly reactive biochar residue containing free radicals	All the above gases

2.5.2.3 Particle size

To improve the efficiency of FP in producing bio-oils, Bridgwater *et al.* (1999) suggested that particle size should be lower than 2 mm. In most cases, the particle size was varied between 0.44-2 mm, and in this range no significant effect on product yields has been reported (Scott and Piskorz., 1982). From research done by Kumar *et al.* (2010) the increase of the particle size decreased bio-oil yield and increased those of biochar and non-condensable gases. This is attributed to the better heat transfer in the inner core of the smaller biomass particles favouring the bio-oil liquid production (Kang *et al.*, 2006). The vital feature of fast pyrolysis is the evolution of all volatiles and complete decomposition of the biomass particles. Shen *et al.* (2009) also reported that the effects of biomass particle size on its FP behaviour can only be compared for biomass particles prepared using similar milling methods and similar types of biomass with the same shape and physical properties. Therefore there is a need to group the different types of biomasses and find optimum particle for each group in order to maximise the liquid yield and quality. The effect of particle size on the bio-oil quality was

also studied by Shen *et al.* (2009) and they found that the smaller particles could give lower yields of light bio-oil components and high yields of heavy bio-oil components.

2.5.2.4 Vapour residence time

It is the average time a vapour gas molecule spends inside the reactor, and is a function of reactor volume and sweep gas flow rate:

$$\tau = \frac{V}{Q}$$

Equation 11

Where V is the reactor volume in m^3 , Q is the sweep gas flow rate in m^3/s and τ is the vapour residence time. Scott *et al.* (1999) and Liden *et al.* (1985) measured the effect of residence time on liquid yield and Antal *et al.* (1983) studied the effect of residence time on bio-oil composition. An increased residence time caused a rapid decrease in bio-oil yield and more tars are produced. It was concluded that the decrease is due to secondary reactions, cracking and polymerisation. During these secondary reactions, polymerisation is promoted, which will ultimately increase the viscosity of the bio-oil product. In essence the vapour residence time should be short, less than 2 seconds (Yaman *et al.*, 2004). The long residence times of the vapours and elevated temperatures (higher than 500°C) cause secondary reactions of the primary products.

2.5 Char and ash separation

As the particles decrease in size during reaction some particles become entrained in the gas. These particles act as vapour cracking catalyst, promoting undesirable secondary reactions, which are unfavourable during bio-oil storage (Das *et al.*, 2004). Therefore the biochar should be separated from the gas as rapidly as possible. Cyclones are used to collect the biochar; however some particles still carry over. Ideally no biochar should end up in the liquid product, as this could cause equipment blockage and failure. According to Bridgwater (1999e), filtration after pyrolysis proves to be difficult. However, successes have been accomplished with ceramic cloth bag house filters, as well as candle filters for smaller laboratory set-ups. The aim is to implement bio-oils in more quality demanding commercial applications, therefore fast pyrolysis technology must be improved to produce a low solid content bio-oil. Hot gas filtration may be used, but this technology is still undergoing development. The ash content of the bio-oil is directly dependent on the biomass ash content, and the efficiency of biochar separation methods used (Bridgwater, 1999e).

2.5.2.6 Liquid collection

Efficient liquid collection poses a challenge in pyrolysis process. This is because the pyrolysis vapours are not true vapours but rather, a combination of vapours, small-sized droplets and polar molecules bonded with water molecules (Bridgwater *et al.*, 1999). Simple heat exchange can cause preferential deposition of lignin derived components leading to liquid fractionation and eventually blockages (Czernik, 2002). Quenching in product bio-oil or in an immiscible hydrocarbon solvent is widely practised. Aerosol capture devices such as demisters are not very effective and electrostatic precipitation is currently the preferred method at smaller scales up to pilot plant (Czernik, 2002). Cooling rate affects the liquid collection; slow cooling rate leads to the production of more lignin compounds, which causes the bio-oil viscosity to increase. It is imperative that quenching of bio-gas is done rapidly, because if this is not done the residence time increases, and secondary reactions may occur (Yaman, 2004).

2.6 Literature review on corn residues fast pyrolysis

Any form and type of biomass can be considered for FP. While most FP work has been done on wood due to its consistency, and comparability between tests, FP tests on nearly 100 different biomass feedstock types have been carried out (Mohan *et al.*, 2006). Many research institutes studied biomass from agricultural wastes such as corn straw, wheat straw, rice straw, olive pits and nut shells to energy crops such as miscanthus, switch grass and sorghum, forestry wastes such as saw dust, bark and solid wastes such as sewage residues and leather wastes (Mohan *et al.*, 2006).

Table 6 presents some recent results obtained from FP of corn residues. From Table 6, the yield of bio-oil is higher than that for biochar and gas at different experimental conditions for both CC and CS biomass. Moreover, the age of the biomass plays a role when comparing the results from fresh and week-old corn stover (Agblevor, 1995). There are slightly higher yields of the liquid and biochar for the old corn stover than the fresh corn stover mainly because of lower water content in the old corn stover (Agblevor, 1995). Therefore, there is a need to study the effect of longer age differences (more than one week) of biomass on the product yields and quality. From Table 6, the yields of bio-oil in fluidised bed reactors (Mullen *et al.*, 2009; Agblevor, 1995) are higher than those produced in fixed bed reactor (Zabaniotou, 2008; Zhang, 2009). This is due to better heat transfer in fluidised bed reactors than in fixed bed reactors. From the study done by Zabaniotou (2008)

on different feedstocks (corn stover and corn cobs), the results showed that under the same operating conditions and type of fast pyrolysis reactor the product yields distribution differs due to differences in modes of heat transfer.

Table 6: Literature review on FP of CC and CS.

Biomass	Conditions	Y_{Liquid} (Wt. %)	Y_{Char} (Wt. %)	Y_{Gas} (Wt. %)	Reference
CC	Fixed bed non-catalytic	40.22	37.31	16.16	Zabaniotou , 2008
CS	N ₂ =100 mL/min 1.5 g of biomass; 0.7 g of glass beads; 500 °C	42.22	32.67	14.47	
Fresh CS	Fluidised bed; 500 °C 80-100 g/h	59.9-61.1	15-15.9	14.6-15.1	Agblevor, 1995
Week old CS		62.5-62.9	19.4-19.5	11.7-14.3	
CC	Static bed; N ₂ =3.4 L/min; 550 °C; 6 g of biomass	56.8	23.2	14.0	Zhang, 2009
CC	Continuous fluidised bed; 100 g of biomass 500 °C	47	23	30	Yanik <i>et al.</i> , 2007
CC	Fluidised bed reactor	61.0	18.9	20.3	Mullen <i>et</i> <i>al.</i> , 2009
CS	Feed rate 1-1.6 kg/hr; 500 °C	61.6	17	21.9	

There are few studies dealing with the influence of lignocellulosic composition on yields and product quality from FP of biomass. Li *et al.* (2004) and other researchers from pyrolysis of biomasses other than corn residues of different lignocellulosic composition concluded that cellulose and hemicelluloses produce more hydrogen than lignin. The pyrolysis of corn residues mixtures have not been researched, showing the vast opportunity for the fundamental research in FP. There are great opportunities in the research of the available South African feedstocks in various areas of FP process.

2.7 Industrial plants

There is an extensive fundamental research work on FP being done in the world at many different institutions (Table 7). They are part of the research groups who are making significant contribution to the researches on FP. Although laboratory studies regarding the thermal decomposition of various organic substances have been carried out for a much longer period, the technology development of fast pyrolysis started only some 20 years ago

(Vendorbosch and Prins, 2010). Ablative fast pyrolysis technology is being developed by German company Pytec, with a pilot plant of 250 kg/hr in operation near Hamburg and plans of a 2 t/hr unit in Mecklenburg-Vorpommern (Scholl et al., 2004)(Table 7).

The simplest method for rapid heating of biomass particles is to mix them with sand particles of a high temperature fluid bed (Vendorbosch and Prins, 2010). The early work on fluidised beds was carried out at the University of Waterloo in Canada, which pioneering the science of fast pyrolysis and established a clear lead in this area for many years (Scott and Piskorz, 1982). Bubbling fluidbeds have been selected for further development by several companies, including Union Fenosa (Cuevas et al., 1995), who built and operated a 200 kg/h pilot unit in Spain based on the University of Waterloo process which was dismantled some years ago (Bridgwater, 2011). The Canadian company, Dynamotive developed and designed the first fluidised bed commercial plant at West Lorne in 2002. In 2006, the company started to build a second plant in Guelph with a design capacity of 200t/day (Table 7). The operational performances for both the plants cannot be found in the open literature (Sandvig et al 2003).

More recent activities include Ikerlan who are developing a spouted fluid bed in Spain (Fernandez, 2010), Metso who are working with UPM and VTT in Finland who have constructed and are operating a 4 MWth unit in Tampere Finland (Lehto et al., 2010) and Anhui University of Science and Technology in China who are overseeing the construction of three demonstration plants in China up to 600 kg/hr (Bridgwater, 2011).

The first circulating fluid bed was developed at the University of western Ontario in the late 1970s and early 1980s (Vendorbosch and Prins, 2010). A fairly large circulating fluid bed pilot plant of 625 kg/hr throughput capacity has been built in Bastardo, Italy (Rossi and Graham, 1997). Special mention should be made of the work at KIT, Germany. They are optimising the already existing FPurgi twin screw reactor of 15 kg/hr capacity with different heat carriers and feed (www.kit-itcvp.edu). They are converting straw to pyrolysis oil and char to serve as a high-energy slurry feedstock for entrained flow gasification (Bioliq Process) (Henrich et al., 2009). The construction of a 500 kg/hr was completed and pilot plant uses sand as a heating medium, whereas the research work was carried out on different heat carriers including stainless steel balls (Table 7).

BTG' technology rotating cone reactor has been a continuous research in Netherlands (Vendorbosch and Prins, 2010). At University of Twente BTG constructed a novel reactor

system (throughput capacity of up to 20 kg/hr) (Vendorbosch et al., 1997). BTG also scaled up Wagenaar's RCR technology from 50 kg/hr in 1997 to 250 kg/hr in 2001. In 2001, BTG had a first detailed design for a 1 t/hr diaper slugde pyrolysis unit for the company Bio-oil Nerderland (BON). In 2004, BTG sold the world's first commercial unit of 50 t/day on empty fruit bunch (EFB) in Malaysia (Vendorbosch and Prins, 2010).

Table 7: Fast pyrolysis research institutes.

Institute	Capacity	References
EFB (Malaysia)	50 t/day	Vendorbosch and Prins, 2010
BON (Netherlands)	1 t/day	
ENEL Energy power (Italy)	650 kg/hr	Trebbi, 1994
VTT (Finland)	20 kg/hr	Vendorbosch and Prins, 2010
Wagenaar' s RCR	50 kg/hr	Vendorbosch and Prins, 2010
Bastardo (Italy)	625 kg/hr	Rossi and Graham, 1997
Karlsruhe Institute of Technology (Germany)	20/500 kg/hr	Henrich, 2007
Dynamotive (Canada)	200 t/day	Vendorbosch and Prins, 2010)
Pytec(German)	250 kg/hr	Scholl et al., 2004
Union Fenosa (Spain)	200 kg/hr	Cuevas et al., 1995
Anhui University of Science and Technology (China)	600 kg/hr	Brigdwat, 2011

2.8 Bio-oil from Fast Pyrolysis

2.8.1 Product description

Fast pyrolysis (FP) of biomass leads to the formation of solid, gaseous and liquid phases. This study focuses on the liquid phase, named, bio-oil. Bio-oil is a dark brown, free-flowing organic liquid that are comprised of highly oxygenated compounds and is immiscible with other hydro-carbonaceous fuels (Czernic et al., 2004; Peacocke et al., 1994a). The synonyms for bio-oil include pyrolysis oils, pyrolysis liquids, bio-crude oils, wood liquids, wood oils, liquid smoke, wood distillates and pyroligneous acid (Mohan et al., 2006). The formed pyrolysis oil consists of different sized and reactive molecules as a result of fragmentation

reactions of cellulose, hemicelluloses and lignin polymers. However, the oils are highly oxygenated, viscous, corrosive, acidic, relatively unstable and chemically very complex. It has a distinctive smoky odour. Because of the high oxygen and water content the heating value is significantly less than that of conventional fossil fuels, 18-22 MJ/kg for bio-oil and 40 MJ/kg for heavy fuel oil (Czernik and Bridgwater, 2004; Mohan *et al.*, 2006; Garcia-Perez *et al.*, 2002; Raveendran and Anuradda, 1996). The main difference between fast pyrolysis and liquefaction process are lower conversion rates and heating values product produced from fast pyrolysis (Demirbas, 2001a).

2.8.2 Chemical nature of bio-oil

Most of the original oxygen in the biomass is retained in the fragments that collectively comprise bio-oil. Small amounts of CO₂ and CO are formed, along with a substantial amount of water. Bio-oil contains 35-40 wt. % of oxygen (Czernik and Bridgwater, 2004; Mohan *et al.*, 2006; Garcia-Perez *et al.*, 2002; Oasmaa and Czernik, 1999), but the oxygen content is dependent on the bio-oil's water content. The difference in oxygen content present in the feed versus that in the bio-oil is related to the oxygen content in the gases and the amount present as water in the oil. Oxygen is present in most of the more than 300 compounds that have been identified in bio-oil (Soltes *et al.*, 1981). The compounds found in bio-oil have been classified into the following five broad categories by Piskorz *et al.* (1988): Hydroxyaldehydes, hydroxyketones, sugars and dihydrosugars, carboxylic acids, and phenolic compounds. Table 8 shows more detailed bio-oil chemical groups and the examples of the compounds in the product.

Table 8: The representative chemical composition of liquid from FP (Bridgwater *et al.*, 2002)

Major components	wt. %
Water:	20-30
Water insoluble lignin fragments: insoluble pyrolytic lignin	15-30
Aldehydes: formaldehyde, acetaldehyde, Hydroxyacetaldehyde, glyoxal	10-20
Carboxylic acids: formic, acetic, propionic, butyric, pentanoic, hexanoic, glycolic	10-15
Carbohydrates: cellobiosan,levoglucosan,oligosaccharides,anhydroglucofuranose	5-10
Phenols: phenols,cresols,guiacols,syringols	2-5
Furfurals:	1-4
Alcohols: methanol, ethanol	2-5
Ketones: acetol(1-hydroxy-2-propanone),cyclo-pentanone	1-5

The bio-oils contain several hundred different chemicals in widely varying proportions, ranging from low-molecular weight to complex high molecular weight such as phenols and anhydrosugars (Diebold, 1999; Meier *and* Faix, 1999). The presence of highly oxygenated compounds in bio-oil such as water, carboxylic acids, water insoluble lignin fragments, ketones, alcohols, furfurals, carbohydrates, aldehydes and phenols is the primary reason for the different physical and chemical properties of hydrocarbon fuels and biomass bio-oils (Diebold, 1999). These differences translate into bio-oils with lower energy content, a higher acidity, and a chemical instability that manifests itself as increased viscosity and decreased volatility with time. Therefore, the efficient removal of oxygen is necessary to transform bio-oil into a liquid transportation fuel that would be widely accepted and economically attractive. Water soluble fraction largely consists of carbohydrate derived products while the water insoluble fraction is a highly viscous phase and mainly derives from lignin (Scholze, 2002). However the separation is not so exclusive. The water insoluble lignin fragments constitutes between 15-30 wt. % of the bio-oil, depending on the feedstock and pyrolysis conditions (Bridgwater *et al.*, 2002). The lignin derived compounds have undesirable effects on bio-oil properties such as high viscosity, phase separation and product instability (Bayerbach *and* Meir, 2009). The acidity of fast pyrolysis bio-oil is the sum of the acidity of its carboxylic compounds which constitutes 10-15 wt. % of the product. Acetic and formic acid are the main acidic components, constituting more than 70% of the carboxylic acids in bio-oil (Czernik *and* Bridgwater, 2004).

2.8.3 Properties of bio-oil

The complex chemical composition of bio-oils induces different chemical and physical properties that are presented in Table 9. The effects of these physical and chemical properties on bio-oil in Table 9 are discussed in the following paragraphs.

2.8.3.1 Moisture content

The water in the bio-oils results from the original moisture in the feedstock and as a product of the dehydration reactions occurring during pyrolysis (Elliott, 1994). The range of the moisture content, 15-30 wt. % is highly dependent on the feedstock and process conditions (Czernik *and* Bridgwater, 2004). At this concentration, water is usually miscible with the lignin derived components because of the solubilising effect of other polar

hydrophilic compounds (low-molecular-weight acids, alcohols, hydroxyaldehydes, and ketones) mostly originating from the decomposition of carbohydrates.

Table 9: Comparison of physical and chemical properties of bio-oil with heavy fuel oil (Czernik and Bridgwater, 2004; Mohan *et al.*, 2006; Garcia-Perez *et al.*, 2002).

Chemical and physical	Bio-oil	Heavy fuel oil
Moisture content, wt. %	15-30	0.1
pH	2.5	-
Density (kg/m ³)	1200	940
Elemental composition, wt. %		
C	54-58	85
H	5.5-7.0	11
N	0-0.2	0.3
O (By difference)	35-40	0.1
Ash (wt. %)	0-0.2	0.1
HHV, MJ/kg	16-19	40
Viscosity (at 50 °C), cP	40-100	180
Solids, wt.%	0.2-1	1
Distillation residue, wt. %	30-50	1

The presence of water has both negative and positive effects on the bio-oil properties. It lowers its heating value, especially the Lower Heating Value (LHV) and flame temperature. It also contributes to the increase in ignition delay and in some cases to the decrease of combustion rate compared to diesel fuels (Elliott *et al.*, 1994). On the other hand, it improves bio-oil flow characteristics (reduces the oil viscosity), which is beneficial for combustion (pumpability and atomisation properties).

2.8.3.2 Elemental composition – Oxygen content

Bio-oil oxygen content is approximately 35-40 wt. %, distributed over all components (more than 300, depending on biomass) (Czernik and Bridgwater, 2004). This high oxygen content is what creates the main difference between bio-oil and conventional hydrocarbons. The high oxygen content results in a low energy density (heating value) that is approximately half that of conventional fuel oils, immiscibility with hydrocarbon fuels and makes it less energy dense (www.pyne.co.uk). The distribution of these compounds mostly depends on the type of biomass used and on the process conditions in terms of temperature, residence time, and heating rate profiles. An increase in pyrolysis temperature and residence time reduces the organic liquid yield due to cracking of the vapours and formation of gases but leaves the organic liquid with less oxygen (Boateng *et al.*, 2007).

2.8.3.3 Volatility distribution

Due to their chemical composition, bio-oils show a very wide range of boiling temperatures because of the many different species present. In addition to water and volatile organic components, biomass pyrolysis oils contain substantial amounts of non-volatile materials such as sugars and oligomeric phenolics. During boiling operations, some of the compounds start evaporating at low temperatures (100°C) and may stop boiling at about 250-280 °C, leaving 30-50 wt. % residues (Czernik *and* Bridgwater, 2004). Thus, bio-oils cannot be used for applications requiring complete evaporation before combustion.

2.8.3.4 Viscosity

The viscosities of bio-oils vary, and are dependent on several parameters, such as water content, aging and temperature. The viscosity of bio-oils can vary over a wide range (35-1000 cP at 40 °C) depending on the feedstock and process conditions, and especially on the efficiency of collection of low boiling components. In a study, Sipila *et al.* (1998) found that viscosities were reduced by higher water content and less insoluble components. Research at the National Renewable Energy Laboratory (NREL) showed that the increase of viscosity during storage could be reduced by adding 10-20 wt. % of an alcohol (methanol or ethanol) to the mixture (Diebold, 2000). A significant reduction in viscosity can also be achieved by addition of polar solvents such as acetone. The viscosity increase, an undesired effect, observed when the oils are stored or handled at higher temperature is believed to result from polymerisation reactions between various compounds present in the bio-oil, leading to the formation of larger molecules (Czernik *and* Bridgwater, 2004).

2.8.3.5 Acidity-pH

Bio-oils contain substantial amounts of organic acids, mostly acetic and formic acids, which result in a pH range of 2-3 (Czernik *and* Bridgwater, 2004). This acidity makes bio-oil corrosive, especially at elevated temperatures in the presence of water. Corrosive resistant materials of construction (e.g non-corrosive stainless steels) should be used in the process designs. Soltes *and* Lin (2001) reported that common construction materials such as carbon steel, aluminium and sealing materials can be affected by the acidity.

2.8.3.6 Heating value

The heating value of bio-oil produced from biomass feedstocks is relatively low compared to conventional fuels, in the region of 16-22 MJ/kg (Czernik *and* Bridgwater, 2004; Mohan *et al.*,

2006; Garcia-Perez *et al.*, 2002; Raveendran *and* Anuradda, 1996). This range of values is directly related to the amount of energy released per kg. Due to its high oxygen content and the presence of a significant portion of water, the heating value of bio-oil is much lower than for fossil derived oils by almost half (Mohan *et al.*, 2006). The Higher Heating Value (HHV) of bio-oil gives a more transportation cost advantage than biomass, carrying a more energy dense product bio-oil. The bio-oil heating value can be improved by removing water from the product and upgrading by oxygen removal.

2.8.3.7 Ash

Some ash remains in the bio-oil, which can cause corrosion as well as other problems. The inorganic part which end up in the ash content is made up of alkali (Na, K), earth alkali (Mg, Ca) and other elements such as S, Cl, N, P, Si, Al and heavy metals (Cd, Zn, As, Pb, Cu, Hg) (Diebold, 2000; Milne *et al.*, 1997). The ash content should preferably be less than 0.1 wt. % for use in engines (Qi *et al.*, 2007). This parameter is very important as the presence of ash causes aging reactions in the product during storage and is affected also by the feedstocks elemental composition. The harvesting methods, transportation, storage and collection of the raw materials also affect the ash content present in the product. Ash content can be reduced by removing the fines particles in the feedstock and by raw materials pre-treatment methods for example de-ashing, alkali or acid treatment, ozonolysis and delignification (Garcia-Perez *et al.*, 2002).

2.8.3.8 Solids content

These are solids entrained in the bio-oil and consist of fine biochar particles that are not removed by the cleaning section of cyclones and filters. The solid biochar can also raise bio-oil viscosity through catalytic reactions during storage, and is likely to be detrimental in most applications. Therefore, efficient removal of solids is necessary for the production of bio-oil of high quality (Park *et al.*, 2004). Hot gas filtration in ceramic cloth bag house filters (Diebold *et al.*, 1993) and candle filters for short runs have achieved success in reducing the solids content in the bio-oil.

2.8.3.9 Density

The density of bio-oil is higher than that of biomass (Table 10). There is a greater increase in energy per unit volume from the raw biomass to the bio-oil by over 4 times as shown in Table 10. The higher energy density of the bio-oils has advantages of making the bio-oils

2.9.1 Composition by solvent fractionation

Bio-oil is fractionated into different groups of compounds before chemical analysis due to their solubility properties. Bio-oil fractionation is the first stage in chemical analysis of bio-oil components. In solvent fractionation, pyrolysis liquid is fractionated into water-soluble (WS) and water insoluble (WIS) fractions. The WS fraction is analysed for volatile carboxylic acids, alcohols, ether-soluble (ES) fraction (aldehydes and ketones), water, and ether-insoluble (EIS), sugars. The WS fraction is further extracted with diethyl ether. Ether-soluble and diethyl ether-insolubles are evaporated ($< 40\text{ }^{\circ}\text{C}$) and residues are dried and weighed. ES is calculated by subtracting the quantities of carboxylic acids, water, alcohols and EIS from WS fraction (Oasmaa and Meir, 2000). The WIS fraction consists mainly of lignin derived materials of varying molecular mass distributions, extractives and solids. WIS are divided by dichloromethane (DCM) extraction further into two fractions having different molecular size distribution. DCM-insoluble material is powder-like HMM (MM < 1050 Da) lignin derived material. There are no GC-eluted compounds. Solids are included in this fraction. The DCM-soluble fraction consists of low molecular-mass lignin material (MM 400 Da) and extractives. GC-eluting compounds of this fraction are poorly WS lignin monomers and lignin dimmers (Oasmaa and Meir, 2000).

2.9.2 Volatile compounds by solid-phase micro-extraction

Solid Phase Micro Extraction (SPME) is a quick technology used to separate volatile compounds from bio-oil (Pinho *et al.*, 2003). It has two vital functions: analyses by extraction and desorbing the sample into an analytical instrument. A fused silica, coated with an adsorbing material, is exposed into the head space of the sample. The sample is drawn back into the needle and introduced into the injector of a GC as reported by Pinho *et al.* (2003) using flame ionisation detector (FID) (Poinot *et al.*, 2007).

2.9.3 Volatile carboxylic acids and alcohols

The acidity of pyrolysis liquids can be determined by the pH. The fouling of electrodes and bio-oil sticking on the probe can cause errors in the result. Hence, pH is recommended to be used mainly for determination of pH level (Oasmaa and Meier, 2005). Quantitative analysis of carboxylic acids and alcohols can be carried out by GC (Shen, 1981). The characterisation of organic acids in pyrolysis liquids often starts by group separation (described in paragraph 2.9.1) steps prior to gas chromatography (GC) (Drozd, 1975).

2.9.4 Extractives

Extractives of bio-oils can be determined as n-hexane-soluble material. Quantitative analysis of extractives is demanding as there is no solvent which could dissolve only the extractives. The accuracy of this method is compromised by lignin monomers (guaiacols) which also dissolve in n-hexane (Oasmaa and Kuoppala, 2003). The quantitative analysis of solids biomass extractives is performed using organic solvents and a Soxhlet apparatus in accordance to ASTM Method 1108-96 (Sluiter *et al.*, 2008). Qualitative chemical analysis of the extractives is performed using gas chromatography mass spectrometry. Quantitative analysis of extractives in liquids is difficult and is recommended to be done in a laboratory specialising in these types of analyses.

2.9.5 Carbonyl groups determination

The carbonyl group of chemicals (aldehydes and ketones) participate in aging reactions during storage; hence it has been suggested to use carbonyl group content as a stability indicator (Meier, 1999). The method is based on the reaction of hydroxylamine hydrochloride with a variety of aldehydes and ketones in the presence of pyridine. The function of pyridine in the reaction is to produce oxime. The acid liberation in the form of pyridine hydrochloride is determined by titration and is a direct measure of the amount of carbonyl groups originally presents in the sample or prior to analyses with GC and HPLC (Meier, 1999).

2.9.6 Molecular mass determination

The average molecular mass (MM) can be also be used as a stability indicator and is determined by Gas Permeation Chromatography (GPC) using successive infra-red (IR) and ultra-violet (UV) detectors. In this analysis, tetrahydrofuran (THF) is used as a solvent. Based on the application of Raoult's law average molecular mass measurements on bio-oil residues are mainly carried out by vapour pressure osmometric method (Gueze and Williams, 1984).

2.9.7 Elemental analysis

Bio-oils elemental analysis of carbon (C), hydrogen (H) and nitrogen (N) is recommended to be carried out according to ASTM D 5291 by an elemental analyser (Scholze, 2002; Oasmaa *et al.*, 1997). In this method, the elements are simultaneously determined as gaseous products (carbon dioxide, water vapour and nitrogen). The elemental analysis accuracy of C

and H in wood pyrolysis is good, but poor for N. This is attributed to low amounts of nitrogen (<0.1wt. %) in wood bio-oils and to the low N detection limit (0.1wt. %) of the method. The bio-oils from agricultural residues and forest residues contain higher (0.2-0.4 wt. %) concentrations of N, S and Cl, and can be determined after ashing and dissolution of the sample according to ASTM D 4208. Metals are analysed by Inductively Coupled Plasma (ICP) or X-Ray Fluorescence Spectroscopy (XRF) (Pouzar *et al.*, 2001). Oxygen is obtained by difference. Due to the small sample size of bio-oil, the reproducibility of the elemental analysis is dependent on the homogeneity of the product. A minimum of 3 samples are recommended, if the bio-oil sample is inhomogeneous.

2.9.8 Sugars

The determination of sugars is performed by Gas Chromatography (GC) and the use of High Pressure Liquid Chromatography (HPLC) allows the determination of levoglucosan which is the main anhydrosugar in bio-oils (Yoichiro *et al.*, 1998). McInnes *et al.* (1958) reported different types of GC methods which have been developed to determine the amount of sugars; the most useful involve coupling gas chromatography and mass spectroscopy. The sugars in pyrolysis liquids are also characterised as EIS using solvent fractionation scheme and by brix method (Oasmaa and Kuoppala, 2008). Oasmaa and Kuoppala (2008) found that the amount of EIS sugar fraction obtained from solvent fractionation correlated well with the brix method.

2.9.9 Organic acids

The samples are derivatised to their benzylic esters prior to GC analysis (Oasmaa *et al.*, 2005). The conversion increases the volatility of compounds and hence the quantity of eluting compounds from the GC column increases (Meier, 2002). Formic and acetic acids form the bulk part of the organic acids with a portion of 70-80 wt. % (Oasmaa and Kuoppala, 2003).

2.9.10 Poly aromatic Hydrocarbons (PAH)

The knowledge of the PAH content is important in order to use the bio-oils in the market. PAH are determined only by GC and High Pressure Liquid Chromatography (HPLC). Samples are fractionated on silica with different solvents. The diethyl ether-soluble fraction is used for analysis. The PAH amount produced is dependent on the pyrolysis operating conditions such as residence time, biomass type and temperature.

2.9.11 Phenols

They are analysed by using a GC with an internal standard calibration method (Meier, 2002). The phenols are extracted with ethyl acetate prior to analysis or directly injecting the pyrolysis oil. From round robin tests by Oasmaa and Meier (2005) fairly good consistency results were obtained from the two methods. The difference in phenol concentrations from extraction method was reported to be due to inadequate ethyl extraction in other samples (Oasmaa and Meier, 2005).

2.9.12 Total acid Number (TAN)

The total acid number determines the purity of the bio-oil and the presence of acidic and corrosive components in the aqueous sample. It is determined by the amount of potassium hydroxide (KOH) base required to neutralise the acid in one gram of an oil sample. The standard unit of measure is mgKOH/g. It does detect both the weak and strong inorganic acids. The commonly used standard methods are ASTM D664 and ASTM D974, which are titration methods based on using the potentiometer to determine an end point. In a bio-oil sample for fuel production, the value should not exceed 0.1 mg of KOH per gram (mg KOH/g) of sample (Rutkowski and Kubacki, 2006).

2.9.13 Esters

The analysis of esters is important in upgrading methods to measure the extent of solvent addition which converts carbonyl compounds into esters and acetals (Oasmaa et al., 2004). These groups of chemicals are also used as a stability indicator as they are products of aging reactions during storage (Oasmaa et al., 2005). The existence of very low concentrations FAME (fatty methyl esters) in bio-oil has been reported by Garcia-Perez et al. (2010). Several methods have been developed for analysing esters during the trans-esterification of vegetable oils (Stavarache et al., 2005; Suppes et al., 2004; Turkan and Kalay, 2006; Darnoko et al., 2000; Knothe, 2000; Hernando et al., 2007). Among these methods already defined, HPLC and GC are the most common analytical techniques used due to their low cost and operational simplicity. The advantage of HPLC over GC is that it requires no time-consuming derivatisation (Knothe, 2000). For HPLC analysis, the sample can be directly injected after simply washing away the catalyst so the overall analysis time is much shorter. Several HPLC methods for the determination of methyl esters have been reported (Neff et al., 1997; Tratthnigg and Mittelbach, 1990; Holcapek et al., 1999) with a variety of detectors.

The quality standard for the production of biodiesel is described in EN 14214. Within EN 14214, method EN 14103 specifies the FAME content determination.

2.10 Methods for physical characterisation

In order to use bio-oils as heating fuels and oil refinery feedstock, fuel standards are needed. Based on feedback from customer end-users and other research institutes the following physical properties have been suggested to specify: solids, stability, homogeneity, water, and flash point (Peacocke *et al.*, 2003). These properties can be influenced during bio-oils liquid production. Physical properties such as density, heating value and viscosity which cannot directly be influenced by the pyrolysis process are important for liquid end-use customers.

2.10.1 Water content

Water is believed to be chemically dissolved in bio-oils. A change in water content indicates a change in moisture of feedstock, process operating conditions, or an oxygen leak into the system. The water content can be easily adjusted by adjusting the initial feedstock moisture levels. Water content in the bio-oils affects other properties for example viscosity, heating value and density of the product (Asadullah *et al.*, 2008). Scholze (2002) recommended water content of the oils to be analysed by Karl-Fischer titration according to the standard ASTM E 203.

2.10.2 Solids and its components

The solids content of the bio-oils originate from feedstock initial ash, pyrolysis biochar, and sand from reactor fluidising bed or from dirt in the feedstock. From a rice straw biomass of < 5 mm particle size, particles with sizes of 10-100 μ m were captured by cyclones and solid content in bio-oil was about 0.03 wt. % (Park *et al.*, 2004). In contrast, the hot filter could catch particle size around 0.1 μ m (Park *et al.*, 2004). Solid content can be influenced e.g. using homogeneous feedstock size, reducing fines particles, efficient cyclones, or effective solids separation technology such as hot vapour filtration. Oasmaa *and* Kuoppala (2003), Oasmaa *et al.* (2009) and Roy *et al.* (1990) recommended that solid content of bio-oils to be analysed as insoluble material in methanol dichloro methane solution (1:1).

2.10.3 Homogeneity

Homogeneity of bio-oil is a very important property for its end-use. The amount of water in the liquids has a negative effect on the homogeneity of bio-oils. During production the homogeneity of the oils can be controlled by visual observations. Microscopic determination

gives possible phase-separation or presence of solid material, e.g. extractive crystals or inorganics, in the liquid. A 7 day test is recommended for homogeneity verification. The method allows a homogeneous sample to stand for a week at room temperature and the water content from different depths are determined by Karl-Fischer titration (Scholze, 2002).

2.10.4 Stability

Stability of bio-oils can be monitored by changes in viscosity and average molecular mass. These properties are related (Oasmaa *et al.*, 2003a). The use of accelerated aging test (24 hours at 80 °C, viscosity at 40 °C) is recommended as a quick test for measuring the stability of oils. The accelerated aging test relates very well with the chemical changes in the liquid (Oasmaa and Kuoppala, 2003). Stability tests should be performed each time, in exactly the same manner. If the weight loss is > 0.1 wt. % during the test, the results should be discarded. Stability testing is recommended for comparison of bio-oils from one specific pyrolysis process. The best comparisons can be obtained when the differences in the amount of water of the samples is negligible.

2.10.5 Flash point

Flash point is the lowest temperature at which the application of an ignition source causes the ignition of vapours under specified test conditions. The test method ASTM D 93 covers the procedure for the determination of flash point of petroleum products by manual Pensky-Martens closed cup apparatus. The method is applicable to all petroleum products with flash point above 40 °C and below 360 °C, except fuel oils. This method has been used with pyrolysis liquids. However, the flash point cannot be measured for bio-oils at 70-100 °C, where the evaporation of water suppresses the ignition (Oasmaa *et al.*, 1997).

2.10.6 Viscosity and pour point

Viscosity of bio-oils can be affected indirectly by changing the water content or by solvent addition (Oasmaa *et al.*, 1997). Viscosity of bio-oil is recommended to be determined as kinematic viscosity according to the standard method ASTM D 445. Dynamic viscosity by rotating viscometers can also be used for measuring the viscosity of the pyrolysis oils. However, it is not as accurate as kinematic viscosity (Oasmaa and Meir, 2000). The lowest temperature at which movement of sample is observed is recorded as the pour point (Li and Zhang, 2003). The test method for pour point is described in the standard method

ASTM D 97. When measuring the pour point of bio-oils pre-heating of the sample should be excluded due to thermal instability.

2.10.7 Heating values

Heating values are defined as the amount of energy contained in a fuel. The heating values are dependent on the phase of water/steam in the combustion products. If H₂O is in liquid form, the heating value is called Higher Heating Value (HHV). When H₂O is in vapour form, the heating value is called Lower Heating Value (LHV). The heating values are measured by DIN 51900 using a bomb calorimeter and depend mainly on the elemental composition of the material (Oasmaa *et al.*, 1997; Oasmaa *et al.*, 2002). The high water content of bio-oils may lead to poor ignition. The information on heating value determination of bio-oil with high water content is currently unavailable. TAPPI (2011) reported that vacuum distillation to remove part of the water content before analysis can be used. Due to the high volatility of bio-oil lighter components, vacuum distillation can be used to reduce the water content at low temperatures. The bio-oil heating value is a function of water content of the liquid (Czernik and Brigdwater, 2004). The extractive group of compounds contains high energy content and their dissolution in the whole product is beneficial to the product energy content (Oasmaa *et al.*, 2003a). The heating values of the bio-oils can also be determined from the chemical analyses (ultimate analyses) using a correlation by Channiwala and Parikh (2002) (Equation 12).

$$\text{HHV}(\text{MJ/kg}) = 0.3491x_C + 1.1783x_H + 0.1005x_S - 0.1034x_O - 0.0151x_N - 0.0211x_{\text{ASH}} \quad \text{Equation 12}$$

Where C is the carbon, H is the hydrogen, S is the sulphur, O is the oxygen and N is the nitrogen.

2.10.8 Density

The density of bio-oils can be determined with a digital density meter according to the standard method ASTM D 4052. The standard method covers the products which can be handled in the liquid state between 15 and 35 °C. Vapour pressure of the samples should be lower than 80 kPa and kinematic viscosity below 0.015 m²/s. The method is based on the effect of change in the mass of the sample tube in oscillatory frequency. The density of bio-oil liquids correlates well with the amount of water in the liquid (Oasmaa *et al.*, 2004). The

lower the water content the more viscous and denser is the bio-oil and the higher the water content the less viscous and dense is the pyrolysis oil.

2.11 Bio-oil applications

The properties of bio-oil also results in several significant problems, during its use as fuel in standard equipment such as boilers, engines, and gas turbines constructed for combustion of petroleum-derived fuels (Chiaramonti *et al.*, 2003). Poor volatility, high viscosity, coking and corrosiveness are probably the most challenging and have so far limited the range of bio-oil applications. The most important criteria for fuel oil quality are: low solid content, good homogeneity and stability, and a reasonably high flash point (Tsiantzi *and* Athanassiadou, 2000; Oasmaa *and* Peacocke, 2001). Some of the advantages of bio-oils are that: it can be produced from a range of biomass feedstocks, it is cleaner than fossil fuel (releases 50% less nitrogen oxides, zero net CO₂ emissions, no sulphur dioxide emissions) (Mohan *et al.*, 2006). It also presents transportation advantages compared to biomass due to energy densification, it has the potential to be upgraded and used as a transport fuel and it can be refined to produce valuable chemicals (Mohan *et al.*, 2006). The opportunities for industrial applications are many to be listed but some immediate applications in primary industries are kilns and boilers in the pulp and paper industries, process heat in boilers in sawmills, metallurgy, oil and gas industries, as well as in secondary industries such as greenhouses, district heating and stationary engines. The special applications of these compounds in industrial processes and manufacturing are just beginning to be explored. They represent a potentially very large market for value-added products derived from bio-oil. Figure 4 shows different uses of pyrolysis liquid. The different uses of bio-oil are detailed in the following paragraphs:

2.11.1 Combustion and electricity production

Although the heating value of bio-oil is about half that of fossil fuel, and contains a significant portion of water, bio-oil has been successfully used as fuel in various institutions (Canmet in Canada, MIT, Neste in Finland) (Hogan, 2002). Problems reported were high viscosity which can be corrected by the addition of methanol and in-line pre-heating. The preheating of bio-oil using conventional fuels is required before it can be used in boiler or furnace (Bridgwater *et al.*, 2000).

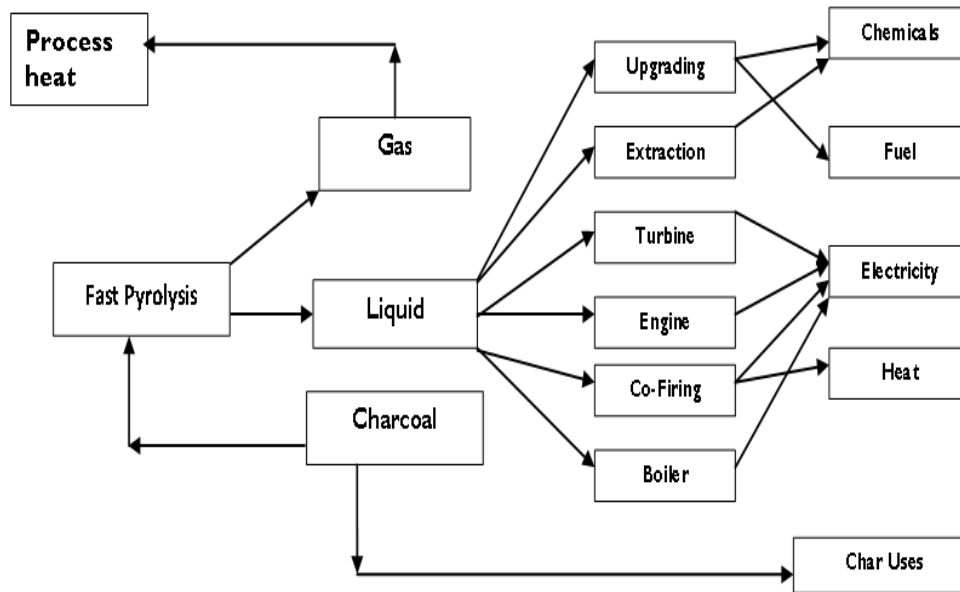


Figure 4: Uses of FP products Redrawn from (IEA Bio-energy, 2002)

Because of the more sophisticated start-up procedure, co-firing of bio-oil in coal utility boilers has also been used (www.btgworld.com). Electricity production is favoured over heat production because of its easy distribution and marketing (Bridgwater *et al.*, 2000). Over recent years numerous diesel engines (laboratory and large scale engines) have been tested with bio-oil (Bridgwater *et al.*, 2002b). These first tests mentioned positive results of engine performance in terms of smooth running. The main problems that still need to be addressed are the acidic nature of the oil, and its tendency to corrode and to re-polymerise, causing a viscosity increase (Bridgwater *et al.*, 2002b). The use of bio-oil requires modification of various parts of the engine; amongst the most important ones are the fuel pump, the linings and the injection system. With these modifications the diesel engine can use bio-oils as an acceptable substitute for diesel fuel in stationary engines. Successful tests have been conducted with a 2 MW gas turbine (Andrews *et al.*, 2007). There is still some uncertainty over the stability, ash and solids properties of bio-oil (Bridgwater and Peacocke, 2000).

In 2002 at University of Florence (Italy) (Chiaramonti *et al.*, 2003a), using a 5.4 kW Lombardini engine. The engine has been successfully operated with use of bioemulsions (bio-oil/diesel oil emulsions) without involving significant modifications to the engine technology (Chiaramonti *et al.*, 2003a). The most important modification to be done was

that the injector and the fuel pump should be made in stainless steel or similar corrosive resistant material.

Ormrod Diesels (Ormrod *and* Webster, 2000) in the United Kingdom have accumulated more than 400 hours of operation on a modified dual fuel low speed diesel engine. Three cylinders of the six-cylinder 250 kW engine have been modified to run on bio-oil using up to 5% diesel as a pilot fuel to initiate combustion. The engine has been successfully operated entirely on bio-oil by shutting off the diesel supply to the un-modified cylinders (Leech, 1997). There were black deposits formed on the pumps and injectors, but they did not appear to affect the performance in any way (Bridgwater, 2004).

In 1993 at VTT Energy, Solantausta et al. (1993) using a 500 cc (maximum power 4.8 Kw) high-speed, single cylinder, direct injection Peter diesel engine with compression ratio of 15.3:1, could not achieve auto-ignition of bio-oil without additives. Further tests at VTT Energy (Solantausta et al., 1994) showed that bio-oil could be efficiently used in pilot-ignited medium speed diesel engines. The most important identified problems were difficulty in adjusting the injection system (due to variation in bio-oil composition), wear and corrosion of certain injection and pump elements (acids and particulates), and high CO emissions. Strenziok et al. (2001) at the University of Rostock (Germany) conducted bio-oil combustion tests in a small commercial gas turbine with a rated power output of 75 Kw. Compared to the operation on diesel fuel, Strenziok et al. (2001) also found that CO and HC emissions were significantly higher and Nox less for dual fuel operation. However, Bridgwater (2004) reported that it is possible to overcome these problems with improvements to the pyrolysis process and use materials for injection nozzles and a catalytic converter for exhaust gases.

2.11.2 Synthesis gas production

Producer gas is a mixture of hydrogen (H_2) and carbon monoxide (CO) produced by gasification of carbon (C) with oxygen (O) and steam. The Fisher-Tropsch (FT) reaction converts synthesis gas derived from coal, methane (CH_4), natural gas or biomass to liquid fuels. Impurities include carbon dioxide (CO_2), CH_4 and higher hydrocarbons which dilute the gas. The concentrations of these trace components should not be too high for the

synthesis reactions of hydrocarbons or alcohols. There are three ways of producing syngas from pyrolysis products by using pure pyrolysis biochar, mixing biochar and bio-oil (Henrich, 2007) and pure bio-oil. The question at mind is whether it is useful to produce producer gas from bio-oil rather than only biomass gasification. For large scale production, it makes sense to use bio-oil because it does not have to be gasified immediately. Off-site production of pyrolysis bio-oil and biochar also reduced the volume of feedstock to be transported by 50%, and thereby significantly decreases transportation costs (Henrich, 2007). After gasification, synthesis gas is fed to the FT process to synthesise fuels.

2.11.3 Boilers

Bio-oil is an effective substitute for diesel, heavy fuel oil, light fuel oil, or natural gas in essentially any type of boiler where these fuels are fired or contemplated to be fired. These are relatively simple applications requiring basic modifications limited mainly to fuel nozzles and transport systems. The only commercial system that regularly uses bio-oil to generate heat is at the Red Arrow products pyrolysis plant in Wisconsin and has operated for over ten years (Freel *et al.*, 1996). A demonstration in 2005 involved firing bio-oil alone in a Dutch oven-type wood fired boiler at the West Lorne's bio-oil plant satisfying steam demand, production and pressure for over an hour as part of the demonstration phase of the West Lorne Bio-oil Cogeneration Project (www.dynamotive.com). The steam produced in the boilers was used to heat Erie Flooring's lumber kilns. Bio-oil seems thus to be a suitable boiler fuel as long as it has consistent characteristics, provides an acceptable emissions level, and is economically feasible. Extensive tests have been performed at Neste Oy (Gust, 1997) in a 2.5 MW Danstoker boiler supplied with a dual fuel burner. The main findings of these tests at Neste Oy showed the need for substantial modifications as follows (Bridgwater, 2004):

- The use of acid resistant material of construction in the boilers.
- Some modifications of the burner and boiler sections were required to improve combustion.
- There is need for preheating the bio-oils to improve its quality as higher water content lead to lower NO_x but higher particulates in flue gas.
- There were clear differences in combustion behaviour and emissions for different bio-oils tested; those with high viscosity and solids content showed significantly

poor flowability. There is need for substantial modifications in the burner to handle high viscosity and solids content.

A constant quality bio-oil is necessary for commercial and large scale boiler applications. Problems of handling (storage, pumping, filtration, and atomisation) and optimisation of boiler design to improve performances and reduce emissions seem to be possible to solve by relatively significant modifications to the existing equipment (Bridgwater, 2004).

2.11.4 Steam reforming

In this process, hydrogen is produced via catalytic reactions of bio-oil vapours. If approximately 80% liquid are obtained from pyrolysis; 6 kg of hydrogen can be produced from 100 kg of pyrolysed biomass. A range of catalysts have been used by different scientists in the field (Ross, 1975; Qi *et al.*, 2007).

2.11.5 Chemicals extracted from bio-oils

The large majority of chemicals are manufactured from petroleum feedstocks (Bridgwater, 2011). A small proportion of the total oil production, around 5%, is used in chemical manufacture but the value of these chemicals is high and contributes comparable revenue to fuel and energy products (Bridgwater, 2011). There is an economic advantage in having flexibility into the biofuels market by devoting part of the biomass production to the manufacture of chemicals. In fact, this concept makes even more sense in the context of biomass because it is chemically more heterogeneous than crude oil and conversion to fuels, particularly hydrocarbons, is not so cost effective (Bridgwater, 2011).

There are many chemical components that can be reclaimed from bio-oil, such as phenols used in the resins industry, levoglucosan, volatile organic acids in formation of chemical anti-icing, furfurals, hydroxyacetaldehyde, some additives applied in the pharmaceutical field, fibre synthesising or fertilising industry and flavouring agents in the food industry (Bridgwater, 1999e; Zhang *et al.*, 2007). Dynamotive Corporation developed a product, biolime, which proved successful in capturing SO_x emissions from coal combustors (Oehr, 1995). Compared to lime, those organic calcium compounds are about four times more efficient in capturing acid gases. In the same way, the water-soluble fraction of bio-oil can also be used to produce calcium salts of carboxylic acids that can be environmentally friendly road de-icers (Oehr *et al.*, 1993). The same aqueous extract of bio-oil includes both low-molecular

mass aldehydes that are effective meat browning agents (especially glycolaldehyde) as well as phenolic compounds that provide smoky flavours.

The water insoluble fraction that usually constitutes 25-30 wt. % of the whole bio-oil is often called pyrolytic lignin because it is essentially composed of oligomeric fragments originating from degradation of native lignin (Radlein *et al.*, 1987; Meier *et al.*, 1997). So far, high value applications of this fraction have not been commercialised; however, using pyrolytic ligninas a phenol replacement in phenol-formaldehyde resins seems to approach that stage. The most important contributions in research and development on pyrolytic lignin based resin formulation have been made at NREL (Chum *and* Kreibich, 1993; Kelly *et al.*, 1997) and Biocarbons (Himmelblau, 1991) in the USA, Ensyn (Giroux *et al.*, 2001) and Pyrovac (Roy *and* Pakdel, 2000) in Canada, and ARI (Tsiantzi *and* Athanassiadou, 2000) in Greece. These resins were successfully used as adhesives in ply wood and particle board manufacturing showing high mechanical strength. In addition to the above applications, the bio-oil has been proposed for use as an alternative wood preservative that could replace creosote (Freel *and* Graham, 2002). Some terpenoid and phenolic compounds present in bio-oil are known to act as insecticides and fungicides (Freel *and* Graham, 2002). The commercialisation of special chemicals from bio-oils requires much effort in developing reliable and effective low cost separation and refining technologies (Brigdwater, 2011).

2.11.6 Emulsification

The easiest way to use bio-oil as a transport fuel seems to be to directly blend it with diesel. Bio-oils are not miscible with liquid hydrocarbons; they can be mixed with the aid of a surfactant (emulsifier). Chiaramonti *et al.* (2003) prepared blends of bio-oil and diesel with ratios of 25, 50 and 75 wt. % and found the emulsions more stable than the original bio-oil. The higher the bio-oil content, the higher the viscosity of the emulsions. The optimal range of emulsifier to provide acceptable viscosity is between 0.5 and 2 wt. % (Zhang *et al.*, 2007). The viscosity of 10-20 wt. % bio-oil emulsions was much lower than that of pure bio-oil, and their corrosiveness was about half that of pure bio-oil alone (Chiaramonti *et al.*, 2003). In emulsification there is no chemical transformation, but the high cost and energy consumption cannot be neglected.

2.12 Bio-oil downstream processes

The use of bio-oils in downstream processes presents many obstacles because of the deleterious properties of high viscosity, product instability and acidic nature and then physical and chemical techniques are required before their application. The properties that affect bio-oil liquid quality are low energy content, incompatibility with liquid hydrocarbons, high solids content, high viscosity and chemical instability of the product (Ahmad *et al.*, 2010). The energy content can be significantly improved, but it requires changes to the chemical structure of bio-oils, which is technically feasible (Lindfors, 2009). These bio-oils characteristics can be improved using chemical and physical techniques. In this section, the recent physical and chemical techniques are described.

2.12.1 Physical techniques

2.12.1.1 Hot gas filtration

Hot gas filtration can decrease the ash levels of the bio-oils to less than 0.01% and the alkali levels to less than 10 ppm which is much lower than reported for biomass oils produced in pyrolysis processes with cyclones for gas cleaning (Scahill *et al.*, 2000). The alkali metals are the main cause of high-temperature corrosion of applications in gas-turbine blades, and they may also affect the long term durability of ceramic filters (Kurkela *et al.*, 1993). The current industrial gas-turbine specification limit for alkali-metal compounds in gas entering a turbine is 0.1 ppm by weight (Mojtadehi *et al.*, 1987, 1991; Mojtahedi and Backman, 1989). Successful results were obtained at VTT reducing the alkali content to less than 0.1 ppm using hot gas filtration (Kurkela *et al.*, 1993).

Brigdwater and Peacocke (2000) reported that diesel engine tests performed on unfiltered oil and on hot filtered bio-oil showed a significant increase in rate of burning and a lower ignition delay for the filtered bio-oil, due to lower average molecular weight for the bio-oil. The presence of solid particles degrades the quality of pyrolysis oils and weakens their ability to penetrate the higher quality fuel markets. As reported by Diebold *et al.* (1996) hot gas filtration has the following advantages:

- The biochar and bio-oil are produced individually and can be marketed separately.
- It reduces amount of solid biochar in the bio-oils.
- This process reduces operating costs by elimination of sludge disposal costs produced from filtering biochar from the bio-oil.

2.12.1.2 Dehydration method

The excess of water and organics (i.e., low molecular mass acids, aldehydes, ketones) which causes the instability of bio-oils can be removed. In laboratory tests, this should be carried out by evaporating the pyrolysis liquid under mild conditions (low temperature and low pressure) in a rotavapor (Oasmaa *et al.*, 2005). In a large scale pyrolysis plant, the removal of water and organics would be carried out by raising the temperature of condensers and, hence, by evaporating the light compounds out of the liquid (Oasmaa *et al.*, 2005). The yield of bio-oil will be reduced by raising the condenser temperature in the fast pyrolysis process (Oasmaa *et al.*, 2005). The evaporation method improves heating value and stability but it also increases the viscosity of the bio-oil which is an undesirable flow property. Oasmaa *et al.* (2005) reported that the viscosity after evaporation technique can be reduced by addition of solvents such as methanol and ethanol.

2.12.1.3 Adsorption separation

Adsorption process is the separation of liquid and gaseous mixtures used in both laboratory and industrial scale for the production of a wide variety of biochemicals, chemicals and materials (Liu *et al.*, 2006). The process has low energy consumption, but the disadvantages of high cost of material, low capacity, low selectivity and possible fouling (Dürre, 1998). Radlein *et al.* (1996) reported the use of molecular sieves to capture the water (reactive-adsorption). This method is usually applied with other methods like reactive distillation (discussed in 2.12.3.2) to remove the water from the bio-oil. Chemical and physical properties determination of the derived bio-oil product showed that the properties were significantly improved by the application of adsorption technology in bio-oil product upgrading (Radlein *et al.*, 1996).

2.12.1.4 Gravimetric filtration

Gravity can be used to separate bio-oil into two phases: a lighter aqueous phase and the heavier viscous tarry phase. The aqueous phase contains mainly water and carbohydrates and the tar phase contains primarily lignin derived compounds. Hydrogen can be produced from carbohydrate solutions by an aqueous phase reforming process (Huber *and* Dumesic, 2006).

2.12.1.5 Membrane separation

It is a separation technology technique considered as one of the most effective and energy-saving processes, highly selective and simple to perform (Dürre, 1998). Its driving force is due the differences of the chemical potential between the feed and permeate sides of the membrane layer. Membrane technology processes are widely used in the petrochemical and water industries (Cheryan *and* Rajagopalan, 1998; Ravanchi *et al.*, 2009). Fouling remains the biggest challenge in the application of membrane-based separations (Cheryan *and* Rajagopalan, 1998; Ravanchi *et al.*, 2009). In bio-oil upgrading microfiltration has been used to remove biochar particles from bio-oil (Javaid *et al.*, 2010). From a study by Javaid *et al.* 2010, bio-oil of 0.1 wt. % ash content was reduced after microfiltration by approximately 60%, to about 0.03 wt. %.

2.12.2 Chemical techniques

2.12.2.1 Polar solvent addition

Addition of alcohols improves the homogeneity, decreases the viscosity and density, lowers the flash point, increases the heating value of pyrolysis liquids and lowers the molecular mass increase during the aging of pyrolysis liquids (Oasmaa *et al.*, 2004; Radlein *et al.*, 1996). The reduction in the viscosity was primarily due to a stabilising effect of alcohols on the water insoluble high molecular mass lignin derived fraction. Other effects include the formation of acetals in reactions of alcohols with aldehydes, ketones, and anhydro-sugars. Low alcohol additions (< 5 wt. %) prevent aging reactions by a few months, while the higher one (> 10 wt. %) retarded them by almost a year. Methanol is the most effective alcohol of those tested namely methanol, ethanol and isopropanol (Boucher *et al.*, 2000; Doshi *et al.*, 2005). Oasmaa *et al.* (2004) reported that in addition to improving solubility, the alcohols also enhanced the separation of the extractive rich top layer in the pyrolysis of biomass by decreasing its volume and increasing the concentration of extractives and solids in the top layer. The main advantage of this method is to reduce the viscosity of the bio-oil and formation of more stable chemical components.

2.12.2.2 Hydro-deoxygenating or Hydro-treatment

The process is performed in hydrogen, providing solvents activated by the catalysts of Co–Mo, Ni–Mo and their oxides or loaded on Al₂O₃ under pressurised conditions of hydrogen and/or CO. Oxygen gas is removed as H₂O and CO₂, and then the energy density is

improved. Pindoria *et al.* (1997; 1998) hydro-treated the volatiles from FP of eucalyptus in a two-stage reactor. Hydro-cracking in the absence of catalysts was operated in the first stage, and catalytic hydro-treatment was operated in the second stage with lower temperature and the same pressure compared to that in the first stage (Pindoria *et al.*, 1997). The chemical analysis indicated that the catalyst deactivation did not result from carbon deposition, but the embodiments of volatile components blocked the activated sites of the zeolite catalyst. This process produced significant amounts of water and complicated the bio-oil with many impurities. Zhang *et al.* (2005) in another study separated the bio-oil with a yield of 70 wt. % into two phases namely: water and oil phase. The oil phase was hydro-treated and catalysed by sulphided Co–Mo–P/Al₂O₃. The reaction was carried out in an autoclave reactor filled with tetralin (as a hydrogen donor solvent) under the optimum operating conditions of 360 °C and 2 MPa pressure. The analysis showed that oxygen content was reduced from 41.8 wt. % of the bio-oil to 3 wt. % of the upgraded one. Apparently the hydro-treating process needs expensive equipment, complex techniques and excess costs. Catalyst deactivation and reactor clogging are problems encountered in this process.

2.12.2.3 Catalytic cracking of pyrolysis vapours

The bio-oils are catalytically decomposed to liquid and gaseous hydrocarbons with the removal of oxygen as H₂O, CO₂ or CO. It was proved that ZnO was a mild catalyst for the conversion of pyrolysis vapours into bio-oils which yield was substantially increased (Nokkosmaki *et al.*, 2000). The upgrading technique had no effect on the water insoluble fraction (lignin derived), it decomposed the diethyl insoluble fraction (water soluble anhydrosugars and polysaccharides). After ageing tests at 80 °C for 24 h, the increase in viscosity was significantly lowered for the ZnO-treated bio-oil (55 % increase in viscosity) compared to the reference bio-oil without any catalyst (129% increase in viscosity). The heating of the product produced separation of the bio-oil into light and heavy organics and polymerisation of the bio-oil to biochar. Guo *et al.* (2003) reviewed various catalyst types used in bio-oil upgrading in detail and believed that although catalytic cracking is a predominant technique, the catalyst with good performance of high conversion and little coking tendency is demanding much effort. Although catalytic cracking is regarded as a cheaper route by converting oxygenated raw materials to lighter product fractions, the

results seem not promising due to high levels of coking 8-25 wt. % and poor quality of the fuels produced (Adaye and Bakhshi, 1995).

2.12.2.4 Esterification of organic acids in bio-oils

Recently, functional ionic liquids, besides being used as a solvent have produced successful results in the area of catalysis. The properties of crude and upgraded bio-oils by ionic liquids are presented in Table I I. The upgraded bio-oil properties were significantly improved than the crude bio-oil by removing of water and acids in the presence of ionic liquid ($C_6(\text{mim})_2\text{-HSO}_4$) (Table I I) (Xiong *et al.*, 2009). Furthermore, large molecule-weight compounds like pyrolysis lignin were removed, and thereby, the viscosity of upgraded bio-oil decreased significantly. The water layer included water, ionic liquid, and a small amount of hydrophilic compounds. With esterifying treatment, high moisture and acidity problems of bio-oil were overcome to some extent under very mild conditions at room temperature and atmospheric pressure. This is a promising treatment for upgrading bio-oil.

Dicationic liquid, for example $C_6(\text{mim})_2\text{-HSO}_4$ is synthesised and used as the catalyst for bio-oil upgrading through the esterification reaction of organic acids and ethanol at room temperature. When the reaction is complete, no coke and deactivation of the catalyst are observed (Xiong *et al.*, 2009). The higher heating value approached 24.6 MJ/kg, the pH value increased from 2.9 to 5.1, and the moisture content decreased from 29.8 to 8.2 wt. % (Table I I). The room temperature ionic liquid (RTIL) offers many advantages from an environmental point of view such as having temperature stability and having the potential for recyclability (Cole *et al.*, 2002; Shi *et al.*, 2005; Smiglak *et al.*, 2007; Welton, 1999). Fischer esterification reactions catalysed by RTIL are extensively studied, and the much development in catalyst recycling and energy conservation has been achieved (Zhang *et al.*, 2007; Pralhad *et al.*, 2008; Li *et al.*, 2008). These reactions demonstrate that the application of acidic dicationic liquid as catalyst for esterification reaction is simple, inexpensive, and easily accessible. From previous studies, the effect of acetalisation reactions of carbonyls and alcohols to the bio-oil stability was not studied in the esterification reactions.

Table 11: Properties of crude and upgraded oils (Xiong *et al.*, 2009)

Properties	Crude bio-oil	Upgraded bio-oil
Moisture (wt. %)	32.8	8.2
Elemental Analysis (wt. %)		
C	41.8	50.6
H	8.8	10.8
O	48.7	38.0
N	0.6	0.4
pH	2.9	5.1
HHV (MJ/kg)	17.3	24.6
Kinematic viscosity (mm ² /s)	13.0	4.9

2.12.3 Physico-chemical techniques

2.12.3.1 Concentration method

The concentration method was developed for improving the storage stability of bio-oils without significantly changing the flash point of the liquid. This method, by which a large part of the water and the light reactive volatiles of FP liquid are replaced by alcohol, proved in laboratory-scale experiments to possess excellent potential to produce a high quality (homogeneous, viscosity similar to light fuel oil and stable) liquid product, removing the unpleasant odour of pyrolysis, and a part of the acidic content, increasing the heating value of the liquid by removing water. Alcohol addition has been suggested as one of the cheapest methods for quality improvement (Oasmaa *et al.*, 1997; Oasmaa and Czernik, 1999; Soltes *et al.*, 1981; Piskorz *et al.*, 1988). However, it also lowers the flash point (Piskorz *et al.*, 1988). It has been suggested that removing light compounds which participate in aging reactions from pyrolysis liquid would improve its stability (Diebold, 2000). These light compounds also cause its unpleasant smell and lower the flash point.

2.12.3.2 Reactive distillation

This upgrading technique is done by reacting crude bio-oil with an alcohol (e.g. ethanol) at mild conditions using sulphuric acid as a catalyst (Radlein *et al.*, 1996; Doshi *et al.*, 2005; Boucher *et al.*, 2000; Oasmaa *et al.*, 2004). From the chemistry point of view, the reactive compounds like aldehydes and organic acids are converted by the reactions with alcohols into more stable compounds such as esters and acetals (Boucher *et al.*, 2000). The removal of water is important to drive the equilibrium to the right. For this purpose, Radlein *et al.* (1996) have proposed the use of molecular sieves technology to capture the produced

water (reactive-adsorption) in order to shift the reaction to the right side. Chemical analysis of the produced bio-oil products showed that, there was an increase in heating value, reduction in water content, reduction in acid content and reduction in viscosity by this alcohol treatment technology (Radlein *et al.*, 1996).

Solids and liquid catalysts are all used in the reactions giving different quality upgraded bio-oil. Mahfud *et al.* (2007) reported that the performance of liquid H_2SO_4 gives a better quality upgraded bio-oil than the solid catalysts except on the acidity which will be higher (pH 0.5 against 3.2); this is due to the relatively low number of solids acid sites (Beltrame *and* Zuretti, 2003; Rios *et al.*, 2005). To prevent a high acidic upgraded bio-oil product, the use of solid acid as catalysts has widely been used to catalyse esterification and other liquid phase acid catalysed reactions (Misono *and* Nosier, 1990; Tanabe *and* Holderich, 1999; Grieco, 1998; Armor, 1991, 2001; Namba *et al.*, 1981; Harmer *et al.*, 1996, 2000; Harmer *and* Sun, 2000; Okuhara, 2002). Nafion SAC13 solid catalyst (Harmer *et al.*, 1996, 2000; Harmer *and* Sun, 2001) was selected to overcome the high acid content in bio-oils and the catalyst recyclability problem when using homogenous acids like liquid H_2SO_4 . To avoid excessive alcohol evaporation, higher boiling point alcohols than that of water are selected. N-Butanol was selected as the best choice in reactive distillation process (Ezeji *et al.*, 2005; 2007) and solidification and polymerisation are prevented at elevated temperatures by applying low pressures. The previous reactions studies indicated that solid acid catalysts have high potential for the reactive distillation concept, although optimisation studies are required to achieve further reductions in bio-oil product acidity and water content.

Other solid acids catalysts ($\text{SO}_4^{2-}/\text{M}_x\text{O}_y$) were prepared and compared in upgrading bio-oil using ethanol and bio-oil as raw materials through reactive rectification (Jun-ming *et al.*, 2008). The properties of upgraded bio-oils were changed by ($\text{SO}_4^{2-}/\text{ZrO}_2$) catalyst and the results are shown in Table 12. The water content decreased from 33% to 0.52% and 5.03%, respectively. The dynamic viscosity of upgraded bio-oils was lowered from 10.5 to 0.46 and 3.65 mm^2s^{-1} . The pH value of light oil was increased from 2.82 to 7.06, while the pH value of heavy oil rose to 5.93. The energy content of two kinds of upgraded oil was increased from 14.3 to 21.5 and 24.5 MJkg^{-1} , respectively (Jun-ming *et al.*, 2008).

Table 12: Comparison of raw bio-oil and upgrading bio-oil after reactive distillation (Jun-ming et al., 2008).

Properties	Original oil	Light oil	Heavy oil
pH	2.82	7.06	5.35
Density (gcm ⁻³)	1.16	0.91	0.95
H ₂ O Content	33.0	0.52	5.03
Calorific value (kJg ⁻¹)	14.3	21.5	24.5
Dynamic Viscosity(mm ² s ⁻¹)	10.5	0.46	3.65
Appearance	Dark brown	Colorless	Dark brown

2.13 Summary of literature

The different waste crops chosen for this study are available in large quantities in South Africa. Biomass feedstocks are a combination of individual components: cellulose, hemicelluloses, lignin and extractives, each of which has its own kinetic characteristics, so it is important to characterise the biomass feedstock before any studies on pyrolysis kinetics and fast pyrolysis experiments. The distribution of these constituents varies from one biomass plant species to another; hence the characterisation information is useful in order to evaluate their suitability as a chemical feedstock in FP processes. The biomass physical properties are differing in terms of brittleness, density, angle of repose and shape of particles. There have been various studies which have looked at the effects of particle size on product yields and distributions. There is need to have a study on every possible feedstock such as corn residues, but the results of other biomasses' prior work can be applied to other type of biomass. As part of this study initial characterisation of the available targeted biomass feedstocks will be determined before any studies on pyrolysis process reactions and kinetics study. The variable initial composition of these feedstocks will allow the production of products with different physical and chemical properties.

The Fast Pyrolysis of CC and CS are comparable and there is no information available on the FP of biomass mixtures of these crop wastes. The description of bio-oils and a list of chemical and physical characterisations have been presented. Some chemical and physical methods to characterise bio-oils are: pH and GC-MS for chemical analysis, and water

content, viscosity, solids content and HHV for physical analysis have been selected in methodology in Chapter 3. The analytical methods were selected from the available facilities at Process Engineering Department (University of Stellenbosch, South Africa) and Karlsruhe institute of Technology (Germany).

It was concluded that the liquid bio-oil product from FP has considerable advantages of being a potential source of a number of valuable chemicals that offer the attraction of much higher added value than fuels. Some chemicals produced from bio-oil such as furfural, phenols, wood resins and esters offer interesting commercial opportunities but the separation methods are currently very expensive. The bio-oil characteristics show it is a complex and chemically unstable mixture with very high oxygen content to be used as a fuel. However, it has been successfully used as boiler fuel and also showed promise in diesel engine and gas turbine applications. The properties of bio-oils also result in several significant problems during its use as a fuel in standard equipment such as boilers, engines and gas turbines constructed for combustion of petroleum-derived fuels. The bio-oil properties of high volatility, high viscosity, stability, high solids content coking and corrosiveness are the most challenging and have limited its applications. Hence, the use of bio-oils as a transport fuel or feedstock for Fischer-Tropsch refinery process still poses several chemical and physical properties challenges. Bio-oil can be upgraded to improve the quality and be compatible and can be blended with the Fischer-Tropsch liquid hydrocarbons products streams.

Upgrading bio-oil to a quality of transport liquid fuel still poses several technical challenges but there are low cost upgrading methods to improve its quality and use it as a fuel or feedstock in Fischer-Tropsch process such as blending with diesel by emulsification, concentration method, alcohol addition and esterification reactions. Emulsification is one of the simplest ways to use bio-oil as a transport fuel with conventional fuel directly but there is high cost and energy consumption in the processes. Hydro-deoxygenation, catalytic cracking and steam reforming of bio-oils are expensive and complex techniques which are under different stages of research. The bio-oil quality from these upgrading processes is low due to high coking and catalyst deactivation. It can be concluded that the concentration method and solvent addition are the cheapest, simple and effective upgrading methods

improving on a wide range of properties in the bio-oil. They improve homogeneity; reduce acidity, increase heating value and the stability of bio-oils by evaporation of water and light reactive volatiles which cause the product instability. The addition of a solvent such as methanol, acetone and ethyl acetate can improve the homogeneity, decreases the viscosity and increases the heating value of the bio-oil. The combined benefits of the two methods can improve the bio-oil properties cheaply using simple processes. Table 13 is the proposed physical technique of the bio-oil to improve its properties for biomass to liquids process feedstock.

Table 13: Proposed bio-oil upgrading strategy (Oasmaa et al., 2005)

Methods	Improvements	Laboratory Set-up
Concentration	<ul style="list-style-type: none"> ▪ Increase heating value ▪ Improve homogeneity ▪ Increase viscosity ▪ Improves stability ▪ Reduce O₂ content 	Heating in a water bath (Buchi system) at low temperature and pressure. Simulated to FP condensers

Chapter 3: Methodology and Materials

In this chapter, the materials and methodology used during the fast pyrolysis of corn residues are described. The thermal behaviour of corn residues were studied by thermogravimetric analysis. Thermogravimetric analysis of the corn residues (CR) at different heating rates was performed and Fast Pyrolysis (FP) on corn residues experiments with similar operating parameters were carried out using two different reactors: a bubbling fluidised bed reactor (BFBR) and Lurgi twin screw reactor (LTSR). The physical and chemical characterisation of corn residues biomass, bio-oil, uncondensed gas and biochar were performed according to ASTM (American Society for Testing and Material) and DIN (Deutschland Institute of Standardisation) methods and a summary of the methods is presented in Appendix C. The upgrading of bio-oil by the evaporation method is also described in this chapter.

3.1 Materials

3.1.1 Corn residues

(a) Experiments at KIT (Germany)

The biomass used in this study was corn residues (corn cobs and corn stover). Corn Stover (CS) and Corn Cob (CC) were collected from the Lichtenburg area in the Northwest province of South Africa, soon after grain harvesting in August 2009. Representative feedstock samples were ground with a Pulverisette 25 mill (Fritch, GmbH Germany), by changing sieves of (8000 μm , 4000 μm , 2000 μm and 1000 μm) to a particle size distribution of <1000 μm for physical and chemical characterisation. 100kg of each biomass (CC and CS) for fast pyrolysis experiments were milled by a two-stage cutting mill Herbneue LD type LM 450/1000 55-2 (Reihen, Germany). The materials were ground to $\leq 5\text{mm}$ particle size as required in the Process Demonstration Unit (PDU) as optimum particle size. Thermogravimetric analysis (TGA) and Fast Pyrolysis (FP) experiments in a LTSR at KIT (Germany) were carried out on the CR from North West province.

(b) Experiments at Process Engineering, SU (South Africa)

Dried CC and CS were collected from a farm in the Free State province in South Africa, soon after grain harvesting in July 2009. Dried samples of both materials were milled using a Retsch Type SM 100, by changing different sieve sizes to less than 2000 μm . This batch of

feedstock was used for the FP experiments in a BFBR at the Department of Process Engineering, Stellenbosch University (South Africa).

3.1.2 Foundry sand

AFS 35 Foundry sand was used as a fluidising medium in the bubbling fluidised bed reactor with a particle size diameter range 75-710 μm and loose bulk density (ρ) of 1526 kg/m^3 . The sand particle size distribution is shown in Appendix M. The sand was purchased from Consol Minerals (Cape Town, South Africa) and contains 99.7 wt. % SiO_2 .

3.1.3 Steel balls

An equal mixture of spherical stainless steel balls, 1.0 mm with a density of 4900 kg/m^3 and 1.5 mm with a density 5 000 kg/m^3 from Germany was used as the heat transfer medium in the LTSR. The mixing of steel balls with different diameters was done to increase the area of contact between the biomass particles and steel balls during the reaction.

3.1.4 Acetone

Industrial grade acetone (purity 95%) was used as a cleaning solvent. This solvent was used in both types of reactors in the LTSR (Lurgi Twin screw reactor) (Germany) and the BFBR (Bubbling fluidised bed reactor) (SA).

3.1.5 Isopar

Isopar G (www.exxonmobil.com, 2010) of density 750 kg/m^3 and flash point of $>40^\circ\text{C}$ was used as the condensing medium in the BFBR. The cooling liquid properties are presented in Appendix A.

3.1.6 Polydimethylsiloxane

A thermostating organic liquid called polydimethylsiloxane with flash point of $>170^\circ\text{C}$ and specific density of 0.97 was used as a heat transfer medium in the LTSR process. Polydimethylsiloxane was used as a heat transfer medium in the condensation section.

3.1.7 Antifrogen, Monoethyleneglycol (1, 2-Ethandiol)

A clear viscous organic liquid called Antifrogen, Monoethyleneglycol (1, 2-Ethandiol) with a flash point of 108.2°C and a specific density of 1.097 was used as a heat transfer fluid in the LTSR process. Antifrogen, Monoethyleneglycol (1, 2-Ethandiol) was used as a heat transfer medium in the second condenser.

3.2 Procedures

3.2.1 Sampling

The CS and CC was packed in 10 separate polypropylene made sack bags, with dimensions of 0.51 * 0.76m, each with an average mass of about 10 kg biomass. Sampling was done by taking 3 sub-samples from each bag, at the top, middle and bottom of the bag into a 20 liter bucket to have a representative sample. The particle size reduction of CC and CS samples from 150 mm to less than 1 mm was done by a Pulverisette 25 mill (Fritch, GmbH Germany). After this milling step, another sampling procedure was carried out to get a sub-sample for compositional analysis. Coning and quarterly method (Allen, 1996) to sub-sample the quantity of each feedstock for analysis was done and consisted of taking a sample of 2 kg from the 20 liter bucket and putting a cone shaped heap on a flat surface. The heap was flattened with a spatula and divided into four identical volumes. One portion was taken and the procedure repeated until only 1/16th of the original volume remained for compositional analysis. Most dry biomasses are hygroscopic (Igathinathane *et al.*, 2009), therefore they rapidly take up moisture, so as a consequence the dried material samples were stored in air tight 200 ml plastic cylindrical vessels before analysis.

3.2.2 Thermogravimetric analysis (TGA)

A representative sample of the biomass was placed in aluminium cup that was supported on an analytical balance located inside the TGA equipment. Purge gas was allowed to flow through the equipment and switched between nitrogen and oxygen in order to control pyrolysis and combustion reactions. Pure nitrogen and air were used as purge gases. A Netzsch STA 409 CD balance was used for TGA. All TGA experiments were conducted at a constant nitrogen purge flow rate of 70 ml/min. Residual weight of the sample and derivative of weight (DTG), with respect to time and temperature, were recorded using TGA7 software. Thermogravimetric experiments were conducted at heating rates of 1, 10, 20, 30, 40 and 50 °C/min. Samples were held at 20 °C for 1h and heated to 700 °C and held at this temperature for 1h. Oxygen was allowed to flow at 15 ml/min during the combustion stage for 1 h at 700 °C. Approximately 20-50 mg (particle size of 125-350 µm) of the corn residue samples were placed in the alumina cup of the TGA microbalance, which was enough to fill the bottom of the cup because of the low density of the ground biomass. Dried samples of the 1000 µm particle size were milled to fines (125-350 µm) with a

cryogenic mill (Freezer mill 6800, Germany). The thermogravimetric experiments were done in duplicates for each heating rate.

3.2.3 Biomass kinetics analysis

The kinetic parameters were determined by the AKTS-Thermokinetics software package Version 3.18. This program among other things facilitates kinetic analysis of thermogravimetric analysis (TGA), differential thermal analysis (DTA) and differential scanning calorimetry (DSC) data for the study of materials and their products. The method determines kinetic parameters (activation energy (E) and pre-exponential factor (A)) of a given solid material and predicts reaction progress under a range of temperature (up to 700 °C) and heating rates (Vyazovkin, 2006). The kinetic parameters, activation energy (E) and pre-exponential factor (A), reaction progress and thermal stability of the corn residues under a temperature range of up to 700 °C were determined. The isoconversional method of Friedman (model-free) under non-isothermal conditions was used to determine the kinetic parameters (Vyazovkin, 2006).

3.2.4 Fast pyrolysis processes

Lurgi twin screwreactor (LTSR) and bubbling fluidised bed reactor (BFBR) are outlined in Figure 5 and 6, respectively. The operating procedures for the plants are presented in appendix B. The biomass feeding rate calibrations results of both types of reactors are presented in appendix G.

(a) Lurgi twin screw reactor (LTSR) process description

The LTSR plant (Figure 5) consisted of a biomass feeding unit consisting of a hopper **(1)** and screw conveying system **(2)** feeding into the LTSR **(3)** of length 1.5 m and capacity of 15 kg/h of biomass feed. The feeding screws were connected to an adjustable-speed drive that were designed for changing speed automatically while the screws were in operation to meet variations in the process. The type of feeding screw depended on the properties of each biomass type, so feeding rate calibrations were determined before a process run. The biomass was pyrolysed in the LTSR at 500-530 °C, under a pressure of 0.98 bars, with 1-2 seconds residence time of pyrolysis gases to prevent secondary reactions. The pyrolysis reactions occurred by contact of biomass (particle size of ≤ 5 mm) with amounts of hot steel balls in a LTSR.

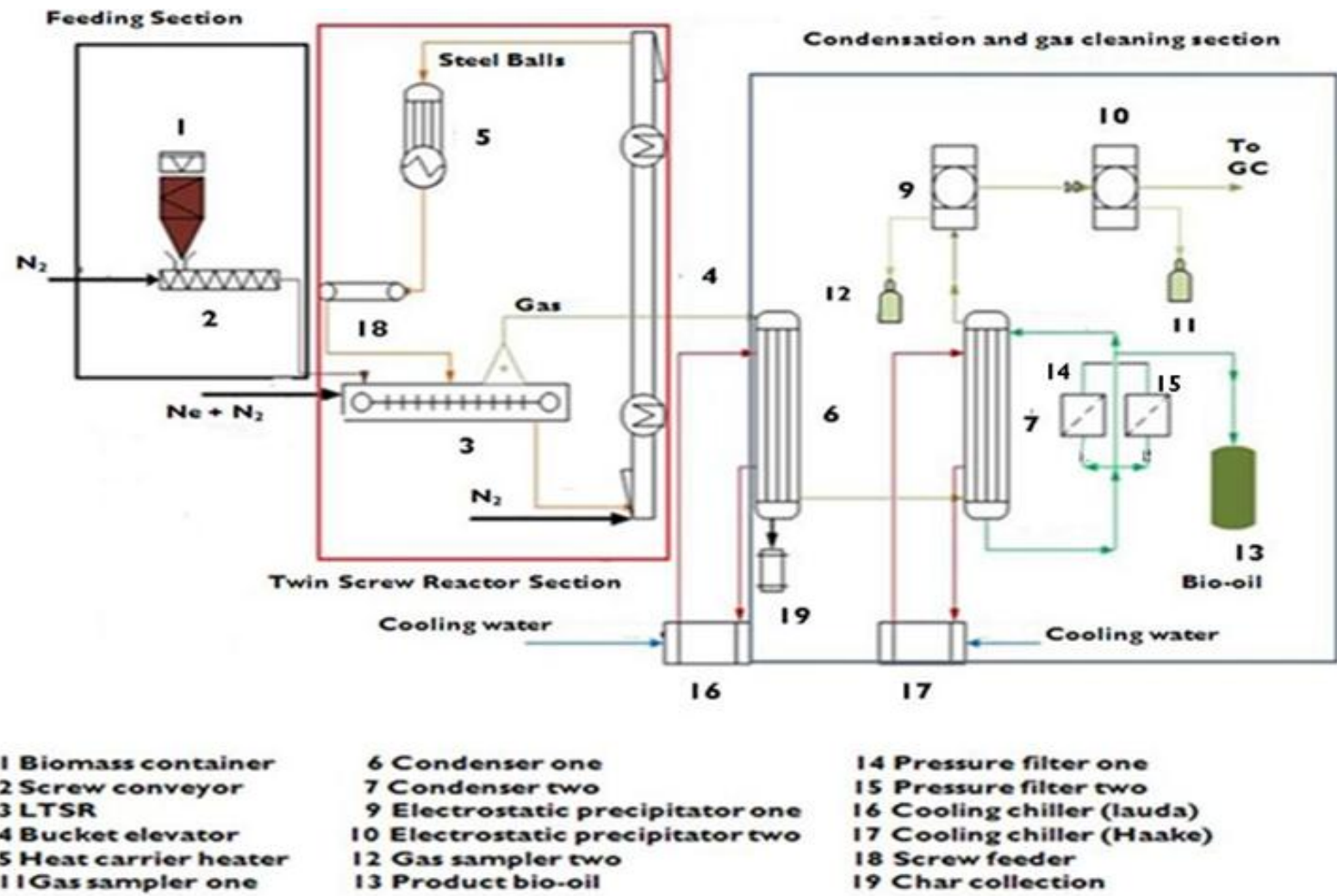


Figure 5: Lurgi Twin screw reactor process flow diagram

The LTSR process at KIT is described from the process flow diagram shown in Figure 5.

The heating supply was from an equal mixture of 1mm and 1.5 mm diameter stainless steel balls as heat carrier at a temperature of 550 °C. Due to the density differences the steel balls were separated from the bottom end of the reactor to the bucket elevator **(4)** at 510 °C where they were conveyed to the top of the heat carrier heater **(5)**. The heat carrier heater was a radial heat exchanger with a conduction hollow cylinder of 8.5 mm internal diameter mounted with 5 electrical heaters at 600 °C. 5 Electrical heaters, 3 of capacity 2400 W from the inside and 2 of a capacity of 1790 W heating from the outside of the heating space were used. The heat carrier steel balls left the heater at 500-600 °C back to the middle of the LTSR through a screw feeder **(18)** which maintained a mass flow rate of 1000 kg/hr of steel balls in circulation from 40 kg equal mixture of 1mm ($\rho=4900 \text{ kg/m}^3$) and 1.5mm ($\rho=5\ 000 \text{ kg/m}^3$) steel balls at a 5 kg/h biomass feed rate.

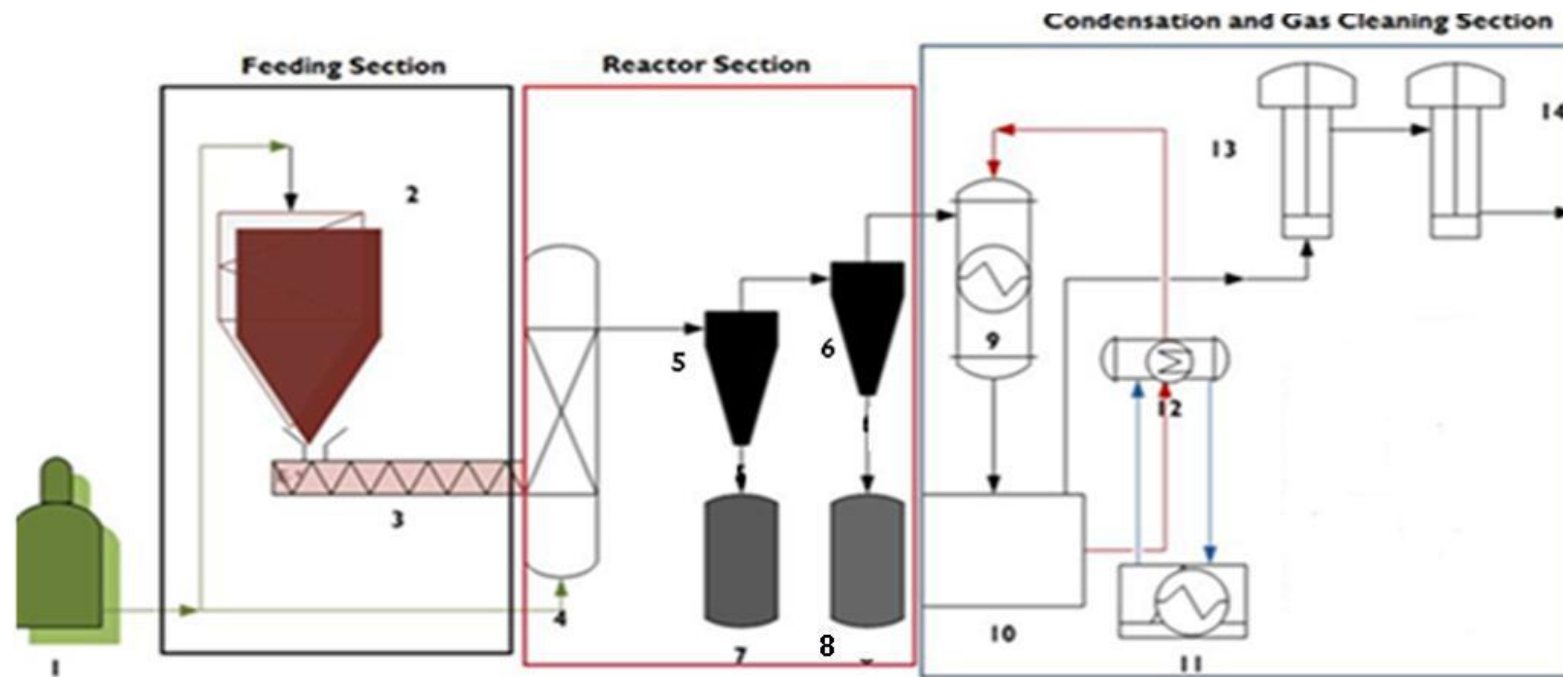
The pyrolysis gas and biochar particles were sucked out of the reactor top at 500-530 °C to the first condenser **(6)** which had both a quenching and condensing effect to about 50-70 °C, depending on the type of feedstock. Condenser (1) is a shell and tube counter current heat exchanger, with an organic liquid polydimethylsiloxane on the shell side of the heat exchanger. The cooling liquid was circulated to a cooling chiller (Lauda) **(16)** cooled with cooling water at 10 °C to lower the thermostating liquid temperature before it goes back into condenser (1). Biochar was drained manually from the bottom of condenser (1) through a flap valve **(19)** into buckets after every 30 minutes during a process run. From the first condenser, the uncondensed and pyrolysis gases go to the second condenser **(7)** at 50-70 °C and leave the condenser (2) at 15 °C. The second condenser was a shell and tube heat exchanger, with a cooling liquid (Antifrogen, Monoethyleneglykol (1.2-Ethandiol)) at 10 °C circulating on the shell side and cooled by a cooling chiller **(17)**. The gas stream was cooled through an indirect contact heat exchanger with filtered bio-oil from the product recycle on the tube side of the heat exchanger. The bio-oil was filtered by two pressure filters and the filtered product was collected in the product tank **(13)**.

The uncondensed gas (mainly CO₂, N₂, CO, H₂ and light hydrocarbons gases) from the second condenser was cleaned through two electrostaticprecipitators **(9, 10)** in series

before the gas chromatography online analysis. Electrostatic precipitators (20 kV and 0.001 mA) remove aerosols suspended in gas streams by direct use of electrical force so that the gas was clean before gas chromatography analysis. Dispersed particles were electrically charged by passing them through an electrostatic field (9, 10). The action of the electrical field causes the particles to migrate to the collection surfaces from which they were subsequently removed manually at the end of each process run. Samples for gas analysis were collected from gas samplers (11, 12).

(b) Bubbling fluidised bed reactor (BFBR) process description

The BFBR process at University of Stellenbosch (US) is described from the process flow diagram shown in Figure 6.



- | | | |
|-------------------------|------------------------|---------------------------------|
| 1 Nitrogen cylinder | 6 Cyclone 2 | 11 Cooling chiller |
| 2 Feeding hopper | 7 Char pot 1 | 12 Cooling bath |
| 3 Screw conveyer | 8 Char pot 2 | 13 Electrostatic precipitator 1 |
| 4 Fluidised bed reactor | 9 Condenser | 14 Electrostatic precipitator 2 |
| 5 Cyclone 1 | 10 Condenser reservoir | |

Figure 6: Bubbling fluidised bed reactor process flow diagram

The BFBR plant consists of a reactor **(4)** with a length of 370 mm and an inner diameter of 100 mm and is heated externally by an electric furnace. Before each run the oven was heated over a period of approximately one and a half hour at which time a steady state was reached. Nitrogen **(1)** was used as the inert gas throughout the process and was supplied to the reactor as the fluidising gas at a rate of 2.4-3 m³/hr. The reactor fluidising gas passed through a porous distributor before coming into contact with 400-500 g foundry sand which acted as heat transfer medium. The feed was transported by a screw conveying system **(3)** into the fluidised bed reactor **(4)**. The plant operated in a batchwise process by feeding 300 g of biomass in a hopper and then letting it pyrolyse. 300 g of biomass feedstock was introduced into the bed of foundry sand. The whole experiment was held for 20 minutes until no further significant release of gas was observed. One hour long runs feeding 1000 g of biomass were also carried out to get a representative bio-oil sample for upgrading. A number of thermocouples were placed within the reactor system to measure the furnace temperature, pyrolysis middle reactor temperature and reactor top temperature.

The reactor operated between 500-530 °C with a vapour residence time of a few seconds for FP. The pyrolysis products which left the reactor (organic volatiles, gases, biochar, aerosols and nitrogen) pass through a dual cyclone system **(5, 6)** to separate biochar and collect the majority of the biochar in the char pots **(7,8)**. The char pots were placed in the furnace so that an isothermal temperature consistency was achieved. The organic vapours, aerosols and gases were then passed into a transition pipe which was maintained at 400 °C by a rope heater, then passed into a condenser **(9)**, to quench and condense the organic vapours from 500 °C to 15 °C using iso-par condensing liquid. The uncondensed gas goes to the electrostatic precipitators **(13, 14)**. The electrostatic precipitators supplied a charge to the mixture of vapours which entered from the condenser. The bio-oil was collected in a reservoir tank **(10)** together with isopar liquid. The bio-oil accumulated in the reservoir was transferred into a 20 l bucket and separation from the isopar was done by a conical separating flask. The remaining liquid product left behind in the reservoir tank, electrostatic precipitators, condenser including all connection tubes were dissolved with acetone. The solvent part of the bio-oil dissolved in acetone was extracted in a beaker. The mixture was left for 12 hours for the acetone to evaporate and the quantity of the bio-oil from acetone washes was obtained. The acetone evaporation time was obtained experimentally as the time when the mixture (bio-oil and acetone) mass loss was constant (Appendix L). The bio-oil comprised of a dark liquid from the acetone washes and reservoir

weighed together. The mass of the biochar in the char pots, cyclones and reactor was weighed. The organic and biochar yields were calculated from the recovered masses and the gas yield was determined by difference. Each experiment was repeated two times. The formulae of yields calculations are described in appendix F.

3.2.5 Process operating conditions

The FP experiments conditions are shown in Table 14 and the results discussed from chapter 5 are an average of two runs from a BFBR and two runs from a LTSR process. Three samples were studied: corn cobs (CC), corn stover (CS) and a mixture of the biomasses in the ratios, 70% of CS and 30% of CC. The corn residues from the plant comprise of 50% stover and 20% cobs (Myers *and* Underwood, 1992), hence the minimum amount of CC blended with CS was determined as 30% from the production tonnages of the plant. The maximum amount of the CC in the mixture will be dependent on the amount of CS retained in the field for soil fertilisation and stock feed manufacture.

Table 14: Fast pyrolysis experimental conditions

LTSR, Karlsruhe Institute of Technology(KIT), ITCVP ,Germany			
Experimental conditions:			
Temperature: 500-530 °C, N ₂ Flow rate, Q: 1-1.2m ³ /hr, Particle size: < 5mm			
Feedstock	Duration (m)	Feed Rate, F, (kg/hr)	Feed (kg)
CC: Run 1	242	5.5	22.3
CC: Run 2	266	5.8	25.5
CS: Run 1	299	5.1	25.2
CS: Run 2	256	4.8	20.3
CRM (70% CS: 30% CC): Run 1	300	4.9	24.5
CRM (70% CS: 30% CC): Run 2	243	6.1	24.6
BFBR: US, South Africa			
Experimental conditions:			
Temperature: 500-530 °C, N ₂ Flow rate, Q: 2.5-3m ³ /hr, Particle Size: <2 mm			
CC: Run 1	20	0.9	0.3
CC: Run 2	20	0.9	0.3
CS: Run 1	20	0.9	0.3
CS: Run 2	20	0.9	0.3
CRM (70% CS: 30% CC): Run 1	20	0.9	0.3
CRM (70% CS: 30% CC): Run 2	20	0.9	0.3

3.3 Physical and chemical characterisations of biomass

3.3.1 Proximate analysis

(a) Analytical method

The proximate analysis is defined as the loss in mass of the corn residue samples heated up to a specified temperature (Okuno *et al.*, 2005). The proximate analysis was done to determine the moisture content (MC), volatile matter (VM), fixed carbon (FC) and ash content (AC) in CC and CS. Corn residue samples (0.5-1g) were dried in an oven at $105 \text{ }^{\circ}\text{C} \pm 2 \text{ }^{\circ}\text{C}$ to a constant weight in order to determine residual moisture by convection oven drying method according to a standard method DIN CEN/TS 14774-1:2004-11. An automatic oven (Analyse Automat MAC-500, GmbH Germany) with an inside electronic balance for weighing samples was used. The sample was heated in a covered crucible (to prevent oxidation) at $900 \text{ }^{\circ}\text{C}$ to a constant mass. The mass loss is referred to VM. The AC for biomasses at $550 \text{ }^{\circ}\text{C}$, $815 \text{ }^{\circ}\text{C}$ and $1000 \text{ }^{\circ}\text{C}$ was determined with the same equipment according to a standard method (DIN CEN/TS 14775:2004-11). The FC was obtained by calculation method according to equation 13.

$$\text{FC}(W_0) = 100\% - (W_1 + W_2 + W_3) \quad \text{Equation 13}$$

Where W_1 is the mass percent of sample evolved after heating at $105 \text{ }^{\circ}\text{C} \pm 2 \text{ }^{\circ}\text{C}$ (WC),

W_2 is the mass percent of sample evolved after heating at $900 \text{ }^{\circ}\text{C}$ (VM),

W_3 is the mass percent of sample remaining after heating at $550 \text{ }^{\circ}\text{C}$ (AC),

And W_0 is the mass percent of sample called fixed carbon (FC).

(b) Thermogravimetric analysis method

Weight loss curve from TGA was used to calculate the proximate analysis using TGA7 software as illustrated in Figure 7. The sample was heated in the N_2 atmosphere. The sample was first heated from room temperature to $700 \text{ }^{\circ}\text{C}$ at specified heating rates ($1\text{-}50 \text{ }^{\circ}\text{C}/\text{min}$) in a N_2 environment to drive off volatile materials, including water from dehydration and low molecular weight hydrocarbons. The temperature profile started with a drying step up to $105 \text{ }^{\circ}\text{C}$ to remove moisture (a, wt. %) shown by a slight mass loss step change (Figure 7). The subsequent mass loss was due to pyrolysis step. Once $700 \text{ }^{\circ}\text{C}$ was reached, the temperature was held constant until the TGA curve became flat, so that the volatile materials (b, wt. %) were completely released (Figure 7). Finally, N_2 flow was stopped; and the flow rate ($15 \text{ ml}/\text{min}$) of oxygen was admitted for an

hour. The oxygen introduced was used to oxidise fixed carbon (c , wt %) in biochar into CO_2 (Figure 7). The entire TGA test was completed when the weight loss was constant.

The component left was ash (d , wt. %) of the sample, which was then allowed to cool naturally (Figure 7). The equation of the proximate analysis is represented inequation 14:

$$100\text{wt. \%} = a(\text{wt. \%}) + b(\text{wt. \%}) + c(\text{wt. \%}) + d(\text{wt. \%}) \quad \text{Equation 14}$$

Where a (wt. %) - Moisture Content, b (wt. %) - Volatilisable Content c (wt. %) - Fixed Carbon Content and d (wt. %) - Ash Content.

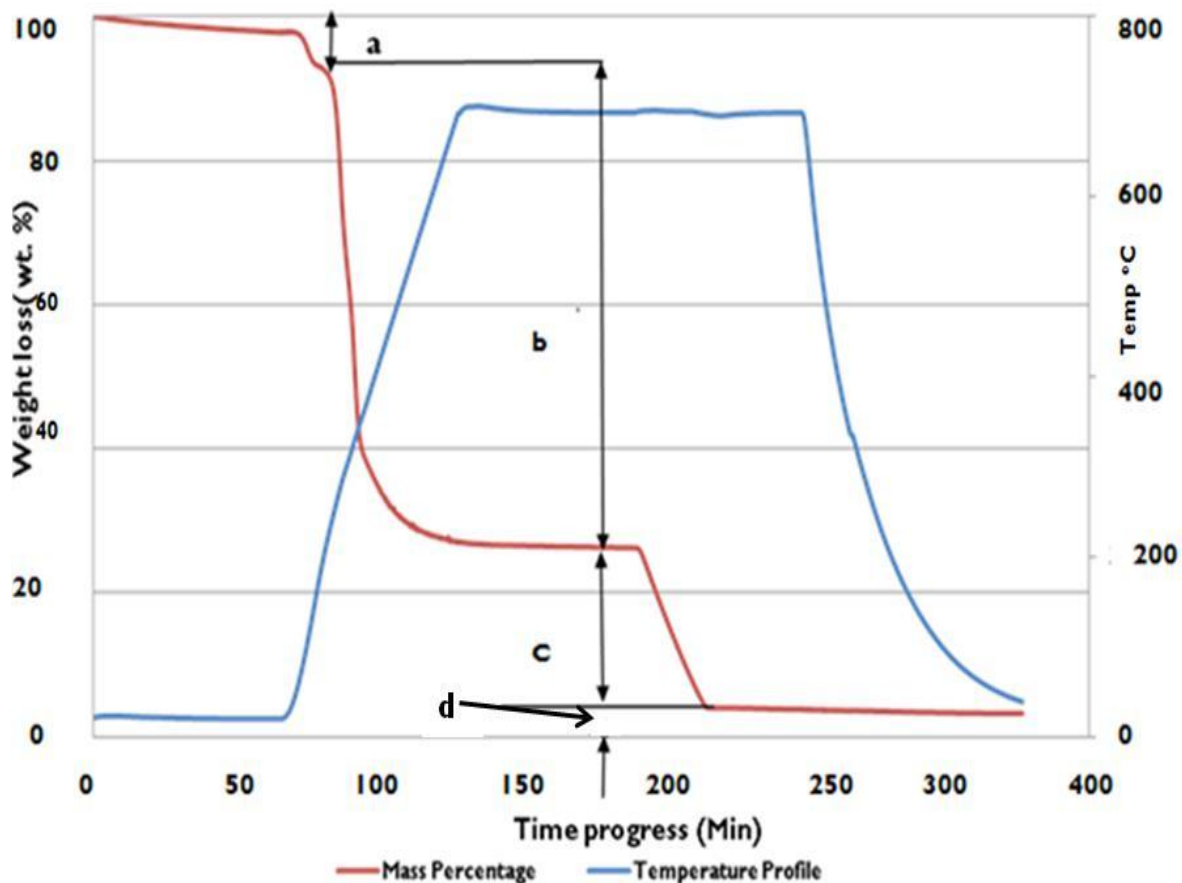


Figure 7: TGA mass and temperature profiles

3.3.2 Heating value

The heating value of corn residues is important when considering the heating efficiency of equipment for producing energy. Biomass from North West province was analysed at Karlsruhe Institute of Technology (KIT) and the corn residues from Free State province was analysed at Department of Forestry and Wood Science, Stellenbosch University (SUN). In this study, the heat of combustion was determined by burning a 0.5-1.0 g sample in an oxygenbomb calorimeter. The heating value was analysed by Kalorimeter system C 4000A at KIT and ECO bomb

calorimeter from CAL2k at SUN according to a standard method DIN CEN/TS 14918:2005-08. The instruments were calibrated with about 0.5 g of benzoic acid before measurements. The test procedure consisted of adding a weighed sample of CR to the cup, installing a fuse, and charging the bomb with approximately 30 bars of oxygen. Using the proper allowance for thermochemical and heat transfer corrections, the heat of combustion was computed from temperature observations before, during, and after combustion. Detailed procedures for bomb calorimeter operation and calculations method equations are presented in appendix D.

3.3.3 Elemental analysis

The purpose of this test is to determine elemental composition of carbon (C), hydrogen (H), nitrogen (N), sulphur (S), chlorine (Cl) and oxygen (O) in the CR. The elemental composition was determined using an elemental analyser, Analyse Automat Leco TRU SPEC (GmbH, Germany) for samples from North West province. The main components of the elemental analyser consisted of a quartz tube reactor, column, gas chromatography oven, front furnace (temperature maximum 1020 °C), the detecting system used thermal conductivity detector and an oxygen trap. Carbon and hydrogen were determined according to standard method DIN CEN/TS 15104:2005-10. N₂ was analysed using the same equipment in solution of HNO₃/HF/H₃BO₃ according to a standard method DIN 22022-1:2001-02. Chlorine was determined separately after combustion as hydrogen chloride in a separate bomb calorimeter analyser Analyse Automat Leco SC-144 DR according to a standard method DIN CEN/TS 15289:2006-07. The O content was determined by calculation.

The elemental analysis for the corn residues from Free State province was done at University of Stellenbosch with different facilities from the analysis in Germany described above. The corn residues samples were analysed with different equipment in the Soil Science Department (University of Stellenbosch) using the following method: 5-10mg samples of biomass were milled in a ball mill to ensure a representative sample. EuroEA elemental analyser from Eurovector was used to analyse the elements. The milled sample was placed in a tin sample cup, crimped to confine it, and introduced into a quartz reactor. The quartz reactor was maintained at 1030°C with a constant flow of He gas. Flash combustion occurred when a pulse of O₂ was injected into the quartz reactor shortly after introduction of the sample. Under these temperature and O₂ conditions, the tin was oxidised to SnO₂, resulting in the temperature increasing to between 1700 and 1800°C, and the complete combustion of biomass organic matter. The combustion products

(CO₂, NO_x and H₂O) were swept by the helium carrier gas through a column of chromium dioxide (CrO₂), to catalyse oxidation of organic fragments, and Co₃O₄ coated with Ag to remove halogens and sulphur oxides. The gases then flow through a heated column (650°C) containing Cu to remove excess oxygen and Mg (ClO₄)₂ to remove H₂O, and then into a chromatographic column which separates N₂ and CO₂. The different gases were detected with a thermal conductivity detector. The instrument was calibrated with sulfanilamide (C₆H₈N₂O₂S) standard from Euro Vector. 8 g biomass pellet was analysed for sulphur content by an XRF Spectrometer, Axios from PAN Analytical and oxygen was determined by calculation method.

3.3.4 Density

The knowledge of biomass bulk density is important in determining the conveying characteristics and storage hopper designs. It is defined as the mass of many particles of the biomass material per unit volume occupied. This property can change depending on how the biomass is handled. After milling of the biomass and the biomass handling and transportation to the process demonstration plant, there was compaction of the biomass particles due to shaking, hence the determination of the tapped bulk density after a specified compaction process was done. The bulk density of the biomasses was determined both as freely settled and tapped densities (where the tapped density refers to the bulk density of the biomass after a specified compaction process, involving vibrating the measuring vessel).

$$\text{Bulk density} = \frac{\text{Mass of biomass (kg)}}{\text{Core volume (m}^3\text{)}}$$

Equation 15

The densities were measured for the biomass particle size of 1 mm. The samples were prepared as corn residues passing through a 1 mm carbon steel made sieve. Biomass was packed into a 500 ml graduated cylinder container until it was full. The mass of biomass was weighed and the density calculated according to equation 15. The bulk densities were determined according to a standard method GEA niro analytical method A 2.

3.3.5 Inorganic composition

(a) Inorganics in biomass

The purpose of this test was to determine inorganic compositions present in the biomass. XRF spectroscopy, an established method was used to analyse the metallic elements in CR (Skoog, 1985). The method is quick and multi-element measurement with minimal sample preparation. In the presence of chlorine atoms, elements can interact each other, resulting in skewed less accurate results as chlorine absorb fluorescent X-Rays (Skoog, 1985). The composition of

inorganics of the raw biomasses was determined by the automatic XRF X-Ray Fluorescence Spectroscopy (XRF) machine, Bruker AXS S4 Pioneer (GmbH, Germany). The experiment was done by putting a prepared sample of <1mm particle size into a spectro membrane perforated thin-film sample support frames prolene according to a standard method DIN 51729-10. XRF proportional detector gas was Argon of energy range of 0.1-8 keV (Be-Cu). The results from the XRF machine were evaluated by Spectra plus Software package.

(b) Inorganics in biochar

The main influences in pyrolysis process are the group 1 and 2. Trace elements and heavy metals were also analysed in order to study the influences of such metals in subsequent uses of pyrolysis products such as catalyst poisoning and flue gas emissions. The inorganic compositions were determined on the ash at 550 °C by three different methods more accurate than XRF, detecting trace elements. Si, Al, Fe, Ca, Mg, Na, K, Ti and P in solution were determined by ICP (Inductively Coupled Plasma) according to the standard method (DIN 51 729) and operating manual (DBI/AUA 003). As, Cd, Co, Cr, Cu, Hg, Mn, Mo, Ni, Pb, Sb, V, Zn, Se, Sn and Ti were analysed by Atomic Absorption Spectroscopy (AAS) according to the standard method DIN 22022-3:2001-02. Sb, As, Se, Te and Hg were determined by Atomic Absorption Spectroscopy Hydrid according to the standard method DIN 22022-4:2001-02. Boron was determined according to the standard method DIN EN ISO 11885(E22):1998-04.

3.3.6 Lignocellulosic composition

There exist many methods for determining the lignocellulosic components of biomass. The corn residues were analysed according to the following procedures.

3.3.6.1 Extractives content

It is necessary to remove non-structural components from biomass before lignocellulosic analysis to avoid interferences with these analytical steps. This procedure used a two-step extraction process to remove water soluble and ethanol (99.9%, Ethanol grade) soluble material. 5-10 g of biomass sample was added to a weighed extraction thimble. The thimble was put inside soxhlet siphon tube and the assembled soxhlet apparatus. 190 ml of distilled water were added to a weighed receiving flask which was part of the soxhlet apparatus. The receiving flasks were on top of heating mantles adjusted to provide a minimum of 4-5 siphon cycles per hour. The biomass was refluxed for 12 h. After the reflux time was complete, the heating mantles were turned off and glassware allowed to cool to room temperature. The flasks were heated without the soxhlet

system until all the water evaporated, the flasks cooled in a desiccator and the mass of extractives determined. A successive ethanol extraction was performed, leaving the thimbles in the soxhlet extractor and changing the weighed flask and adding 190 ml of ethanol. The extraction was repeated using the same procedure for ethanol extraction. The content in the flask was evaporated into the atmosphere till there was no alcohol and the flasks were weighed to determine the alcohol soluble extractives. The extraction was done according to the standard method ASTM E1690. The calculation is shown in equation 16.

% Total Extractives

$$= \frac{[(\text{Weight}_{\text{flask+waterextractives}} - \text{Weight}_{\text{flask}}) + (\text{Weight}_{\text{flask+ethanolextractives}} - \text{Weight}_{\text{flask}})]}{\text{ODW}_{\text{Sample}}}$$

Equation 16

$\text{ODW}_{\text{Sample}}$ = Oven Dried Weight Sample

3.3.6.2 Lignin content

The procedure used for determining lignin involved adding 0.5 g dry extractive free biomass in the 50ml glass and slowly adding, while stirring, 7.5 ml cold (12-15°C) 72% sulphuric acid. The mixture was well mixed by constantly stirring for one minute (primary hydrolysis). The mixture was stirred at ambient temperature for 2 h, then the biomass was washed in the round bottom flask with 280 cm³ distilled water to dilute the acid to 3%. The content was boiled under reflux for 4 h (secondary hydrolysis) and washed with 500 ml boiling water. The samples were dried in an oven at 105°C for 2 h. The percentage of Klason lignin on the oven dry and extractive free biomass was calculated. The analysis was done according to a standard method T222 om-88 (Bridgwater, 1994). The calculation is shown in equation 17.

$$\text{KlasonLignin}(\text{wt. \%}) = \frac{[(\text{Weight}_{\text{Driedsample+Container}} - \text{Weight}_{\text{Container}})]}{\text{Weight}_{\text{Initial extractive free sample}}} \text{Equation 17}$$

3.3.6.3 Holocellulose content

Holocellulose comprises the cellulose and hemicelluloses. The procedure used for determining holocellulose involved the treatment of milled extractive free biomass (4 g) with an acid solution (160 ml sodium acetate solution) at 75°C for 5 h. This first step subjects the biomass sample to a concentrated acid that destroys the non-covalent interactions between biomass components. Sodium chlorite (4 ml) was added every hour during 4 hours. This stage was to optimise the whole polymer hydrolysis and minimise the decomposition of monomeric sugars. Once the

mixture is cooled, the residue was filtered and washed firstly with water (one litre) and with acetone (15 ml). The residue was dried at 105^o C for the determination of the holocellulose. The experiment was done according to a standard method from the Institut du Bois' (France). The calculation is shown in equation 18.

$$\text{Holocellulose (wt. \%)} = \frac{[(\text{Weight}_{\text{Driedsample+Container}} - \text{Weight}_{\text{Container}})]}{\text{Weight}_{\text{InitialExtractivesfree sample}}} \quad \text{Equation 18}$$

3.3.6.4 α -Cellulose content

α -Cellulose is defined as the residue of holocellulose that is insoluble in 17.5 wt. % NaOH solution. 5 g sample of extractive free holocellulose were added to a 17.5 wt. % NaOH solution (100 ml) at room temperature for a 30 min incubation period. The residue was filtered and washed firstly with water (two times with 200 ml) and then filtered again. Then the addition of 15 ml of a 10 wt. % acetic acid solution allowed the hydrolysis of degraded cellulose and hemicelluloses. The residue was filtered and washed with hot water (500 ml), and dried at 105^o C. The α -cellulose amount was determined gravimetrically and hemicelluloses were determined by difference as they were more readily hydrolysed compared to cellulose because of its branched and amorphous nature. The analysis was done according to a standard method from the Institut du Bois'. The calculation is shown in equation 19.

$$\text{Cellulose (wt. \%)} = \frac{[(\text{Weight}_{\text{Driedsample+Container}} - \text{Weight}_{\text{Container}})]}{\text{Weight}_{\text{InitialExtractivesfree sample}}} \quad \text{Equation 19}$$

3.3.7 Particle size distribution

The same procedure was used for both biomasses for LTSR and BFBR processes. A Retsch model AS 200 was used for particle size sieving on a sample volume of 200 ml, amplitude of 1 mm and analysis time of 10 min.

3.4 Characterisation of bio-oil

Characteristics of the bio-oil product include density, water content, heating value, pH and ash. The elemental analysis of the total C, H, N and O of bio-oil was also determined.

3.4.1 Density of bio-oil

Density is a basic physical property that can be used together with other properties to characterise the bio-oil liquids. The determination of the density of bio-oil is important for the conversion of measured volumes at the standard temperature. The density of bio-oil was determined by using a 25ml measuring cylinder at a temperature of 25^o C and calculated the

density as the mass of bio-oil per unit volume of 25ml. The procedure was repeated three times and the average was obtained.

3.4.2 Ash

Knowledge of the amount of ash material present in bio-oils can provide information as to whether or not the product is suitable as a fuel. Ash can be included in bio-oil as water-soluble metallic compounds or from extraneous solids such as entrained solids biochar. In this study, the sample, contained in a suitable vessel, was ignited and allowed to burn until only ash and carbon remain according to a standard method DIN CEN/TS 14775:2004-11. The carbonaceous residue was reduced to ash by heating in a furnace at 550 °C with a heating time of 4 hours, followed by cooling and weighing. The mass of the ash was calculated as a percentage of the original samples as follows (equation 20):

$$\text{Ash, wt. \%} = \frac{w}{W} * 100 \quad \text{Equation 20}$$

Where w = mass of ash in g and W = mass of sample in g.

3.4.3 Moisture content

Information on the water content of bio-oil products can be useful to predict the quality and performance characteristics of the product. In this study, water content of the bio-oil product was measured using Karl-Fischer Titrator, type Metrohm 774 oven sample processor and 841 Titrando based on ASTM D 1744. A mixture of Karl-Fischer reagent Hydranal composite-5 titrant and methanol as a solvent was used. Bio-oil sample (50-60mg) was titrated and an electrometric end point method was used.

3.4.4 Heating value

The heat of combustion is a measure of the energy available from the fuel. Knowledge of this value is essential when considering the energy content of the bio-oil (section 3.4.2). In this study, the bio-oil produced from the LTSR had very high water content and the one from the BFBR had lower water content. Two different methods were used to determine the heating values. The procedure for operating a bomb calorimeter and sample calculation for heating value determination is presented in appendix D.

3.4.4.1 Bio-oil from LTSR

The heating values of bio-oil from the LTSR were estimated from the elemental and ash analyses, using the correlation from Channiwala *and* Parikh (2002) (equation 12)

3.4.4.2 Bio-oil from BFBR

AIKA C200 bomb calorimeter at the Department of Inorganic Chemistry, University of Stellenbosch was used to measure the heating values of bio-oils. The test procedure consisted of adding the weighed sample of bio-oil to the cup (approximately 0.3–0.5 g), installing a cotton firing thread, and charging the bomb with oxygen to approximately 30 bars. The heat of combustion was computed from temperature observations before, during, and after combustion, with proper allowance for thermochemical and heat transfer corrections. The procedures were done according to a standard method (ASTM D2015).

3.4.5 pH

In order to evaluate the corrosive property of the bio-oil products, the pH of the bio-oil was measured using a pH-meter (type Metrohm 691). The electrode was directly dipped into 30 ml of the bio-oil sample.

3.4.6 Elemental analysis

The purpose of this test is to determine elemental percentage of carbon (C), hydrogen (H), nitrogen (N) and oxygen (O) in the bio-oil.

3.4.6.1 Bio-oil from LTSR

The elemental analysis was determined using an elemental Analyser (Analyse Automat Leco TRU SPEC (GmbH, Germany)). The main components of the Elemental Analyser consisted of a quartz tube reactor, column, gas chromatography oven, front furnace (maximum temperature 950 °C), the detecting system which used a thermal conductivity detector and an oxygen trap. Separation of elemental C, H₂, and N₂ was determined by using a Gas Chromatography Column. Carbon and hydrogen were determined according to standard method DIN 51721 by infrared detector and the TruSpec Software program was used to determine the elemental composition. The O content was determined by difference.

3.4.6.2 Bio-oil from BFBR

The elemental analysis for bio-oil from BFBR was not analysed as C, H, N, S and O. The available laboratories were able to analyse total organic carbon, nitrogen and sulphur. Total Organic Carbon (TOC) was used to determine the total content of organically bound carbon in dissolved and undissolved components of the bio-oil and was analysed by Spectroquant Cells. By digestion with sulphuric acid and peroxodisulphate, carbon containing compounds were transformed into

carbon dioxide and reacting with an indicator solution and the end point determined photometrically. The analysis was done according to the standard method DIN 38402 A51. Nitrogen was determined using the Spectroquant Cell tests according to standard method DIN 38402 A51. Organic and inorganic nitrogen compounds in the bio-oil were transformed into nitrate according to Koroleff's method by treatment with an oxidising agent in a thermoreactor. In a solution acidified with sulphuric and phosphoric acid, this nitrate reacts with 2, 6-dimethylphenol (DMP) to form 4-nitro-2, 6-dimethylphenol that was determined photometrically.

3.4.7 Viscosity

The viscosity was analysed with a Rheometer (Physica MCR 501, Anton Paar). A bio-oil sample volume of 20ml was put in a stainless steel cup. The viscosity was measured for up to 5 minutes at a temperature of 22 °C and the data analysed with Rheoplus software.

3.4.8 Dehydration of bio-oil liquids

The effect of dehydration of bio-oils on properties such as heating value, water content and acidic content were studied. The bio-oil was concentrated by evaporating the light volatiles and water in a water bath. The water bath used was Bibby RE 200 from Rotaflow (England UK). The temperature of the water was maintained at 40 °C to prevent decomposition of sugars. Evaporation was started at atmospheric pressure for 4 hours, and then gradually the pressure was decreased to vacuum condition. At vacuum condition (10 kPa), the bio-oil was evaporated for 4 hours. The viscometry, water content and pH of the original bio-oil, condensate and evaporated oil were analysed according to methods described in sections (3.5.7, 3.5.3 and 3.5.5).

3.5 Characterisation of biochar

3.5.1 Elemental analysis

3.5.1.1 Biochar from LTSR

The purpose of this test is to determine the elemental percentage of carbon (C), hydrogen (H), nitrogen (N) and oxygen (O) in the biochar (Refer section 3.4.3). A sample of extracted biochar was made by using an extraction method with methanol on a 10-20 mg crude biochar (unextracted) sample using ASE 200 Accelerated solvent extractor equipment. The unextracted char elemental analysis was performed with LECO True Spec CHN equipment (GmbH, Germany) by a standard method DIN 51721. The C and H contents were analysed by infrared detector and N by thermal conductivity detector. A sample mass of 100 mg was combusted at a temperature of 950 °C and a True Spec software program was used for analysis of the results.

The extracted char was analysed for elemental analysis of CHN by an elementalAnalyser (Analyse automat Leco TRU SPEC) using the same procedure as in section 3.4.3

3.5.1.2 Biochar from BFBR

The biochar was analysed for C, S, N and H at Stellenbosch University by a Eurovector EA elemental analyser in duplicate (see section 3.4.3)

3.5.2 Heating value

The purpose of this test is to determine the heating value of the biochar. In this study, the heat of combustion was determined by burning a weighed biochar sample in an oxygen bomb calorimeter under controlled conditions according to procedures in section 3.4.2.

3.5.3 Ash content

3.5.3.1 Biochar from LTSR

The extracted biochar sample was used to determine ash content of the biochar. The ash content for the biomasses was determined by Analyse automat MAC-500 equipment according to a standard method (DIN CEN/TS 14775:2004-11) using a LECO TGA7 equipment at 575 ± 25 °C.

3.5.3.2 Biochar from BFBR

The ash contents of the biochar were analysed in a muffle furnace (Gallenkamp, Muffle Furnace Size 2) at 575 ± 25 °C according to a procedure described in section 3.5.2. ASTM E1755-01 was used for this analysis. An electronic balance (Mettler AE 200) sensitive to 0.1mg was used for weighing the samples. The ash was also determined from TGA analysis of the biochar using the same method as in section 3.4.1. For each experimental run, samples were held at room temperature for 1 hour. At this stage, the sample mass would have stabilised at a constant dried weight and was then heated to 700 °C at a heating rate 10°C/min. The purge gas, nitrogen, was set to a flow rate of 15 ml min⁻¹. Subsequent to heating to 700 °C the purge gas was switched to oxygen at the same flow rate of 15 ml min⁻¹ and the biomass maintained at 700 °C for a further 30minutes, to allow combustion of the remaining biochar for the subsequent determination of ash content.

3.5.4 Surface area and total pore volume

Nitrogen adsorption experiments were conducted to determine the specific surface area and pore volume of the biochars using an ASAP 2010, Micromeritics USA, multipoint Brunauer-

Emmet-Teller (BET) surface area instrument. The BET surface area and total pore volume were obtained by measuring their nitrogen adsorption-desorption isotherms at 77K. The analytical method consisted of three steps, namely dehydration of samples, degassing of sample under low pressure and nitrogen gas adsorption at $-196\text{ }^{\circ}\text{C}$ as described in the following section. The BET surface area was only analysed on biochar from BFBR. Dehydration of the biochar sample was conducted overnight in a furnace at a temperature of $105\text{ }^{\circ}\text{C}$. This procedure is done to remove any traces of contaminants such as oil and water on the surface or within the pores of the biochar particles. The biochar was put in a sample holder and placed at the bottom prior to the degassing step.

The solid biochar in the sample holder and Degas system (Micromeritics Vac Prep 061, Sample Degas System) was heated to a temperature of $90\text{ }^{\circ}\text{C}$ under a vacuum for one hour in order to remove volatiles for one hour. The degassing was continued at $250\text{ }^{\circ}\text{C}$, under vacuum conditions for an extended period of time, usually 2 to 3 days to ensure effective removal of volatiles from the sample before analysis. Degassed samples were directed to the analysis port almost immediately after degassing to prevent any exposure to the atmosphere. The biochar sample was analysed by using adsorptive nitrogen gas which was added in incremental dosages. For the initial experiment, adsorption isotherm, BET surface area (Brunauer *et al.*, 1938), t-plot (De Boer *et al.*, 1966) and Barret-Joyner-Halenda (BJH) desorption were chosen because these methods were suitable for microporous material such as biochar.

Total pore volumes (V) were estimated from the amount of nitrogen adsorbed at the highest relative pressure $\left(\frac{p}{p_0}\right) = 0.98$. This involved the selection of a suitable relative pressure range in accordance to the type of material. Relative pressure, $\left(\frac{p}{p_0}\right)$, which is the actual gas pressure, p divided by the vapour pressure p_0 of the adsorbing gas at the temperature at which the test was conducted. Data were automatically collected, displayed and analysed by computer. The determination of the pore size distribution and surface area by the machine was based on the relative pressure applied to effect penetration of the nitrogen into the pores. The resulting isotherm was analysed using BET method, while pore size distributions were carried out by BJH desorption method.

3.5.5 Particle size distribution

3.5.5.1 Biochar from LTSR

The LTSR produced biochar in a mixture with bio-oil and in order to determine the particle size distribution, slurry of 34 wt. % solids was made. A special 1.5kW colloid mixer (MAT, Mischanlagentechnik, Type: sc-05-M) well known for the preparation of a very homogeneous cement mortar was used to prepare a pumpable biochar/bio-oil mixture for both CC and CS (Henrich, 2007). This colloid mixer has high shearing stress ($> 10^4 \text{ s}^{-1}$) to completely destroy the solid biochar agglomerates and form a stable paste of slurry without adding additives. The slurry mixtures were milled in a colloid mill at 50-60Hz frequency (Model DMTT 02 ATEX E 026) to study the effect of biochar particle size on the homogeneity and stability of slurries. The mixed and milled samples were analysed for particle size distribution by an XPT-C Particle Analyser. The analyser was installed with a standard gross camera taking photos of the solid particles. A 10mg sample of the solids is put in a cylinder and methanol was topped up to three quarter full. A stirring rod was used to stir the solution as the measurement progresses. The slurry viscosity measurements (within a small temperature range on the mixed and milled biochar slurries) were studied by a Brookfield R/S Rheometer. The viscometer agitator or vane was immersed in a sample of a depth twice that of the vane height and the vane-container diameter ratios was lower than 0.75 to obtain best results.

3.5.5.2 Biochar from BFBR

The biochar from BFBR was dry due to separation of the gas and solid particles in the dual cyclone system prior to condensation of the organic vapours. A Retsch Model AS 200 was used for particle size sieving on a sample volume of 200 ml, amplitude of 1 mm and analysis time of 10 min.

3.6 Gas analysis

3.6.1 Corn residues non condensable gas product

Micro gas chromatography (GC) (Rosemount Analytical process gas chromatograph, model 700) was used to analyse qualitatively and quantitatively the gas components from fast pyrolysis of biomass in a LTSR. A quantitative and qualitative analysis of non-condensable gas was not carried out in a BFBR the process was not coupled to an online GC-MS. The gas quantity was determined by the injection of a constant flow of helium (He) (internal standard) as a calibration gas to calculate the mass of each gas component in the non-condensed gas stream. A volume of

1 l litre of the carrier gas, He, was injected per hour. A sample from the pilot plant was also taken for analysis on GC Agilent 5890 series 2 with thermal conductivity detector on PoraBond Q column from Varian for organic gases. A flame ionisation detector on the Carboxen 1000 column from Supelco for permanent gases was used. The oven was programmed to hold at 35°C for 6 min, ramp to 225°C and hold at this temperature for 14.5 min. The flow rate was 40 mL/min of He. The results were evaluated by the Chemstation software.

3.6.2 Pyrolysis vapour analysis

The chemical signature of gas products from FP of biomass was investigated by the analysis of complex pyrolysis gas mixture prior to condensation. An on-line process analysis of pyrolysis gases by fragmentation-less soft photo-ionisation Time-Of-Flight Mass spectrometry was used. The schematic diagram of the pyrolysis-Resonance Enhanced Multi Photon Ionisation (REMPI) system illustrates the experimental set-up (Figure 8). The pyrolysis gas prior to condensation was trapped and diluted by nitrogen. A series of cyclones, bag filters and fine filters were used to clean the gas stream before Time-Of-Flight Mass spectrometry analysis. A Nd-YAG-Laser, (266 nm) was used for nonlinear generation of Ultra-violet laser pulses for REMPI.

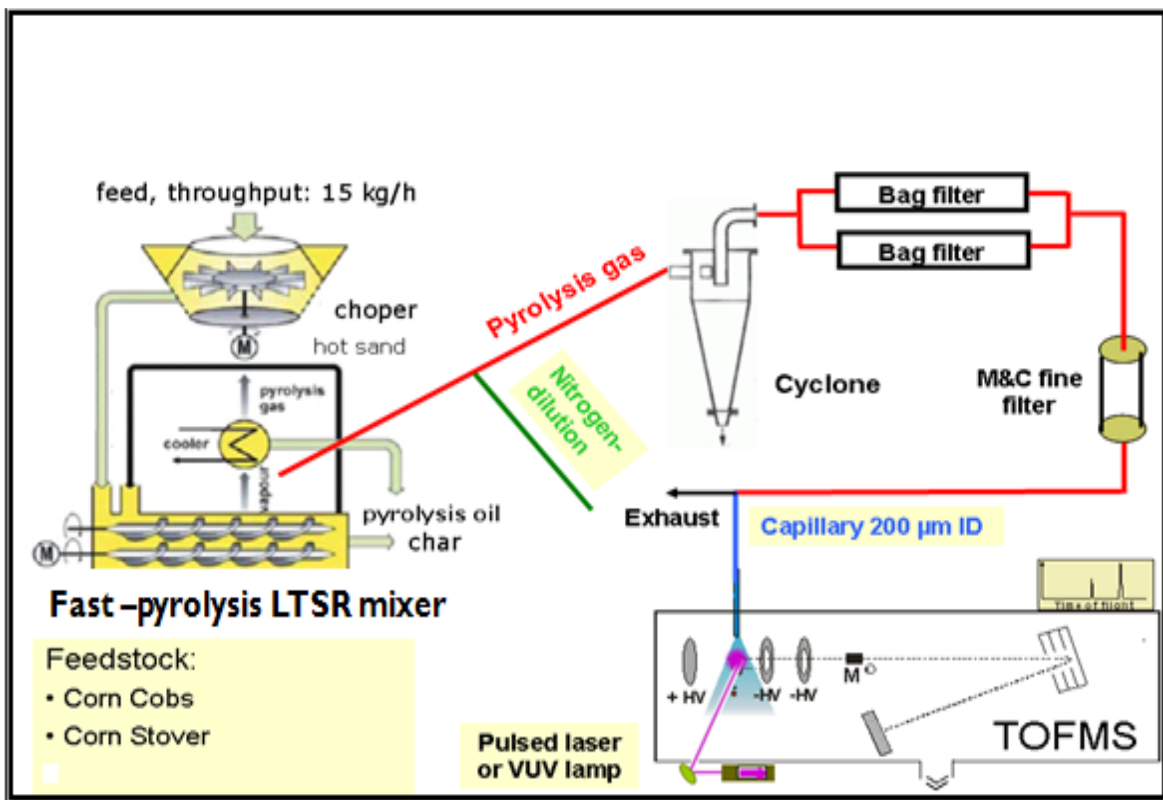


Figure 8: Scheme of the on-line process gas analysis

Chapter 4: Characterisation of biomass feedstocks

4.1 Results and Discussion

This chapter deals with results and discussion of the characterisation of the corn residues from South Africa. Characterisation of the corn residues includes proximate analysis, heating value, densities, mineral composition and ultimate analysis. The physical and chemical properties of the corn cob and corn stover were determined and compared, to evaluate their suitability as a chemical feedstock in pyrolysis processes. The analytical results were important for data interpretation and prediction of the quality of pyrolysis products, and also give an understanding of thermal characteristics of corn residue (CR) biomass.

4.1.1 Lignocellulosic compositional analysis

Hemicelluloses, cellulose and lignin compositions and their standard deviations (SD) for both feedstocks were determined (Table 15).

Table 15: Lignocellulosic composition of corn cob (CC) and corn stover (CS) (wt. %. df)

Component	CS	SD	CS (Literature)	CC	SD	CC (Literature)
Extractives	7.7	0.6	-	8.6	0.2	-
Analyses below were done on extractives free samples						
Lignin	13	1	11-16.6	15	1	18.8
Cellulose	37	2	28-51	48	2	34.3
Hemicelluloses	42	2	22.6-30.7	33	2	40.5
Holocellulose	79	5	50.6-81.7	81	4	74.8
References	This Study		Lynd <i>et al.</i> , 1999 Dermibas, 1997 Trautman <i>and</i> Richard, 2007	This Study		Garrote <i>et al.</i> , 2003

From these analyses, it has been found that extractives, lignin, cellulose and hemicelluloses contents in CS were 7.7 wt. %, 13 wt. %, 37 wt. % and 42 wt. % and 8.6 wt. %, 15 wt. %, 48 wt. % and 33 wt. % for CC, respectively. The results obtained in CS were in agreement with other researchers (Lynd *et al.*, 2009; Dermibas, 1997; Trautman *and* Richard, 2007). In CC lignocellulosic composition there were large differences compared to a study by Garrote *et al.*

(2003) having relative differences of 13.7 wt. % cellulose, 7.5 wt. % hemicelluloses and 3.8 wt. % lignin. There is limited data information in the literature for the CC lignocellulosic composition. Previous studies on lignocellulosic compositional analysis of corn residues presented in Table 15 were done by Technical Association of Pulp and Paper industry (TAPPI) methods. The lignocellulosic composition in this study on corn residues (CR) was done by using methods developed by the TAPPI, ASTM and Institut du Bois' methods for extractives, lignin, cellulose and holocellulose. The TAPPI and ASTM methods are known to produce very accurate results for wood feedstocks but are generally unsuitable for agricultural residues (Brigdwat, 1994). The major drawbacks of the TAPPI and ASTM standards for agricultural feedstocks analysis is the interference from the ash during the lignin determination. This could be the reason for a large variation in lignocellulosic compositions from different studies (Table 15). The ash is retained with the lignin and higher results of lignin content in agricultural residues are obtained (Brigdwat, 1994). The lignocellulosic composition of corn stover varied for different studies due to large variation of ash content in agricultural residues (Table 14).

Major fractions of biomass, holocellulose (cellulose and hemicellulose) are converted into the volatile fraction during thermal decomposition and into bio-oil upon condensation (Mohan *et al.*, 2006; Asadullah *et al.*, 2008). Jung *et al.* (2008)'s study on rice straw and bamboo found that higher volatiles content biomass could be expected to produce higher bio-oil yield. CC and CS have almost the same holocellulose content, 81 wt. % and 79 wt. % respectively, and is expected to have a slight difference in bio-oil yields at the same fast pyrolysis operating conditions. The carbon content that produces biochar is called the fixed carbon (FC), and is formed from different components of biomass in the order of lignin>hemicellulose>cellulose (Asadullah *et al.*, 2008). The pyrolytic conversion of lignin leads to a higher biochar yield (Wenzl *et al.*, 1970). The formation of biochar from lignin under pyrolysis reaction conditions is a result of the breaking of the relatively weak bonds, like the alkyl-aryl ether bonds, and the formation of more resistant condensed structures (Domburg *et al.*, 1974). It has been found that corn residues have slight differences in lignin, hemicelluloses and cellulose; hence it would be expected to produce same FC and fast pyrolysis biochar yields. The physical and chemical properties of CR are shown in Table 16.

Table 16: Physical and chemical properties of CR

Reference	This study	This study	Kumar <i>et al.</i> ,2008	Tartosa <i>et al.</i> ,2007	Gaur <i>et al.</i> ,1998	Feng <i>et al.</i> ,2005
Feedstock	CC	CS	CS	CS	CC	CC
Country	South Africa	South Africa	United States of America	Netherlands	United States of America	China
Proximate analysis (wt. %)* (<i>* By difference and calculated from ash at 550°C</i>)						
Moisture	4.6	8.5	5.3	7.4	-	3.8
Volatiles	79.9	76.7	74.9	73.2	80.1	77.7
Fixed carbon*(by calculation)	13.7	8.2	11.7	19.2	18.5	17.0
Ash at 550°C	1.8	6.6	8.2	7.7	1.4	1.5
Ash at 815°C	1.6	6.1	-	-	-	-
Ash at 1000°C	1.6	6.1	-	-	-	-
HHV(MJ/kg)	19.14	18.06	18.45	17.68	18.77	-
LHV(MJ/kg)	17.88	16.84	-	16.4	-	-
Ultimate analysis (wt. %, daf)						
C	50.21	48.9	51.8	48.8	47.3	47.6
H	5.90	6.01	5.50	6.41	6.02	4.91
O*(by calculation)	43.5	44.4	41.6	44.1	46.2	46.48
N	0.42	0.61	0.84	0.65	0.48	0.84
S	0.03	0.05	0.34	0.08	0.01	0.41
Cl	0.22	0.41	-	0.64	-	-
H/C molar ratio	1.41	1.47	1.27	1.58	1.53	1.24
O/C molar ratio	0.65	0.68	0.60	0.68	0.73	0.73
Empirical Formula	CH_{1.41}O_{0.65}N_{0.007}	CH_{1.47}O_{0.68}N_{0.01}	CH_{1.3}N_{0.014}O_{0.6}S_{0.002}	CH_{1.6}N_{0.01}O_{0.7}S_{0.006}	CH_{1.53}N_{0.009}O_{0.73}	CH_{1.24}N_{0.02}O_{0.73}S_{0.003}
Tapped density (kg/m ³)	390	210	-	-	-	-
Freely settled density	290	170	-	-	-	-
Particle size (mm)	<1	<1	-	-	-	-
Energy density (GJ/m ³)	5.6-7.5	3.1-3.8	-	-	-	-

4.1.2 Proximate and ultimate analyses:

Table 16 shows the proximate and ultimate analyses of CR. The ultimate analysis is used to determine combustion air requirements and emission levels. From this analysis, it has been found that CC contains 50.2 wt. % of carbon slightly higher than CS, 48.9 wt. % and equal hydrogen content, 5.9 wt. % and 6 wt. % from CC and CS respectively (Table 16). The results showed that CR are environmentally friendly energy sources, since it contains only trace amounts of nitrogen (0.42 wt. % daf for CC and 0.61 wt. % daf for CS) and sulphur (0.03 wt. % daf for CC and 0.05 wt. % daf for CS), compared to South African coal (nitrogen 0.8-1.9 wt. % daf and sulphur 0.7-1.2 wt. % daf) (Alessio *et al.*, 2000; Tola and Cau, 2007; Bosch, 1998) (Table 17). If the biomass itself or the pyrolysis products derived from the biomass are burnt for energy, the amounts of nitrogen oxides and sulphur oxides given off will be much lower than when burning fossil fuels. The nitrogen and sulphur oxides into the atmosphere give rise to greenhouse effect and international long-term climate change. It is beneficial to the environment when using CR for energy production.

The H/C and O/C ratios of CC were 1.41 and 0.65 and of CS were 1.47 and 0.68, respectively, in between the range of previous reports on CR from various parts of the world with O/C (0.6-0.73) and H/C (1.27-1.58) (Kumar *et al.*, 2008; Gaur *et al.*, 1998; Fenget *et al.*, 2005; Tortosa *et al.*, 2005). The range of CR O/C and H/C ratios were the same for other biomasses illustrated on a Van Krevelen diagram for various fuels presented by Prins *et al.* (2007). The higher O/C ratios in biomasses compared to fuels like coal is due to the presence of structurally well-defined compounds, hence relatively more work may be required decomposing such fuels (Prins *et al.*, 2007). If considering only the main elements (C, H, O, N, S), the molecular formulae of the samples based on one N atom can be written as $\text{CH}_{1.41}\text{O}_{0.65}\text{N}_{0.007}$ for CC and $\text{CH}_{1.47}\text{O}_{0.68}\text{N}_{0.01}$ for CS (Table 16). The empirical formulae of biomass are important in predicting the products produced from fast pyrolysis process. Due to the slight differences in elemental composition of the biomasses, the empirical formulae remain different between each CR biomass source (Table 16). The oxygen content of the CR biomass is between 43.5-44.4 wt. %, significantly higher than those for coal (8-19.7 wt. %) (Table 17). This latter content should

lead to a high oxygen content in the pyrolysis liquid products and then much lower heating values than those of fossil fuels (Pattiya *et al.*, 2007). Accordingly, removal of oxygenated species during or after the pyrolysis reactions is necessary to obtain a higher fuel grade product. The only difference between the South African CR and the ones studied in other countries are the variation in ash content (Table 15). The ash content is varied due to different methods of harvesting and the amounts of nutrients (fertilisers) applied to the corn plant in different parts of the world.

Volatile matter evolves gases and light hydrocarbons during the pyrolysis process (Asadullah *et al.*, 2008). Higher volatiles content in the initial biomass makes it more reactive as it is more readily devolatilised than lower volatiles content solid fuels, liberating less fixed carbon, hence making them more useful for pyrolysis process (Graboski *and* Bain, 1981). The volatile matter, fixed carbon and ash content were 79.9 wt. %, 13.7 wt. % and 1.8 wt. % for CC and 76.7 wt. %, 8.2 wt. % and 6.6 wt. % for CS, respectively. There is a slight difference in the CR volatiles content hence it is expected to have almost the same reactivity and liquid yields. The volatiles content of CR is higher than that of coal (Table 16).

The moisture content of CC, 4.6 wt. % was lower than for CS, 8.5 wt. % (Table 16). The differences of moisture content in CR could be due to CS being more hygroscopic than CC it absorbs moisture from the atmosphere (Igathinathane *et al.*, 2009). Morris *and* Johnson(2000) reported that to ensure rapid heat transfer rates in a fast pyrolysis reactor, the moisture content should be less than 10 wt. %. The CR biomass was within the recommended moisture content levels for FP. For pyrolysis, higher moisture content in the feedstock has an adverse effect such as additional heat is required for vaporising the water and it increases the water content of the bio-oil (Asadullah *et al.*, 2008). Dry biomass, however, can cause problems such as dust that fouls equipment and can even cause an explosion hazard. High moisture content biomass has a tendency to decompose during storage resulting in energy loss and transportation of high moisture biomass is also costly (Jenkins *and* Ebeling, 1985). The moisture

content of biomass also has a marked effect on the conversion efficiency in pyrolysis processes, and the energy content of the biomass and the pyrolysis product bio-oil.

The CS has higher ash content than CC due to the association with soil during harvesting. Several methods exist to remove the unwanted soil and ash from biomass. The high soil content in CS can be removed by a washing step. Alternatively it can be pre-treated to remove ash by means of water leaching under mildly acidic conditions (Das *et al.*, 2004). The other method for reducing ash content is by discarding the smallest particle size fraction (fines) as mentioned in Chapter 1 (section 2.8.3.7).

4.1.3 Heating values

In this study, the heating value of the CC and CS was determined to evaluate the potential energy content of the biomass used during pyrolysis. The results obtained showed that the heating values of CR were almost similar, with CC having a HHV of 19.14 MJ/kg and a LHV of 17.88 MJ/kg, and CS having a HHV of 18.06 MJ/kg and a LHV of 16.84 MJ/kg. There are slight differences in chemical and physical properties of biomass (Table 16), hence in this study energy content of corn residues were compared with fossil fuel such as coal. From Table 17, heating values of CR are lower than those of other South African coals and higher than low grade coal with higher ash content. This is mainly because of the higher oxygen content in the biomass (43.5-44.4 wt. %, daf basis) than for coal (8-19.7 wt. %, daf basis) (Mohan *et al.*, 2006). The slightly higher heating value of CC is mainly due to its lower ash content than CS, as reported by Jenkins *et al.* (1998) who found out biomass ash content can drastically lower energy output and then decrease the heating value. In a similar study, it has been reported that heating values are inversely related to ash content, with every 1% increase in ash concentration decreasing the heating value by 0.2 MJ/kg (Cassida *et al.*, 2005).

Table 17: South African coal properties

Ultimate analysis (wt. % daf basis)	Alessio et al., 2000	Tola and Cau, 2007	Bosch, 1998	CR
C	69.6	71.6	47	-
H	3.8	4	2.4	-
N	0.7	1.6	1.1	-
S	0.6	1	0.5	-
O (By difference)	8.8	6.8	12.5	-
Ultimate analysis (wt. %, daf basis)				
C	83.4	84.2	74	48.9-50.21
H	4.6	4.7	3.8	5.90-6.01
N	0.8	1.9	1.7	0.42-0.61
S	0.7	1.2	0.8	0.03-0.05
O	10.5	8	19.7	43.5-44.4
Proximate analysis (wt. %, basis)				
Moisture	2.5	8	5.6	4.6-8.5
Ash	16.5	15	36.5	1.8-6.6
Volatiles	23.3	23	21.1	76.7-79.9
Fixed carbon (By difference)	57.8	54	36.8	8.2-13.7
Proximate analysis (wt. %, daf basis)				
Volatiles	28.7	28.9	36.4	-
Fixed carbon	71.3	71.1	63.6	-
HHV (MJ/kg)	24.4	25.9	16.2	18.06-19.14

There are a number of formulae proposed in the literature to estimate the HHV of biomass from basic analysis data, i.e. proximate, ultimate and lignocellulosic composition (Sheng and Azevedo, 2005; Dermibas, 1997; Channiwala and Parikh, 2002; Jenkins and Ebeling, 1985; Shafizadeh and Degroot, 1976; Dermibas, 2001b). In this study, these correlations were used to calculate the heating values (Table 18) using the analytical results in Table 15 (Lignocellulosic composition) and Table 16 (ultimate and proximate composition). It has been found that the correlations based on ultimate analysis were the most accurate with a difference of less than 0.7 MJ/kg compared to the heating value obtained from the analytical method for both feedstocks (Table 18). Correlations based on the proximate analysis data were the least accurate with difference of up to 3.69 MJ/kg. The correlations based on lignocellulosic compositions produced reliable heating values of less than 2 MJ/kg difference and thus more accurate than proximate analysis correlations, in disagreement to findings by Sheng and Azevedo (2005) who found larger differences (more than 3 MJ/kg).

Table 18: Heating values correlations

Correlation (HHV,MJ/kg)	HHV (MJ/kg)	Differences	Name of Author
$\text{HHV} = -3.04 + 0.22\text{VM} + 0.26\text{FC}$ <i>Equation 21</i>	CC 18.18	0.96	Based on proximate analysis: Sheng <i>and</i> Azevedo,2005
	CS 16.05	2.01	
$\text{HHV} = 0.312\text{FC} + 0.153\text{VM}$ <i>Equation 22</i>	CC 16.50	2.64	Dermibas,1997
	CS 14.32	3.69	
$\text{HHV} = 0.349\text{C} + 1.178\text{H} + 0.1\text{S} - 0.103\text{O} - 0.015\text{N} - 0.021\text{Ash}$ <i>Equation 23</i>	CC 19.60	0.46	Based on ultimate analysis: Channiwala <i>and</i> Parikh,2002
	CS 18.06	0.00	
$\text{HHV} = -0.763 + 0.301\text{C} + 0.525\text{H} + 0.064\text{O}$ <i>Equation 24</i>	CC 19.82	0.68	Jenkins <i>and</i> Ebeling,1985
	CS 18.52	0.46	
$\text{HHV} = 0.1739\text{C}_e + 0.266\text{L} + 0.3219\text{E}$ <i>Equation 25</i>	CC 20.84	1.70	Based on chemical composition: Shafizadeh <i>and</i> Degroot,1976
	CS 19.67	1.61	
$\text{HHV} = 0.0889\text{L} + 16.823$ <i>Equation 26</i>	CC 18.15	0.99	Dermibas,2001b
	CS 17.97	0.09	
Analytical Method	CC 19.14	-	This Study
	CS 18.06	-	

Biomass composition, VM (Volatiles), FC (Fixed Carbon), Ash, C, H, O, S are weight percent on dry biomass basis (wt. %.db). C_e, L, E are weight percent of holocellulose (Cellulose + Hemicelluloses), lignin and extractives on wt. %.df, respectively.

4.1.4 Particle density and shape

The freely settled and tapped bulk densities of the biomass are important for the determination of the storage space and hopper volume in a fast pyrolysis (FP) plant. Bulk density includes the volume of biomass particles, total void volume, and interstitial volume between the particles and is often dominated by the latter. The density and particle size of biomass fuel particles are vital, as they affect the pyrolysis results by influencing the heating rate and moisture vaporisation during the FP process (Okuno *et al.*, 2005). The tapped density were equal to 390 kg/m³ and 210 kg/m³ for CC and CS, respectively (Table 16). Freely settled densities were slightly lower and equal to 290 kg/m³ and 170 kg/m³ for CC and CS (Table 16). CC is heavier than CS, hence the flow properties and feeding systems into the process were expected to be different.

One of the major limitations of biomass for energy is the low densities. These low densities make biomass material more costly to transport and store. To overcome this limitation, the density of biomass can be increased by densification using extrusion processes, pelletising and briquetting presses (Tumuluru *et al.*, 2010). Pelletising can be used to improve the storage properties of biomass and can be easily transported and fed into a fast pyrolysis process. CR biomass after milling has irregular shapes with a wide variety of aspect ratios (Ma *et al.*, 2007). Corn stover (CS) particles are a fibrous and thin material, whereas corn cobs (CC) are spherically shaped and brittle after milling. Due to the above physical property differences CS has poor flow characteristics as the particles tends to bridge more than CC during feeding into the fast pyrolysis process. The size and shape of biomass particles are significant as they affect the amount of material that can be pelleted and the energy required for the compression process (Tumuluru *et al.*, 2010). The CR differences in shapes, particle size and geometry are also expected to influence the various physical properties such as moisture content and bulk density. From both bulk densities, the energy density is estimated as 5.55-7.5 GJ/m³ for CC and 3.07-3.8 GJ/m³ for CS. Comparing the CR bulk densities, CC have 1.8-2 times greater energy content per unit volume making transportation of CC much cheaper and cost effective than the transportation of the CS. The energy densities were much higher than estimated by Mullen *et al.* (2009) (for CR 0.7-1.4GJ/m³). The difference was due to lower bulk densities used in the

energy density calculation than the ones obtained in this study. The low bulk densities of 40-80 kg/m³ obtained by Mani *et al.* (2006) were used in the energy density calculations by Mullen *et al.* (2009) compared to higher bulk densities, 170-290 kg/m³ obtained in this study. The differences in bulk densities could be due to different procedures applied in the researches.

4.1.5 Biomass inorganic composition

The XRF technique has been used to determine the elemental composition of inorganic components of both the raw biomass feedstocks (Table 19). The biomass ash after heating at 550 °C was analysed by atomic absorption spectroscopy (AAS) and inductively coupled plasma-atomic emission spectroscopy (ICP-AES) (Table 20). The elemental composition of raw biomass indicated that K, 0.86 wt. % (43.37% on 100% ash basis), and Si, 3.03 wt. % (43.04% on 100% ash basis), were the most abundant elements in the inorganic fraction of CC and CS, respectively. The silicon constitutes about 43.04 % in CS and 33.28 in CC biomasses. Silicon is associated with the soil from harvesting and it's a contaminant not an inherent part of the biomass. The soil in the corn residues can be removed by a washing step and discarding of the fines particles by sieving (Garcia-Perez *et al.*, 2002). The removal of soil from the corn residues can reduce the ash content of CC from 1.8 wt. % to 1.14 wt. % and CS from 6.6 wt. % to 3.57 wt. %. The inorganic elemental composition of CR in this study was compared to the ones from United States of America analysed by the same method (XRF). The inorganic analyses were in agreement with an American corn residues elemental composition by Mullen *et al.* (2009), who found that K, 1.04 wt. % and Si, 2.79 wt. %, were the most abundant elements in the inorganic fraction of CC and CS, respectively (Table 2). Cu and Zn, levels were lowest at less than 0.05 wt. % for each feedstock and other significant mineral elements including Ca, Mg and Al were more concentrated in CS biomass. Ti and Mn were detected in CS only and Zn was only detected in CC. There were slight differences in the inorganic elemental composition in this study compared to the feedstocks studied by Mullen *et al.* (2009). Ti was detected in both feedstocks by Mullen *et al.* (2009) and only identified in CS in this study. Ba and Sr were not detected in South African CR and were identified in American CR. The amount of fertilisers applied and soil type are the main reasons for the differences in the elemental composition of the CR.

Table 19: Biomass elemental composition

Element		CC (wt. % dry In biomass)	CC (% on 100% ash basis)	CS (wt. % dry In biomass)	CS (% on 100% ash basis)
Si	Silicon	0.66	33.28	3.03	43.04
Al	Aluminium	0.06	3.03	0.23	3.27
Mg	Magnesium	0.04	2.02	0.56	7.96
P	Phosphorous	0.01	0.50	0.04	0.57
S	Sulphur	0.02	1.01	0.06	0.85
Cl	Chlorine	0.28	14.12	0.77	10.94
K	Potassium	0.86	43.37	1.33	18.89
Ca	Calcium	0.02	1.01	0.87	12.36
Ti	Titanium	-	-	0.01	0.14
Mn	Manganese	-	-	0.01	0.14
Fe	Iron	0.02	1.01	0.11	1.56
Cu	Copper	0.01	0.50	0.01	0.14
Zn	Zinc	0.003	0.15	-	-
Br	Bromine	-	-	0.01	0.14

The ash content of biomass ranges from less than 1 wt. % in wood biomass to 15 wt. % in agricultural residues (Yaman, 2004). During CR pyrolysis, these inorganics, especially K and Ca, catalyse biomass decomposition and biochar forming reactions. Biochars formed during these reactions invariably end up in the bio-oils liquids as submicron solid particles with inorganic elements in it. If a hot gas filter is used, secondary biochar formation will be removed and will not end up in the quenched bio-oils (Diebold *et al.*, 1993). The presence of the ash in the bio-oils makes them release these particles in its application such as boilers, combustion and other thermochemical applications and reduce equipment efficiency (Agblevor and Besler, 1996). Studies on various biomass types by Ahuja *et al.* (1996) showed that, in general, ash removal (pre-treatment) increased the volatiles yield, initial decomposition temperature and rate of pyrolysis. The higher ash and mineral contents in CS biomass should lead to lower volatiles, lower pyrolysis rate, higher slagging, fouling and corrosion tendencies than CC biomass. The higher ash content in the CS is mainly due to the harvesting method where the raw material is associated with soil from the ground.

4.1.6 Char inorganic composition

Table 20: Ash inorganic composition

Element		CC	CC wt.%	CS wt.%	CS	Element		CC	CS
ICP		wt.%	dry	dry	wt.% dry	AAS		ppm	ppm
		dry after	on 100%	dry after	on 100%				
		heating	ash basis	heating at	ash basis				
		at 550		550 °C					
Aluminium	Al	0.9	1.8	1.5	3	Antimony	Sb	-	-
Barium	Ba	0.1	0.2	0.1	0.2	Arsenic	As	3	8
Calcium	Ca	0.8	1.6	6.6	13	Lead	Pb	26	25
Iron	Fe	0.6	1.2	1.3	2.6	Boron	B	-	-
Potassium	K	30.2	59	9.7	19.1	Cadmium	Cd	1.1	-
Magnesium	Mg	1.5	2.9	4.3	8.5	Chromium	Cr	263	0.7
Manganese	Mn	0.1	0.2	0.1	0.2	Cobalt	Co	3	116
Sodium	Na	0.2	0.4	0.4	0.8	Copper	Cu	263	8
Phosphorous	P	1.6	3.1	0.7	1.4	Molybdenum	Mo	6	849
Silicon	Si	15	29.3	25.8	50.8	Nickel	Ni	117	342
Titanium	Ti	0.1	0.2	0.2	0.4				

Higher concentrations of inorganic were obtained due to the loss of volatiles and moisture after heating at 550 °C. The K has the highest concentration in CC followed by Si and in CS Si has the highest concentration followed by K. It was found that Cr, Cu, Ni, Sr and Zn are present in significant concentrations due to the chemical treatments (pesticides and insecticides spraying) of corn plant. In CC and CS, it was found that there were differences in concentrations for the following metals, Cr, Cu and Mo. The source of these metals are from soil parent rocks, Cr higher concentrations is in soil derived from volcanic rocks, Mo higher concentrations in granitic and acid magmatic rocks and Cu higher in mafic and intermediate rocks (Pendias *et al.*, 2000). The inorganic elements in plants vary between different regions and countries depending on the soil parent rocks. Elevated contents of these metals in some phosphate fertilisers may be a significant source of these metals in soils. The inorganic metal content in plant parts is depended mainly by the soluble metal content of the soils. However, the rate of metal uptake by the corn plant is dependent on the type of soil, stages of plant growth and plant tissues (Mertz *et al.*, 1974). Due to the differences of plant tissues in the CR, the mechanism of metal uptake between CS and CC is different due to metal solubility and

absorptive properties in stover and cobs. In a similar study, Pendas *et al.* (2000) found that Cu accumulates in reproductive organs of plants, but this however differs widely among plant species. Cu was higher in CC than in CS in agreement with a study by Loneragan *et al.* (1981) who found that Cu concentrations were highest in corn grains and corn cobs. These findings were not in agreement with those reported by Liu *et al.* (1974), who found a more uniform distribution of Cu throughout the barley plant due to different species. The AAS and ICP-AES are more accurate techniques than XRF detecting trace elements such as arsenic, cadmium and lead. Arsenic, a heavy metal naturally occurring in soil, is a highly deleterious as it is an environmentally hazardous substance if emitted into the atmosphere. This metal can be released to the flue gas through pyrolysis, and can also poison the catalysts in subsequent uses such as bio-oil upgrading and biochar gasification. CR feedstock contained trace amounts of arsenic (< 10 ppm) (Table 20). Pavish *et al.* (2010) reported that arsenic in solid fuels can be reduced by fixed bed limestone.

The devolatilisation percentages of the raw biomass after heating at 550 °C were calculated and the results are shown in Table 21. Positive devolatilisation percentage means that the elements were vaporised into the atmosphere and a lower amount of ash was produced after heating at 550 °C. Negative devolatilisation percentage means that the inorganics amounts were higher in the ash after heating at 550 °C than in biomass samples. Phosphorous in both biomasses and potassium in CS produced negative devolatilisation. This could be due to differences in equipment used, XRF equipment being less accurate than the AAS and ICP. XRF equipment could have measured a lower value metal content than present in the raw biomass. There were differences in the inorganics identified in the raw biomass and the one after heating at 550 °C. In both feedstocks S, Cl and Br were not detected after burning at 550 °C and 100% devolatilisation percentages obtained (Table 20). This is due to the volatilisation into the vapour phase of these elements at 550 °C. Gibb (1983) studied pyrolysis of British coal and found that chlorine vaporises at relatively low temperatures with, 71 wt. % of the total chlorine vaporised at 258 °C. In another study Bjorkman and Stromberg (1997) found that chlorine from inorganic salts will not leave below their melting point, approximately 750 °C, while organic chlorine would vaporise at lower temperatures. The chlorine in the CR can be mainly from the organic part of biomass as all the chlorine was vaporised at 550 °C. Devolatilisation occurred to most

of the elements by positive devolatilisation percentages (Table 20). Al and Cu had high devolatilisation percentages, more than 70% in both biomasses.

Table 21: Devolatilisation % of total inorganic elements at 550°C

Element	CC	CS
S	+100	+100
Cl	+100	+100
Br	+100	+100
Si	59.1	67.3
Al	73.0	74.2
Ca	28.0	93.9
Fe	46.0	64.0
K	36.8	-49.9
Mg	32.5	82.3
Mn	-	34.0
P	-188	-164
Ti	-	34.0
Cu	95.3	82.6

Chapter 5: Thermal behaviour of corn residues

5.1 Results and Discussion

This chapter deals with results and discussion of the thermal and pyrolytic behaviour of corn residues. In order to design the reactor for fast pyrolysis, information is needed about the hydrodynamics of the biomass particles, kinetic parameters and the gases in the reactor and heat transfer to the particles during the process (Bramer and Brem, 2007). In this study, there was no design of fast pyrolysis done but more information was needed about the thermal characteristics of the corn residues in order to understand their fast pyrolysis. The activation energies of corn residues decomposition were obtained to compare the reactivities of the biomass and the yields of expected products. Thermo-analytical techniques, in particular the thermogravimetric analysis (TGA) allowed this information to be obtained. The objective was to obtain properties of CR related to thermochemical decomposition, and to compare the two biomass feedstocks.

5.1.1 Analysis of thermo-analytical curves

There are no major differences in the thermal decomposition temperatures between the two feedstocks. Characteristics of thermal decomposition of biomass data with regards to weight loss (TG) and derivative weight loss (DTG) for CR at different heating rates were compared. An example of the TG/DTG curves is illustrated in Figure 9 and a summary of the peak temperature ranges and biomass components devolatilisation stages are shown in Table 22. The curves at heating rates from 1 °C/min to 40 °C/min for both feedstocks, plotted against temperature are shown in Figure 10, 11, 12 and 13. They are pyrolysed in the same range of temperatures within ± 12 °C differences on maximum peak temperatures. From the curves, three distinct weight loss stages could be identified (water evaporation, main pyrolysis and slow decomposition), in agreement with previous findings (Kumar *et al.*, 2008; Vutharulu, 2004). The first stage (I) goes from room temperature to 130 °C; a slight weight loss in the weight loss curve (TG curve) and a small peak in the rate of weight loss curve (DTG curve) (Figure 11 and 13) is observed.

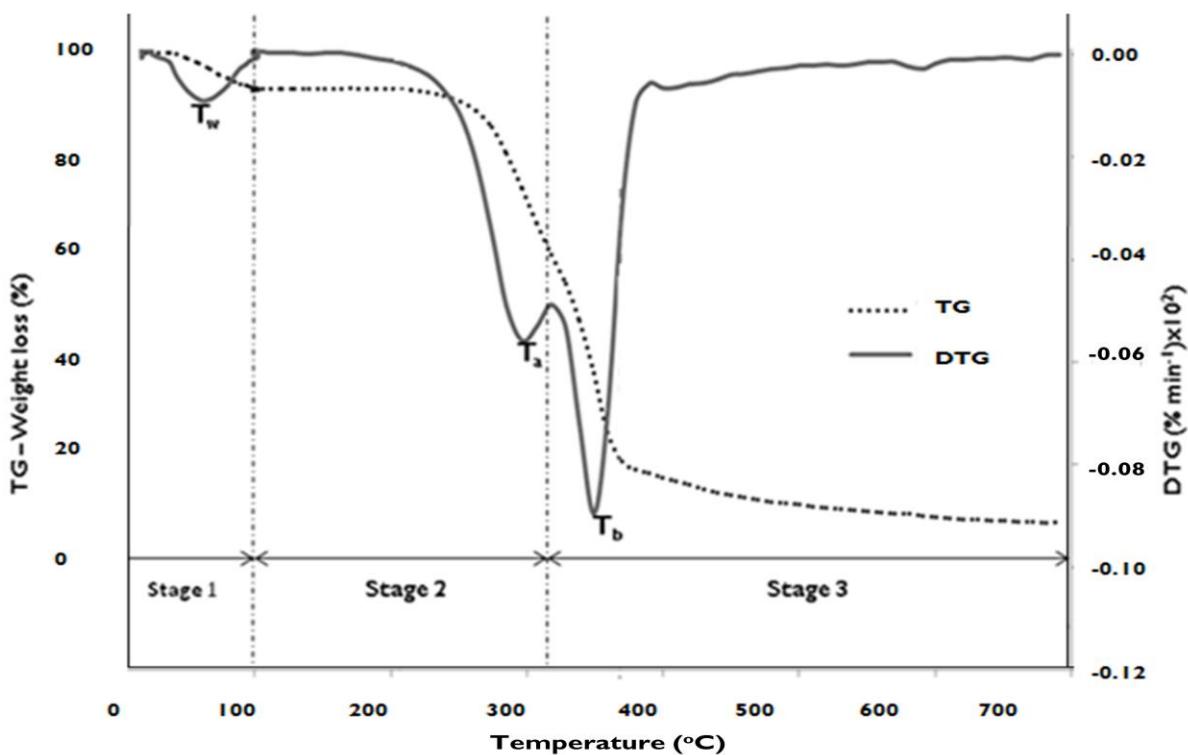


Figure 9: CC TG/DTG curve temperature illustration graph

Table 22: Temperature devolatilisation parameters for CC and CS at different heating rates

Sample	Heating rate (°C/min)	T_a (°C)	T_b (°C)	T_w (°C)	Stage 2 (°C)	Stage 3 (°C)
CC	1	252	295	60	157-266	266-700
	10	276	324	105	172-302	302-700
	20	290	343	114	188-318	318-700
	30	298	344	119	192-326	326-700
	40	307	348	125	195-333	333-700
CS	1	251	298	60	145-264	264-700
	10	279	334	103	170-303	303-700
	20	288	346	114	186-319	319-700
	30	299	353	115	188-325	325-700
	40	307	357	122	191-327	327-700

T_w , T_b and T_a are the maximum peak temperatures of hemicelluloses, cellulose degradation and water evaporation.

This could be due to the loss of water and light volatile components (Mansaray and Ghaly, 1999) and the maximum water loss temperature is denoted by T_w in Table 22 and illustrated in Figure 9. Using data from various heating rates, the average weight loss for the moisture devolatilisation stage was 9.2 ± 0.8 wt. % for CS and 6.9 ± 0.6 wt. % for CC. The second stage (II) goes from 145 to 333 °C. Stage II which was characterised by a major weight loss from 65 to 71 wt. % for CC and 63 to 69 wt. % for CS mass reduction, corresponding to the main pyrolysis process. According to Roque-Diaz *et al.* (1985) the degradation of most of the heavier components in biomass, the breaking down of C-C bonds and formation of biochar occur in this stage. There is a characteristic peak in the derivative weight loss curve, with a peak temperature T_a (Figure 9), at which the rate of weight loss attains a maximum.

The third stage (III) goes from around 264°C to the final temperature 700°C with a peak temperature denoted and illustrated by T_b in Figure 9 and defined in Table 22. In this third stage, inorganics mass loss occurred and the lignin in the biomass continuously decomposes at a very slow rate. A slight continued loss of weight is shown in the weight loss curves (Figure 11 and 13). Kumar *et al.* (2008) gave curves of similar shapes for CR.

The devolatilisation stages have been shown to correspond mainly to the degradation of the biomass components (cellulose and hemicellulose) (Yang *et al.*, 2007; Sonobe *et al.*, 2008). The analysis of the rate of weight loss curve shows that, during the pyrolysis process, two characteristic peaks corresponding to the degradations of cellulose and hemicelluloses (Kumar *et al.*, 2008). As shown in Table 22, hemicelluloses typically decomposed in the range of 145-333 °C, while cellulose degrades at a higher temperature range from 264 °C in agreement to findings by Varhegyi *et al.* (1989) on sugar cane bagasse. Caballero *et al.* (1997) and Antal and Varhegyi (1995) found that lignin decomposed throughout the whole temperature range and could not be assigned a distinct peak. The DTG curves for CC have distinct peaks and for CS at 40 °C/min the first peak is merged.

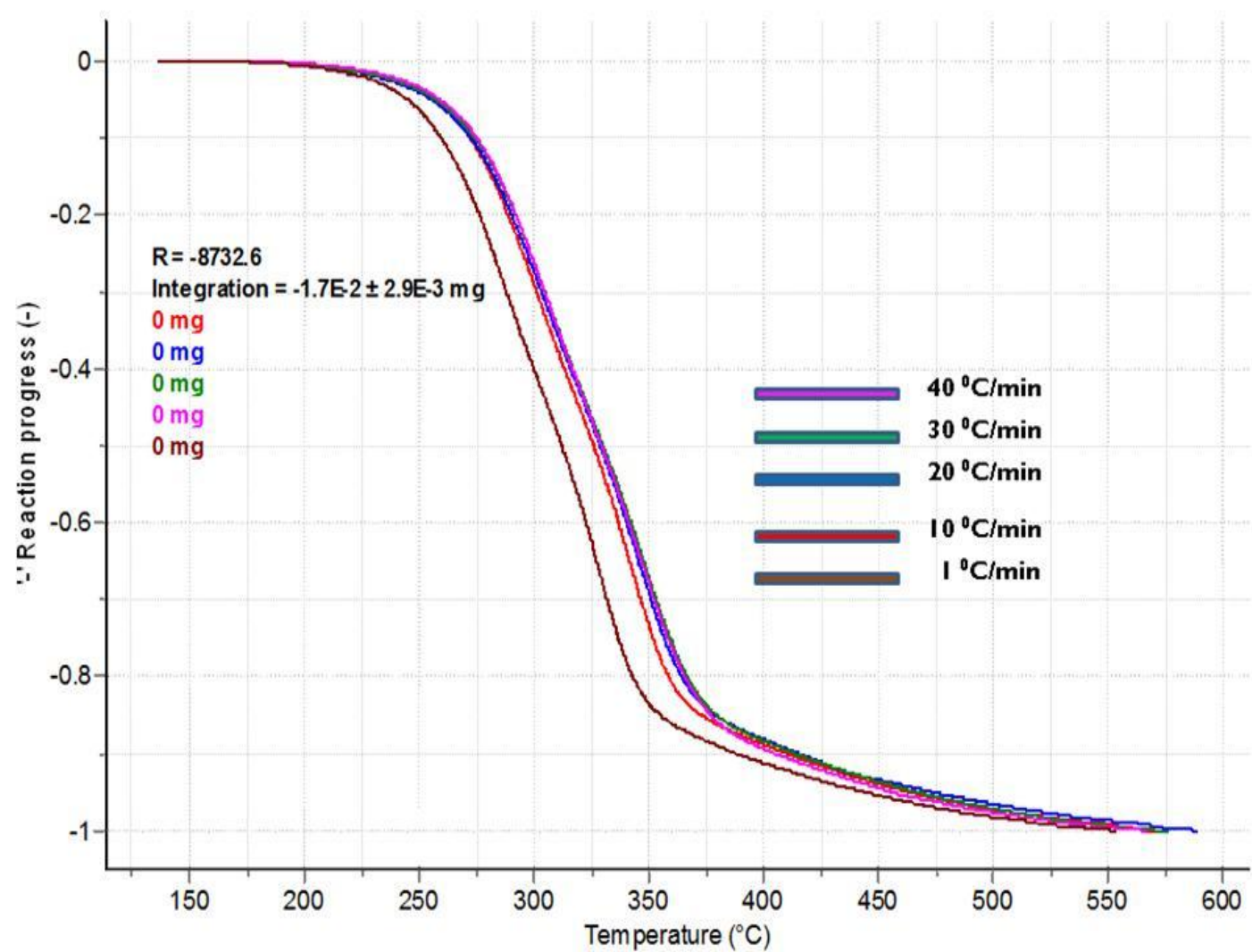


Figure 10: TG curve for CC

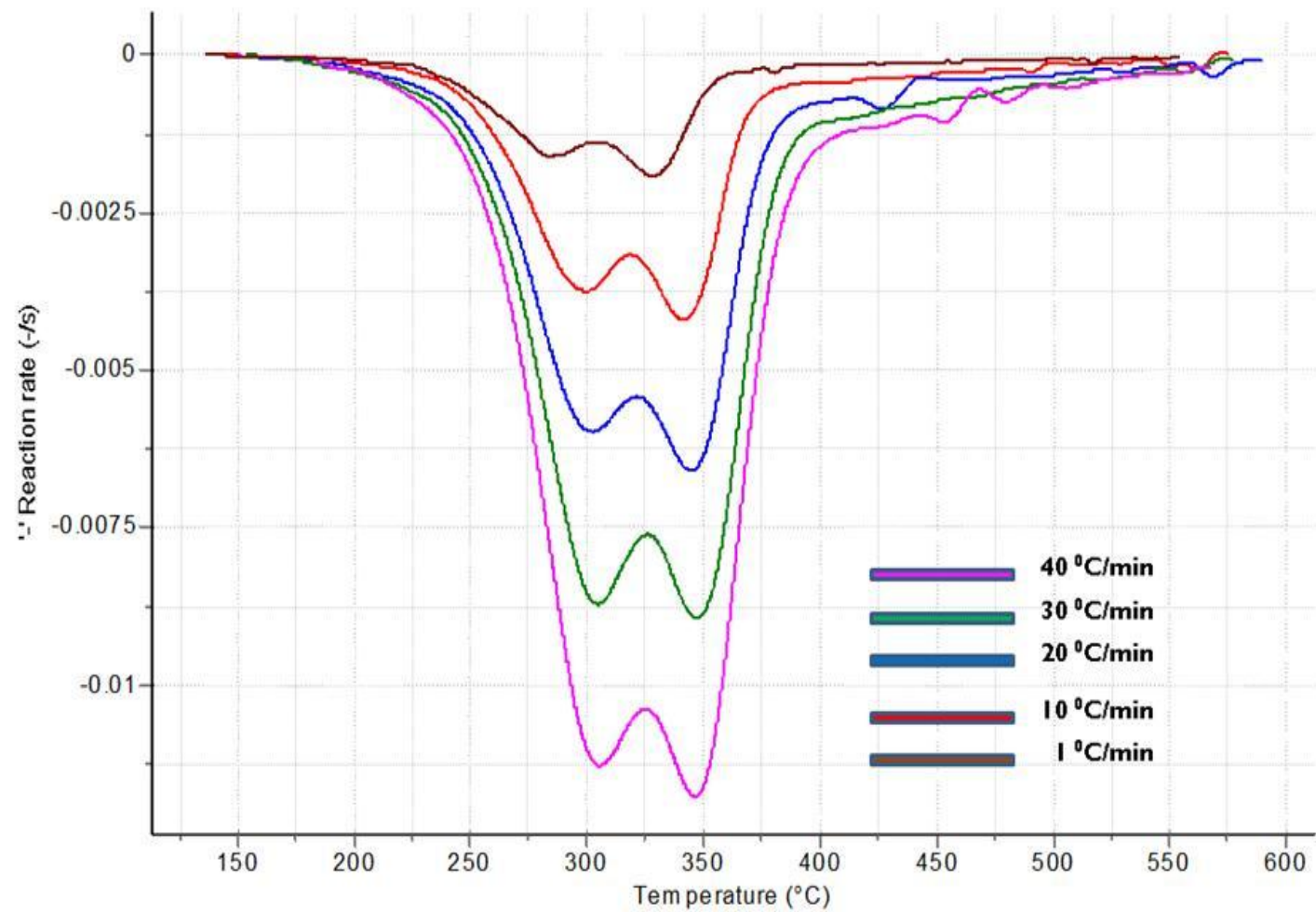


Figure 11: DTG curve for CC

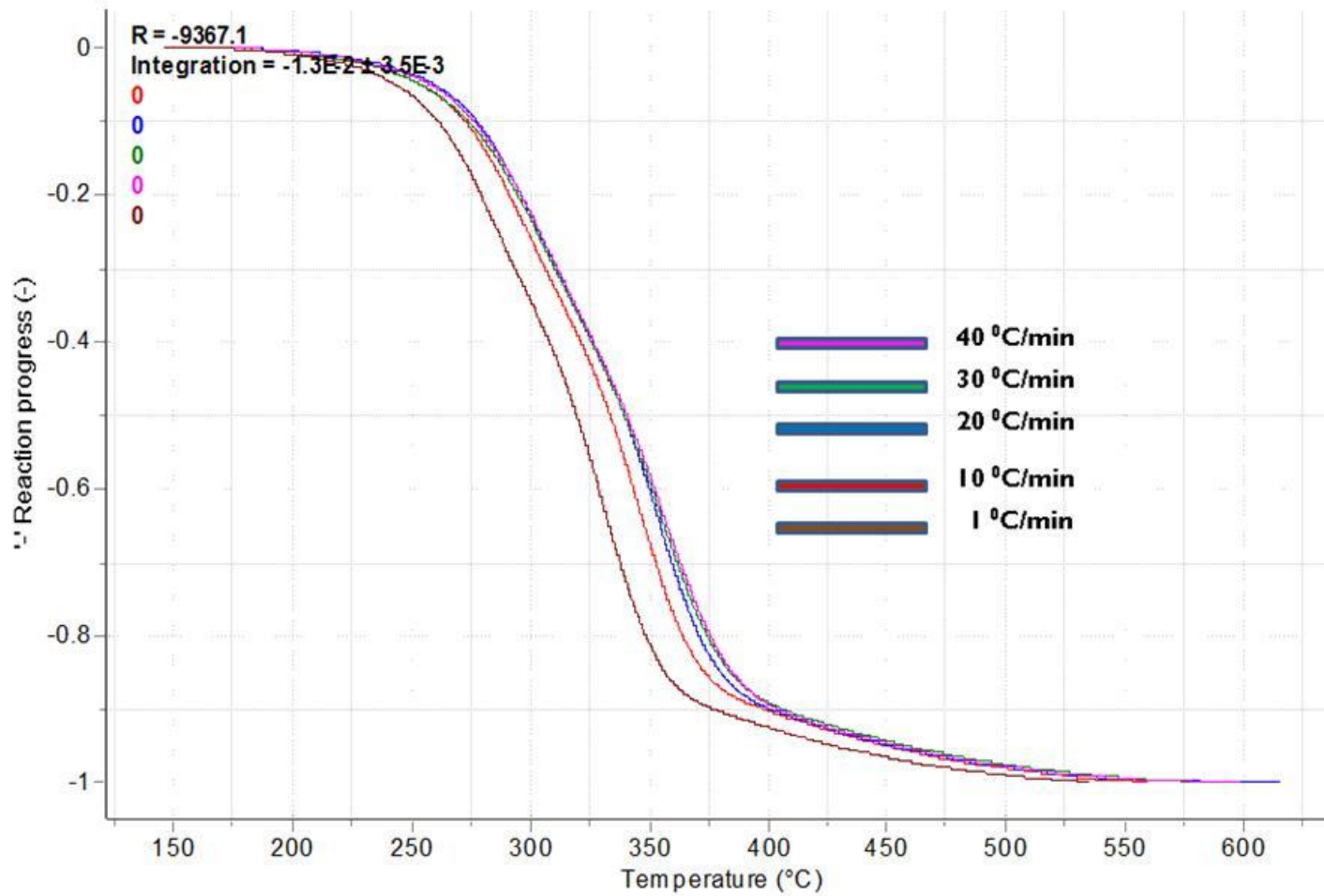


Figure I2: TG curve for CS

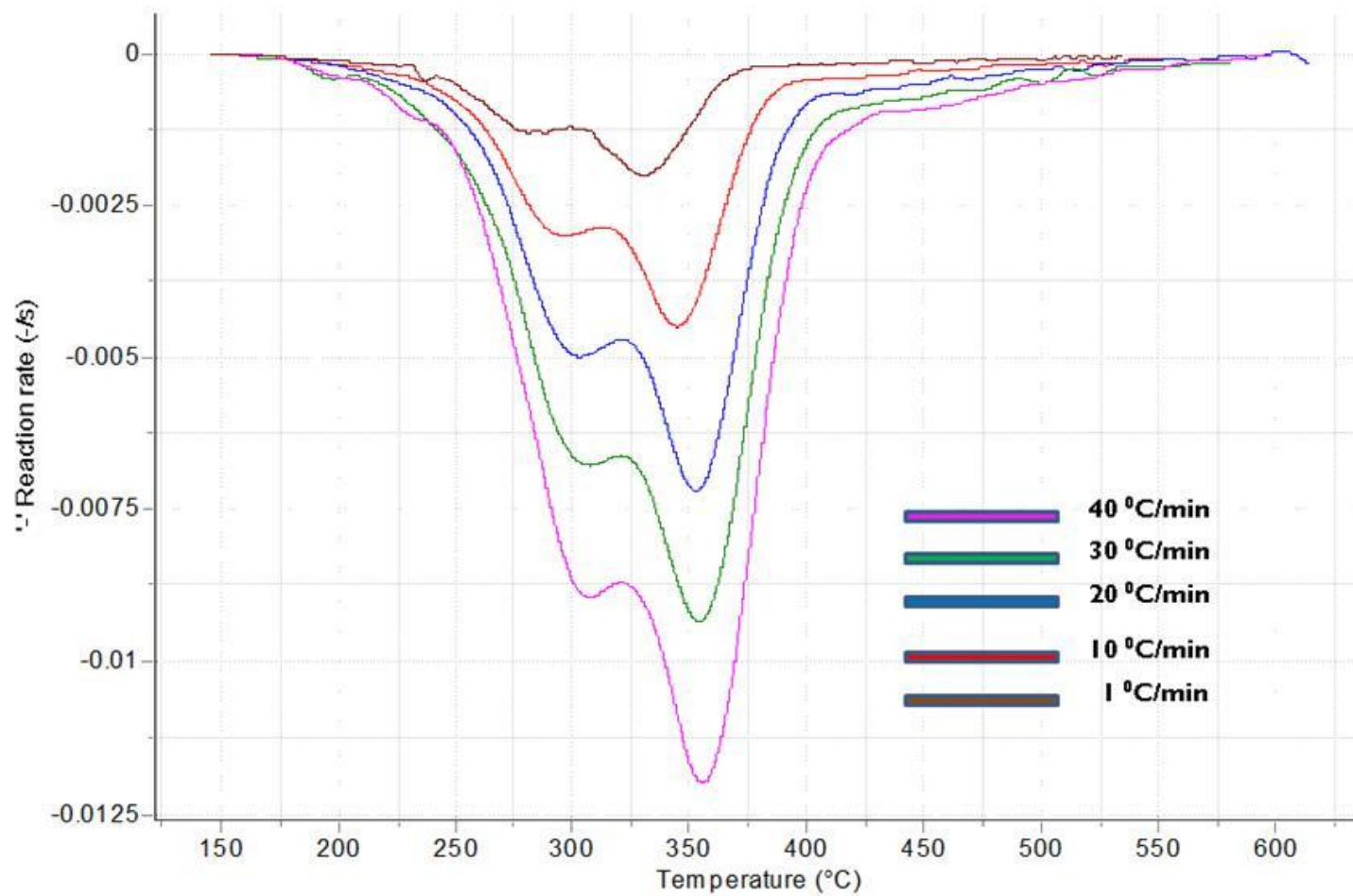


Figure 13: DTG curve for CS

The cause of merged DTG peaks is the ash presents in the biomass, which catalyses the biomass pyrolytic decomposition (Varhegyi et al., 1988). The higher ash content in CS explains the reason why CC exhibited distinct peaks up to 40°C/min heating rate while the peaks merged for CS at the highest heating rate. The composition of the ash is believed to have an effect on the thermal decomposition of biomass components. Yang *et al.* (2006) studied thermal decomposition of palm oil wastes and found that the addition of potassium metal as K_2CO_3 caused the overlapping of cellulose and hemicellulose peaks. The addition of potassium inhibits the hemicellulose decomposition and enhanced that of cellulose greatly by shifting its peak to a lower temperature. Bradbury *et al.* (1979) and Diebold (1994) found that the thermal decomposition of cellulose occurs in two stages: (1) conversion of highly crystallised cellulose to more reactive and less crystalline at lower temperatures; (2) thermal decomposition to gas, solid and liquid products at higher temperature. The presence of the inorganics, cellulose thermal decomposition occurred at lower temperature, which might have been due to the elimination of the first stage. In the first step, there is change in physical and chemical structure of the cellulose due to the presence of inorganics. From Chapter 4, CS (1.33 wt. %) had higher potassium content than CC (0.86 wt. %) making it overlap at a high heating rate of 40 °C/min. Shafizedah and DeGroot (1984), in a similar study on cotton wood found that potassium reduces the temperature of the maximum decomposition, while calcium treatment increases it.

During the first pyrolysis stage, the CS started decomposition at a slightly lower temperature than CC and this may be due to differences in their physical properties; CS being lighter, thinner and fibrous shaped (Table 22). Hagge *and* Bryden (2002) also reported that the density of biomass had an effect on the pyrolysis time, shrinkage, cracking and heat transfer. The CC has a lower heat transfer due to brittle and rounded particles of a higher particle size range than the CS (Hagge *and* Bryden, 2002). Due to the differences in physical properties and particles aspect ratios of CR, the heat flux in CS will be slightly higher than in CC and the shrinkage will develop faster (Sheng *et al.*, 2009). The higher density of CC than CS could also be a reason for heat transfer limitations in pyrolysis and slight delays in the thermal decomposition (Sheng *et al.*, 2009). The higher density CC biomass has less particles voidage than CS and limits the heat transfer between particles during devolatilisation. The differences in

thermal properties such as thermal conductivity and heat capacity of the corn residues biomass could also be reason for the lower decomposition temperature of CS than CC (Blasi, 1997). Thermal conductivity not only vary with biomass type but also, for corn cobs and corn stover, along, across and tangential to the grain (Siau, 1984). The amount and composition of ash could also be the reason for the delay of decomposition of CS. Similar observation was found in previous studies on the influence of K and Fe in thermal decomposition of biomass (Varhegyi *et al.*, 1997; Yang *et al.*, 2006).

5.1.2 Effect of heating rate on devolatilisation

The effect of heating rate on the TGA curves is shown in Figure 10, 11, 12 and 13. The TG and DTG curves tended to shift towards higher temperatures with increasing heating rates. The DTG peaks also shifted to higher temperatures with increasing heating rates, from 251^oC to 357^oC for CS and from 252^oC to 348^oC for the maximum weight loss of CC hemicelluloses and cellulose (Figure 11 and 13). The CC, behaved the same as CS with a difference of $\pm 3^{\circ}\text{C}$ for the hemicelluloses peak temperature and $\pm 13^{\circ}\text{C}$ for the cellulose peak temperature at each heating rate.

An increase in the heating rate delayed the thermal decomposition processes towards higher temperatures (Kumar *et al.*, 2008). Heating rate could affect the pyrolysis of the sample from the following aspects: with an increase in heating rate, a larger instantaneous thermal energy is provided in the system and a longer time is required for the sample biomass to reach equilibrium with the temperature because of heat transfer limitations (Milosavljevic and Suuberg, 1995). Biomass also being a poor conductor of heat, results in a temperature gradient throughout the cross-section. At lower heating rate, the temperature profile along the cross-section can be assumed linear as both the surface and the inner core of the biomass material attain the same temperature at a particular time as sufficient time is given for heating. On the other hand, at a higher heating rate, a substantial difference in temperature profile exists along the cross-section of the biomass and the maximum rate of decomposition is delayed. This has been also reported by Maiti *et al.* (2007). The calculation to illustrate the existence of the thermal gradients in corn residues biomass thermal decomposition is shown in appendix H.

For CS biomass, the maximum hemicelluloses DTG peak at 40 °C/min in the cellulose DTG peak also merged due to the increase in heating rate. The tendency for the DTG peaks to overlap at higher heating rates was also observed with wood by Di Blasi (2008) and rape seeds by Haykiri-Acma *et al.* (2006). The overlapping of DTG peaks was probably due to sufficiently high heating rates allowing less time for each individual component in the biomass to decompose at its own peak temperature, while at lower heating rates decomposition is gradual and such peaks at each heating rate are separated to form distinct peak temperatures.

Typical pyrolysis behaviour predicts that an increase in heating rate will cause a slight increase in volatiles production, and a slight decrease in biochar production (Kumar *et al.*, 2008). From Figure 14, it is evident that this statement holds. However, an increase in heating rate increased the volatiles yield (Basak and Putun, 2006). The volatiles yield increased from 70 wt. % to 79 wt. % in the range of 1 °C/min to 50 °C/min heating rate (Figure 12). The biochar yield decreased from 26 wt. % to 19 wt. % in the range of 1 °C/min to 50 °C/min heating rate (Figure 14). High heating rates of CR made solid particle pass charring stage at lower temperature more quickly to reduce char production, and improved the volatiles production. The lower heating rates simulate slow pyrolysis (SP), which produces mainly char, while fast heating rates simulate Fast Pyrolysis (FP), with the highest volatiles and liquid yields. The moisture and ash contents were almost constant for all the biomass from 1 °C/min to 50 °C/min heating rates. CS had a bigger variance in the ash content and this was mainly due to the variability of the samples ash content. CS comprises of stalk, leaf, tassel and silk, and each of these physical components had different physical and chemical properties. The ash content varies in each sample because the different components are incorporated with different amounts of ash. The compositional variability of CS can affect the process strategy and inconsistency of products quality (Agblevor, 1995).

5.1.3 Proximate analysis

The TGA data from corn residues (CR) were used to calculate on average the proximate analysis obtained at different heating rates and the results are shown in Table 23. There are ASTM procedures to determine the proximate analysis of biomass and this method can be used as an internal comparative method to analytical methods. The TGA method in this study is not the definitive procedure for measurement of proximate analysis as can be seen by the

variations due to changes in heating rate. For CS, the water and ash values differ slightly from the values obtained during the initial characterisation of the biomass. The water is slightly less (0.7%) which is most possibly caused by the drying effect of the nitrogen purge gas. The ash content is slightly lower (2%) mainly due to the fine particles blown out of the alumina cup and have a smaller effect on the ash content. Shuangning *et al.* (2005) reported an average of approximately 20.4% of char and 79.6% of volatiles which are in agreement with proximate analysis obtained on CS in this study using the TGA method. For CC, the water and ash values differ slightly from the analytically determined ones. The particle size of biomass for TGA was finer (125-323 μm) compared to 1000 μm for the analytical method. The 1000 μm biomass was further milled to a finer particle size using a cryogenic mill. The water is slightly less than 3.2%, which is most possibly caused by the drying effect of the cryogenic mill. Cao *et al.* (2004) reported approximately 80.66% of volatiles and char of 19.34% on ash-free and dry basis which compares well with the results obtained on CC in this study (Table 23). The slight differences in the biomass proximate analysis could also be attributed to different particle sizes of the CR used for analytical and TGA methods. Studies by Chouchene *et al.* (2010) on olive wastes and Mani *et al.* (2010) on wheat straw found that the particle size has an effect on the biomass proximate analysis.

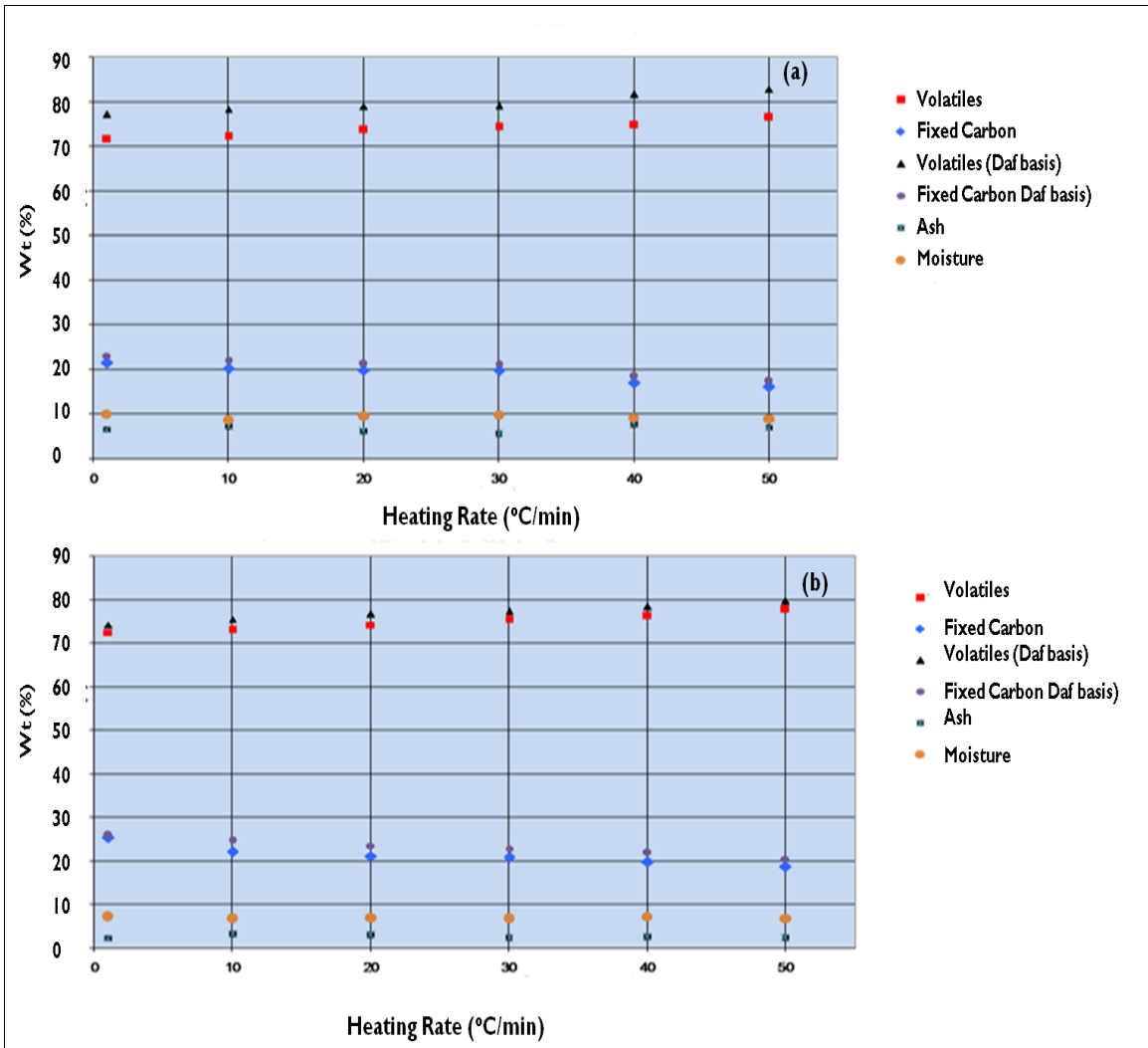


Figure I4: The trend of proximate analysis from CS (a) and CC (b) according to the heating rate.

Table 23: Proximate analysis obtained from TGA and analytical method

	Water (wt. %)	Volatiles (wt. %)	Fixed Carbon (wt. %)	Ash (wt. %)	Particle size(µm)
Corn Stover					
Analytical method	8.5	77	8	7	1000
SD	0.5	1	1	2	
TGA	7.8	74	19	5	125-325
SD	0.8	1	2	2	
TGA (daf basis)	-	79.56	20.45		
Shuangning et <i>al.</i> ,2005		79.6	20.4		117-173
Corn Cobs					
Analytical method	4.6	79.9	13.7	1.8	1000
SD	0.4	0.2	0.6	0.7	
TGA	1.4	74.8	21.2	2.6	125-325
SD	0.6	0.4	0.8	0.8	
TGA (daf basis)	-	76.87	23.13	-	
Cao et <i>al.</i> ,2004	-	80.66	19.34		250

The particle sizes used to determine proximate analyses from TGA in this study and literature were almost in the same range (<325 µm) (Table 23). Hence there was an insignificant difference in the proximate analyses obtained.

5.1.4 Kinetic study using an isoconversional method

The apparent overall activation energies were calculated for CR using Friedman's method (Vyazovkin, 2006). The slope of the isoconversional lines from the Friedman's plot for the conversion range of 0.1-0.9 was obtained (Figure 15 and 16). The Friedman's plots were used to determine the relationship of the extent of conversion (α), and activation energies (E), (Figure 15). The relationship was obtained from equation 4, plotting $\ln \frac{d\alpha}{dt}$ against $\frac{1}{T}$ and obtaining $\frac{E}{R}$ as the gradient of the slope. From Friedman plot, the activation energies were obtained at conversion from 0 to 1 and variation of activation energy against conversion is

shown in Figure 17 and 18. The kinetic parameters, activation energies (E) and pre-exponential factor (A), were obtained for both materials, CC and CS, at different conversions. The trend of activation energy dependence on α was quite similar for both CC and CS (Figure 17 and 18). Activation energy varied with the extent of conversion for biomass and Vyazovkin (2006) has previously interpreted it as evidence of the existence of a multi-step reaction mechanism. The range of activation energies, as determined, is not the actual activation energy of any particular single reaction step, but is rather an aggregate value reflecting the contributions of the individual reaction steps to the overall reaction rate.

At the start of devolatilisation ($\alpha < 0.2$), the apparent activation energy for both corn residues increased from 160 kJ/mol to 255 kJ/mol for CS and from 175 kJ/mol to 270 kJ/mol for CC in the region $0 < \alpha < 0.2$. Activation energies reduced in the range $0.2 < \alpha < 0.8$. CC's activation energies reduced from 270 kJ/mol to 237 kJ/mol and that for CS from 255 kJ/mol to 220 kJ/mol. At extents of conversions higher than 0.8 the apparent activation energy behaved irregularly and increased rapidly to 250 kJ/mol for CC and 255 kJ/mol for CS. Higher activation energies in this region can be due to the decomposition of the less reactive components in the biomass, with the more reactive fractions having been decomposed at lower conversions (Biagini *et al.*, 2008). The activation energy of CS (220-255 kJ/mol) is slightly lower than the one for CC (220-270 kJ/mol). This could be due to higher ash content in CS, having a catalytic effect changing the chemical structure of the biomass and thermal decomposition rate (Vargheyyi *et al.*, 1997). CS had higher concentrations of the reactive cations (Ca and K) having a catalytic effect than CC. The range of overall activation energy values obtained for CR agreed well with those obtained by Ramajo-Escalera *et al.* (2006) on sugarcane bagasse using the same isoconversional method (Table 24). The kinetic parameters at different conversions of the CR are presented in appendix E. There were limited literature available to compare the CR kinetics results obtained using the same iso-conversional method. Most kinetic parameters found from literature used the model-fitting approach (Cao *et al.*, 2004; Zabaniotou *et al.*, 2007; Kumar *et al.*, 2008). The two biomass feedstocks have a similar range of activation energies hence the same thermal stability indicating that the pyrolysis occurred through the cleavage of linkages with similar energy bonds (Garcia-Perez *et al.*, 2001). The slightly lower activation energy range of CS (220-255 kJ/mol) shows that it is slightly more reactive than CC (237-270 kJ/mol).

Table 24: Kinetic parameters of the biomass thermal decomposition

Biomass	Method	Heating Rate (°C/min)	E (kJ/mol)	Reference
CC	Isoconversional method $0.2 < \alpha < 0.8$	10,20,30,40,50	237-270	This Study
CC	Single first order	20	75	Zabaniotou <i>et al.</i> , 2007
CC	Single first order	5,10,30	119.6-135.3	Cao <i>et al.</i> , 2004
CS	Isoconversional method $0.2 < \alpha < 0.8$	10,20,30,40,50	220-255	This Study
CS	Single first order	5,20,50	57.3.4-139.1	Kumar <i>et al.</i> , 2008
Sugarcane bagasse	Isoconversional method $0.2 < \alpha < 0.8$	5,10,30	250-300	Ramajo-Escalera <i>et al.</i> , 2006
Wood	Isoconversional method $0.2 < \alpha < 0.8$	2,5,10,15	144.7-204.9	Gasparovic <i>et al.</i> , 2009

5.1.5 Quality of fit

The quality of fit of the CR thermal decomposition experimental data was compared with kinetic iso-conversional method predictions using non-linear regression analysis using a procedure by Caballero *and* Conesa. (2005) (described in appendix I). The graphs of conversion vs temperature for experimental and expected thermogravimetric (TG) data are shown in appendix K. Table 25 represents the quality of fit percentages of predicted TG data by the iso-conversional method and experimental TG data of CR. The quality of fit of the experimental data to the model was (93-99.5% for CC and 90-96% for CS).

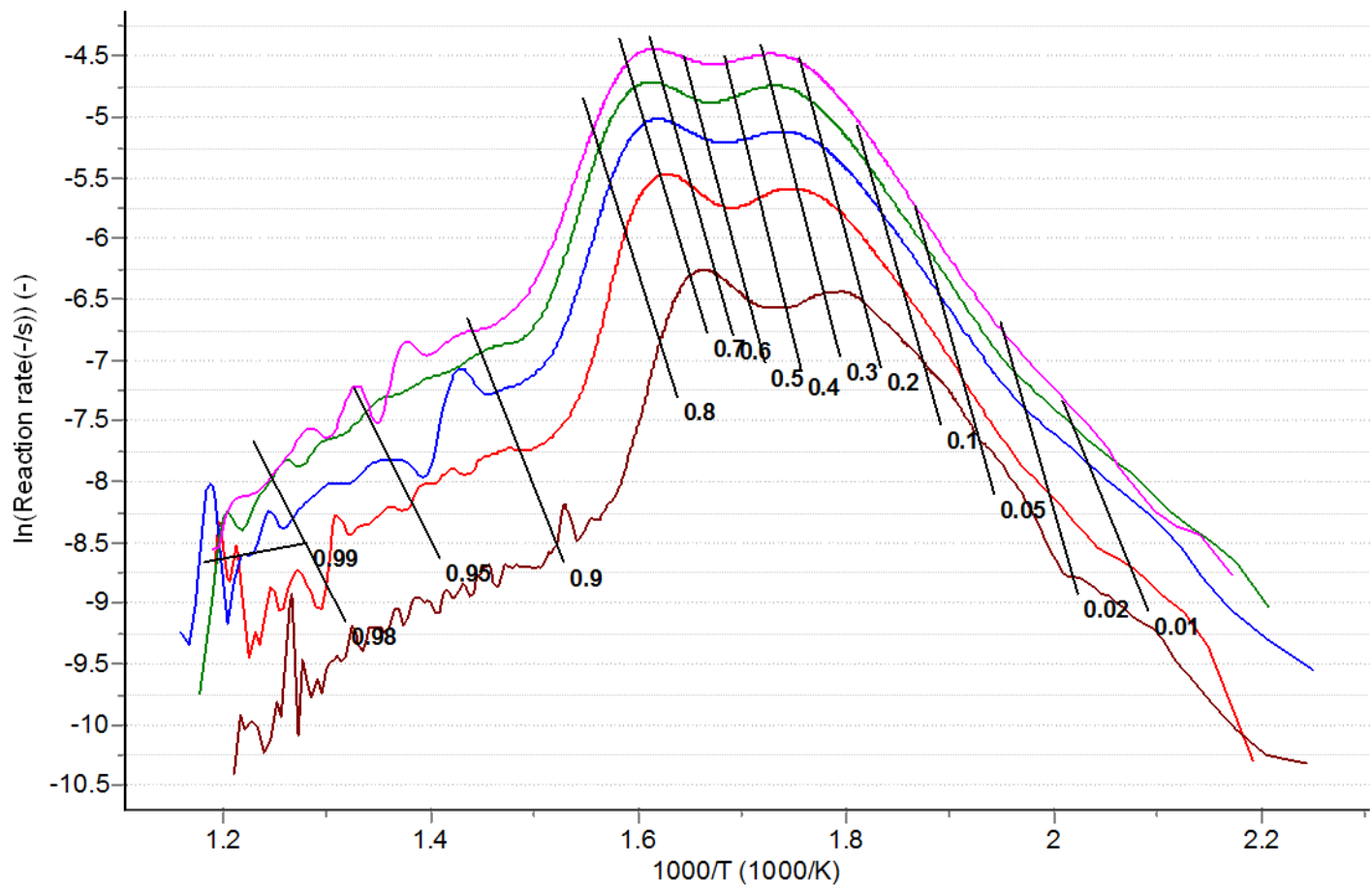


Figure 15: Friedman's plots for CC

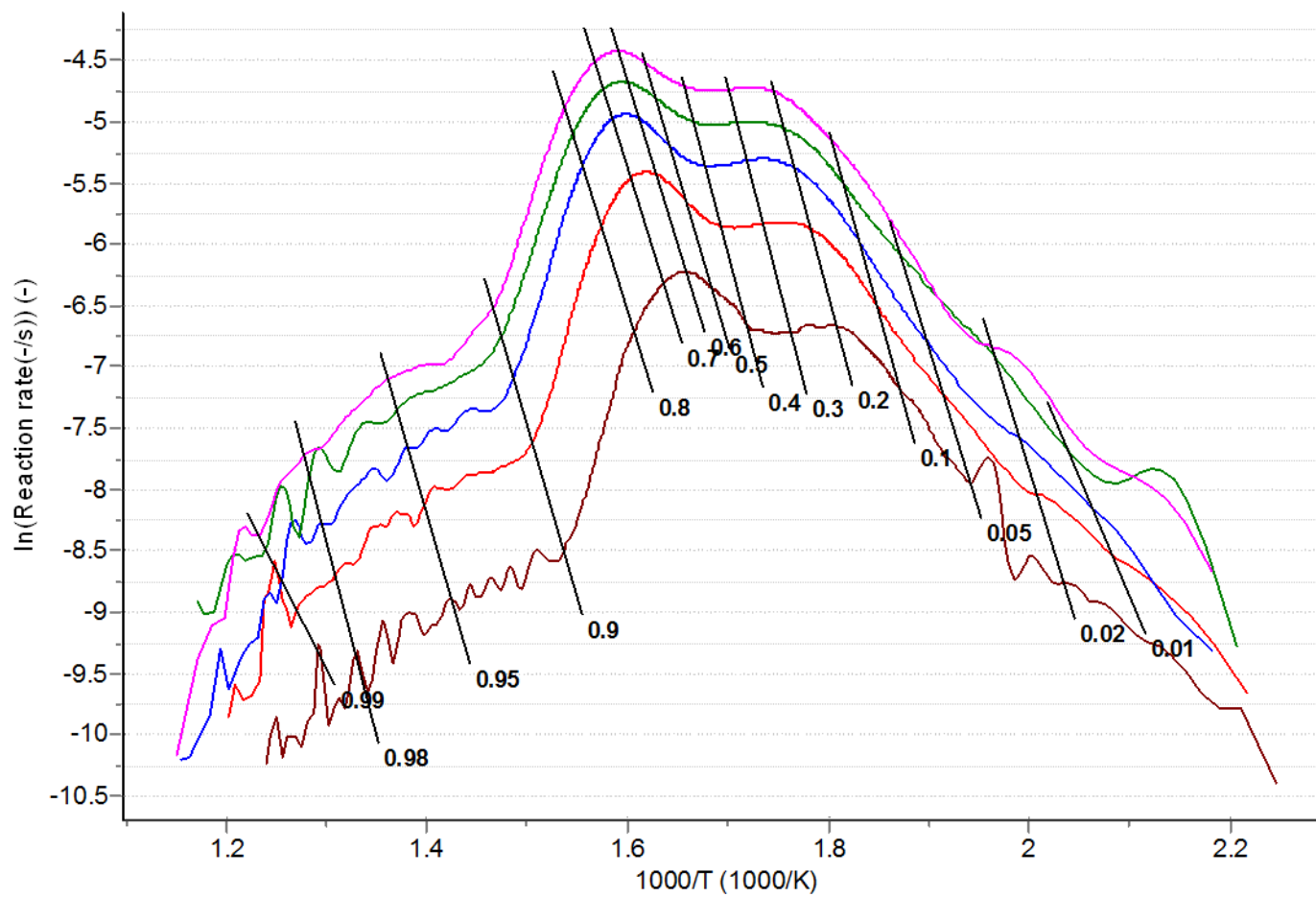


Figure 16: Friedman's plots for CS

A reasonably good fit was obtained to within 10% error for CR (Table 25). The error percentage was in agreement with obtained values by Branca *et al.* 2005. They found errors within 10%, from 91.3 to 96.8% quality of fit. The quality of fit of the model was higher at low heating rates than at high heating rates in both biomasses, which could be due to less thermal gradients in biomass at lower heating rates. The source of error is the systematic procedure which may vary from experiment to experiment. When experiments are performed at different heating rates it is possible that some systematic errors are introduced by the thermobalance (Caballero *and* Conesa, 2005).

Table 25: Quality of fit percentages (%) of kinetic model predictions for CR

Quality of fit (%)		
Heating Rate (°C/min)	CS	CC
10	96.1	99.5
20	90.8	98.9
30	92.0	93.9
40	92.0	93.7
50	94.1	93.1

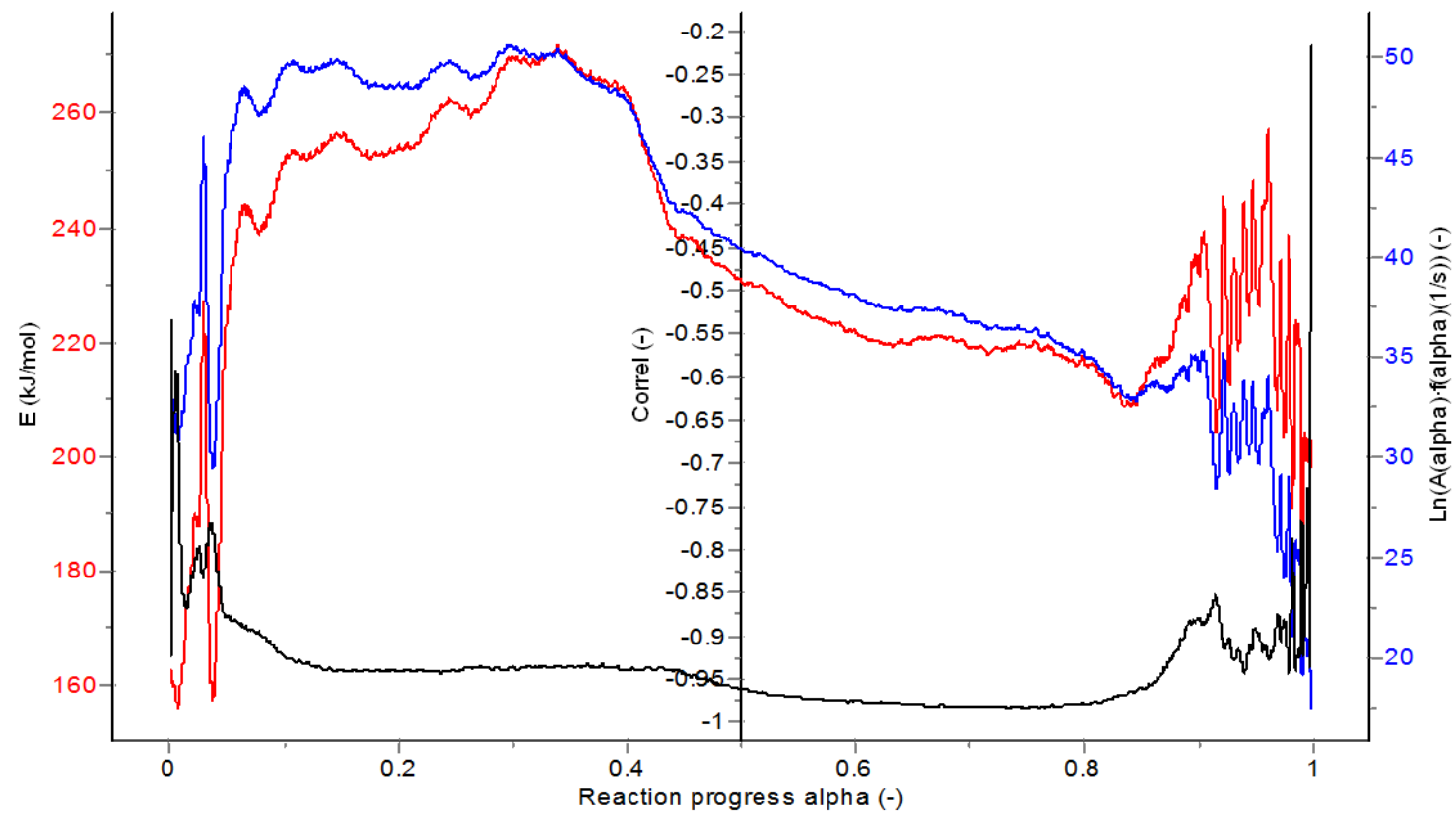


Figure 17: Apparent activation energy dependence on conversion for CC.

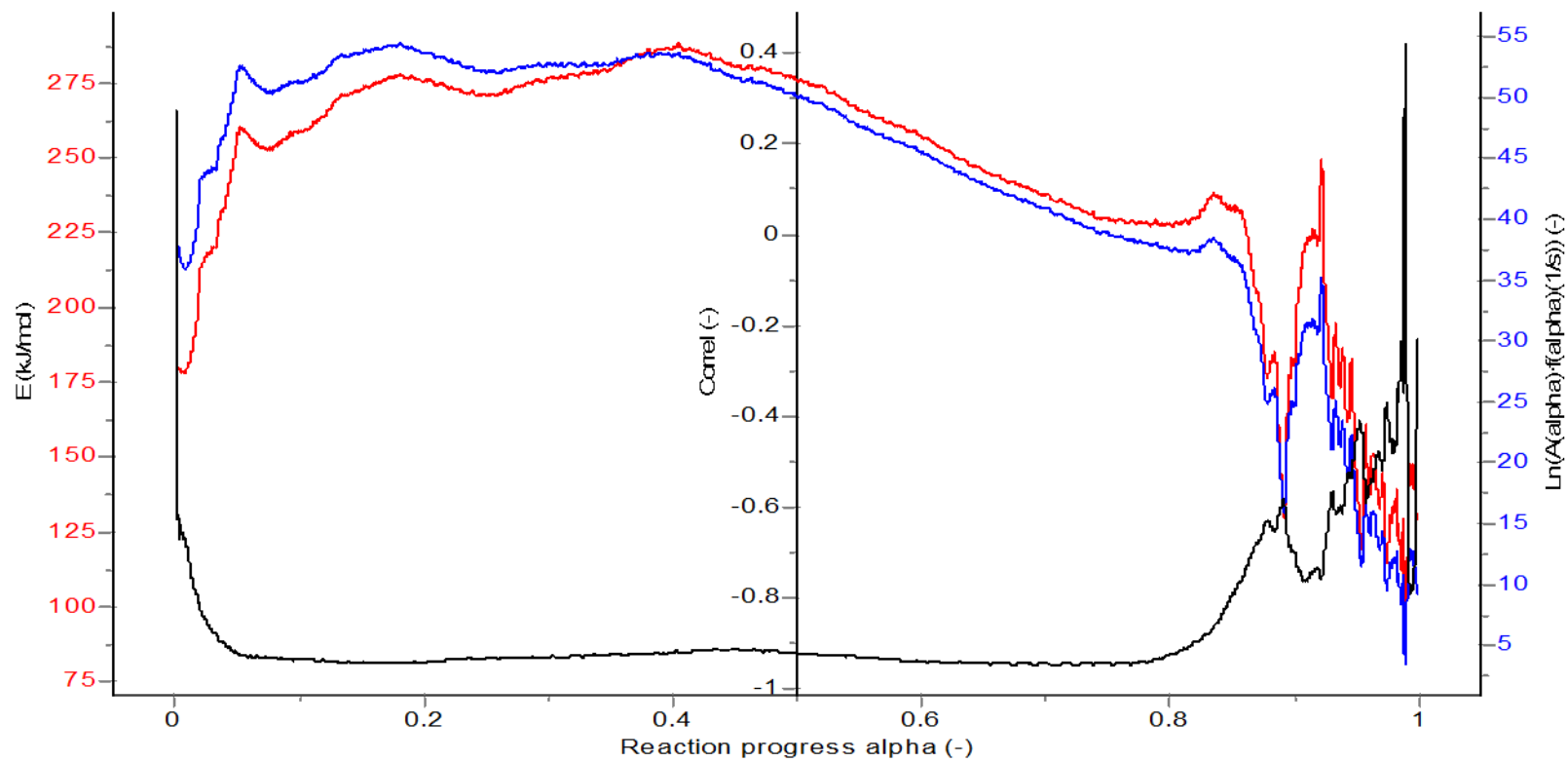


Figure I8: Apparent activation energy dependence on conversion for CS.

Chapter 6: Fast pyrolysis products characterisation

6.1 Results and Discussion

The products obtained from the fast pyrolysis (FP) of corn residues (CR) were distributed into bio-oil, biochar, water and non-condensable gaseous materials. The yields and compositions of end products of pyrolysis are highly dependent on various such as biomass properties, particle size and type of reactor. In this study, the effect of different types of biomass, particle size distribution and fast pyrolysis reactors on pyrolysis product yields and quality were investigated. The key differences between the two FP process reactors are: particle size distribution (Figure 19 and 20), the method of heat transfer and the biomass properties fed in each type of reactor (Table 26).

6.1.1 Biomass physical and chemical properties

As previously highlighted in Chapter 3, the CR feedstock was from different parts of South Africa. The corn residues properties from Free State and North West province are shown in Table 26. CS from Free State province had twice the ash content than that from North West province, 13.1 wt. % against 6.6 wt. % (Table 26). Due to the difference in ash content the heating value of CS from Free State (14 MJ/kg) was lower than the one from North West province (18.06 MJ/kg). The CC from all the provinces had almost similar properties. The elemental analyses for CR from both sources were similar.

Table 26: Physical and chemical properties of corn residues (CR)

Reactor type	Bubbling fluidised bed reactor		Lurgi twin screw reactor	
Origin	Free State Province		North west province	
Age (Months)	12		2	
Elemental analysis (wt.%, daf basis)				
Biomass type	CC	CS	CC	CS
C	51.1	47.9	50.2	48.9
H	5.7	6.3	5.9	6
S	0.11	0.13	0.03	0.05
N	0.34	0.55	0.42	0.61
O*	42.8	45.7	43.5	44.4
H/C	1.34	1.58	1.41	1.47
O/C	0.63	0.72	0.65	0.68
HHV (MJ/kg)	21.3	14.1	19.14	18.06
Proximate analysis (wt. %)				
Moisture	4.3	7.6	4.6	8.5
Volatiles	79.4	69.5	79.9	76.7
Ash	1.9	13.1	1.8	6.6
Fixed Carbon*	14.4	9.8	13.7	8.2

* Determined by difference.

6.1.2 Particle size distribution

Figure 19 and 20 shows the results of the corn residues particle size distribution prior to fast pyrolysis process. The physical properties (shape, hardness and bulk densities described in Chapter 4) of CC and CS are different hence the particle size distribution are not in the same ranges. The CC is more brittle and spherically shaped than the thin fibrous CS. From Figure 19, the CC has a higher particle size than the CS, for the LTSR above 51.1% corn cobs particles were more than 2 mm against 37.7% CS particles more than 2 mm for biomass milled by the same milling equipment. For the CC used in the BFBR, above 67.1% of the particles were larger than 0.85 mm against 19.1% of CS particles larger than 0.85 mm (Figure 20). The particle size distributions and particles shapes are suitable for the production of FP products and expected to significantly influence the product yields and product quality at the operating conditions studied.

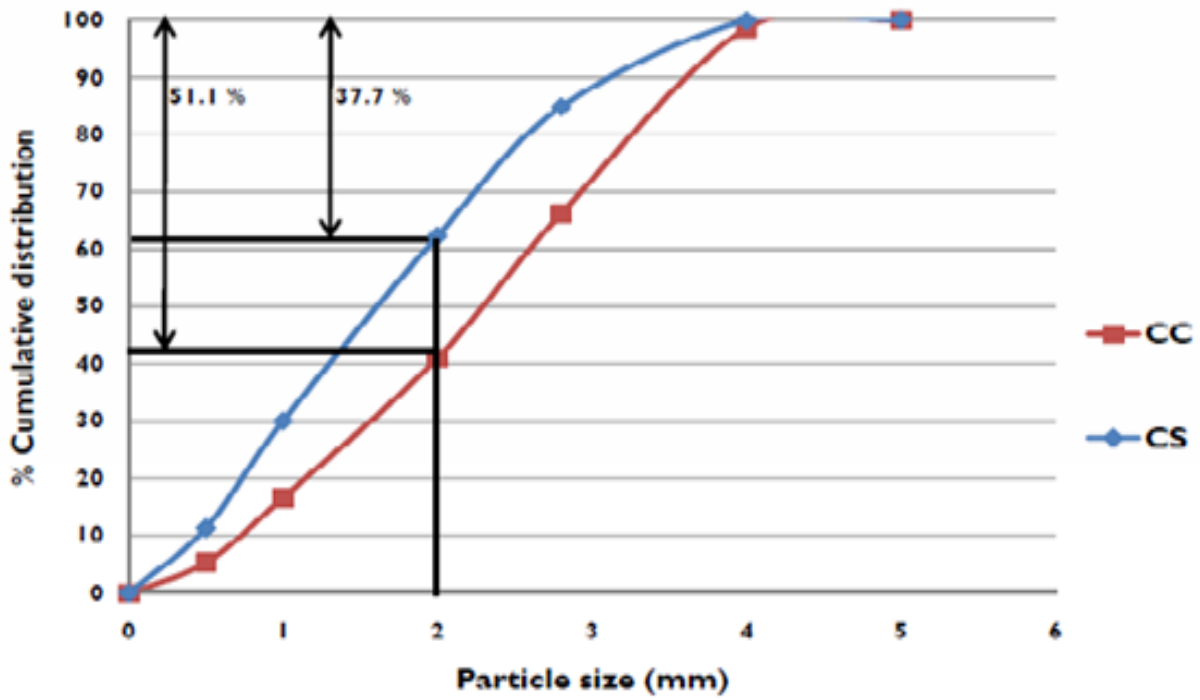


Figure 19: Particle size distribution of biomass feedstock in a LTSR

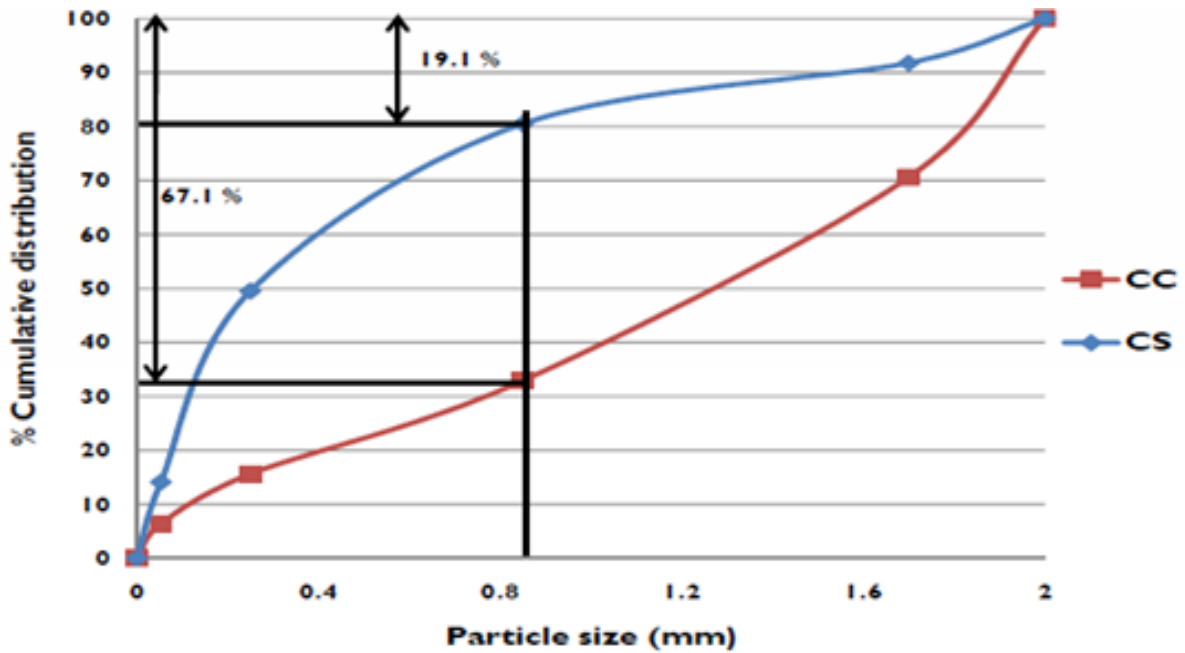


Figure 20: Particle size distribution of biomass feedstock in a BFBR

6.1.3 Mode of heat transfer

In both reactors, the main mode of heat transfer is by conduction (90% for BFBR and 95% for LTSR) (Brigdwater, 1999e), however LTSR, operated by transporting biomass (particle size of ≤ 5 mm) with amounts of hot steel balls to achieve pyrolysis reactions. The primary products are deposited on the surface of moving screws which then subsequently decompose and give rise to volatiles products. In the BFBR, the biomass is directly fed in a bed of hot sand fluidising medium and released into the vapour phase. There are different modes of volatiles formation and heat transfer in the reactors, which can lead to differences in the products quality and yields.

6.1.4 Products yields

The product yields are reported, taking into account only the portion of biomass that was pyrolysed during the process and the results are from an average of 2 runs in a LTSR and 2 runs in a BFBR (Table 27). In this study, the bio-oils yield described excludes water produced. From Table 26, it was shown that the FP of CR was carried out on biomass with varying moisture and ash contents. Due to this variation, the yields of FP have been compared on an ash and dry free basis biomass. The yields on weight basis were also calculated and presented.

Most previous studies calculated their yields on weight basis hence the comparison with literature was done on weight basis yields and the product yields of CR results discussion was on an ash and dry free basis. Table 27 presents the average yields of fast pyrolysis products at 500-530 °C of CC and CS biomass samples of < 2 mm and < 5 mm particle size ranges on an ash and dry free basis and weight basis. The actual recovery yield of bio-oil in a LTSR averaged 37.0 wt. % of the feedstock for CC, 35.5 wt. % for the CS and 36 wt. % CRM. The bio-oil yields from the BFBR were higher 51.2% for CC, 47.8% for the CS and 45.9% for CRM. The parameters such as the reactor type (LTSR and BFBR), ash content in biomass and particle size could affect the thermal degradation of biomass and then bio-oil yields. The higher bio-oil yields in a BFBR can be due to better heat transfer of smaller particle size of < 2 mm compared to < 5 mm in a LTSR. The larger particle size for biomass fed into LTSR causes larger temperature gradients inside the particle so that at a given time the inner core temperature is lower than the surface, and actual heating rates will be much slower (Fraga *et al.*, 1991; Okuno *et al.*, 2005).

The lower actual heating rates could give rise to an increase in the biochar yields, and a decrease in liquids and gases as low heating rate may favour charring reactions over the formation of volatiles. When the smaller particles (< 2 mm) were fed into the fast pyrolysis BFBR, they were pyrolysed up quickly and almost instantly increasing the actual heating rate. Indeed it is known that heating rate is more sensitive to biomass particle size in the smaller particle size ranges than larger particle size ranges (Di Blasi, 2002). For larger particles, the heating rate in pyrolysis reactions would differ little with change in particle size, explaining why there is a smaller difference in bio-oil yield for large particles (< 5 mm) in a LTSR than smaller particles (< 2 mm) in a BFBR. Particle size is known to influence FP products and similar results were found by Encinaret *al.* (2000) on cardoon (*Cynara cardunculus*), Ate *et al.* (2004) on sesame stalk and Shen *et al.* (2009) on mallee woody biomass. However, in this work it was also observed that in both reactors the CC pyrolysis led to higher bio-oil yield than CS and CRM. This observation could be due to higher ash content in CS and CRM which acts as a catalyst favouring vapour cracking and then decreasing the liquid yield (Oasmaa *et al.*, 2003; Shafizadeh, 1968; Nowakowski *et al.*, 2007). Previous researchers (Williams and Horne, 1994; Agblevor and Besler, 1996; Blasi *et al.*, 2000; Raveendran *et al.*, 1995) found that certain minerals (such as Ca, K, Na, Mg, and Fe) exert a significant catalytic effect, and even a small amount of them is sufficient to influence pyrolysis behaviour. From Chapter 4 on biomass characterisation, it was found that CS (Ca 0.87 wt. %, K 1.33 wt. %, Mg 0.56 wt. % and Fe 0.11 wt. %) had higher amounts of these inorganics than CC (Ca 0.02 wt. %, K 0.86 wt. %, Mg 0.04 wt. % and Fe 0.02 wt. %). The main difference on the corn stover having a more catalytic effect in pyrolysis than CC is due to the higher composition of active cations (K and Ca). Sodium was not detected in both feedstocks. Corn stover had higher ash content than corb cobs and also higher concentrations of the inorganic elements that have catalytic influence on pyrolysis yields.

Table 27: Product distribution yields obtained at 500-530 °C using a bubbling fluidised bed reactor (BFBR) and Lurgi twin screw reactor (LTSR) on CS, CC and CRM.

wt. % ,daf																
Biomass	Type of reactor	Particle size (mm)	Ash content wt. %	Char	SD	Bio-oil	SD	Water	Liquid	SD	Gas as det	SD	Gas by diff	SD	Pyrolytic water	SD
CS	LTSR	<5	6.6	25.0	3	35.5	0.4	21.3	56.8	0.4	27	9.0	19.0	3.0	9.2	0.4
CRM	LTSR	<5	5.2	25.0	2	36.0	5.0	25	61.0	3.0	30	2.0	14.0	1.0	13.0	2.1
CC	LTSR	<5	1.8	15.2	0.5	37.0	7.0	26	63.0	3.0	25	12	22.0	10.0	13.7	5.4
CS	BFBR	<2	13.1	25.4	0.5	47.8	0.3	16.6	64.4	4.7	NA	-	10.3	5.2	7.9	4.5
CRM	BFBR	<2	8.2	24.1	0.3	45.9	0.9	30.5	66.1	0.9	NA	-	9.9	1.3	9.5	0.6
CC	BFBR	<2	1.9	20.0	0.4	51.2	0.1	17.74	68.9	3.2	NA	-	11.1	3.6	9.6	1.2
CC (LR)	BFBR	<2	2.1	19.7	-	45.4	-	26.7	72.1	-	-	-	8.2	-	21.2	-
CS (LR)	BFBR	<2	7.3	25.7	-	44.1	-	23.6	67.8	-	-	-	6.5	-	11.7	-
<i>Det- as detected, By diff- by difference, LR- Long Run</i>																
CS	LTSR	<5	6.6	21.1	1.7	30.5	0.6	18.3	48.8	-	-	-	30.1	1.2	8.0	0.7
CRM	LTSR	<5	5.2	21.9	1.4	31.3	4.2	21.1	52.4	-	-	-	25.7	21	11.2	2.4
CC	LTSR	<5	1.8	19.9	12.1	36.7	2.6	14.4	51.1	-	-	-	29.0	0.9	20.0	10.8
CS	BFBR	<2	13.1	20.1	0.4	38.0	0.3	13.1	51.1	3.7	-	-	28.7	4.0	6.3	3.6
CRM	BFBR	<2	8.2	20.0	0.1	38.1	0.1	16.7	54.8	0.2	-	-	25.24	0.4	7.9	0.7
CC	BFBR	<2	1.9	18.1	0.4	46.3	2.0	15.9	62.2	0.3	-	-	19.7	0.1	8.7	1.41
CC (LR)	BFBR	<2	2.1	21.3	-	36.5	-	19.6	56.1	-	-	-	22.6	-	9.7	-
CS (LR)	BFBR	<2	7.3	18.3	-	42.2	-	24.8	66.9	-	-	-	14.8	-	19.7	-

The differences in bio-oil yields could also be due to the different condensation systems in the two processes and condensation temperatures. Tsai *et al.* (2007) studies on rice husk found out that the condensation temperature has an effect on the product yield. The FP experiments were performed with different condensation systems and temperatures. The BFBR process used direct contact of isopar condensing medium at 15 °C. The LTSR process used a dual condensation system indirect contact with Polydimethylsiloxane at 50-70 °C and bio-oil direct contact heat exchanger at 15 °C in series. The higher bio-oil yields in BFBR can be due to a better heat exchange/condensation system than in a LTSR, condensing more volatiles to liquids products than in a LTSR. The biochar yields from the LTSR were 25%, 25% and 15.2% for CS, CRM and CC, respectively (Table 27). The higher biochar yields in CS were due to the higher ash content in the feed than in CC. The biochar yields from a BFBR were 25.4%, 24.1% and 20% for CS, CRM and CC respectively (Table 27) and slightly higher than the biochar yields in the LTSR. This observation can be explained by the larger size involved in the LTSR. The biochar remained in the LTSR reactor, bucket elevator and piping of the system and was not physically recovered which could also explain the higher standard deviations found in biochar yields in LTSR compared to BFBR. A comparison of biochar yields from the two types of reactors is then difficult.

The pyrolytic water yields from BFBR were 9.6 wt. % for CC, 7.9 wt. % for CS and 9.5 wt. % lower than ones from LTSR, 13.7 wt. % for CC, 13 wt. % for CRM and 9.2 wt. % for CS. The results of pyrolytic water yield showed that the yields from LTSR with a larger particle size range had a slightly higher pyrolytic water yield than from BFBR, in agreement with findings by Shen *et al.* (2009) and Garcia-Perez *et al.* (2008). They found that the pyrolytic water yield increased with the increase in biomass particle size. This is due to the differences in surface areas of particles; larger particles could catalyse more the dehydration reactions of some primary pyrolysis products to form water. The slight difference in pyrolytic water yield in this study was also in agreement with Shen *et al.* (2009) who observed a small difference in pyrolytic water yield for biomass with the same particle size range of 0.18-5.6 mm. Apart from the effect of particle size, the CC with lower ash content had a higher pyrolytic water yield which is the opposite trends as observed in a study by Di Blasi *et al.* (2007) who found that inorganic elements catalyse the reactions and tend to produce water at the expense of organic liquids.

The analysis of gas yields in a LTSR was done by two methods (calculation method and gas chromatography method) as the process was coupled to a gas chromatography online process analysis. The BFBR process was not coupled to an online gas chromatography and the yields of gas were obtained using the calculation method only. The gas yields were 19 wt. %, 14 wt. % and 22 wt. % by difference and 27 wt. %, 30 wt. % and 25 wt. % as detected for CS, CRM and CC, respectively. The analytical method led to higher standard deviations in the non-condensable gas yields detected up to 12 wt. % and mass balance closures of more than 100 %. The mass balance closures were 108.8%, 116% and 103.2% with only one within the acceptable tolerance of $100\% \pm 5\%$. This was mainly due to oxygen leakages into the system after the pyrolysis reactor section of the process. The oxygen leakage gives a less accurate gas composition on the gas chromatography and also the calculated yields of gas as detected. The mass balance closures were also used as an indication of the extent of oxygen leakages into the process.

The gas yields from a bubbling fluidised bed reactor were determined by difference only and were 10.3 wt. %, 9.9 wt. % and 11.1 wt. %, CS, CRM and CC respectively. The higher gas yields in a LTSR than in a BFBR could be due to oxygen leakages in the system. Due to the larger size of LTSR than BFBR there were more oxygen leakages into the system especially during the removal of biochar during the process. The presence of oxygen in fast pyrolysis led to combustion reactions increasing the amount of carbon dioxide and lighter hydrocarbon gases thereby increasing the yield of gas (Brunner *and* Roberts, 1980). The over-estimation of the gas yields could also be due to poor liquids and biochar recovery due to the larger size of the plant. The comparison of product yields with literature was done with weight basis results (Table 27). The CS liquid yields from BFBR in this study were lower than the results obtained in previous studies (Table 28), 51.1 wt. % against 61.6 wt. % (Mullen *et al.*, 2009) and 58.1-62.9 wt. % (Agblevor *et al.*, 1995). This could be due to the catalytic effect as previously mentioned of higher ash content CS in this study, 13.1 wt. % against 4.9 wt. % and 5.4 wt. % ash in previous studies (Table 28). The ash content could also be the reason for CS higher biochar yield in this study than the yields found by Mullen *et al.* (2009) and Agblevor *et al.* (1995). The CC yields in this study were in agreement with those obtained in a previous study by Mullen *et al.* (2009).

They were 62.2 wt. % for liquids, 19.7 wt. % for gas and 18.1 wt. % for biochar in agreement to those obtained by Mullen *et al.* 2009, 61 wt. %, 20.3 wt. % and 18.9 wt. %, liquid, gas and biochar respectively. The yields for CC were almost similar and could be due to the same ash content of feedstock at 1.9 wt. % (Table 25 and 27), same type of reactor and operating conditions. There was no information on fast pyrolysis of corn residues in a LTSR process but the results were comparable to other biomass type pyrolysed in the same pilot plant (www.itc-cpv.kit.edu) (Table 28). Any small differences in the yields observed can be explained by the differences in feedstock, fast pyrolysis conditions, reactor type and experimental error.

Table 28: Product yields from previous studies on Fast Pyrolysis of biomass.

Biomass	Ash content (wt. %)	Type of reactor	Biochar	Liquid	Gas	Particle size (mm)	Temperature (° C)	Plant capacity (g/hr)	References
CC	1.94	BFBR	18.9	61	20.3	2	500	1000	Mullen et al.,2009
CS	4.9	BFBR	17	61.6	21.9	2	500	1000	Mullen et al.,2009
CS	5.4	BFBR	15-19.1	58.1-62.9	11.7-15.1	2	500	80-100	Agblevor et al.,1995
Biomass: Wheat straw, Miscanthus, Eucalyptus, rice straw and wheat	Up to 15	LTSR	15-25	45-70	15-30	5	500-530	15 000	www.ltc-cpv.kit. edu

6.1.5 Characterisation of bio-oil

The properties of the bio-oil were determined according to different fast pyrolysis reactors and same operating conditions and the results obtained are discussed in this section (Table 29). The results were an average of 2 runs in a bubbling fluidised bed reactor (BFBR) and 2 runs in a Lurgi twin screw reactor (LTSR).

6.1.5.1 Properties of bio-oil

The liquid product obtained from Fast pyrolysis (FP) of CC and CS, (usually termed bio-crude oil) is a red-brown coloured liquid with irritable odour. The appearance and smell are common to all bio-oil liquids from biomass wastes (Tsai *et al.*, 2006; Nokkosmaki *et al.*, 2000). Bio-oils produced in a LTSR and BFBR contained equal amounts of water. Lindfors (2009) reported that the water content in bio-oil results from the original moisture in the biomass and product of the dehydration reactions occurring during FP. As can be seen in Table 29, the moisture content of bio-oil varied between 21.3 wt. % and 30.5 wt. %. The highest moisture content of bio-oil obtained is 30.5 wt. % on corn residues mixture (CRM) in a BFBR. Furthermore, the lowest moisture content of bio-oil obtained is 21.3 wt. % on CS in a LTSR. CR bio-oils are acidic with pH of between 3.8 and 4.3. This acidity is due to the presence of low-molecular weight carboxylic acids mainly formic and acetic acid (Karimi *et al.*, 2010).

The ash contents of bio-oils from BFBR and LTSR were 0.1-0.4 wt. % and 3.2-7.3 wt. %, respectively. The main source of ash in bio-oils is the solid particles carried over by the pyrolytic vapours. The higher ash content in a LTSR could be due to the absence of cyclones for solids separation before condensation whilst the BFBR had two cyclones in series. Both solids and ash are highly undesirable because they can bring many negative effects to the storage and combustion of the bio-oil (Oasmaa *and* Czernik, 1999). During storage of the bio-oils an ageing process occurs mainly due to the presence of oxygenated organic compounds which are very reactive. The presence of solid particles and inorganics (ash) as well as the acidity of the bio-oils accelerate bio-oil ageing. During ageing, etherification and esterification reactions occur between hydroxyl and carbonyl components (Diebold *and* Czernik, 1997; Sharma *and* Bakhshi, 1989). The ageing process causes the instability of bio-oil product. The

presence of ash in the bio-oil can also cause erosion and corrosion problems (Sadiki *et al.*, 2003). Boucher *et al.* (2000) reported that ash content is problematic for gas turbines applications and the limit is 0.1 wt. %.

Table 29: Physical and chemical properties of bio-oils from Fast pyrolysis of Corn residues

Reactor type	Bubbling Fluidised Bed Reactor: Temperature 500-530 °C						Lurgi Twin screw reactor: Temperature 500-530 °C					
	CC	SD	CS	SD	CR	SD	CC	SD	CS	SD	CR	SD
Biomass type												
Water content (wt. %)	25.6	1.1	25.5	1.8	30.5	0.4	26.0	3.0	21.3	0.4	25.0	3.0
Density(g/c m ³)	1.21	0.10	1.20	0.20	1.17	0.11	1.06	0.01	1.11	0.01	1.11	0.1
pH	3.9	0.9	4.0	0.4	4.3	0	3.8	0	3.8	0	4.0	0.2
Ash (wt. %)	0.1	0	0.2	0	0.4	0.1	3.2	0.4	7.3	0.1	7.0	0.5
Elemental Analysis (wt. %,daf Basis)												
C	58.1	-	50.7	-	-	-	64.7	6.7	56.4	1.2	57.7	3.2
H	4.2	-	4.9	-	-	-	4.2	0.7	4.9	0.1	5.2	0.3
N	0.4	0.19	0.65	0.15	0.5	1.8	0.5	0.2	0.7	0.3	0.7	0
O (By difference)	36.3	-	44.7	-	-	-	27.5	8	30.9	1.3	29.6	3.9
S	0.03	0.02	0.04	0.03	0.03	0.04	0	0	0	0	0	0
H/C molar Ratio	0.87	-	1.16	-	-	-	0.78	-	1.04	-	1.08	-
O/C molar Ratio	0.47	-	0.66	-	-	-	0.32	-	0.41	-	0.38	-
Empirical Formula	$\text{CH}_{0.87}\text{N}_{0.006}\text{O}$		$\text{CH}_{1.16}\text{N}_{0.01}\text{O}$		-		$\text{CH}_{0.8}\text{N}_{0.007}\text{O}_0$		$\text{CH}_{1.042}\text{N}_{0.01}\text{O}$		$\text{CH}_{1.1}\text{N}_{0.01}\text{O}_{0.38}$	
(HHV,MJ/kg)	20.2	0.47	18.7	0.7	19.6	0.7	25.3	1.5	22.3	0.41	22.6	0.7
(HHV, MJ/kg)*	21.5	-	18.8	-	-	-	24.6	-	22.0	-	23.0	-

Note: The heating values (HHV) of bio-oils with water, * Determined by Channiwala equation

The ash content of CR bio-oil was above 0.1 wt. % and does not meet the specifications for gas turbine fuels. Stringent limit on solid content will be required to ensure low metal contents in the CS bio-oil in applications such as gas turbines. Solids separation processes such as hot vapour filtration should be applied in fast pyrolysis to reduce solids content in bio-oil (Diebold *et al.*, 1993). The bio-oil produced from CS had higher ash content than from CC due to their differences in initial feedstock (CS 13 wt. % against CC 1.9 wt. %). The bio-oils are slightly denser than water, 1.06-1.11 g/cm³ for bio-oils from LTSR and 1.17-1.21 g/cm³ for bio-oils from BFBR. The lower densities for bio-oils from LTSR are due to use of water in the first run as a condensing medium in second stage condensation. The project objectives in LTSR process was to produce char-bio-oil slurries for gasification. Water was used as a condensing medium and improving the viscosity of the slurries. The initial amount of water for condensing was subtracted in order to determine the actual amount of bio-oil produced.

6.1.5.2 Ultimate and proximate analyses

As shown in Table 29, the percentage of total carbon (TC) for bio-oils from LTSR ranged from 50.7 to 64.7 wt. %, comparable to 55.1 to 53.9 wt. % reported by Mullen *et al.* (2009) for CR. The highest percentage of carbon obtained was 64.7 wt. % from CC in a LTSR. Total organic carbon (TOC) is the carbon which is bound in bio-oil organic compounds and inorganic carbon (TIC) is the dissolved carbon as carbon dioxide, carbonate and bicarbonate ions. TOC content can be measured directly or can be determined by difference if the total carbon content and inorganic carbon contents are measured (equation 29). Bio-oils from BFBR's TOC were analysed and the TIC was estimated as equal to the values from corresponding samples from the LTSR process.

$$\text{Total Carbon(TC)} = \text{Total Inorganic Carbon} + \text{Total Organic Carbon(TOC)}$$

Equation 27

The total carbon was estimated according to equation 29, by adding the total inorganic carbon of the corresponding sample from a LTSR to the TOC for the samples of CC and CS.

The estimated TC for bio-oil from BFBR was 58.1 wt. % for CC and 50.7 wt. % for CS. The hydrogen content for FP in the BFBR process could not be measured and estimated values from

corresponding samples from LTSR was used. These estimated values for bio-oil from BFBR process were used for the calculation of oxygen by difference.

The percentage of oxygen ranged from 27.5-30.9 wt. % with the highest percentage obtained 30.9 wt. % for CS in a LTSR. The oxygen content levels were much lower than reported by Mullen *et al.* (2009) for CR (36.9-37.9 wt. %, daf basis). The estimated oxygen for bio-oil from BFBR was much higher 36.3% for CC and 44.7% for CS. The differences in oxygen levels could be due to the amount of water in the bio-oils and the initial oxygen content in the feedstocks. The high oxygen and water contents make bio-oil incompatible with conventional fuels although it may be utilised in a similar way. Bio-oil upgrading by oxygen and water removal and stabilisation are necessary to give a product that is fully compatible with conventional fuels. Actually, the high oxygen content in the bio-oil is not attractive for transport fuels (Sensoz and Kaynar, 2006). An alternative approach is to reduce the oxygen content to a sufficiently low level that it may be satisfactorily blended with conventional fuels. This might be achieved by evaporation and catalytic hydrogenation (Oasmaa *et al.*, 2005; Nokkosmaki *et al.*, 2000). The evaporation method was used in this study to improve the properties of the bio-oil.

The percentage of hydrogen obtained in bio-oil from a LTSR was 4.2-5.2 wt. % and nitrogen ranged from 0.5-0.7 wt. %. The highest hydrogen and nitrogen contents obtained were 5.2% and 0.7% in a LTSR and BFBR for CRM, respectively. There was no sulphur detected in the bio-oils from LTSR and up to 0.03 wt. % for bio-oils from the BFBR. The empirical formulas of the bio-oil based on one nitrogen atom are listed in Table 28. The elemental composition analysis, H/C molar ratio are also listed in Table 29. The H/C ratios of bio-oil were changing between 0.78 and 1.16. The highest H/C ratio of bio-oil obtained was 1.16 for CS bio-oil from a BFBR process. The O/C ratios of bio-oil ranged between 0.32 and 0.66. The highest O/C ratio of bio-oil obtained was 0.66 for CS in a BFBR. The molar ratios of H/C and O/C are used to characterise fuels. The Van Krevelen diagram for conventional fossil fuels can be found elsewhere (Apaydin-Varol *et al.*, 2007; Sharma *et al.*, 2004). The corn residues bio-oils are not in the same region as the CR feedstocks, coal and biochars. This is due to higher oxygen content

than coal and biochar, slightly lower oxygen content and higher carbon content than biomass, and lower carbon content than coal.

6.1.5.3 Heating values

In contrast to fossil fuels, bio-oil contains a large amount of oxygen (27.5-30.9 wt. % for bio-oil from LTSR). The oxygen for bio-oil from BFBR was 36.3% for CC and 44.7% for CS. The high oxygen content in bio-oil is the main reason for the differences between hydrocarbon fuels and bio-oil. Due to the high oxygen content, the heating value of bio-oil 18.7-25.3MJ/kg (Table 29), which is lower than that for fossil fuels and it is immiscible in conventional fuels (Oasmaa and Czernik, 1999; Czernik and Bridgwater, 2004). The high water content in the CR bio-oils has a negative impact on the heating value, but on the other hand it improves the bio-oil flow characteristics like viscosity (Czernik and Bridgwater, 2004).

6.1.5.4 Chemical analysis of pyrolysis gas

The pyrolysis gas analysis by GC-MS was done to study the pyrolysis gas quality of corn residues. The pyrolysis gas before condensation at 500 °C for South African CC and CS was analysed and the components identified by the GC-MS are listed in Table 30.

Table 30: Gas components identified from FP of CR at 500 °C

m/z	Biomass pyrolysis products	m/z	Biomass pyrolysis products
42	Propene	108	Methylphenol (Cresol) / Anisole
43	Carbohydrate fragment: C ₃ H ₇ ⁺ , C ₂ H ₃ O ⁺	112	Methyl-dihydro-pyranone / Hydroxy-pyranone
56	Butene	114	4-Hydroxy-5,6-dihydro-(2H)-pyran-2-one
57	Carbohydrate fragment / 2-Propen-1-amine	120	4-Vinylphenol
58	Acetone	122	Xylenol / Ethylphenol / Methylanisole
60	Ethen-1,2-diol, acetic acid	124	Guaiacol
68	Furan / Isoprene	126	5-Hydroxymethylfurfural / Maltol / Levoglucosenone
70	2-Butenal	128	Hydroxymethyldihydropyranone
72	2-oxo-Propanal / 2-Butanone	134	4-Allylphenol / Cinnamic alcohol
74	Hydroxy-Propanal / -Propanone	136	Dimethylanisole / Anisaldehyde
82	Methylfuran / 2-Cyclopenten-1-one	138	4-Methylguaiacol
84	Furanone	144	2-Hydroxymethyl-5-hydroxy-2,3-dihydro-(4H)-pyran-4-one
86	2,3-Butanedione / Tetrahydrofuran-3-one	148	Cumarylaldehyde
96	Furfural	150	4-Vinylguaiacol
98	Dihydro-methyl-furanone / 2-Furanmethanol	152	Vanillin / 4-Ethylguaiacol
100	2,3-Pentanedione / Tetrahydro-4-methyl-3-furanone	162	Methoxy cinnamic aldehyde
120	Ethylphenol	166	4-Propylguaiacol / 4-Acetylguaiacol
		182	Syringaldehyde / Trimethoxytoluene

The GC-MS identified the various chemical components from the CR biomass. These pyrolysis gas components were analysed prior to condensation hence they resemble some of the chemical analysis of bio-oil product. The chemicals that are conveyed to the GC-MS are not fully representative of the pyrolysis liquids as over 60 wt. % of the chemicals will remain such as other lignin components, sugars and larger phenolic compounds (Zhang et al., 2009). The lignin derived components produced from corn residues were identified as, 4-vinylphenol, Ethylphenol, Methylphenol (Cresol), 4-ethylguaiacol, 4-propylguaiacol, 4-acetylguaiacol, 4-methylguaiacol and 4-allylphenol, which are mostly derivatives of phenol. It has been found that most of the pyrolysis gas components from lignin include high molecular weight compounds above 100 (m/z). Similar lignin derived components such as cresol, Ethyl phenol and guaiacol were identified in bio-oil from corn residues by Mullen *et al.* (2009). Other components from

cellulose and hemicellulose were identified as 2-oxo-propanal, 4-hydroxy-5,6-dihydro-(2H)-pyran-2-one, Hydroxy-propanal, Propanone, Methylfuran, 2-cyclopenten-1-one, furanone, 2,3-butanedione, Tetrahydrofuran-3-one, furfural, 2,3-pentanedione, tetrahydro-4-methyl-3-furanone, levoglucosenone, Hydroxymethyl-dihydropyranone and Tetrahydro-4-methyl-3-furanone. The composition of the pyrolysis gas or bio-oil is dependent on the composition of the biomass feedstock (Zhang *et al.*, 2008). The presence of the reactive and low-molecular weight carbonyl compounds (2-oxo-propanal, 2-butanone, hydroxy-propanal, propanone and dihydro-methyl-furanone, etc.), is the main reason for the aging and instability properties of the bio-oil (Oasmaa *et al.*, 2005). These compounds are reported to react during storage (Oasmaa and Kuoppala, 2003).

6.1.5.5 Viscosity and solids content of bio-oil

The viscosity variation against shear rate was analysed for CR bio-oil samples of different water content. In Figure 21 and 22, it was found that the viscosity of bio-oils from CR ranged from 1.39 to 11.2 mPa.s for a shear rate of up to 1000 s⁻¹. In both bio-oils from CS and CC the increase in water content increased the viscosity range of the bio-oils. These results were not in agreement with previous studies (Oasmaa and Meier, 2002). Sipila *et al.* (1998) in a similar study found that viscosities were reduced by higher water content and also less insoluble components. The samples were not analysed immediately after a process run, instead they were stored in a fridge for 2 weeks before viscosity analysis. The viscosity change, an undesired property, is also observed when the bio-oils are stored or handled at higher temperature (Chaalal *et al.*, 2004). It is believed to result from polymerisation reactions between various compounds present in the bio-oil, leading to the formation of larger molecules (Czernik and Bridgwater, 2004). High level of reactive species and water content of CR bio-oils makes them unstable under normal storage conditions, which led to increased viscosity over time (Hilten *et al.*, 2010). Hence, the trend could have been due to the polymerisation reactions occurring at higher water content producing higher molecular weight components in the product. The water could also be the reason for the trend due to the fact that higher water content samples probably means that more reactive, smaller aldehydes were also recovered, which lead to more polymerisation of the lignin fragments.

The presence of inorganic ash content, 0.1-0.4 wt. % for BFBR (Table 29), also acts as a catalyst in the polymerisation reactions. The solids content were also analysed in the bio-oil samples to study the factors which could have affected the higher viscosity obtained for higher water content bio-oils. Table 31 shows the solids content of the bio-oil samples. There was no significant difference in solids content (less than 0.25 wt. %) for CR bio-oil samples to cause the unusual trend of viscosity variation. The viscosity tests were done at the same temperature of 22 °C hence the differences were not due to temperature.

Table 31: Solids content (wt. %) of CR bio-oils

Bio-oil sample	Solids content (wt. %)
CC 1	0.02
CC 2	0.11
CC 3	0.17
CS 1	0.23
CS 2	0.13
CS 3	0.01

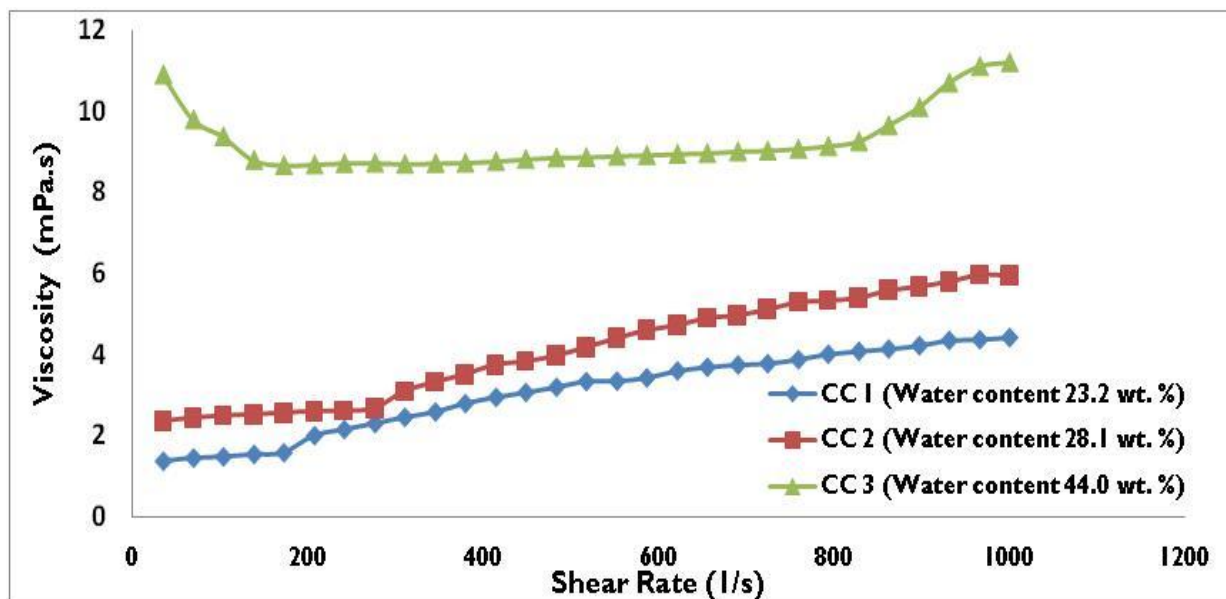


Figure 21: Viscosity vs Shear rate for CC bio-oils

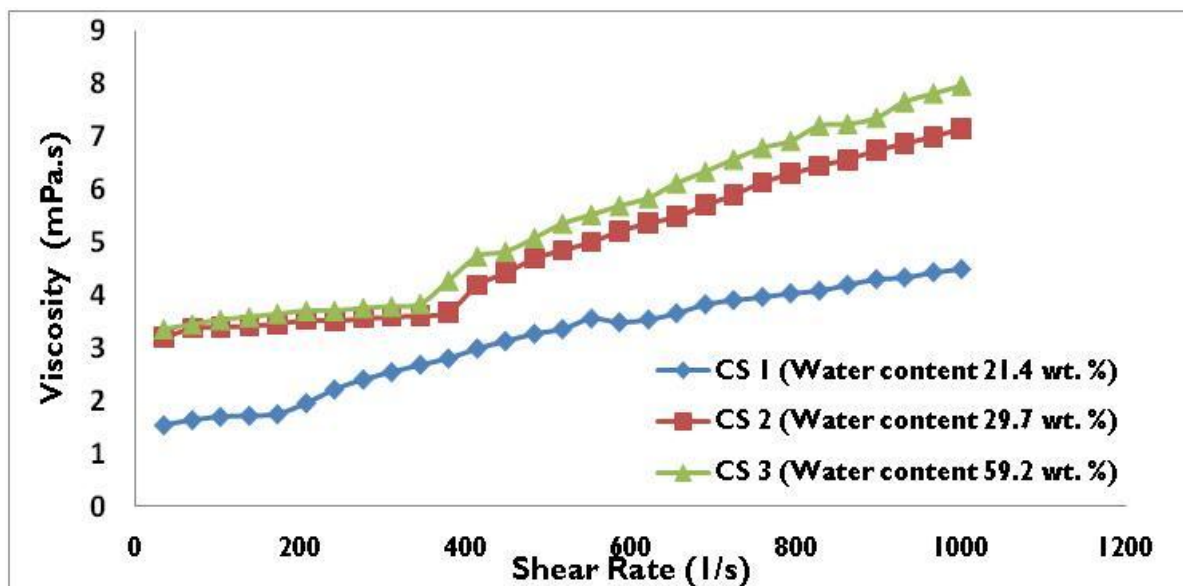


Figure 22: Viscosity vs Shear rate for CS bio-oils

6.1.5.6 Dehydration of bio-oil

The evaporation method was developed for improving the physical and chemical properties of the bio-oil. The aim of this objective was to study the removal of unwanted compounds (excess water and acids) (Oasmaa *et al.*, 2005). The results of the feed bio-oil, upgraded oils and condensate are shown in Table 32. The major changes in properties when employing the evaporation method are a decrease in water content, increase in viscosity and increase in heating value. The water content reduced from 37 wt. % to 17.6 wt. % in CC bio-oil and from 34.9 wt. % to 21.8 wt. % in CS bio-oil. There was a very slight reduction of the pH in both feedstocks and this can be due to the loss of low molecular acids (Oasmaa *et al.*, 2005). Due to the removal of water content the heating values increased from 20.8 MJ/kg to 22.5 MJ/kg in CC bio-oils and from 17.8 MJ/kg to 20.8 MJ/kg in CS bio-oil.

When the water is removed by evaporation the viscosity is increased and addition of solvents can be used to reduce the viscosity (Oasmaa *et al.*, 2005). There is higher increase in CC bio-oil viscosity than in CS bio-oil after evaporation due to different chemical components, amount of water and solids content in the bio-oil. The higher solids content and lower water content can be the reason for the higher viscosity range. The differences in the bio-oil solids content from

CR were small hence the differences in viscosity could be attributed mainly to the water content. The solids content can also raise bio-oil viscosity through catalytic reaction during storage, and is likely to be detrimental to most bio-oil applications. Therefore efficient removal of solids is necessary for the production of bio-oil of high quality. This upgrading method has been tested and achieved the same results in a process demonstration unit pilot plant by condenser temperature optimisation (Oasmaa *et al.*, 2005).

Table 32: Properties of upgraded bio-oil from FP of CR.

Parameters	Original oil	Upgraded oil	Extraction (wt. %)	Condensate
CC				
pH	4.1	4.4	<i>It is the extraction yield on the original bio-oil</i>	3.9
Water content (wt. %)	37	17.6		52.4
Heating values (MJ/kg)*	20.8	22.5		-
Viscosity (mPa.S) at 25° C	2.78-6.94	47.2-57.6		-
Solids content (wt. %)	0.10	0.17		
CS				
pH	3.9	4.1	<i>It is the extraction yield on the original bio-oil</i>	3.7
Water content (wt. %)	34.9	21.8		45
Heating values (MJ/kg)*	17.8	20.8		-
Viscosity(mPa.S) at 25° C	2.5-6.5	4.7-8.6		-
Solids (wt. %)	0.001	0.01		
Forestry Residues (Oasmaa <i>et al.</i>, 2005)				
Viscosity at 40° C (mPa.S)	18-60	120-240		-
Water content (wt. %)	15-30	9-10		-
Heating values (MJ/kg)	15-20	20-22		-

* Experimentally determined

6.1.6 Characterisation of biochar

The properties of biochar according to different FP reactors and same operating conditions were determined and the results obtained are presented in this section. The FP experiments

were done in a BFB and LTS reactors, and feedstocks with corn cobs (CC), corn stover (CS) and corn residue mixture (CRM) (Table 26). The properties of the biochar from CR from different type of reactors were determined and the results obtained are given in Table 33.

6.1.6.1 Ultimate and proximate analyses

As shown in Table 33, the percentage of carbon ranged from 67.4–84.7 wt. %, comparable to 53.9-77.6 wt. % reported by Mullen *et al.* (2009) for CR. The highest percentage of carbon obtained was 84.7 wt. % from CS in a BFBR. The percentage of oxygen ranged from 9.2-18.8 wt. % with the highest percentage obtained 18.8 wt. % for CC in a BFBR. The amount of oxygen in biochar decreased after the FP process from a range of 42.8-45.7 wt. % in biomass to 9.2-18.8 wt. % in biochar much higher than reported by Mullen *et al.* (2009), (5.11-5.45 wt. %, daf basis). The difference can be due to feedstock moisture content, feedstock oxygen content and the amount of organic volatiles in the biochar. The empirical formula of the biochar based on one nitrogen atom is listed in Table 33.

The biochar from BFBR contained on average higher carbon content and lower hydrogen content, than the biochar from LTSR for each sample. The carbon content differences were about 1.3 wt. %, 17.3 wt. % and 8.8 wt. % for CC, CS and CRM respectively. This can be attributed to the longer holding time of biochar at pyrolytic conditions: 4 hour at BFBR compared to 30 minutes in a LTSR. The biochar in a BFBR take a longer period for the temperatures to decrease from 500 °C to room temperature after a process run and carbonisation reactions were occurring. Ash also acts as a catalyst which could favour carbonisation reactions and reduce the hydrogen content and increase carbon content (Savage, 1940). The highest difference on biochar carbon content was on CS due to the large difference in ash content of feedstocks, 6.6 wt. % for LTSR feed against 13.1 wt. % for fluidised bed reactor feed (Table 26). The difference between ash content for CC was 0.1 wt. %, which was small to cause a large difference in carbon content. The H/C ratios of biochar were changing between 0.47 and 0.59 in a LTSR. The highest H/C ratio of biochar obtained was 0.59 for CS. The O/C ratios of biochar were ranged between 0.09 and 0.11 in a LTSR. The highest O/C ratio of biochar obtained was 0.11 for CRM. The percentage of hydrogen (H) and nitrogen (N)

ranged from 3-3.4 wt. % and 0.7-1 wt. % respectively. The highest H and N contents obtained were 3.4 wt. % and 1 wt. % for CRM and CS, respectively. There was no sulphur detected in the biochar and this is important information for predicting emissions from combusting biochar. The H/C ratios of biochar were changing between 0.004 and 0.06 in a BFBR. The highest H/C ratio of biochar obtained was 0.06 for CRM. The O/C ratios of biochar were ranging between 0.12 and 0.18. The highest O/C ratio of biochar obtained was 0.18 for CC.

The percentage of H and N ranged from 0.03-0.4 wt. % and 1.98-5.60 wt. % respectively. The highest H and N contents obtained were 0.4 wt. % and 5.6 wt. % for CRM. Biochar produced from Fast pyrolysis had higher nitrogen content in a BFBR (1.98-5.60 wt. %) than in a LTSR (0.7-1.0 wt. %). This could be due to longer holding time (4 hours, nitrogen flow rate 0.5 m³/hr) of biochar after reaction in a BFBR than 30 minutes during the reaction in a LTSR. The biochar in a LTSR after the reaction was cooled by natural air, methanol extracted and dried at 105 °C before chemical and physical analysis. The drying step for biochar in a LTSR drives off all the trapped gases including absorbed nitrogen during the process, whereas for biochar from a BFBR were analysed without any pre-treatment step. The trapped nitrogen also increased the content of nitrogen in biochar from BFBR.

As can be seen from Table 33, biochar is a carbon rich fuel with a freely settled bulk density of 205-310 kg/m³ slightly higher than the densities of their biomasses (170-290 kg/m³) due to the evolution of light components volatiles. When CR biomass and biochar are compared after the FP process, carbon rich solid fuel is obtained with higher amounts of fixed carbon and ash content, but lower amounts of volatiles than CR feedstocks. Table 33 shows the volatiles content of biochar from different particle sizes of biomass and different types of reactor. It has been observed that the volatiles differences of biochar in BFBR for the particle size of (<2 mm) and in a LTSR for the particle size of (<5 mm) were insignificant. The biochar in a LTSR had slightly higher volatiles (> 27 wt. %) than those in a BFBR with less than 26 wt. % volatiles (Table 32).

Table 33: Characterisation of biochar from FP of CR

Reactor Type	BFBR: Temperature 500-530 °C						LTSR: Temperature 500-530 °C					
Biomass Type	CC	SD	CS	SD	CRM	SD	CC	SD	CS	SD	CRM	SD
	wt. %											
Moisture (TGA)	2.2	0.2	2.5	0.9	2.1	0.2	2.1	0.1	2.31	0.2	-	-
Moisture (Analytical method)	2.1	0.9	2.2	3	1.9	0.4	-	-	-	-	-	-
Fixed Carbon(TGA)	54.9	2.7	38.8	7.6	43.1	1.9	62.9	1.6	48.3	1.9	-	-
Ash (TGA)	14.7	2.1	33.0	8.3	31.3	2.9	7.3	1.4	13.2	1.9	-	-
Ash (Analytical method)	10.6	0.3	33.7	2.5	31.5	1.7	10.1	0.3	16.6	1.4	16.1	1
Volatiles (TGA)	25.9	2.4	21	4.1	24	2.5	27.7	1.2	36.3	1.8	-	-
BET surface area (m ² /g)	158.8	61	96.7	28.1	98.7	18.3		-	-	-	-	-
Total pore volume (cm ³ /g)	0.09	0.02	0.06	0	0.06	0		-	-	-	-	-
Bulk density (kg/m ³)	310	15	205	5	240	6		-	-	-	-	-
	Elemental analysis (wt. %,dafbasis)											
C	78.5	4.4	84.7	8.6	78.6	1.46	77.2	0.5	67.4	0.9	69.8	3.1
H	0.03	0	0.03	0	0.4	0.5	3	0	3.3	0.4	3.4	0.3
N	2.7	0.6	1.98	0.24	5.6	0.16	0.7	0	1	0.2	0.9	0
S	0	0	0	0	0	0	0	0	0	0	0	0
O ^(a)	18.8	1.4	13.3	2.1	13.3	1.6	9.2	0.9	11.9	1.9	9.9	1.7
H/C Molar Ratio	0.005	-	0.004	-	0.060		0.47	-	0.59	-	0.58	-
O/C Molar Ratio	0.18	-	0.12	-	0.13		0.09	-	0.13	-	0.11	-
Empirical Formula	C_{33.9}H_{0.16}NO_{6.1}		C_{49.9}H_{0.21}NO_{5.9}		C_{16.4}HNO_{2.1}		C_{128.7}H₆₀NO_{11.5}		C_{78.7}H_{46.2}NO_{10.}		C_{90.9}H_{53.1}NO_{9.7}	
Heating Value (HHV,MJ/kg)	27.4	2.2	19.8	0.3	21.6	3.1	29.3	0.4	25.8	0	26.9	1
(HHV,MJ/kg) ^(b)	25.1	-	27.5	-	25.8		29.3	-	25.8	-	27	-

(a) -Determined by difference

(b)- Calculated from Channiwala equation

The ash content in the biochar from the BFBR is higher than from the LTSR due to different ash contents in the feedstocks which limited the comparison of CC and CS biochars. There was higher ash content in the feedstocks from Free State province than from North west province (Table 26), CS 13.1 wt. % against 6.6 wt. % and CC 1.9 wt. % against 1.8 wt. %. The biochar ash contents were reflective of the initial feedstocks ash contents. The ash content of biochar is considerably higher than that of bio-oil.

6.1.6.2 Heating value

Heating value is a major quality index for fuels. Calorific value obtained defines the energy content of a fuel. The heating values of biochar obtained from the same operating conditions are changing between 19.8 and 29.3MJ/kg. The highest calorific value of biochar obtained was 29.3MJ/kg with ash content of 10.1 wt. % in a LTSR for CC and the lowest was obtained for CS at 19.8MJ/kg with an ash content of 33 wt. % in a BFBR. There is a significant effect of biomass type and ash content on calorific value of char. The latter is known for decreasing the fuel heating value (Dermibas, 2002). The biochar from LTSR with a lower ash content of 10.1-16.6 wt. % had higher heating values of 25.8-29.3MJ/kg. Whereas, biochar from BFBR with higher ash content of 14.7-33 wt. % had lower range of heating values (19.8-27.4MJ/kg).

The estimation of heating value from elemental composition of the fuel was calculated using a correlation by Channiwala *and* Parikh (2002) and the values obtained correlated well with the analytically determined heating values for biochar from LTSR (Table 33). The differences for biochar heating values (analytically and calculated) from LTSR were 0 MJ/kg for CC, 0 MJ/kg for CS and 0.1 MJ/kg for CRM. There were large differences in the biochar heating values from the two methods in a BFBR (7.7 MJ/kg for CS, 4.2 MJ/kg for CRM and 2.3 MJ/kg for CC). The biochar from BFBR had more volatiles than the ones from LTSR due to differences in the two processes. The gases and biochar were separated in a BFBR with a dual cyclone separation system which was less effective than the one from LTSR. In the LTSR the biochar and pyrolysis gas were condensed together in first condenser and biochar was extracted with methanol and dried at 105 °C before chemical analysis. The heating value analysis from bomb calorimeter is carried out on dry basis hence the first stage was drying step which removed most of the

trapped volatiles in the biochar. The elemental composition of biochar included the volatiles which are mostly, composed of lighter hydrocarbons adding more carbon to the biochar elemental composition. Higher values of carbon content were obtained than could have been obtained for a sample of biochar undergone drying step before chemical analysis. All biochars have a low moisture content (<3 wt. %), which is desired in thermochemical processes. The heating values of biochar from FP obtained in the present study were in the same range as previous reports ranging from 21 MJ/kg to 30 MJ/kg for CR biochar (Mullen *et al.*, 2009).

The South African coal, fast pyrolysis biochar and CR biomass chemical and physical properties were compared and the values are summarised in Table 34. As expected, in terms of moisture, elemental analysis (C, H, N, S, and O), heating values and volatiles, the data in Table 34 clearly show that biochar generally have better fuel qualities than dried biomass due to higher elemental carbon. Biochar from CR energy content were comparable to South African coal (16.2-25.9 MJ/kg) (Alessio *et al.*, 2000; Tola and Cau, 2007; Bosch, 1998), against 18.7-29.3 MJ/kg for biochar. This renewable energy source can be used as a feedstock in coal to liquid gasification process as it has higher heating value, lower ash content and lower sulphur content than coal. The biochar energy densities are 4.06-8.5 GJ/m³ for biochar from a BFBR, 5.3-9.1 GJ/m³ for biochar from a LTSR and CR biomass, were in the range of 2.4-6.2 GJ/m³ (Table 33). The biochar energy densities based on freely settled bulk density are slightly higher than that of biomass making it cheaper to transport. The energy density of coal is 2.5-4 times higher than that of biochar which makes it more costly to transport biochar than coal to a gasification plant.

6.1.6.3 Surface area

BET surface area gives an indication of the extent of porosity as highly porous structures, especially microporous structures have high surface area. It is one of the most important parameters to evaluate chemical kinetics in processes such as gasification of biochar. Increasing the surface area of a substance generally increases the rate of a chemical reaction (Campbell *et al.*, 2002). This characteristic was determined to evaluate the quality of biochar for potential activated carbon production and reactivity in thermochemical processes such as gasification. The BET surface areas were only analysed on biochar from BFBR. The BET surface area and

pore volume for CC and CS pyrolysed at 500-530 °C in a BFBR were 158.8 m²/g, 0.09 cm³/g and 61 m²/g, 0.02 cm³/g, respectively (Table 33). The CR biochar surface areas in this study were higher than unactivated CR biochar (1.1 m²/g for CC and 3.1 m²/g for CS) and lower than activated CR biochar values (249 m²/g for CC and 455 m²/g for CS) reported previously (Lima *et al.*, 2010). The BET surface areas determined for CR biochars in this study were also much higher than those determined in a similar study by Mullen *et al.* (2009), 0m²/g for CC and 3.1 m²/g for CS and in the same range with those determined by Hugo (2010), 255-282 m²/g and Das *et al.* (2004), 98-243m²/g for the pyrolysis of sugar cane baggase at 500-530 °C.

The higher BET surface area than the ones in literature could be due to the longer holding time of more than 4 hours in the BFBR at US favouring further development of chars' porous structure. However, surface area of some samples could not be determined, because the volatile contents of these samples were too high and difficulties were experienced during the degassing step. The surface areas of CC biochar were higher than those for CS making it more valuable feedstocks for the production of adsorbents. The differences could be due to higher ash content in CS than CC. Devnarain *et al.* (2002) reported that the ash content of biochar caused a decrease in surface area after activation, which could explain the differences in BET surface area of CC and CS. This study shows that the CR biochar from FP can be a feedstock for adsorbents manufacture because of the high surface areas.

Table 34: Comparison of properties of coal, CR biomasses and CR biochars

	South African Coal(Alessio <i>et al.</i> , 2000; Tola <i>and</i> Cau, 2007; Bosch, 1998)	CR biochar	CR biochar	CR biomass
Source		BFBR	LTSR	
Ultimate analysis (wt.%,daf basis)				
C	74-84.2	78.5-84.7	67.4-77.2	47.9-51.1
H	3.8-4.7	0.03-0.40	3.0-3.4	5.7-6.3
N	0.8-1.9	1.98-5.60	0.7-1.0	0.34-0.61
S	0.7-1.2	0	0	0.03-0.13
O ^(a)	8-19.7	13.3-18.8	9.2-9.9	42.8-45.7
Proximate analysis (wt. %)				
Moisture	2.5-8	1.9-2.2	n.d.	4.3-8.5
Volatiles	21.1-23.3	21-25.9	17.9-36.3	69.5-79.9
Ash	15-36.5	15.3-33.7	10.1-16.6	1.8-13.1
Fixed Carbon ^(a)	36.8-57.8	38.8-54.9	48.3-73.9	8.2-14.4
Heating value(MJ/kg) ^(b)	16.2-25.9	19.8-27.4	25.8-29.3	14.01-21.3
Bulk densities(kg/m ³)	800-1000	205-310	205-310	170-290
Energy densities(GJ/m ³)	12.9-25.9	4.06-8.5	5.3-9.1	2.4-6.2

(a) Determined by difference; (b) Experimentally determined heating value; n.d. Not determined

6.1.6.4 Particle size distribution

(a) Biochar from BFBR.

The biochar from BFBR was dried to a moisture content of less than 3 wt. %. Table 35 shows the particle size distribution of biochar from BFBR.

Table 35: Particle size distribution of biochar from BFBR (μm)

Biomass type	Mean	SD	<10%	<25%	<50%	<75%	<90%
CC	713	140	53	250	850	1000	1700
CS	321	450	<53	53	250	400	850

Mean particle size was 713 μm and 321 μm for CC and CS biochar, respectively with the CC biochar presenting a broader range of sizes. Ninety percent of the mass were smaller than 1700 μm and 850 μm for the CC and CS biochar, respectively. There was a higher particle size range for CC than CS due to the differences in feedstocks particle size distribution. CC had a higher particle size range than CS feedstocks.

(b) Biochar from LTSR

The objective of the Karlsruhe Institute of Technology (KIT) research was to develop biochar and bio-oil slurry with a higher heating value for gasification process. The biochar from LTSR was wet with condensate oil from first condenser. The bio-oil and biochar were mixed together to form a slurry of 34 wt. % solids and the samples were analysed for particle size distribution. The slurries were milled to reduce particle size and improve the homogeneity of the slurry. The particle size distribution and viscosity measurement were done. Table 36 shows the particle size distribution of biochar from BFBR.

Table 36: Particle size distribution of biochar slurries from LTSR (μm)

Biomass type	Comment	Mean	SD	<10%	<25%	<50%	<75%	<90%	Particles analysed
CC	Mixed	155.7	89.1	63	91	133	210	320	588771
	Milled	237.2	136.5	56	106	230	350	420	479035
CS	Mixed	304.6	130.5	126	200	320	390	500	503362
	Milled	137.3	69.8	56	84	126	190	270	1105351

Mean particle size for mixed slurries was 155.7 μm and 304.6 μm for CC and CS biochars, respectively with CS biochar presenting a broader range of particle sizes. Ninety percent of the particles were smaller than 320 μm and 500 μm for the CC and CS biochars, respectively. Mean particle size for milled slurries reduced for CS to 137.5 μm and increased for CC to

237.2 μm , with the CC biochar presenting a broader range of sizes. Ninety percent of the milled particles were smaller than 420 μm and 270 μm for the CC and CS biochar, respectively. The differences in CR biochar particle size ranges are expected to affect slurry properties such as viscosity and homogeneity.

6.1.6.5 Slurry viscosity

(a) CS slurries

Viscosity is one of the most important rheological properties of slurries for gasification and it is desired to be as low as possible (www.itc-cpv.kit.edu). Viscosity affects the fluidity of the slurries and depends on the biochar particle size and bio-oil homogeneity. The flow and stability characteristics of the slurries were studied by analysing the viscosity. The effect of biochar particle size range on the slurry properties was also studied by milling the mixed slurry. The viscosity for CS and CC slurries studied from LTSR are shown in Figure 23 and 24.

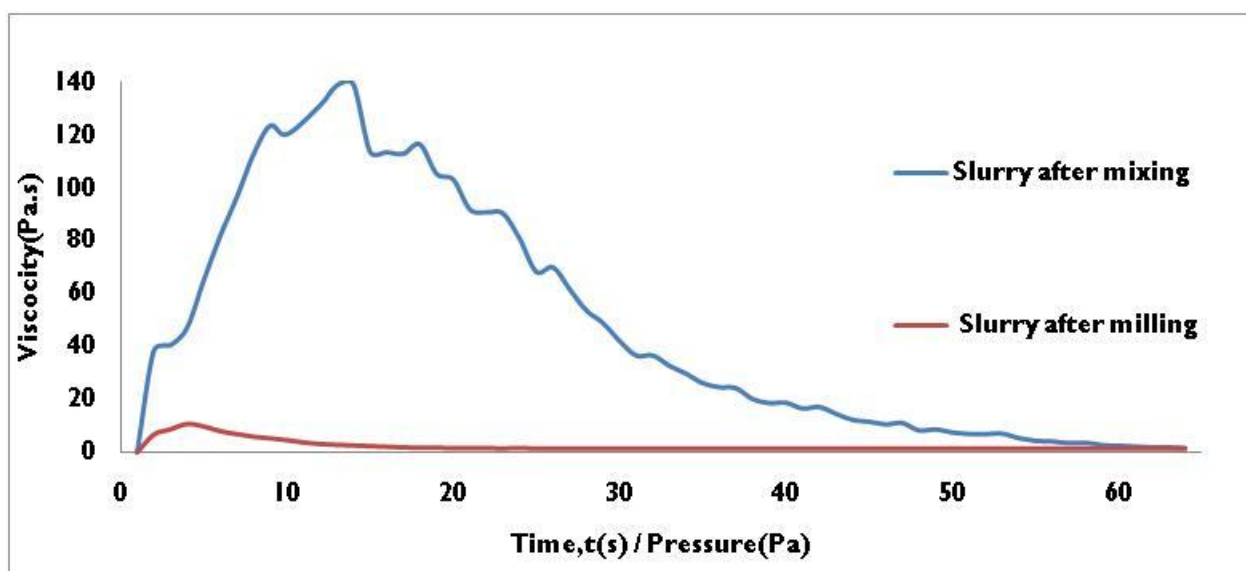


Figure 23: Viscosity variation for CS slurries

From the graph of CS slurry after mixing as the shear rate increases during the first few seconds it can be seen that the viscosity rises up to a maximum of 140 Pa.s and then after applying 15 Pa pressure the viscosity starts to decrease and equilibrate at a consistent range of less than 5 Pa.s viscosity around 55 Pa pressure. After milling, the slurry's behaviour changed and became more homogeneous. The viscosity varied in a narrow range of less than 5 Pa.s after a few seconds of applying pressure. After mixing and milling, from the CS fast pyrolysis

products there was an increase in the number of detected biochar particles (Table 35), showing an increase in the number of biochar agglomerates broken down to form smaller particles.

(b) CC slurries

The graph for CC shows that the slurries were inhomogeneous as the agglomerates were not broken by the colloid mixer to form a uniform product. The agglomerates were not broken by the viscometer agitator leading to wide range of viscosity as pressure was increased to 60 Pa. The milling of the slurry to a finer particle size distribution (Table 35) did not improve the homogeneity of the slurry as it behaved in the same way. The viscosity increased to 13 kPa.s after 10 seconds for mixed slurry and 23 seconds for the milled slurry. The stability of the slurries could be due the unstable chemical components in the bio-oil, inhomogeneity of the liquid product and phase separation. These results showed that the bio-oil from CC was less stable than that from CS as it was forming an unstable and inhomogeneous slurry shown by the behaviour of the shear rate against viscosity graphs (Figure 24).

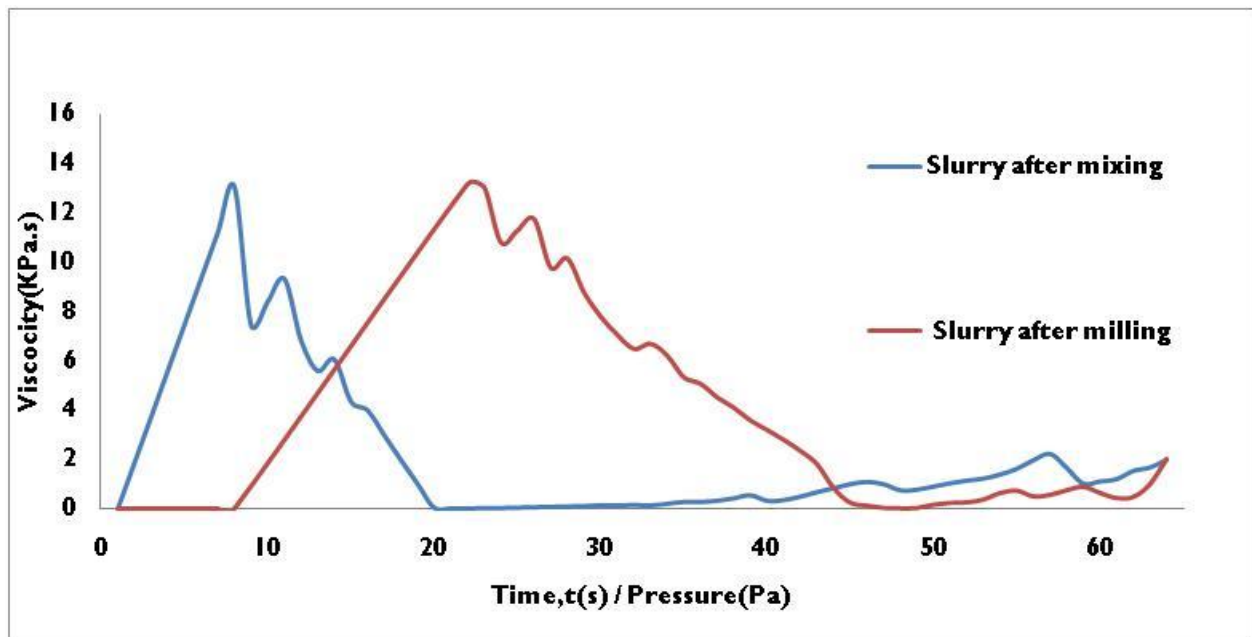


Figure 24: Viscosity variation for CC slurries

Junming *et al.* (2008) in a previous study found that water content results in a phase separation and the water insolubles could be easily separated at higher levels of water. The higher water content of CC 26 wt. % against CS 21.3 wt. % (Table 28) could be one of the reasons for the

unstable CC biochar slurry. Oasmaa *et al.* 2004 found that the stability of bio-oil can be caused by the chemical components, carbonyl and lignin derived compounds being some of the sources of instability. The variation in feedstock composition of CC and CS highlighted in Chapter 4 can be the cause of different chemical components in the bio-oils and different product stabilities. The slurry properties of CC can be improved by directly or indirectly adding additives such as alcohols like methanol or the use of surfactants (Benter *and* Arnoux, 1997). In this case, the particles get caught between the droplets in the continuous phase, which prevents them from settling. The unstable components of the bio-oil the carbonyl compounds under goes acetalisation and esterification reactions with alcohol homogenising the mixture and increasing the product viscosity by forming more stable esters and acetals (Oasmaa *et al.*, 2004).

6.1.7 Characterisation of gas

6.1.7.1 Non-condensable gas composition

In this study, the FP gas characterisation was only carried out in a LTSR for three samples of CC, CS and CRM. The results are an average of two runs for each sample. The elemental analysis and gas composition from a LTSR are presented in Table 37 and Figure 25.

Table 37: GC non-condensable gas analysis

Biomass Type	CC	SD	CS	SD	CRM	SD
Gas density	1.40	0.01	1.37	0.01	1.39	0.03
Heating value	8.86	0.50	8.82	0.90	8.85	0.40
Elemental Analysis (wt. %)						
C	37.2	0.6	37.5	1.0	37.7	0.5
H	2.4	0.2	2.2	0.2	2.25	0.1
O	60.4	0.8	60	1.8	60.1	0.6
H/C molar ratio	0.77	-	0.70	-	0.72	-
O/C molar ratio	1.22	-	1.61	-	1.2	-
Empirical formula	$C_{1.3}HO_{1.6}$	-	$C_{1.4}HO_{1.7}$	-	$C_{1.4}HO_{1.7}$	

The percentage of carbon (C) and hydrogen (H) ranged from 37.2-37.7 wt. % and 2.2-2.4 wt. %, respectively. The oxygen (O) content was the highest in this stream ranging from 60-60.4 wt. %. The H/C and O/C ratios of the three corn residue samples were 0.70-0.77 and 1.2-1.61 for the three samples, respectively. If considering only the main elements C, H and O, the molecular formula of the samples based on one H atom can be written as $C_{1.3}HO_{1.6}$ for CC and $C_{1.4}HO_{1.7}$ for CS and CRM feedstock. The gas consisted mainly of CO_2 , CO, CH_4 , H_2 and C_5^+ hydrocarbons. These compounds represent more than 96 vol % of the total non-condensable product stream and the rest are quantified as both saturated and unsaturated hydrocarbons. The high CO_2 content is due to the high amount of O_2 in the feedstock 41.6-46.5 wt. % on daf basis and O_2 leakages in to the process.

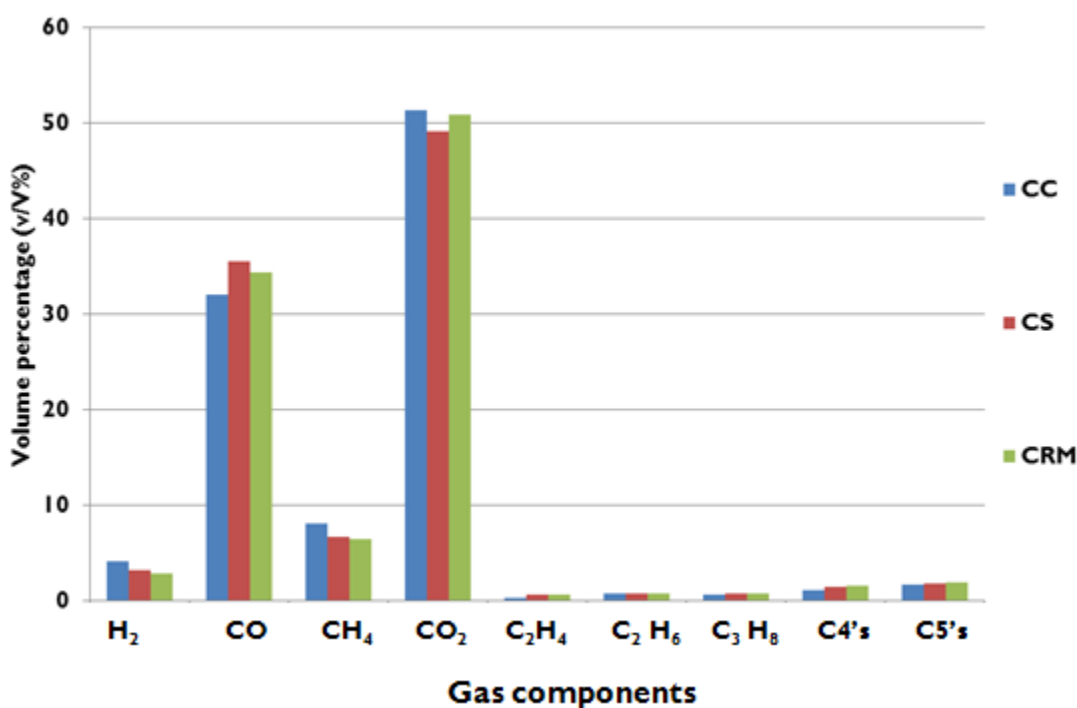


Figure 25: The non-condensable gas compositions of corn residues

The gases from the biomass contained almost the same non-combustible CO_2 (49.1% for CS, 51.4% for CC and 50.9% for CRM) making them an almost same quality low heating value process gas. Calculated heating values for the product gases were 8.82MJ/kg for CS, 8.86MJ/kg for CC and 8.85MJ/kg for CRM. The gas composition was found to be almost similar for the different biomasses and corresponds very well to the values reported for other CR subjected

to similar pyrolysis conditions (Mullen *et al.*, 2009). The gas is a low to medium heating value stream that can be used for process heat (e.g. for drying feed) or power generation on the plant. The energy content of this stream can be improved by removing the CO₂ using absorption with solutions such as potassium carbonate, potassium bicarbonate, diethanolamine and potassium vanadate. Desorption of the carbon dioxide from the solution and recycling the regenerated solution using membrane technologies (nanofiltration, ultrafiltration and reverse osmosis) can be used (Hesseet *al.*, 2001). Biomass material consists basically of three types of polymers: Cellulose, hemicelluloses and lignin (Fushimi *et al.*, 2003). From a previous study done by Williams and Besler (1993) cellulose mainly produces CO₂, CO and H₂ while lignin produces mainly CO₂, CO and CH₄. The lignocellulosic composition of the biomass affects the product gas composition and quality. There were negligible differences in the pyrolysis gas composition due to slight differences in the CR lignocellulosic composition discussed in Chapter 4.

6.1.7.2 Non-condensable gas adiabatic flame temperatures

This is the temperature that the flame would attain if the energy liberated by the chemical reaction that converts the non-condensable gas components into combustion products were fully utilised. Combustion of hydrocarbon fuels occurs in many practical devices, such as internal combustion engines, gas turbine engines and industrial furnaces. In any combustion process, flame temperature is one of the most important properties that controls the rate of chemical reaction and also has an important influence on the design and performance of combustion devices. In design and optimisation of the hot parts of gas turbine engines, for example, the maximum liner temperature and maximum turbine inlet temperature are critical parameters, and are largely determined by the maximum adiabatic flame temperature (Gulder, 1986).

It is a function of the fuel composition characterised by the number of hydrogen and carbon atoms in a fuel molecule, fuel–air equivalence ratio (ϕ), temperature (T) and pressure (P) of the reactants. Based on the law of thermodynamics and chemical equilibrium, the adiabatic flame temperature was calculated using NASA-Glenn Chemical Equilibrium Program (GCEP) in air and oxygen at a pressure of 1.01 bar and temperature of 298.15 K (Figure 26 and 27). The CS non-condensable gas adiabatic flame temperatures in air combustion were 636 K to 2092 K.

The lower temperature was at 0.2 equilibrium ratio and oxygen-fuel ratio of 23.2. The highest temperature was attained at equilibrium ratio of 1 and oxygen-fuel ratio of 2.5. The gas combustion in oxygen produced higher range adiabatic temperatures from 1490 K to 2714 K. The lower temperature was at 0.2 equilibrium ratio and oxygen-fuel ratio of 5.3. The highest temperature was attained at equilibrium ratio of 1 and oxygen-fuel ratio of 0.6. The CC non-condensable gas adiabatic flame temperatures in air combustion were 1142 K to 2062 K. The lower temperature was at 0.3 equilibrium ratio and oxygen-fuel ratio of 7.5. The highest temperature was attained at equilibrium ratio of 1 and oxygen-fuel ratio of 2.4. The gas combustion in oxygen produced higher range adiabatic temperatures from 1446 K to 2681 K. The lower temperature was at 0.1 equilibrium ratio and oxygen-fuel ratio of 5.2. The highest temperature was attained at equilibrium ratio of 1 and oxygen-fuel ratio of 0.6. There were higher ranges of adiabatic flame temperatures in oxygen than in air. The presence of nitrogen gas (79 %) in air has a cooling and diluting effect in fuel combustion. The highest adiabatic flame temperature was obtained at equilibrium ratio of 1. Combustion reaches a maximum temperature at this value when the fuel and oxidant ratio permits all of the hydrogen and carbon in the fuel to be burnt to H_2O and CO_2 (stoichiometric combustion).

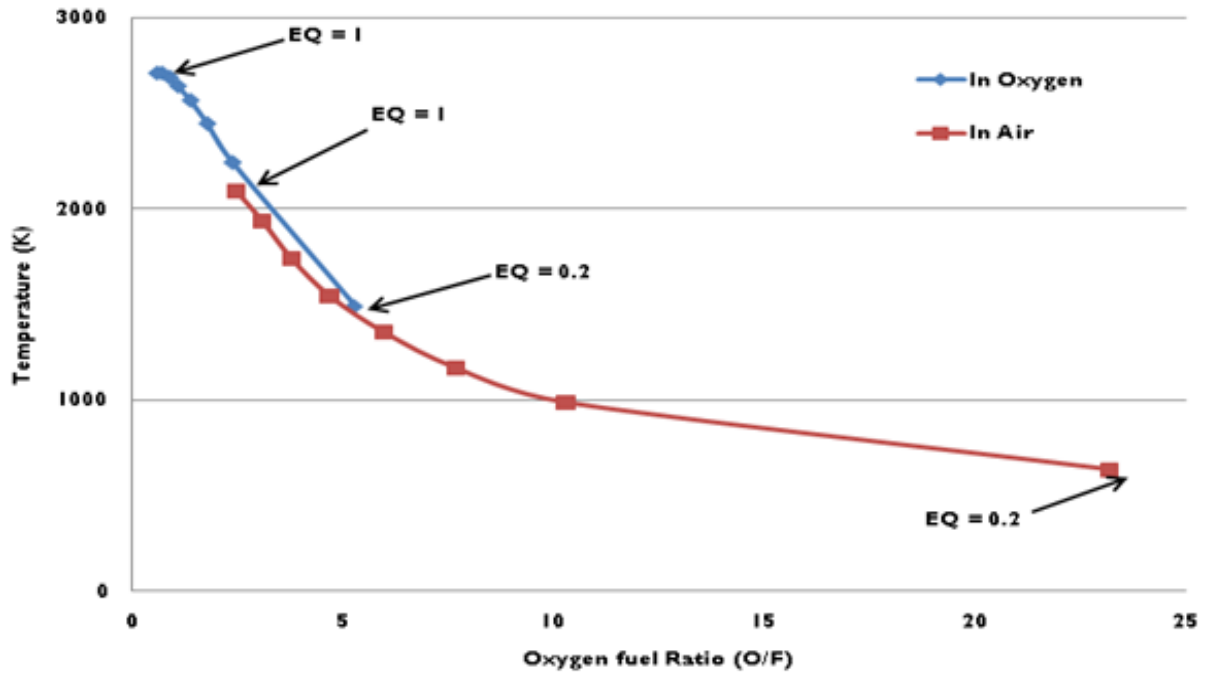


Figure 26: Corn stover non-condensable gas flame temperatures

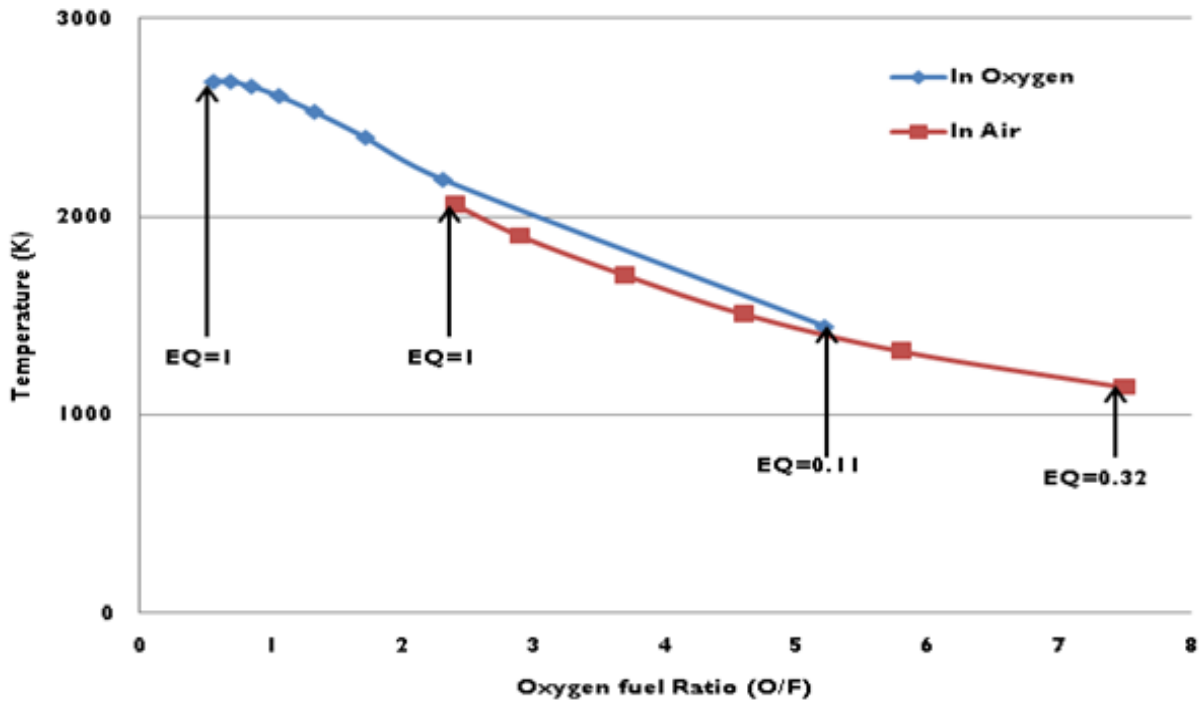


Figure 27: Corn cobs non-condensable gas flame temperatures

6.1.8 Product energy distribution

In FP it is interesting to determine the product energy distribution. The energy in the product streams constitutes the useful energy recovered from the input energy and contained in the bio-oil, biochar and non-condensable gas. The amount of energy input that is recovered in these products constitutes the energy efficiency. Table 38 gives a summary of the energy distribution among products (bio-oil and biochar) from FP at 500-530°C. The average energy distribution for the bio-oil and biochar is almost similar for both LTSR and BFBR. The bio-oil energy content in a LTSR was 67.4% for CC and 60.3% for CS. In a BFBR, the bio-oil energy content was 58.7% for CC and 67.4% for CS. The bio-oil product had the highest energy content followed by the biochar. The biochar energy content in a LTSR was 29.3% for CC and 29.9% for CS. In a BFBR, the biochar energy content was 23.1% for CC and 28% for CS. Combining the bio-oil and biochar products into a single slurry mixture the energy content of a single product can be increased to above 70% of the original biomass energy. Lange (2007) obtained 79% of biomass energy for slurry production from straw pyrolysis on LTSR.

Table 38: Energy recoveries of products from CR

	HHV	x	h	Recovered Energy
	MJ/kg	kg/kg (wt. %)	MJ/kg biomass	(%)
CC	19.14	1	19.1	100
LTSR				
Bio-oil	25.3	0.51	14.2	67.4
Biochar	29.3	0.19	5.6	29.3
CC	21.3	1	21.3	100
BFBR				
Bio-oil	20.2	0.62	12.5	58.7
Biochar	27.4	0.18	4.93	23.1
CS	18.06	1	18.06	100
LTSR				
Bio-oil	22.3	0.49	10.9	60.3
Biochar	25.8	0.21	5.4	29.9
BFBR				
CS	14.1	1	14.1	100
Bio-oil	18.7	0.51	9.5	67.4
Biochar	19.8	0.2	3.96	28

Chapter 7: Conclusions and recommendations

This study focused on the initial characterisation of corn cob and corn stover and their conversion by fast pyrolysis (FP) with the objective to determine the potential of corn residues (CR) as a potential thermochemical feedstock. Fast pyrolysis of the corn residues (CR) was performed in two different reactors: Lurgi twin screw and bubbling fluidised reactors. The main products were bio-oil, biochar and gas, yields of which were calculated and products analysed for a variety of properties. A summary of the conclusions and recommendations are given in this section.

7.1 Biomass characterisation

- Corn residues biomass are potential thermochemical feedstocks, with the following properties: carbon 50.2 wt. %, hydrogen 5.9 wt. % and HHV 19.14 MJ/kg for corn cob and carbon 48.9 wt. %, hydrogen 6.01 wt. % and HHV 18.06 MJ/kg for corn stover. The corn residues biomass energy content was comparable to low grade South African coal (16 MJ/kg) and it is a potential energy feedstock. The South African corn residues were different from other corn residues in the world only on the amount of ash present.
- The elemental composition of raw biomass indicated that the most abundant elements in the inorganic fraction of corn residue were silicon (0.66 wt. % for CC and 3.03 wt. % for CS) and potassium (0.86 wt. % for CC and 1.33 wt. % for CS). The CS (6.6 wt. %) had higher ash content than CC (1.9 wt. %). The CS biomass had higher ash amounts of Ca and K than CC and expected to have a more catalytic effect in fast pyrolysis.
- The corn residues have a lower sulphur (< 0.06 wt. %) and nitrogen (< 0.7 wt. %) content than coal (0.7-1.2 wt. % for sulphur and 0.8-2 wt. % for nitrogen) which makes them more environmentally friendly energy sources. It was concluded that corn residues will emit amounts of nitrogen oxides and sulphur oxides much lower than burning of coal.
- Corn cob has higher density (290 kg/m³ for CC and 170 kg/m³ for CS) and energy density (5.6-7.5 GJ/m³ for CC and 3.1-3.8 GJ/m³ for CS) than corn stover, which could make it more cost effective to transport and store. It was concluded that corn residues are more costly to store and transport than fossil fuels such as coal with energy densities of 12.9 to 25.9 GJ/m³.

7.2 Thermogravimetric analysis

- The thermal decomposition of corn residues were characterised in 3 stages: (i) stage 1 from room temperature to 130 °C corresponding to moisture and light components vaporisation. (ii) Stage 2 from 145-333 °C corresponding to main pyrolysis process. (iii) Stage 3 from 264 °C to maximum temperature corresponding to the slow decomposition of heavier biomass components.
- The derivative thermogravimetric (DTG) and thermogravimetric (TG) curves of corn residues shifted to higher temperatures as the heating rate increased.
- The presence of higher ash composition of Ca and K in CS than CC caused merging of derivative thermogravimetric (DTG) peaks at higher heating rates than CC.
- The CC and CS reactivities were almost similar from the same range of activation energies (220-255 kJ/mol for CS and 237-270 kJ/mol for CC. It was concluded that the corn residues biomasses have the same thermal stability and pyrolysis occurred through the cleavage of linkages of similar bond energy.
- The corn residues experimental thermal decomposition TG data and the expected TG data from the model were within 10% error with higher quality of fit at lower heating rates.

7.3 Fast pyrolysis products

- The differences in corn residue physical properties (bulk density, shape and brittleness) had an effect on the milled particles size ranges (Higher range of particles from CC than CS, for LTSR (51.1% > 2 mm against 37.7% > 2mm) and BFBR (67.1% > 0.85 mm against 19.1% > 0.85 mm)).
- The mode of heat transfer and the particle size range in BFBR and LTSR had an effect on the yields (35-37 wt. % for LTSR and 47.8-51.2 wt. % for BFBR).
- The presence of higher ash (Ca and K) in corn stover has got a catalytic effect on fast pyrolysis reducing the bio-oil liquid yields than from CC.
- It can be concluded that the bubbling fluidised bed reactor's direct spraying with isopar condensation system was more effective than the Lurgi twin screw reactor's two-stage condensation system, thereby resulting in higher bio-oil yields.

- The fast pyrolysis of corn residues produced acidic bio-oils with higher ash content in the Lurgi twin screw reactor than the bubbling fluidised bed reactor.
- Corn residues bio-oil energy content produced from fast pyrolysis was 18.7-25.3 MJ/kg, and the product can be combusted in existing heating application systems or as a mixture with other fuels. Its low nitrogen and sulphur content is promising for its evaluation as a fuel from an environmental point of view.
- The bio-oil from corn residues before application in various uses it must be upgraded reduce the high oxygen content (27.5-44.7 wt. %), reduce the acidic content (pH 3.8-4.3) and reduce water contents (21.3-30.5 wt. %).
- The dehydration of bio-oil can be used to improve the quality by increasing the heating value and reducing the water content of the oil.
- Biochars from corn residues have properties comparable to coal and can be used as a feedstock in the coal to liquid gasification process.
- The biochar carbon content depends on the length of time the particles are held at the final temperature, the temperature and the ash composition.
- Combining the bio-oil and biochar products into a single slurry mixture the energy content of a single product can be increased to above 70% of the original biomass energy.
- The corn residues biochars are potential feedstocks for productions of adsorbents (BET Surface area, $158.8 \pm 61 \text{ m}^2/\text{g}$ for CC and $96.7 \pm 28.1 \text{ m}^2/\text{g}$ for CC).
- The heating value can be improved by removing carbon dioxide from this stream. The gas may be used for drying biomass feedstock, process heating and power generation.

7.4 Recommendations

- It is recommended that an Ash Flow Temperature (AFT) analysis be done on the corn residues biomass or biochar to study the composition and structure of minerals in order to understand the mineral transformations and agglomerate formation during heat treatment processes such as combustion or gasification which are the main potential uses of biochar in energy production.

- There was a large variation in the physical properties of the corn residues which can affect the product quality. The study of particle size distribution of the corn residue is recommended in order to understand the effect on reaction kinetics, drying properties, dust formation, bridge-building tendencies and operational safety during feedstock transportation.
- Corn residue from different farms was used in fast pyrolysis and it was shown that there was a large ash content variation. Studies of harvesting methods from different farms and develop methods to reduce the inconsistency in ash content and product quality.
- It is also recommended to study the variation of the corn residue physical and chemical properties with age (storage time after harvest) and understand the effect on the product quality and yield of pyrolysis.
- It is recommended that thermo-gravimetric analysis be studied on the biomass mixtures and in order to understand the interaction effect of different lignocellulosic components in biomasses. Lignocellulosic composition should be determined from thermo-gravimetric analysis. The coupling of Mass Spectrometry (MS) to thermogravimetric analysis equipment will allow product identification at different temperatures and heating rates. It will be interesting to study specific chemical products which can be obtained at different process conditions by thermo-gravimetric analysis.
- To improve the closure of the mass balance, it is recommended that an electronic balance accurate to weigh milligrams be used for weighing the equipment before and after a run.
- In a bubbling fluidised bed reactor, the longer runs (1000 g of biomass fed) produced more than 500 g of bio-oil. Therefore, it is recommended to maintain a long process run in order to obtain a representative bio-oil sample.
- In the bubbling fluidised bed reactor, it is recommended to modify the condensation unit designing a two condenser system with optimised temperatures in order to improve the quality of the bio-oil by removing the water and light volatiles content in the liquid product.
- It is recommended to study the effect of ash content and composition, temperature and holding time of the corn residues biochar on carbonisation process after fast pyrolysis reaction.

- The biochar from the BFBR is trapped with nitrogen and lighter hydrocarbon gases. It is recommended to oven dry it at 105 °C to drive off these gases before chemical analysis.
- To study the pre-treatment effects on corn residues cation content and their effects on product yields and the chemical composition of the liquids.

References

- Adjaye, J.D.; Bakhshi, N.N. (1995). *Fuel Processing Technology*, 45, 161-183.
- Agblevor, F.A.; Besler, S. (1996). *Energy Fuels*, 10, 293-298.
- Agblevor, F.A.; Besler, S.; Wiselogel, A.E. (1995). *Energy and Fuels*, 9(4), 635-640.
- Ahmad, M.M.; Fitriir, M.; Nordin, R.; Azizan, M.T. (2010). *American Journal of Applied sciences*, 7(6), 746-755.
- Ahuja, P.; Humar, S.; Singh, P.C. (1996). *Chemical Engineering and Technology*, 19, 272-282.
- Ahuja, P.; Singh, P.C.; Upadhyay, S.N.; Kumar, S. (1996). *Indian journal of chemical technology*, 3, 306-312.
- Aiman, S.; Stubington, J. (1993). *Biomass and Bioenergy*, 5, 113-120.
- Alen, R.; Kuoppala, E.; Oesch, P. (1996). *Journal of Analytical and Applied pyrolysis*, 36, 137-148.
- Alessio, A. D.; Vergamini, P.; Benedetti, E. (2000). *Fuel*, 79, 1215-1220.
- Allen, T. (1996).ed.Davies.R.1996; *Kluwer Academic Publishers*, pp. 824.
- Andrews, R.G. D.; Fuleki, S.; Patnaik, P.C. (1997). *Proceedings of the Third Biomass Conference of the Americas*, 425-436.
- Antal, M.J.; Varhegyi, G. (1995). *Industrial and Engineering Chemistry Research*, 34, 703-703.
- Antal, M.J.; Milne, R.P.; Mudge, L.K.; Eds. (1983). *Elsevier*, New York, 511-537.
- Apaydin-Varol, E.; Putun, E.; Putun, A.E. (2007). *Fuel*, 86, 1892-1899.
- Appell, H.R.; Fu, Y.C.; Friedman, S.; Yavorsky, P.M.; Wender, I. (1980). *Biochemical Engineering Journal*, 16, 287-297.
- Armor, J.N. (2001). *Applied Catalysis General*, 222(1-2), 407-426.
- Armor, J.N. (1991). *Applied Catalysis*, 78(2), 141-173.
- Asadullah, M.; Rahman, M.A.; Ali, M.M.; Motin, M.A.; Sultan, M.B.; Alam, M.R.; Rahman, M.S. (2008). *Journal of Bioresource and Technology*, 99, 44-50.
- Asif, M.; Muneer, T. (2007). *Renewable and Sustainable Energy Review*, 7(11), 1388-1413.
- Ate, F.; Putin, E.; Putun, A.E. (2004). *Journal of Analytical and Applied pyrolysis*, 71(2), 779-790.
- Azeez, A.; Meier, D.; Odermatt, J.; Willner, T. (2010). *Energy and Fuels*, 24, 2078-2085.
- Banchorndhevakul, S.; Rad, S. (2002). *Radiation Physics and Chemistry*, 64, 417-422.

- Bapat, D.W.; Kulkarni, S.V.; Bhandarkar, V.P. (1997). *ASME Proceedings of the 14th International Conference in fluidised bed combustion*, Vancouver, New York, NY, pp. 165-74.
- Basak, B.; Putun, E. (2006). *Bioresource Technology*, 97(4), 569-576.
- Bayerbach, R.; Meir, D. (2009). *Journal of Analytical and Applied pyrolysis*, 85, 98-107.
- Beltrame, P.; Zuretti, G. (2003). *Applied Catalysis A: General*, 248(1-2), 75-83.
- Benter, M.M.G.; Arnoux, A.I. (1997). *Biomass and Bio-energy*, 12(4), 253-261.
- Bergmann, P.C.A.; Kiel, J.H.A. (2005). *Energy Research Centre of the Netherlands (ECN)*. Available at: <<http://www.techtp.com>>.
- Biagini, E.A.; Fantei, A.; Tognotti, L. (2008). *Thermochimica acta*, 1-2, 55-63.
- Bjorkman, E.; Stromberg, B. (1997). *Energy and Fuels*, 11, 1026-1032.
- Black, J.W.; Brown, D.B. (1990). *Preliminary Mass Balance Testing of the Continuous Ablation Reactor in Biomass Thermal Processing*, 23-25 October, Ottawa, Canada, pp. 123-125.
- Blasi, C.D. (1997). *Fuel*, 76(10), 957-964.
- Blasi, C.D.; Branca, C.; Errico, G.D. (2000). *Thermochimica Acta*, 364, 133-142.
- Boateng, A.A.; Anderson, W.F.; Philips, J.G. (2007). *Energy and Fuels*, 21(2), 183-1187.
- Boerrigter, H.; Kiel, J.; Bergman, P. (2006). *Third Thermal Net Meeting, Energy research Centre of the Netherlands (ECN)*, 3-5 April, Lille, France.
- Boman, C.; Nordin, A.; Ohman, M. (2004). *Energy and Fuels*, 18, 338-348.
- Bosch, F. (1998). *Flue gas conditioning-SO₃ injection rates for South African coal ashes*.
- Boucher, M.E.; Chaala, A.; and Roy, C. (2000). *Biomass and Bioenergy*, 19(5), 337-350.
- Boukis, I.; Maniatis, K.; Bridgwater, A.V.; Kyritsis, S.; Flitris, Y.; Vassilators, V. (1993). In: Bradbury, A.W.; Sakai, Y.; Shafizadeh, J. (1979). *Journal of Applied Polymer Science*, 23, 3271-3280.
- Bramer, E.A.; Brem, G. (2007). *15th European Biomass Conference and Exhibition*, 7-11 May 2007, Berlin, Germany.
- Branca, C.; Albano, A.; Di blasi, C. (2005). *Thermochimica acta*, 429, 133-141.
- Bridgeman, T. G.; Jones, J. M.; Shield, I.; Williams, P. T. (2008). *Fuel*, 87, 844-856.
- Brigdwater, A.V. (2004). *Review paper, BIBLID*, 2(8), 21-49.
- Bridgwater, A.V. (2003). *Chemical Engineering Journal*, 91(2-3), 87-102.
- Bridgwater, A.V.; Toft, A.J.; Brammer, J.G. (2002). *Renewable and Sustainable Energy Reviews*, 6, 181-248.

- Bridgwater, A.V. (ed.), (2002b) *CPL Press*, Chippenham, UK, pp. 23-40 and pp. 59-67.
- Bridgwater, A.V. (2001). Thermal Conversion of biomass and waste: The status, *Bio-energy Research Group*, Aston University Birmingham (UK).
- Bridgwater, A.V.; Peacocke, G.V.C. (2000). *Renewable Sustainable Energy Review*, 4, 1-73.
- Bridgwater, T.; Czernik, S.; Piskorz, J. (1999). *Handbook-volume 1-CPL Press*, 1-22.
- Bridgwater, A.V.; Czernik, S.; Diebold, J.; Meir, D.; Oasmaa, A.; Peacocke, C.; Pirkorz, J.; Radlein, D. (1999a). *A handbook, Vol. 1*, CPL Press, Newbury Berkshire, UK.
- Bridgwater, A.V. (1999e). *Journal Analytical and Applied pyrolysis*, 51(1), 3-22.
- Bridgwater, A.V. (1994). Advances in thermochemical conversion. *Blackie Academic and Professional, Technology & Engineering*.
- Brown, M.E. (2001). *Kluwer Academic Publishers*.
- Brunauer, S.; Emmett, P.; Teller, E. (1938). *Journal of the American Chemical Society*, 60, 309-315.
- Brunner, P.H.; Roberts, P.V. (1980). *Carbon*, 18, 217-224.
- Caballero, J.A.; Conesa, J.A.; Font, R.; Marcilla, A. (1997). *Journal of Analytical and Applied pyrolysis*, 42, 159-175.
- Caballero, J.A.; Conesa, J.A. (2005). *Journal of Analytical and Applied pyrolysis*, 73, 85-100.
- Cai, J.; Alimujiang, S. (2009). *Industrial and Engineering Chemistry Research*, 48, 610-624.
- Cai, J.; Chen, S. (2008). *Drying technology*, 26, 1464-1468.
- Campbell, P.A.; Mitchell, R.E.; Ma, L. (2002). *Proceedings of the Combustion Institute*, 29, 519-526.
- Cao, Q.; Xie, K.; Bao, W.; Shen, S. (2004). *Bioresource Technology*, 94, 83-89.
- Cassida, K.A.; Muir, J.P.; Hussey, M.A.; Read, J.C.; Venuto, B.C.; Ocumpaugh, W.R. (2005). *Crop Science*, 45, 682-692.
- Cetin, E.; Gupta, R.; Moghtaderi, B.; Wall, T.F. (2005). *Fuel*, 84 (10), 63-69.
- Chaalal, A.; Ba, T.; Garcia-Perez, M.; Roy, C. (2004). *Energy and Fuels*, 18, 1535-1542.
- Channiwala, S.A.; Parikh, P.P. (2002), *Fuels*, 1051-1063.
- CGPL (Combustion, Gasification, and Propulsion Laboratory), (2006). "Project completion report on torrefaction of bamboo". Available online at <<http://cgpl.iisc.ernet.in>>. Accessed 12 April 2009.
- Chen, G.; Andries, J.; Luo, Z.; Spliethoff, H. (2003). *Journal of Energy Conversion and Management*, 44, 1875-1884.
- Cheryan, M.; Rajagopalan, N. (1998). *Journal of Membrane Science*, 151(1), 13-28.

- Chiaramonti, D. ; Bonini, M. ; Fratini, E. (2003). *Biomass Bioenergy*, 25, pp. 85-99 and pp. 101-111.
- Chiaramonti, D.; Bonini, M.; Fratini, E.; Tondi, G.; Gartner, K.; Bridgwater, A.V.; Grimm, H.P.; Soldaini, I.; Webster, A.; Baglioni, P. (2003a). *Biomass and Bioenergy*, 25, 101-111.
- Chouchene, A.; Jeguirim, M.; Khiari, B.; Zagrouba, F.; Trouve, G. (2010). *Resources Conservation and Recycling*, 54, 271-277.
- Chum, H.L.; Kreibich, R.E. (1993). Patent: U.S. Patent 5,091'499.
- Coats, A.W.; Redfern, J.P. (1965). *Journal of Polymer Science Part B*, 917-920.
- Cole, A.C.; Jensen, J.L.; Weave, J.; Forbes, D.C.; Davis, J.H.J. (2002). *Journal of American Chemical Society*, 124, 5962-5963.
- Coulter, J.A.; Nafziger, E.D. (2008). *Agron Journal*, 100, 1774-1780.
- Cuevas, A.; Reinoso, C.; Scott, D.S. (1995). Pyrolysis oil production and its perspectives. In: *Proc. Power production from biomass 2*, Espoo, VTT.
- Cuevas, A. (1993). Proceedings of EC JOULE Contractors Meeting, Athens, June 1993.
- Czernik, S.; Bridgwater, A. V. (2004). *Energy Fuels*, 18, 590-598.
- Czernik, S. (2002). Review of fast pyrolysis of biomass, 1617 Cole Boulevard, Golden, CO80401.
- Czernik, S.; Johnson, S.; Black, S. (1994). *Biomass and Bioenergy* 7(1-6), 187.
- Czernik, S.; Scahill, J.W.; Diebold, J. (1993). *Proceedings of the 28th Intersociety Energy Conversion Engineering Conference, American Chemical Society*, 429-436.
- Darmstadt, H.; Garcia-Perez, M.; Chala, A.; Cao, N.Z.; Roy, C. (2001). *Carbon*, 39, 815-825.
- Darnoko, D.; Cheryan, M.; Perkins, E.G. (2000). *Journal of liquid chromatography RT*, 23, 2327-2335.
- Das, P.; Ganesha, A.; Wangikarb, P. (2004). *Biomass and Bioenergy*, 27, 445-457.
- De Boer, J.H.; Lippens, B.C.; Linsen, B.G.; Brokhoff, J.C.P.; Van Der Heuvel, A.; Osinga, T.J. (1966). *Journal of Colloid Interface Science*, 21, 405-414.
- Dermibas, M.F. (2009). *Applied Energy*, 86, S151-S161.
- Dermibas, A. (2002). *Energy Exploration and Exploitation*, 20(1), 105-111.
- Demirbas, A. (2001a). *Energy Conversion and Management*, 42(2), 183-188.
- Demirbas, A. (2001b). *Energy Conversion Management*, 42(11), 1357-1378.
- Demirbas, A. (2000a). *Energy Conversion and Management*, 41, 633-646.

- Demirbas, A. (2000b). *Energy Education Science Technology*, 5, 21-45.
- Demirbas, A. (1997). *Fuel*, 76(5), 431-434.
- Devnarain, P.; Arnold, D.; Davis, S. (2002). *Proceedings of South African Sugar technologists Assosiation*, 76, 477- 489.
- Di Blasi, C. (2008). *Progress in Energy and Combustion Science*, 34, 47-90.
- Di Blasi, C.; Branca, C.; Galgano, A. (2007). *Industrial and Engineering Chemistry Research*, 46, pp. 430.
- Di Blasi, C. (2002). *Aiche Journal*, 48, 2386-2397
- Diebold, J.P. (2000). Report number: NREL/SP-570-27613, *National Renewable Energy Laboratory*, Colorado, USA.
- Diebold, J. (1999). *A handbook-volume 1-CPL Press*, 135-163.
- Diebold, J.P.; Czernik, S., (1997). *Energy and Fuels*, 11, pp. 1081.
- Diebold, J.P.; Scahill, J.; Czernik, S.; Philips, S.D.; Feik, C.J. (1996). In: Bridgwater and E.N., Hogan, eds., *CPL Scientific Information Services, Ltd*, Newbury, UK, pp 66-81.
- Diebold, J.P. (1994). *Biomass and Bioenergy*, 7, 69-74.
- Diebold, J.P.; Czernik, S.; Scahill, J.W.; Philips, S.D.; Feik, C.J. (1993). Report number: NREL-CP-430-7215, 90–108. In: Milne, T.A. (Ed.), *Biomass Pyrolysis Oil Properties and Combustion Meeting*.
- Domburg, G.; Rossinskaya, G.; Sergseva, V. (1974). In: *Proceedings of the 4th International Conference on Thermal Analysis*, Budapest, Vol. 2 pp. 221.
- Doshi, V.A.; Vuthaluru, H.B.; Bastow, T. (2005). *Fuel Processing Technology*, 86(8), 885-895.
- Drozd, J.J. (1975). *Journal of chromatography*, 113, 303-305.
- Drummond, A.R.F.; Drummond, I.W. (1996), *Industrial and Engineering Chemistry Research*, 35, 1263-1268.
- Dürre, P. (1998). *Annals of the New York Academy of Sciences*, 353-362.
- Duvvuri, M.S.; Muhlenkamp, S.P.; Iqbal, K.Z.; Welker, J.R. (1975). Report number: CONF-750458-4. *Conference-Joint states section of the combustion institute*, San Anonio, TX, USA.
- Edwards, W.; Smith, D. (2008). Report number: File A3-10. Available at <http://www.extension.iastate.edu/publications/FMI698>. Iowa State University. Accessed date 13 Nov 2009.
- Elliott, D. (1994). *Biomass bioenergy*, 7, 179-185.

- Encinar, J.M.; Gonzalez, J.F.; Gonzalez, J. (2000). *Journal of Fuel Processing Technology*, 68, 209-222.
- EurActive, 2008. Available at: <http://www.euractive.com/eu/climate-change/industry-set-win-eu-climate-concessions/article-178003>. Accessed date 18 Nov 2008.
- Ezeji, T.; Qureshi, N.; Blaschek, H.P. (2007). *Process Biochemistry*, 42(1), 34-39.
- Ezeji, T.C.; Qureshi, N.; Blaschek, H.P. (2005). *Journal of Biotechnology*, 115(2), 179-187.
- Faaij, A. (2006). *Springer*, 147-170.
- Fahmi, F.; Bridgwater, A.V.; Donnison, I.; Yates, N.; Jones, J.M. (2008). *Fuel* 87, 1230-1240.
- Feng, J.; YuHong, Q, Y.; Green, A.E.S. (2005). *Biomass and Energy*, 30(5), 486-492.
- Fernandez, A, R. (2010). Fast pyrolysis pilot plant: bio-oil and char production from biomass, PYNE newsletter 26, 8-10, June. Aston university Bioenergy Research Group, Available on PyNe: www.pyne.co.uk.
- Fraga, A.R.; Gaines, A.F.; Kandiyoti, R. (1991). *Fuel*, 70, 803-809.
- Freel, B.; Graham, R.G. (2002). Patent: *US Patent* 6, 485, 841.
- Freel, B. A.; Graham, R. G.; Huffman, D. R. (1996). In: Bio-oil Production and Utilisation; Bridgwater, A. V.; Hogan, E.; Eds., CPL Press, Newbury, UK, pp. 86-95.
- Freeman, E.S.; Carroll, B. (1958). *Journal of Physical Chemistry*, 62, 394-397.
- Friedmann, J.H. (1964). *Journal of Polymer Science*, 6, 183.
- Fushimi, C.; Arak, K.; Tsutsumi, A. (2003). *Industrial and Engineering Chemistry Research*, 42, 3920-3930.
- Garcia-Perez, M.; Adams, T.T.; Goodrum, J.W.; Das, K.C.; Geller, D.P. (2010). *Bioresource Technology*, 101(15), 6219-6224.
- Garcia-Perez, M.; Wang, X.S.; Shen, J.; Rhodes, M.J.; Tian, F.; Lee, W.J.; Wu, H.; Li, C. (2008). *Industrial Engineering and Chemistry Research*, 47, 1846-1854.
- Garcia-Perez, M.; Chala, A.; Roy, C.J. (2002). *Analytical and Applied pyrolysis*, 65, 111-136.
- Garcia-Perez, A.; Chala, A.; Yang, J.; Roy, C. (2001). *Fuel*, 80, 1245-1258.
- Garrote, G.; Cruz, J.M.; Dominguez, H.; Parajo, J.C. (2003). *Journal Chemical Technology and Biotechnology*, 78, 392-398.
- Gasparovic, L.; Korenova, Z.; Jelemensky, L. (2009). *36th International Conference of SSCHE*, May 25-29, Slovak.

- Gaur, S.; Reed, T.; Marcel, D. (1998). Data for natural and synthetic Fuels. Available at <http://www.woodgas.com/proximat.htm>. Accessed date 12 March 2010.
- Gibb, W.H. (1983). International conference corrosion resistant materials for coal conversion, *Applied science publishers*. pp. 25-45.
- Girard, P.; Fallot, A.; Dauriac, F. (2005). Available at: http://hq.unep.org/stapgef/documents/Wshop_do_cs/liquid_bio-fuels_2005. Accessed date 13 May 2009.
- Giroux, R.; Freel, B.; Graham, R. (2001). Patent number: *U.S. Patent 6,326,461*.
- Goudriaan, F.; Peferoen, D.G.R. (1990). *Chemical Engineering Science*, 45, 2729-2734.
- Goyal, H.B.; Seal, D.; Saxena, R.C. (2006). *Renewable and Sustainable Energy Reviews*, 12, 504–517.
- Graboski, M.; Bain, R. (1981). In: Reed TB, Editor, Biomass gasification: principles and technology, *Noyes Data Corporation*, New Jersey, USA, 154-182.
- Grieco, P.A. (1998). *Blackie Academic and Professional*, London, New York, pp. 310.
- Grønli, M.G.; Va' rhegyi, G.; Di Blasi, C. (2002). *Industrial and Engineering Chemistry Research*, 41, 4201–4208.
- Gronli, M., (2000). *Energy and Fuels*, 14(4), 791-800.
- Grønli, M. (1996). P.hD Thesis, *Norwegian University of Science and Technology*, Norway.
- Guieze, P.; Williams, J.M. (1984). *Journal of Chromatography*, 312, 261-272.
- Gülde, L. (1986). *Journal of Engineering for Gas Turbines and Power*, 108, 376–380.
- Guo, X.Y.; Yan, Y.J.; Ren, Z.W. (2003). *Acta Energiæ Solaris Sinica*, 124(12), 206–212.
- Gust, S. (1997). Combustion Experiences of Flash Pyrolysis Fuel in Intermediate Size Boilers, in: *Developments in Thermochemical Biomass Conversion* (Eds. A. V. Bridgwater, D. G. B. Boocock), Blackie Academic & Professional, London, 1997, pp. 481-488
- Hagge, M.J.; Bryden, K.M. (2002). *Chemical Engineering Science*, 57, 2811-2823.
- Hall, D.O.; Rosillo-Calle, F. (1991). *Proceedings of the Sixth E.C. Conference in biomass for Energy, Industry and Environment*, Woods Journal, London, pp. 89.
- Han, J.T. (1998). Available at: <http://www.fpl.fs.fed.us/documents/pdf1998/han98a.pdf>. Accessed date 23 September 2009.
- Harmer, M.A.; Sun, Q. (2001). *Applied Catalysis A: General*, 221(1-2), 45-62.

- Harmer, M.A.; Sun, Q.; Vega, A.J.; Farneth, W.E.; Heidekun, A.; Hoederich, W.F. (2000). *Green Chemistry*, 2(1), 7-14.
- Harmer, M.A.; Farneth, W.E.; Sun, Q. (1996). *Journal of the American Chemical Society*, 118(33), 7708-7715.
- Hayes, D. (2008). *Catalysis today*, 142, 138-151.
- Haykiri-Acma, H.; Yaman, S.; Kucukbayrak, S. (2006). *Renewable Energy*, 31, 803-810.
- He, B.J.; Zhang, Y.; Funk, T.L.; Rutkowski, G.L.; Yin, Y. (2000). *Transactions of American Society of Agricultural Engineering*, 43(6), 1827-1833.
- Heisler, M.P. (1946). *Trans ASME*, 69, pp. 227.
- Henrich, E.; Dahmen, N.; Dinjus, E. (2009). *Biofuels bioprod bioref*, 3, 28-41.
- Henrich, C. (2007). 2nd European summer school on Renewable Motor Fuels Warsaw, Poland, August 2007.
- Hernando, J. ; Leton, P. ; Matia, M.P. ; Novella, J.L. ; Alvarez-Builla, J. (2007), *Fuel*, 86, 1641–1644.
- Herold, I. (2007). *New Energy Finance Ltd*. Available at: <http://www.newenergyfinance.com>. Accessed 14 January 2009.
- Hesse, A.; Smit, J.M.; du Toit, J.F. (2001). Patent number: US 6312655, Sasol Technology (Pty) Ltd, South Africa.
- Hilten, R.N.; Bibens, B.P.; Kastner, J.R.; Das, K.C. (2010). *Energy Fuels*, 24, 673-682.
- Himmelblau, A. (1991). Patent number: U.S.Patent 5,034,498.
- Hisham, F.M.; Eid, M. A. (2008). Available at: <http://www.imc-egypt.org/studies/fullreport/lignocellulosic>. Accessed 19 April 2010.
- Huber, G.W.; Dumesic, J.A. (2006). *Catalysis Today*, 111(1-2).
- Hogan, E. (2002). Bio-oil Briefing workshop, August 16, 2002. Concord, New Hampshire. *CANMET Energy Technology Centre, Natural Resources Canada, Ontario, Canada*.
- Hugo, T. (2010). Masters Thesis, *University of Stellenbosch*, South Africa.
- Holcapek, M.; Jandera, P.; Fischer, J.; Prokes, B. (1999). *Journal of Chromatography A*, 858, 13-31.
- Hopkins, C. (2008). (*North Carolina State University*), and James, J.; (*Agri-Tech Producers, LLC*), Available at

:<http://www.scbiomass.org/Publications/TorrefiedWoodPresentation_208>. Accessed date 18 December 2009.

IEA Bioenergy. (2003). Available at http://www.pyne.co.uk/?_id=76. Accessed date 15 May 2009.

Igathinathane, C.; Pordesimo, L.O.; Womac, A.R.; Sokhansanj, S. (2009). *Applied Engineering in Agriculture*, 25(1), 65-73.

Javaid, A.; Ryan, T.; Berg, G.; Pan, X.; Vispute, T. (2010). *Journal of Membrane Science*, 363, 120-127.

Jenkins, B.M.; Baxter, L.L.; Miles, T.R. (1998). *Fuel Processing Technology* 54, 17-46.

Jenkins, B.M. (1993). In: Biomass energy fundamentals, Report number: EPRI TR-102107, *Electric Power Research Institute*, Palo Alto, California.

Jenkins, B.M.; Ebeling, J.M. (1985). *Symposium energy from biomass and waste*, pp. 371.

Johnson, E. (2009). *Environmental Impact Assessment Review*, 29, 165-168.

Jun, S.; Xiao-Shan, W.; Mauel, G.D.M.; Rhodes, M.; Chun-Zhu, I. (2009). *Fuel*, 88(10), 1810-1817.

Jung, S.; Kang, B.; Kim, J. (2008). *Journal of Analytical and Applied pyrolysis*, 82(2), 240-247.

Junming, X.; Jianchun, J.; Yunjuan, S.; Yanju, L. (2008). *Biomass and Bioenergy*, 32, 1056-1061.

Kang, B. S.; Lee, K. H.; Park, H. J.; Park, Y. K.; Kim, J. S. (2006). *Journal of Analytical and Applied pyrolysis*, 76, 32-37.

Karaosmanoglu, F.; Tetik, E.; Gollu, E. (1999). *Fuel Processing Technology*, 59(1), 1-12.

Karimi, E.; Gomez, A.; Kycia, S.W.; Schlaf, M. (2010). *Energy Fuels*, 24(4), 2747-2757.

Kawser, J.; Hayashi, J.; Li, C.Z. (2004). *Journal of Fuel*, 83, 833-843.

Kelly, S.; Wang, X.; Myers, M.; Johnson, D.; Scahill, J.; Bridgwater, A.V.; Boocock, D.G.B. (1997). Eds. *Blackie Academic and Professional*, London, 557-572.

Kersten, S. R. A.; Wang, X.; Prins, W.; Swaaij, W. P. M. (2005). *Industrial and Engineering Chemistry Research*, 44, 8773-8785.

Klass, D. L. (1998). *Academic Press*, pp. 91-157 and pp. 495-542.

Kluwer. 2005. Engineering data. *Nassau*, Bahamas.

Knothe, G. (2000). *Jaocs*, 77, 489-493.

Kumar, G.; Panda, A.K.; Singh, R.K. (2010). *Journal of Fuel Chemistry and Technology*, 38(2), 162-167.

- Kumar, A.; Wang, L.; Dzenis, Y.A.; Jones, D.D.; Hanna, M.A. (2008). *Biomass and Energy*, 32, 460-467.
- Kurkela, E.; Stahlberg, P.; Laatikainen, J.; Simell, P. (1993). *Bioresource Technology*, 46, 37-47.
- Lange, S. (2007). P.hD Thesis, Karlsruhe University, Germany.
- Lapuerta, M.; Hernandez, J.J.; Rodriguez, J. (2004). *Biomass and Bioenergy*, 27(4), 385-391.
- Leask, W.C.; Daynard, T.B. (1973). *Canadian Journal of Plant Science*, 515-522.
- Leech, J. (1997). Running a Dual Fuel Engine on Pyrolysis Oil, in: *Biomass Gasification and Pyrolysis, State of the Art and Future Prospects* (Eds. M. Kaltschmitt, A. V. Bridgwater), CPL Press, Newbury, UK, 1997, pp. 495-497.
- Li, X.Z.; Wu, M.J.; Eli, A. (2008). *Journal of Molecular Catalysis A: Chemical*, 279, 159-164.
- Li, S.; Xu, S.; Liu, S.; Yang, C.; Lu, Q. (2004). *Fuel Processing Technology*, 85(8-10), 1201-1211.
- Li, L. H.; Zhang, J. (2003). *Fuel*, 82, 1387-1397
- Liang, X. H.; Kozinski, J. A. (2000). *Fuel*, 79, 1477.
- Lima, M.I.; Boateng, A.A.; Klasson, K.T. (2010). *Journal of Chemical Technology and Biotechnology*, 85(11), 1515-1521.
- Linden et al.; Li, J.; Henriksson, G.; Gellerstedt, G. (2005). *Biochemistry and Bioengineering*, 125, 175-188.
- Lindfors, C. (2009). Report Number: FI-02044 VTT. The 2nd Nordic wood Biorefinery Conference, September 2009, VTT Technical Research Centre of Finland, Finland.
- Liu, D.J.; Robbins, G.S.; Pomeranz, Y. (1974). *Cereal Chemicals*, 51, 309-315.
- Liu, J.; Fan, L.; Seib, P.; Friedler, F.; Bertok, B. (2006). *Industrial and Engineering Chemistry Research*, 45(12), 4200-4207.
- Loneragan, J.F.; Robson, A.D.; and Graham, R.D. (1981), Eds., *Academic Press, New York*, pp. 165.
- Luangkiattikhun, P.; Tongsathitkulchai, C.; Tongsathitkulchai, M. (2008). *Bioresource Technology*, 99, 986-997.
- Lynd, L.R.; Wyman, C.E.; Gerngross, T.U. (1999), *Biotechnology Progress*, 15(5), 777-793.
- Ma, L.; Jones, J.M.; Pourkashanian, M.; Williams, A. (2007). *Fuel*, 1959-1965.
- Mahfud, F.H.; Melian-Cabrera, I.; Manurung, R.; Heeres, H.J. (2007). *Process Safety and Environmental Protection*, 85(5), 466-472.
- Maiti, S.; Purakayastha, S.; Ghosh, B. (2007). *Fuel*, 86, 1513-1518.

- Mani, T.; Murugan, P.; Abedi, J.; Mahinpey, N. (2010). *Chemical Engineering Research and Design* 88, 952-958.
- Mani, S.; Tabil, L.G.; Sokhansanj, S. (2006). *Bioresource and Technology*, 97, 1420-1426.
- Maniatis, K.; Baeyens, H.; Peeters, H.; Roggeman, G. (1993). In: Bridgwater, A.V.; (Ed) *Advances in Thermochemical Biomass Conversion*, Blackie, pp. 1257-1264.
- Mansaray, G.K.; Ghaly, A.E. (1999). *Biomass and Energy*, 17, 19-31.
- Marrero, T.M.; McAuley, B.P.; Sutterlin, W.R.; Morris, S.; Manahan, S.E. (2004). *Waste management*, 24(2), 193-198.
- Matthews, J. A. (2008). *Energy policy*, 36(3), 940-945.
- McCarthy, J.; Islam, A. (2000). In: *Historical, biological and materials perspectives*; Glasser, W.G.; Northey, R.A.; Schultz, T.P.; ACS Symposium Series 792; American Chemical Society; Washington, DC, pp. 2-100.
- McKendry, P. (2002). *Bio-resource Technology*, 83, 37-46.
- McInnes, A.G.; Ball, D.H.; Cooper, J.P.; Bishop, C.T. (1958). *Journal of Chromatography*, 1, 556-557.
- Mertz, W.; Angino, E.E.; Cannon, H.L.; Hambidge, K.M.; Voors, A.W. (1974). Vol.1, Mertz, W.; Ed.; N.A.S.; Washington, D.C.; pp. 29.
- Meier, D. (2002). in: *Fast Pyrolysis of Biomass—A Handbook-Volume 2*. ed. By Bridgwater, A.V. CPL Press, UK.
- Meier, D. (1999). *A handbook-volume 1-CPL Press*, pp. 92-101.
- Meier, D.; Faix, O. (1999). *Bioresource Technology*, 68, 71-77.
- Meir, D.; Scholze, B.; Kaltschmitt, M.; and Bridgwater, A.V. (1997). Eds., CPL Press, Newbury, pp. 431-441.
- Mengeloglu, F.; Kabakci, A. (2008). *International Journal of Molecular Sciences*, 9(2), 107-119.
- Myers, D.K.; Underwood, J.F. (1992). Report number: AGF-003-92. *The Ohio State University Extension*. Available at <http://www.ag.ohiostate.edu/~ohioline/agf-fact/0003.html> . Accessed 15 December 2009.
- Miller, R. (1999). General Technology Report number: FPL-GTR-113. *Department of agriculture, forest service, Forest products laboratory, Madison, US*, pp. 463.

- Milne, T.A.; Elam, L.C.; Evans, R.C. (1997). Report number: IEA/H2/TR-02/001, NREL Golden, USA.
- Milosavljevic, I.; Suuberg, E.M. (1995). *Industrial and Engineering Chemistry Research*, 34, 1081-1091.
- Moffat, J.M.; Overend, R.P. (1985). *Biomass*, 7, 99-123.
- Mohan, D.; Pittman, C.U.; Steele, P.H. (2006). *Energy and Fuels*, 20, 848-889.
- Mojtahedi, W.; Kurkela, E.; Nieminen, M. (1991). *Journal of the energy institute*, 63, 95-100.
- Mojtahedi, W.; Backman, R. (1989). *Journal of the energy insitute*, 62, 189-196.
- Mojtahedi, W.; Kurkela, E.; Nieminen, M. (1987). *KemiaKemi*, 14, 835-840.
- Morf, P.O. (2001). P.hD Thesis, Swiss Federal Institute of Technology, Zurich, Switzerland.
- Morris, K.W.; Johnson, W.L. (2000). 1st world conference on biomass for energy and industry, Sevilla, Spain, 5-9 June 2000. *James and james (Sceince publishers)*, pp. 1519-1524.
- Misono, M.; Nojiri, N. (1990). *Applied Catalysis*, 64(1-2), 1-30.
- Mullen, C.A.; Boateng, A.; Goldberg, N.M.; Lima, I.M.; Laird, D.A.; Hicks, K.B. (2009). *Biomass and Bioenergy*, 34(1), 67-74.
- Naber, J.E. ; Goudriaan, F. ; Louter, A.S. (1997). *Proceedings 3rd Biomass of the Americas*, pp. 1651-1659.
- Namba, S.; Hosonuma, N.; Yashima, T. (1981). *Journal of Catalysis*, 72(1), 16-20.
- NationMaster.(2003). Available at<http://www.nationmaster.com/red/pie/agr_gra_cor_pro_agriculture-grains-corn-production. Accessed date 12 April 2010.
- Neff, W.E.; Jackson, M.A.; List, G.R.; King, J.W. (1997). *Journal of Liquid Chromatography and Related Technologies*, 20, 1079-1090.
- Nokkosmaki, M.I.; Kuoppala, E, E.T.; Leppamaki, E.A.; Krause, A.O.I. (2000). *Journal of applied Pyrolysis*, 55, 119-131.
- Nowakowski, D.J.; Jones, J.M.; Brydson, R.M.D. (2007). *Fuel*, 86(15), 2389-2402.
- Oasmaa, A.; Elliot, D.C.; Muller, S. (2009). *Environmental Progress and Sustainable Energy*, American Institute of Chemical Engineers, 28(3), 404-409.
- Oasmaa, A.; Kuoppala, E. (2008). *Energy and Fuels*, 22, 4245-4248.
- Oasmaa, A.; Sipila, K.; Solantausta, Y.; Kuoppala, E. (2005). *Energy and Fuels*, 19, 2556-2561.

- Oasmaa, A.; Meir, D. (2005). *Journal of Analytical Technology and Applied pyrolysis*, 73(2), 323-334.
- Oasmaa, A.; Kuoppala, E.; Selin, J.F.; Gust, S.; Solantausta, Y. (2004). *Energy and fuels*, 18(5), 1578-1583.
- Oasmaa, A.; Kuoppala, E. (2003). *Energy and Fuels*, 17, 1075-1084.
- Oasmaa, A.; Kuoppala, E.; Gust, S.; Solantausta, Y. (2003). *Energy and Fuels*, 17(1), 1-12.
- Oasmaa, A.; Gust, S.; McLellan, R.; Meier, D.; Peacocke, G.V.C. (2003a). *Pyrolysis and Gasification of Biomass and Waste - The Future for Pyrolysis and Gasification of Biomass and Waste: Status, Opportunities and Policies for Europe*. Strasbourg, FR, 30 Sept. - 1 Oct. 2002. Bridgwater, A.V., (Ed.). CPL Press, 161-168.
- Oasmaa, A.; Kuoppala, E.; Gust, S.; Solantausta, Y. (2003b). *Energy and Fuels* 17(1), 1-12.
- Oasmaa, A.; Meier, D. (2002). In: Bridgwater, A.V. Editor, *Fast Pyrolysis of Biomass: A Handbook vol. 2*, CPL Press, Newbury, Berkshire, pp. 23–40.
- Oasmaa, A.; Peacocke, C. (2001). *VTT Publication 450*, VTT. Espoo, Finland, pp 65 and pp 34.
- Oasmaa, A.; Czernik, S. (1999). *Energy and Fuels*, 13, 914-921.
- Oasmaa, A.; Leppämaäki, E.; Koponen, P.; Levander, J.; Tapola, E. (1997). *VTT Publication 306*, VTT. Espoo, Finland, pp 46 and pp 30.
- Oehr, K. (1995). Patent number: *U.S Patent 5,458, 803*.
- Oehr, K.H.; Scott, D.S.; Czernik, S. (1993). Patent number: *U.S. Patent 5,264,623*.
- Okuhara, T. (2002). *Chemical reviews*, 102(10), 3641-3665.
- Okuno, T.; Sonoyama, N.; Hayashi, J.; Li, C-Z.; Sathe, C.; Chiba, T. (2005). *Energy Fuels*, 19, 2164-2171.
- Onay, O.; Kockar, M. (2003). *Energy sources*, 25, 879-892.
- Ormrod, D., Webster, A. (2000). *Progress in Utilisation of Bio-Oil in Diesel Engines*, *PyNe Newsletter*, 10 (2000), Aston University, Birmingham, UK, p.15
- Othmer, K. (1980). *Encyclopedia of chemical technology, third edition*, 11, 347-60.
- Pach, M.; Zanzi, R.; Bjørnbom, E. (2002). *Proceedings of the Sixth Asia-Pacific International Symposium on Combustion and Energy Utilisation*, Kuala Lumpur, Malaysia, May 20–22.
- Pakdel, H.; and Roy, C. (1988). *American Chemical Society Symposia Series*, 376, 203-219.

- Park, Y-K.; Jong-Ki J.; Senngdo K.; Joo-Sik K. (2004). *American Chemical Society and Division of Fueland Chemistry*, 49(2), 800.
- Pattiya, A.; Titiloye, J.O.; Bridgwater, A.V. (2007). *Journal of Energy and Enviroment*, 08(2), 496-502.
- Pavish, J.H.; Hamre, L.L.; Zhuang, Y. (2010). *Fuel*, 89, 838-847.
- Peacocke, G.V.C.; Meier, D.; Gust, S.; Webster, A.; Oasmaa, A.; McLellan, R. (2003). Final report number: 4.1030/C/00-015/2000.
- Peacocke, G. V. C.; Russel, P. A.; Jenkins, J. D.; Bridgwater, A.V. (1994a). *Biomass Bioenergy*, 7, 169-178.
- Peacocke, G.V.C.; Meier, D.; Gust, S.; Webster, A.; Oasmaa, A.; McLellan, R. (1994b). EU Contract Nnmber: 4.1030/C/00-015/2000, Final report, 2003.
- Peacocke, G. V. C.; Madrali, E. S.; Li, C.-Z.; Guell, A. J.; Kandiyoti, R.; Bridgwater, A. V. (1994c), *Biomass Bioenergy*, 7(1-6), 155-167.
- Pendias, A.K.; Pendias, H. (2000). 3rd Edition, *CRC Press*, New York.
- Perez, M.; Chaala, A. ; Roy, C.J. (2002). *Analytical pyrolysis*, 65, 111-136.
- Pindoria, R.V.; Megaritis, A.; Herod, A.A., et al (1998). *Fuel*, 77(15), 1715-1726.
- Pindoria, R.V.; Lim, J-Y.; Hawkes, J.E. et al (1997). *Fuel*, 76(11), 1013-23.
- Pinho, O.; Peres, C.; Ferreira, M.P. (2003). *Journal of Chromatography*, 1011(1-2).
- Piskorz, J. (2002). A Handbook Vol. 2, Bridgwater, A.V., (ed.), *CPL Press*, Chippenham, UK, pp. 103-140.
- Piskorz, J.; Scott, D. S.; Radlien, D. (1988). *American Chemical Society*, 167-178.
- Poinot, P.; Grua-Priol, J.; Arvisenet, G.; Rannon, C.; Semenon, M.; Bail, A.L.; Prost, C. (2007). *Food Research International*, 40(9), 1170-1184.
- Pouzar, M.; Cernohorsky, T.; Krejcova, A. (2001). *Talanta*, 54, 829-835.
- Pralhad, A.G.; Gigi, G.; Jagannath, D. (2008) *Journal of Molecular Catalysis A: Chemical*, 279, 182-186.
- Prins, M.J.; Ptasinski, K.J.; Janssen, F.J.J.G. (2007). *Energy*, 32, 1248-1259.
- Prins, M. J.; Ptasinski, J. K.; Janssen, F. J. J. G. (2006). *Journal of Analytical and Applied pyrolysis*, 77, 35-40.
- Qi, Z.; Jie, C.; Tiejun, W.; Ying, X. (2007). *Energy Conversion and Management* 48, 87-92.

- Rabe, R.C. (2005). Masters' Thesis, Stellenbosch University, South Africa.
- Radlein, D.J.; Piskorz, J.; Majerski, P. (1996). (ed), Patent number: CA2165858. Available at <[http://: www.techtp.com](http://www.techtp.com)>. Accessed date 16 March 2009.
- Radlein, D.; Piskorz, J.; Scott, D.J. (1987). *Journal of Analytical and Applied pyrolysis*, 12, 39-51.
- Ramajo-Escalera, B.; Espina, A.; García, J.R.; Sosa-Arno, J.H.; and Nebra, S.A. (2006). *Thermochimica Acta*, 448, 111-116.
- Ravanchi, M.T.; Kaghazchi, T.; Kargari, A. (2009). *A review, Desalination*, 235(1-3), 199-244.
- Raveendran, K.; Ganesh, A. (1996). *Fuel*, 75(15), 1715-1720.
- Raveendran, K.; Ganesh, A.K.; Khilar, C. (1995). *Fuel*, 74, 1812-1822.
- Rios, L.A.; Weckes, P.P.; Schuster, H.; Hoelderich, W.F. (2005). *Applied Catalysis A: General*, 284(1-2), 155-161.
- Roel, J.M.; Westerhof, D.W.F.; Wim P. M.; Sacha, R.A. (2010). *Industrial and Engineering Chemistry Research*, 49, 1160-1168.
- Roque-Diaz, P. U.; Central University, Villas, L Zh. Shemet, C.V.; Lavrenko, V.A.; Khristich, V.A. (1985). *Thermochimica Acta*, 93, 349-352.
- Ross, J.R.H. (1975). *The Chemical Society*, London, 4, pp. 34.
- Rossi, C.; Graham, R. (1997). Fast Pyrolysis at ENEL, in biomass gasification and pyrolysis: State of the art and future prospects ed by Kaltschmitt, M.; Bridgwater, A.V. *CPL Scientific Ltd, Newbury, Berkshire, UK (1997)*.
- Rossi, C.; Graham, R.; Kaltschmitt, M.; Bridgwater, A.V.; Eds. (1997). *CPL Press, UK*, 300-306.
- Roy, C.; Pakdel, H. (2000). Patent number: *U.S. Patent 6,143,856*.
- Roy, C.; Pakdel, H.; Brouillard, D.; (1990). *Journal of Applied Polymer Science*, 41, 337-348.
- Rutkowski, P.; Kubacki, A. (2006). *Energy Conversion and Management*, 47(6).
- Sadiki, A.; Sky, W.K.; Halim, H.; Bekri, O. (2003). *Journal of Analytical and Applied pyrolysis*, 70, 427-435.
- Salter, L. (s.a). Available at http://www.streetdirectory.com/food_editorials/cuisines/international_cuisin/south_african_corn_and_small_grains.html. Accessed 13 April 2010.

- Sandvig, E.; Walling, G.; Brown, R.C.; Pletla, R.; Radlein, D.; Johnson, W. (2003). Intergrated pyrolysis combined cycle biomass power system concept definition Final Report, Report DE-FS26-01NT41353.
- Savage, W.J. (1940). Report number: Vol vi-No.3. Chemical and process Engineering resource.
- Scahill, J.; Diebold, J.P.; Feik, C. (2000). National renewable energy laboratory, USA.
- Scholl, S.; Klaubert, H.; Meier, D. (2004). Wood liquefaction by flash-pyrolysis with an innovative pyrolysis system.DGMK proceeding 2004-I contributions to DGMK-meeting, Energetic utilisation to Biomasses, April 19-21, 2004 Velen/Westf (2004).
- Scholze, B. (2002). P.hD Thesis, University of Hamburg, Hamburg, Germany, pp. 157.
- Scholze, B.; Meier, D. (2001). Journal of Analytical and Applied pyrolysis, 60, 41-54.
- Scott, D.S., et al. (1999). Journal of Analytical and Applied pyrolysis, 51, 23-37.
- Scott, D. S.; Piskorz, J. (1982). Canadian Journal of Chemical Engineering, 60, 666-674.
- Sensoz, S.; Demiral, I.; Gercel, H.F. (2006a). Journal of Bioresource Technology, 97, 429-436.
- Sensoz, S.; Kaynar, I. (2006b). Industrial Crops and Products, 23, 99-105.
- Shafizedah, F.; De groot, W. (1984). Journal of analytical and applied pyrolysis, 6, 217-232.
- Shafizedah, F. (1982). Journal of Analytical and Applied pyrolysis, 3, 283-305.
- Shafizadeh, F.; Degroot, W.G. (1976). Academic Press, New york, pp. 1-18.
- Shafizadeh, F. (1968). Advances in Carbohydrate Chemistry and Biochemistry, 23, 419-74.
- Sharma, R.K.; Wooten, J.B.; Baliga, V.L.; Lin, X.; Chan, W.G.; Hajaligol, M.R. (2004). *Fuel*, 83, 1469-1482.
- Sharma, R.K.; Bakhshi, N.N. (1989). Report number: 058sz-23283-8-6116. *Bio-energy Development Program, Energy, Mines and resources*, Canada, pp. 79.
- Shen, D.K.; Gu, S.; Bridgewater, A.V. (2010). *Journal of Analytical and Applied pyrolysis* 87, 199-206.
- Shen, J.; Wang, X.; Garcia-Perez, M.; Mourant, D.; Rhodes, M.J.; Zhu-li, C. (2009). *Fuel*, 88, 1810-1817.
- Shen, J. (1981). *Analytical Chemistry*, 53, 475-477.
- Sheng, D.K.; Gu, S.; Luo, K.H.; Brigdwater, A.V. (2009). *Energy and Fuels*, 23, 1081-1088.
- Sheng, C.; Azevedo, J.L.T. (2005). *BiomassandBioenergy*, 28, 499-507.
- Sheppard, S.E. (1930). *Journal of Physical Chemistry*, 34(5), 1041-1052.

- Shi, F.; Zhang, Q.H.; Li, D.M.; Deng, Y.Q. (2005). *European Journal of Chemistry*, 11, 5279-5288.
- Shuangning, X.; Weiming, Y.i.; Baoming, L.I. (2005). *Biomass Bioenergy*, (29), 135-141.
- Siau, J.F. (1984). *Springer Verlag*.
- Sims, R. E. H.; Bassam, N. E.; Overend, R. P.; Lim, K. O.; Liwn, K.; Chaturvedi, P. (2004). *Elsevier*.
- Sipilae, K.; Kuoppala, E.; Fagernas, L.; Oasmaa, A. (1998). *Biomass Bioenergy*, 14,103-113.
- Skoog, D.A. (1985). 3rd Ed, *New York: Saunders*.
- Sluiter, A.; Ruiz, R.; Scarlata, J.; Templeton, D. (2008). Technical report: NREL/TP-510-42619, *National renewable Energy Laboratory*.
- Smiglak, M.; Metlen, A.; Rogers, R.D. (2007). *Accounts of Chemical Research*, 40, 1182-1192.
- Smith, R.D.; Pert, R.M.; Liljedahl, J.B.; Barrett, J.B.; Doering.(1985). *Transactions of American Society of Agricultural and Biological Engineers*, 28(3), 937-942, 948.
- Solantausta, Y., Nylund, N.-O., Westerholm, M., Koljonen, T., Oasmaa, A. (1993). *Bioresource Technology*, 46 (1993), pp. 177-188
- Solo, M. L. (1965). *Aikakawsh*, 37, pp. 127
- Soltes, E. J.; Lin, J.-C.K. (2001). *In: Progress in Biomass Conversion; Tillman, D.*
- Soltes, E. J.; Elder, T. J.; Goldstein, I. S.; Ed. (1981). *CRC Press, Boca Raton, FL*, 63-95.
- Sonobe, T.; Worasuwanarak, N.; Pipatmanomai, S. (2008). *Fuel Processing Technology*, 89, 1371-1378.
- Stavarache, C.; Vinatoru, M.; Nishimura, R.; Maeda, Y. (2005). *Ultrasonics Sonochemistry*, 12, 367-372.
- Strenziok, R., Hansen, U., Künster, H. 2001). Combustion of Bio-Oil in a Gas Turbine, in: *Progress in Thermochemical Biomass Conversion* (Ed. A. V. Bridgwater), Blackwell Science, Oxford, UK, 2001, pp. 1452-1458.
- Sukiran, A.M.; Chow, M.C.; Nor, K.A. (2009). *American Journal of Applied sciences* 6(5), 869-875.
- Suppes, G.J.; Dasari, M.A.; Doskocil, E.J.; Mankidy, P.J.; Goff, M.J. (2004). *Applied Catalysis A General*, 257, 213-223.
- Swatloski, R. P.; Spear, S. K.; Holbrey, J. D.; Rogers, R. D. (2002). *Journal of American Chemical Society*, 124(18), 4974-4975.
- Tanabe, K.; Holderich, W.F. (1999). *Applied Catalysis A: General*, 181(2), 399-434.
- TAPPI (2011). Report number: T 684 om-06.

- Toft, A.J. (1996). PhD Thesis, *Aston University*, Birmingham, UK.
- Tola, V.; Cau, G. (2007). Report number: Piazza d'Armi, 09123. *University of Cagliari, Department of mechanical Engineering, Clean coal technologies*.
- Tortosa, M.; Buhre, B.J.P.; Gupta, R.P.; Wall, T.F. (2007). *Fuel Processing Technology*, **88**, 1071-1081.
- Toubul, Y. (2008). *Akalemiai kiado, co-published with springler science*, **91**, 641-647.
- Tratthnigg, B.; Mittelbach, M. (1990). *Journal of Liquid Chromatograph*, **13**, 95-105.
- Trautman, N.; Richard, T. (2007). *Cornell University Ithaca, New York*. Available at: <http://compost.css.cornell.edu/calc/lignin.noframes.html>. Accessed 5 November 2009.
- Trebbi, G. (1994). *ENEL, Private communication*, May 1994.
- Troxler, S. (s.a). North Carolina Department of Agriculture and Consumer. Available at www.agr.state.nc.us/drought/documents/corn_stover. Accessed 01 May 2010.
- Tsai, W.T.; Lee, M.K.; Chang, Y.M. (2007). *Bioresource Technology*, **98**, 22-28.
- Tsai, W.T.; Lee, M.K.; Chang, Y.M. (2006). *Journal of Analytical and Applied Pyrolysis*, **76**, 230-237
- Tsai, W.T.; Cheng, C.Y.; Lee, S.L.; Wang, S.Y. (2001). *Journal of Thermal Analysis and Calorimetry*, **63**, 351-357.
- Tsiantzi, S.; Athanassiadou, E. (2000). *PyNe Newsletter*, 10 November 2010.
- Tumuluru, J.S.; Wright, C.T.; Kenney, K.L.; Hess, J.R. (2010). Report Number: INL/CON-10-18636. *2010, ASABE Annual International Meeting*.
- Turkan, A.; Kalay, S. (2006). *Journal of Chromatograph A*, **1127**, 34-44.
- Turner, M. B.; Spear, S. K.; Holbrey, J. D.; Rogers, R. D. (2004). *Biomacromolecules*, **5**(4), 1379-1384.
- Uslu, A. (2008). Masters' Thesis, *Utrecht University*, Netherlands.
- Uzun, B.B.; Putun, A.E.; and Putun, E. (2007). *Journal of Analytical and Applied Pyrolysis*, **79**, 147-153.
- Vamvuka, D.; Kakaras, E.; Kastanaki, E.; Grammdis, P. (2003). *Fuel*, **82**, 1949-1960.
- Van de Velden, M.; Baeyens, J.; Brems, A.; Janssens, B.; Dewil, R. (2010). *Renewable Energy*, **35**, 232-242.
- Van Soest, P. J. (1964). *Journal of Animal Science*, **23**, 838-845.
- Varhegyi, G. (2007). *Journal of Analytical and Applied pyrolysis*, **79**, 278-288.

- Varhegyi, G.; Antal, M.J.; Jakab, E.; Szabo, P. (1997). *Journal of Analytical and Appliedpyrolysis*, 42, 73-87.
- Varhegyi, G.; Antal, M.J.; Szekely, T.; and Szabo, P. (1989). *Energy and Fuels*, 3, 329-335.
- Varhegyi, G.; Antal, M.J.; Szekely, T.; Till, F.; Jakab, E. (1988). *Energy and Fuels*, 2, 273-277.
- Venderbosch, R.H. (2010). *Society of chemical industry and John Wiley and sons*, 4, 178-208.
- Venderbosch, R.H.; Janse, A.M.C.; Radovanovic, M.; Prins, W.; Van Swaaij, W.P.M. (1997). *Pyrolysis of pine wood in a small integrated pilot plant rotating cone reactor*, in *Biomass Gasification & Pyrolysis, State of the art and future prospects*, ed by Kaltschmitt M and Bridgwater AV. CPL Scientific Ltd, Newbury, Berkshire, UK.
- Vutharulu, H.B. (2004). *Bioresource Technology*, 92(2), 187-195.
- Vyazovkin, S. (2006). *Journal of Thermal Analysis and Calorimetry*, 83, 45-51.
- Wagenaar, B.M.; Prins, W.; van Swaaij, W.P.M. (1994). *Chemical Engineering Science*, 49, 5109-5126.
- Welton, T., (1999). *Chemical Reviews*, 99, 2071-2083.
- Wenzl, H.F.J.; Brauns, F.E.; Brauns, D.A. (1970). *The Chemical Technology of Wood*. Academic Press, New York; pp. 1-692.
- White, L.P.; Plasket, L.G. (1981). *Academic Press, New York*, 123-133.
- Widyorini, R.; Xu, A.; Kawai, S. (2005). *Wood science*, 51, 648-654.
- Williams, P.T.; Horne, P.A. (1994). *Renewable Energy*, 4, 1-13.
- Williams, P.T.; Besler, S. (1993). *Fuel*, 72, 151-159.
- Xiong, W-M.; Zhu, M-Z.; Deng, L.; Fu, Y.; and Guo, Q-X. (2009). *Energy and Fuels*, 23, 2278-2283.
- Yaman, S. (2004). *Energy Conversion and Management*, 45(5), 651-671.
- Yang, H.; Yan, R.; Chen, H.; Lee, H.D.; Zheng, C. (2007). *Fuel*, 86(12-13), 1781-1788.
- Yang, H.P.; Van, R.; Chen, H.P.; Zheng, C.G.; Ho, L.; Tee, L.D. (2006). *Energy Fuel*, 20, 388-393.
- Yanik, J.; Kornmayer, C.; Saglam, M.; Yüksel, M. (2007). *Fuel Processing Technology*, 88, 942-947.
- Yoichiro, H.; Hiroki, N.; Mika, K.; Toshihisa, S.; Xi, X.; and Kuniko, Y. (1998). *Analytical Biochemistry*, 265, 42-48.

- Yu, F.; Ruan, R.; Steele, P. (2008). American Society of Agricultural and Biological Engineers, 51(3),1023-1028.
- Zabaniotou, A.; Ioannidou, O.; Antonakoub, E.; Lappasb, A.(2008). *International Journal of Hydrogen Energy*, 33, 2433-2444.
- Zabaniotou, A.; Skoulou, V.; Karagiannidis, A. (2007). *Proceedings of the 11th International Waste Management and Landfill Symposium*, Sardinia, Italy, 2007.
- Zanzi, R.; Krister, S.; Bjornbo, E. (1996). *Fuel*, 75(5), 545-550.
- Zhang, H.; Xiao, R.; Huang, H.; Xiao, G. (2009). *Bioresource Technology*, 100, 1428-1434.
- Zhang, B.; Keitz, M.V.; Valentas, K. (2008). *Biotechnology and Bioengineering*, 101(5), 903-912.
- Zhang, H.B.; Xu, F.; Zhou, X.H. (2007). *Green Chemistry*, 9, 1208-1211.
- Zhang, S.P.; Yongjie, Y.; Li T, et al.(2005). *Bioresource Technology*, 96, 545-550.
- www.btgworld.com (January 2011).
- www.dynamotive.com (February 2009).
- www.exxonmobil.com (May 2010).
- www.itc-cpv.kit.edu(August 2009).
- www.pyne.co.uk (January 2010).
- www.solcomhouse.com/fossilfuels.htm

Appendices

Appendix A: Cooling liquid properties (www.exxonmobil, 2010)

Properties	Values
Density	750kg/m ³
Flash point	>40 °C
Auto ignition temperature	365 °C
Boiling point range	155-179 °C
Vapour pressure (20 °C)	0.195kPa
Solubility in water	Negligible
Viscosity (40 °C)	1.21cSt
C _p (10 °C)	2.013kJ/kg ⁰ C
Heat of vaporisation (1.2 bar/10 ⁰ C)	1942.2kJ/kg

Appendix B: Fast pyrolysis operating procedures

Safety, health and environment

This is to ensure safe, efficient and environmentally friendly operation of the fast pyrolysis plants. Bio-oil is a corrosive substance which can affect the human skin in case of contact and destroy vegetation as well. The bio-oil spillages can pollute ground water. Any spillages should be contained. Biomass has got a lot of dust. Protective clothing to suit the dust hazard, liquid hazard or heat hazard in each section is to be used i.e. laboratory coat, closed shoes, gloves, goggles and respirators.

Scope

The procedures and work instructions that follow apply to the bubbling fluidised bed at Stellenbosch University, Department of Chemical Engineering and twin screw reactor at Karlsruhe Institute of Technology, Germany for the production of bio-oil, biochar and gas.

Operating procedures for BFBR

Preparation of a process run:

- Analysis of the biomass feed in terms of ash and moisture contents.
- Calibrate feeder for the type of biomass. Run continuously for 5min in duplicates and take average flow rates at each power setting (20%, 50% and 80%).
- Check if the pressure in the N₂ cylinder (>10000 kPa) is high enough to complete a process run.
- Weigh the electro-precipitators, tower top, char pots, cyclones and Teflon section before each run.
- Assemble the units lubricating stainless steel fittings with Ni-spray and electro-precipitators and Teflon sections using vaseline and teflon thread.
- Add sand (400-500 g) to the reactor and connect the feeder to the reactor using a gasket connection.
- Test for leaks in the system at high N₂ flow rate of 8m³/hr.
- Connect the thermocouples and assemble the oven with a fibre glass insulation seal.

Starting the process:

- Switch on the oven and wait to reach equilibrium at around 500 °C and it will take 1-2hours.

- Add the biomass to the feeder and flush out the system with N₂ gas for 3 minutes at 0.5 m³/hr.
- When the oven is close to the set temperature, open the water from the chiller to flow into the sink and switch on the chiller.
- Once the oven is at set temperature, increase the N₂ flow at a flow rate of 2.4-4m³/hr.
- Start the isopar flow at 1.8-3kPa pressure.
- Attach the pipe heater between the reactor and condenser and set the temperature at 400 °C using a rope heater.
- Insert a memory device to store process data, check the system for leaks and start the electrostatic precipitators voltages 15kV and 12kV respectively for electrostatic precipitators 1 and 2.
- When the temperature difference between T3 (reactor middle temperature) and T4 (reactor top temperature) is less than 10 °C, start the biomass feeder at calibrated feeding rate.
- Monitor the process during experiment and check if the gas is being vented through a sucking fan into the atmosphere.
- Once all the biomass has been fed, continue feeding for five minutes.
- Reduce N₂ flow to 0.5m³/hr maintaining the inert atmosphere during cooling.
- Switch off the chiller and electrostatic precipitators.
- Remove memory device and open the oven top when the temperature is below 300 °C.
- Switch off N₂ flow when the temperature in the reactor is below 100 °C.

Recovering the products:

- Collect the bio-oil from the reservoir and separate the isopar from the bio-oil using the conical separating flask.
- Clean the condenser components and electrostatic precipitators with acetone.
- Weigh the dirty condenser components and electrostatic precipitators after cleaning with acetone.
- Leave the bio-oil and acetone mixtures for at least 12 hours to evaporate acetone.
- Weigh the biochar from the cyclones, char pots and the sand after the reaction.

Operating procedures for the LTSR

Preparation of a process run:

- Choose the best feeding screw and calibrate feeder for the type of biomass. Run continuously for 30 minutes in duplicates and take average flow rates at each power setting.
- Check if the pressure in the N₂ pressure is high enough to complete a run on the feeding unit and reactor.
- Weigh the biochar collecting containers and bio-oil bottles before each run.
- Assemble the units by closing the reactor, bucket elevator and feeding hopper.
- Add 40kg of stainless steel balls to the reactor.

Starting the process:

- Start heating and wait for the temperature to be above 500 °C in the reactor.
- Add the biomass to the feeder when the temperature in the reactor is above 500 °C.
- When the temperature of the reactor is close to 500 °C, open the chillers on both condensers.
- When the temperature difference between T3 (reactor middle temperature) and T4 (reactor top temperature) is less than 10 °C start the biomass feeder at calibrated feeding rate.
- Monitor the process during experiment and check if there are no leakages in the system.
- After every hour, remove the biochar through the first condenser using a flapping valve and after every 30 min command the control system to print out a gas composition from the Gas Chromatography (GC).
- Once all the biomass has been fed, continue feeding for 10 more minutes to ensure all the biomass in the system reacted.
- Stop the two chillers and switch off the electrostatic precipitators.

Recovering the products:

- Collect the bio-oil from the second condenser, weigh and store in glass bottles.
- Clean the condenser components and electrostatic precipitators with acetone.
- Weigh the dirty condenser components and electrostatic precipitators after cleaning with acetone.
- Leave the bio-oil and acetone mixtures for at least 12 hours for the acetone to evaporate.
- Weigh the biochar from the buckets, bucket elevator and in the reactor.

Appendix C: Analytical standards methods procedure for analysis.

Analysis	Karlsruhe Institute of Technology, Germany	University Of Stellenbosch, South Africa
Proximate Analysis: (wt. %) Ash Moisture Volatiles Fixed Carbon (By difference)	Oven dry method and TGA CEN/TS 14775:2004-11 for ash DIN CEN/TS 14774-1:2004-11 for moisture	Oven dry method and TGA ASTME1755-01 for moisture
Elemental Analysis: (wt. %) C H N S O (By difference) Cl	DIN CEN/TS 15104:2005-10 DIN CEN/TS 15104:2005-10 DIN 22022-1:2001-02 - DIN CEN/TS 15289:2006-07	NIST and SARM Certified Standards
Heating values: (MJ/kg) Higher heating value (HHV) Lower heating value (LHV)	Calorimeter DIN CEN/TS 14918:2005-08	 DIN CEN/TS 14918:2005-08
Bulk densities: (kg/m³) Tapped density Freely settled	 GEA niro analytical method A 2	
Ash composition XRF (wt. %) AAS (ppm) -(As, Cd, Co, Cr, Cu, Hg, Mn, Mo, Ni, Pb, Sb, V, Zn, Se, Sn and Ti) AAS (ppm) -Hydrid (Sb, As, Se, Te and Hg) AAS (ppm) -Hydrid (Boron) ICP (wt. %)	DIN 51729-10 DIN 22022-3:2001-02 DIN 22022-4:2001-02 DIN EN ISO 11885(E22):1998-04 DIN 51 729	
Lignocellulosic composition: (wt. %) Extractives Lignin	ASTM E1690 Tappi T222 om-88 Institut du Bois'standard Method	

Cellulose Holocellulose	Institut du Bois' standard Method Institut du Bois' standard Method	
Bio-oil analysis methods		
Ash content (wt. %)	DIN CEN/TS 14775:2004-11	DIN CEN/TS 14775:2004-11
Water content (wt. %)	Karl-Fischertitration: ASTM D 1744	ASTM D 1744
COD (wt. %) TOC (wt. %)	Oxidation correlation: DIN ISO 15705 DIN EN 1484	Bomb calorimeter: ASTM D 3286-91a
Elemental analysis (wt. %): C H N S O*		DIN 38402 A5I DIN 38402 A5I *By difference
pH	E70-07	E70-07
Char extraction	Methanol Extraction: DIN 51721	

Appendix D: Heating value determination from bomb calorimeter

Procedure

1. Rinse the inside of the bomb and add 2 litres of distilled water to the calorimeter bucket. Place the crucible in the bomb. The fuse wire should be in contact with the sample.
2. With the sample and fuse thread in place, close the bomb, and add oxygen to a consistent pressure of 30 bars. Use the same pressure for calibration and the actual tests.
3. Adjust the calorimeter water temperature to 1-1.4 °C below room temperature.
4. Transfer the bomb to the calorimeter. Make sure the bomb is gas tight, and connect it to the firing circuit. Close the cover and start the experiment.
5. The initial calorimeter temperature is recorded as t_a , and the wetted thermometer length or scale reading to which the thermometer is immersed (L). The final temperature attained in the calorimeter is recorded as (t_f) and the room temperature (R) observed 5 minutes after firing the charge.
6. Remove the bomb and release the pressure at a uniform rate such that the operation will require not less than a minute. Examine the bomb interior for evidence of incomplete combustion. Discard the test if unburnt sample or sooty deposits are found.

7. Calculation:

(a) Corrected temperature rise

Calculate the corrected temperature rise, as follows:

$$t = t_f - t_a + t_s$$

Where t = corrected temperature rise, °C

t_f = final temperature at which three successive readings at 60 minute intervals are the same, corrected in accordance with the calibration certificate of the thermometer, °C.

t_a = temperature when the charge was fired, corrected in accordance with the calibration certificate of the thermometer, °C.

And

$$t_s = \text{Emergent stem correction} = Kd(t_a + t_f - L - R), \text{ } ^\circ\text{C}$$

Where

$$K = 0.00016, \text{ } 1/^\circ\text{C}$$

d = temperature rise ($t_f - t_a$), $^{\circ}\text{C}$

L = Scale reading to which the thermometer was immersed, $^{\circ}\text{C}$. This should be constant for bomb calorimeter calibration and each subsequent sample analysis.

R = Room temperature, $^{\circ}\text{C}$

(b) Titration correction

Determine the heating value due to formation of nitric acid from the volume of standard alkali solution used to neutralise the bomb washings: $e_1 = (\text{J/g}) (\text{g}) = \text{ml}$

Of standard alkali * (6.0 J/g) (g/ml of standard alkali)

This correction is applied only if the calibration runs with benzoic acid.

(c) Correction of cotton thread

This correction is calculated as follows: $e_2 = 2.326 * \text{Energy content of thread} \left(\frac{\text{BTU}}{\text{lb}}\right)$.

The energy from combustion of cotton thread is 17 500 J/g.

Old systems use chromel wire and cotton thread combusts completely so this correction factor becomes a constant.

(d) Calibration

Determine the water equivalent of the bomb calorimeter as the average of a series of 10 individual runs with standard benzoic acid samples, made over a period of at least three days. The standard deviation should be less than $15.1 \text{ J}^{\circ}\text{C}$. Discard any individual run if there is evidence indicating incomplete combustion.

The mass of the benzoic acid pellet should be about 1.1 g.

Following the procedures above for titration correction for nitric acid and correction for the firing wire, substitute into the following equation:

$$W = \frac{(H_B)(g_B) + e_1 + e_2}{t}$$

Where W = water equivalent of calorimeter, J°C

H_B = Heat of combustion of benzoic acid, as stated in the NBS certificate, J/g of benzoic acid.

g_B = Mass of benzoic acid, g

t = Corrected temperature rise, $^{\circ}\text{C}$

e_1 =Titration correction (see b)

e_2 =Firing cotton thread correction (see c)

(C) Heating value

Compute the higher heating value by substituting in the following equation:

$$H_G = \frac{(t)(W) - e_1 - e_2 - e_3}{g_s}$$

Where

H_G =Higher heating value, J/g of Corn residues biomass

t = corrected temperature rise, °C

W = water equivalent of calorimeter, J/°C

e_1 = Titration correction

e_2 =Cotton thread correction

e_3 = Heating value of standard used (Standard weight of combustion of benzoic acid * weight used) = (J/g)*(g)

g_s = weight of sample

Appendix E: Corn residues kinetic parameters

Biomass	Conversion (α)	E_A (kJ/mol)	$\ln A$ (s^{-1})
CS	0.2	255	45
	0.5	230	40
	0.8	220	35
CC	0.2	270	51
	0.5	270	50
	0.8	237	37

Appendix F: Calculations of yields

The yields calculations have been determined from the bubbling fluidised bed reactor and the same principle has been applied to the lurgi twin screw reactor.

The different definitions of yield related variables are the following:

Feedstock (M_0) = Initial mass of feedstock used in an experimental run.

Char (M_{char}): Residue left after a pyrolytic run in the reactor (4), cyclones (5, 6), char pots (7, 8) and screw conveyor (3).

M_c : Mass of liquids condensed by isopar in the condenser (9) which consists of a mixture of an aqueous and tarry phases separated from the isopar.

M_A : Mass of the liquids condensed as a thin film in the following equipment electrostatic precipitator (1), electrostatic precipitator (2), condenser (9), Teflon seals, condenser top and the final cleaning of the reservoir after decanting the isopar and bio-oil mixture. These liquids are recovered using acetone and the bio-oil is weighed after acetone evaporation.

M_L : Total liquids are determined as the sum of the M_c and M_A fractions.

Other variables that have an influence on the yield calculations are as follows:

Initial water content of feed (WC_0): determined prior to FP experiments.

Initial ash content of feed (AC_0): determined prior to FP experiments.

Ash content in char (AC_{char}): determined by proximate analysis and analytical methods after each experimental run.

Water content of liquid (WC_L): Determined by Karl-Fischer titration.

Method of yield calculation on weight basis (wt. %):

$$\text{Yield of char (wt\%)} = \frac{M_{CHAR} * 100}{M_0}$$

Equation 28

$$\text{Yield of liquid (wt \%)} = \frac{M_L * 100}{M_O} \quad \text{Equation 29}$$

$$\text{Yield of bio - oil (wt \%)} = \frac{M_L - \left(M_L * \frac{WC_L}{100} \right) * 100}{M_O} \quad \text{Equation 30}$$

$$\text{Yield of pyrolytic water (wt \%)} = \frac{M_L * WC_L * 100}{M_O} \quad \text{Equation 31}$$

$$\text{Yield of gas (wt \%)} = 100\% - (\text{Yield of char} + \text{Yield of liquid}) \quad \text{Equation 32}$$

The pyrolytic water is considered to be present in the total liquids. It is the difference between the water content by Karl-Fischer titration and the initial water content of the feedstock.

Method of yield calculation on a dry/ash-free basis (wt %, daf):

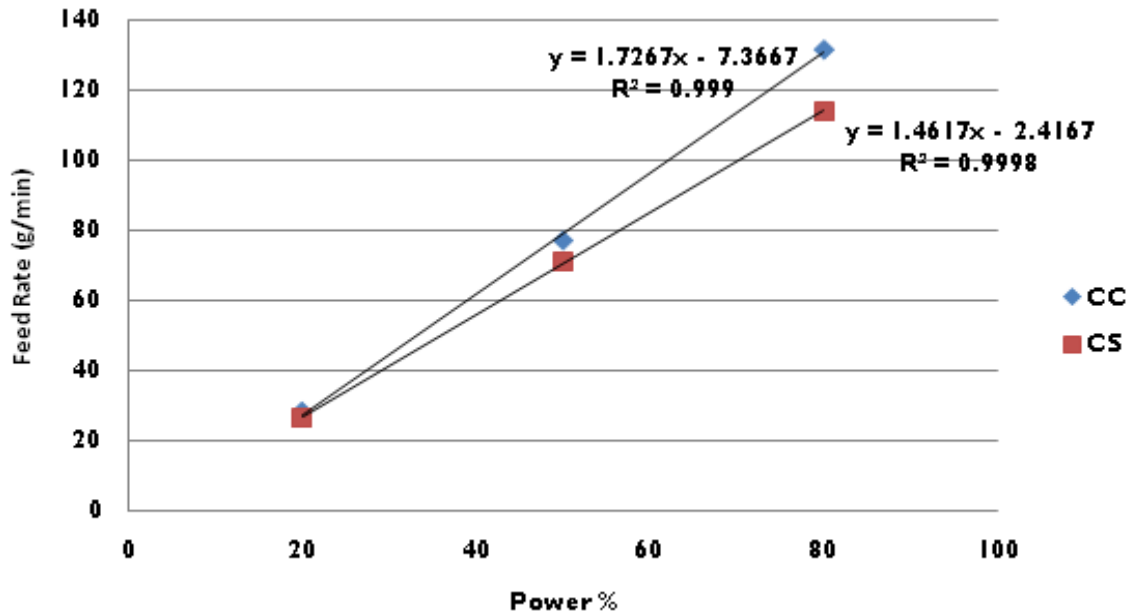
$$\text{Yield of char (wt \%)} = \frac{M_{CHAR}}{M_O - \left(M_O * \frac{AC_O}{100} \right) - \left(M_O * \frac{WC_O}{100} \right)} * 100 \quad \text{Equation 33}$$

$$\text{Yield of liquid (wt \%)} = \frac{M_L}{M_O - \left(M_O * \frac{AC_O}{100} \right) - \left(M_O * \frac{WC_O}{100} \right)} * 100 \quad \text{Equation 34}$$

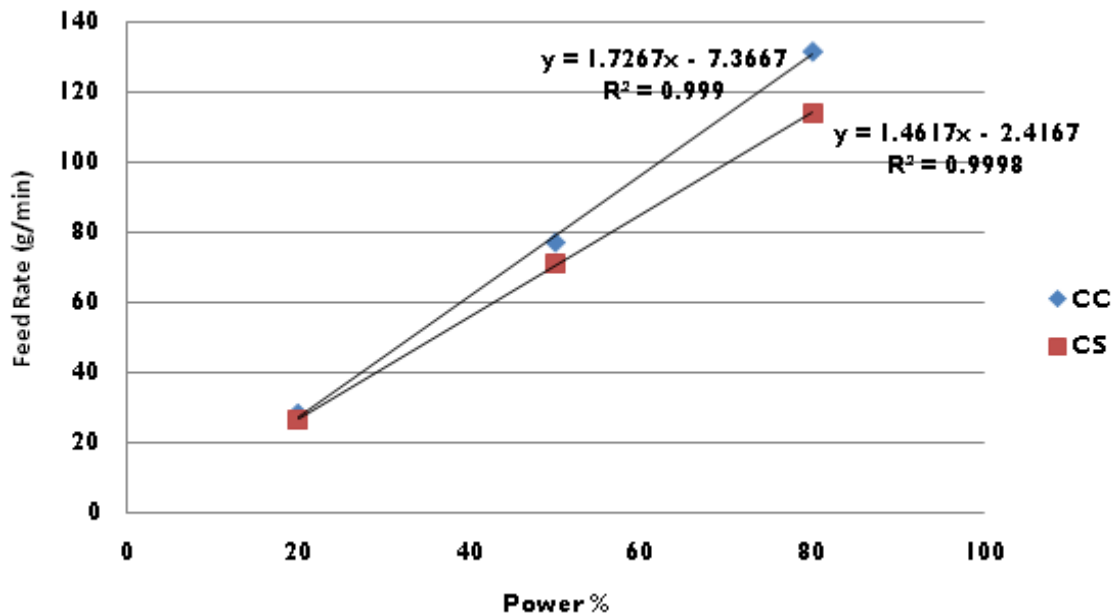
$$\text{Yield of bio - oil (wt \%)} = \frac{M_L - \left(M_L * \frac{WC_L}{100} \right)}{M_O - \left(M_O * \frac{AC_O}{100} \right) - \left(M_O * \frac{WC_O}{100} \right)} * 100 \quad \text{Equation 35}$$

$$\text{Yield of ash devolatilisation} = \frac{M_O * \frac{AC_O}{100} - M_{CHAR} * \frac{AC_{CHAR}}{100}}{M_O * \frac{AC_O}{100}} \quad \text{Equation 36}$$

Appendix G: Biomass feeding rates calibrations



Corn residues feedstocks feeding calibrations in a LTSR



Corn residues feedstocks feeding calibrations in a BFBR

Appendix H: The influence of temperature gradients in the biomass particle

Fast pyrolysis process is achieved by fast and uniform heating of the biomass particles.

This is achieved by preventing thermal gradients in and around the particles. The temperature uniformity throughout the biomass particles can be determined by the heat conduction law of Fourier, here applied in non-stationary regime and for simple case of a spherical particle:

$$\frac{dT}{dt} = \frac{k_p}{\rho_p c_p} \left(\frac{d^2 T}{dr^2} + \frac{2}{r} \frac{dT}{dr} \right) = D \left(\frac{d^2 T}{dr^2} + \frac{2}{r} \frac{dT}{dr} \right) \quad \text{Equation 37}$$

With k_p : heat conductivity of biomass at temperature T (W/mk), c_p : specific heat capacity of biomass at temperature T (J/kgK), ρ_p : density of biomass (kg/m³), D : thermal diffusivity of the particle (m²/s).

The general general solutions are therefore expressed by a dimensional analysis. For asphere of radius r , initially at temperature T_0 and suddenly exposed to the surroundings at T_s , the temperature distribution, at any time t and position x , is given by:

$$\frac{T_s - T}{T_s - T_0} = f \left(\frac{hr'}{k_p}, D \frac{t}{r^2}, \frac{x}{r} \right) \quad \text{Equation 38}$$

With h : external heat transfer coefficient at surface of sphere (W/m²K)

Since the evolution of the biomass particle is up to the core of the sphere (T_c at $x=0$) and introducing the Biot-number = $\left(\frac{r}{k_p}\right) / \left(\frac{1}{h}\right)$ reduces equation to:

$$\frac{T_s - T}{T_s - T_0} = f \left(\text{Bi}, D \frac{t}{r^2} \right) \quad \text{Equation 39}$$

For intermediate biomass biot numbers, results are presented by Heisler (**Heisler, 1946**) in the form of charts, expressing $\frac{T_s - T}{T_s - T_0}$ in terms of $D \frac{t}{r^2}$ (the Fourier number) with $\frac{1}{\text{Bi}}$ as a parameter. The application of the chart for corn residues biomass is given in the table below, with characteristic properties of corn residues at 500 °C, i.e. k_p (0.14 W/mK for CC and 0.12 W/mK for CS) (Kluwer, 2005) and for average fluidised bed heat transfer coefficient at the surface of the sphere i.e. 500 W/mK (Van de Velden *et al.*, 2010).

Fast pyrolysis requires the reaction to take place within 2-2.5 s, it is clear that only very small particles will meet the conditions of fast heating to a uniform temperature. From table below

particles of above 200 μm diameter (radius 100 μm) takes 0.43 s in CC and 0.48 s in CS to warm up which is about 20-24% of the proposed reaction time of pyrolysis. These calculations show that temperature differences between the corn residues biomass surface and core are very limited, certainly when considering that the surrounding temperature is 500 $^{\circ}\text{C}$ and that the heating rates varies. To obtain a fast heating of the whole biomass particle, it is appropriate thus to use small particles and no significant thermal gradient will occur.

Time required for the core of a spherically corn residue particle to reach temperature of surroundings

When $T_c = T_s$, initial temperature T of the sphere is 20 $^{\circ}\text{C}$ then the thermal diffusivity of the particle was determined by using the Biot graph as $1.86 * 10^{-7} \text{ m}^2/\text{s}$.

r (μm)	CS			CC		
	Bi-number	$\frac{Dt}{r^2}$	t(s)	Bi-number	$\frac{Dt}{r^2}$	t(s)
50	0.18	14	0.19	0.2	15	0.2
100	0.36	8	0.43	0.42	9	0.48
150	0.54	4	0.48	0.63	6	0.73
300	1.07	5	2.4	1.25	3	1.45

Appendix I: Procedure for calculation of quality of fit (%) by non-linear regression.

The method involves the application of the least-squares method. Denoting the experimental data by X^{EXP} and the corresponding points of the calculated functions by X^{CALC} , in these methods we look for the values of the unknown parameters that minimise the following:

$$\min S = \sum_{J=1}^{NC} \sum_{i=1}^{NPJ} Z_{ij} \frac{(X_{i,j}^{EXP} - X_{i,j}^{CALC})^2}{NPJNC}$$

Where NC is the number of TG curves to be simultaneously fitted and NP_j is the number of experimental points in the j th curve. Z_{ij} is a weighting factor. The quality of the fit can be expressed as:

$$q.f.(\%) = 100 \frac{S^{0.5}}{X_{highest}^{EXP}}$$

Where $X_{highest}^{EXP}$ is the absolute value of the highest experimental value (initial weight fraction).

Appendix J: The expected and experimental TG curves for corn residues at heating rate from 1 °C/min to 50 °C/min

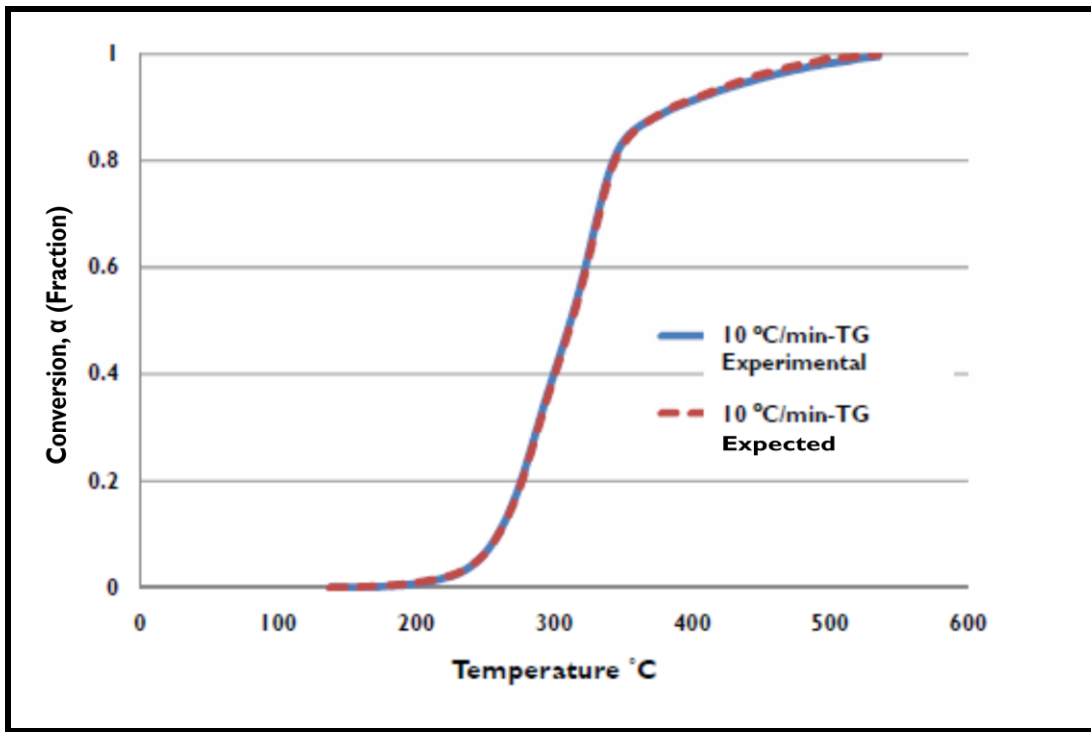


Figure J1: Expected and experimental curves for CC at 10 °C/min

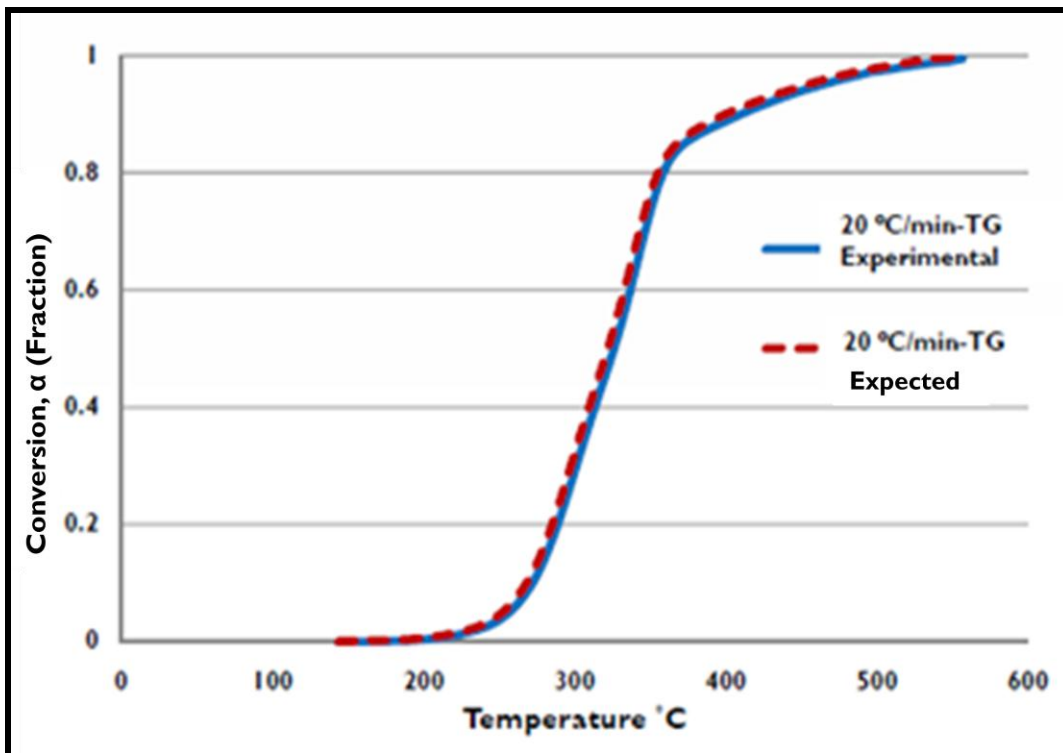


Figure J2: Expected and experimental curves for CC at 20 °C/min

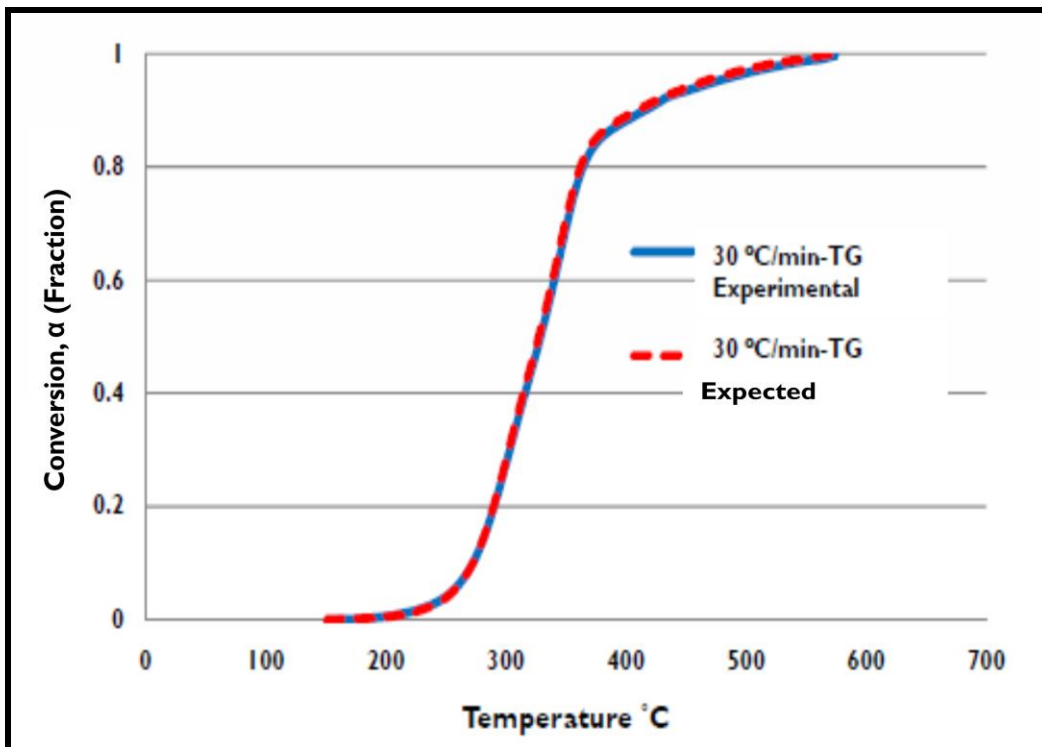


Figure J3: Expected and experimental curves for CC at 30 $^{\circ}\text{C}/\text{min}$

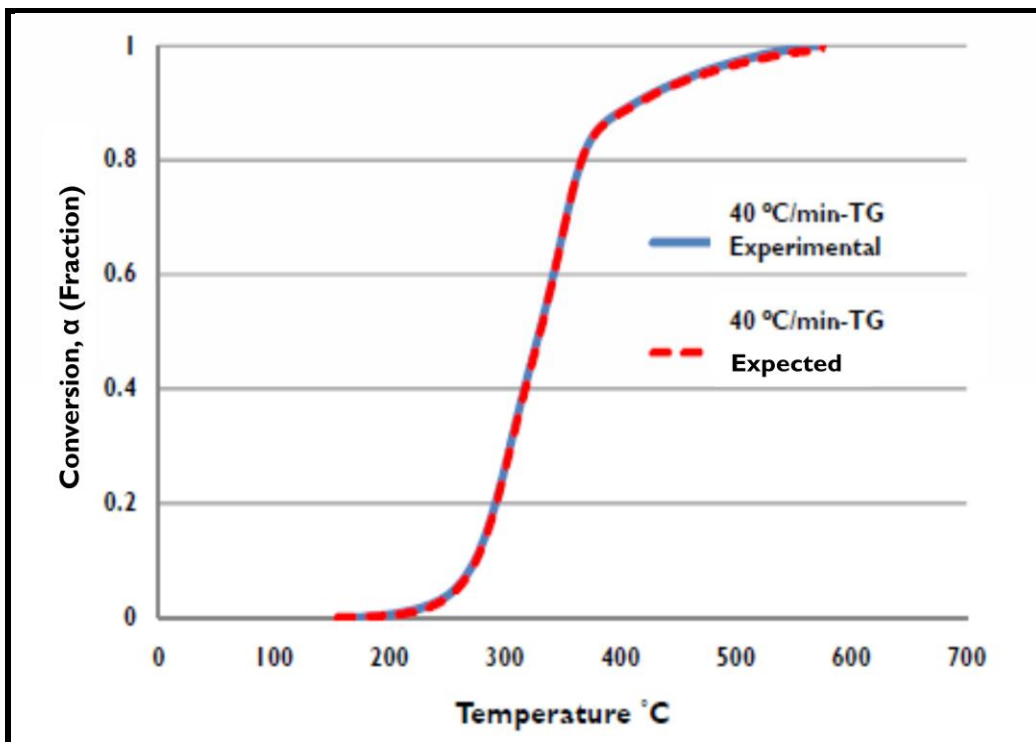


Figure J4: Expected and experimental curves for CC at 40 $^{\circ}\text{C}/\text{min}$

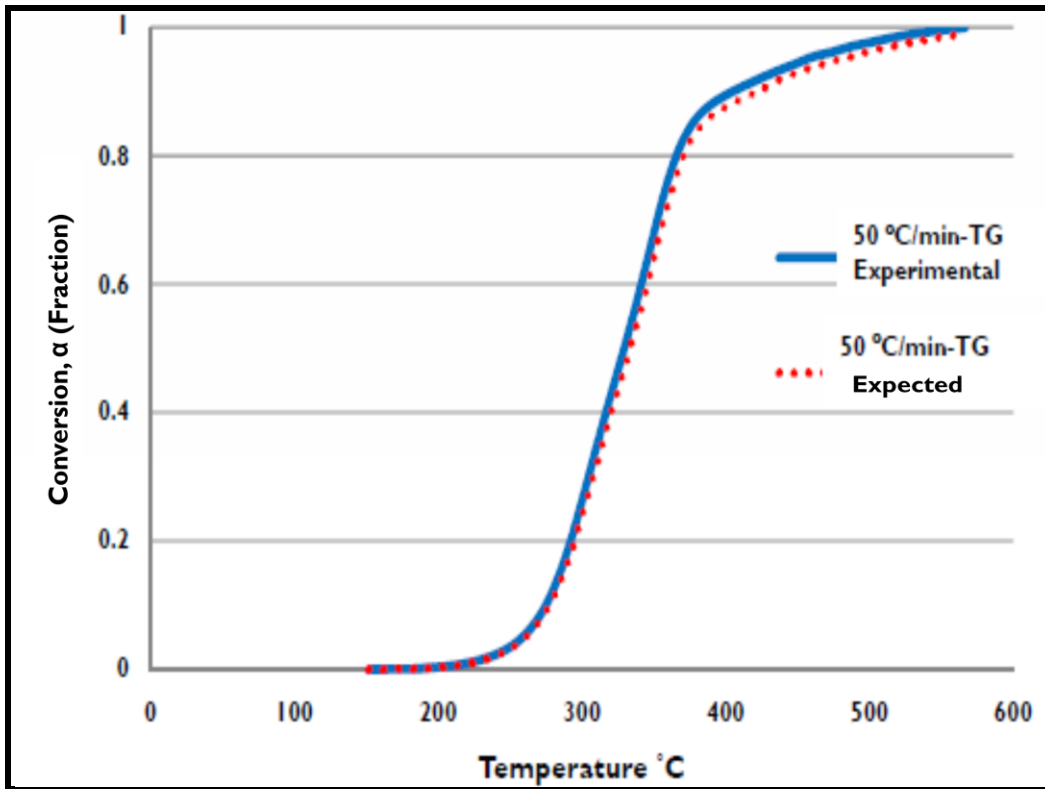


Figure J5: Expected and experimental curves for CC at 50 $^{\circ}\text{C}/\text{min}$

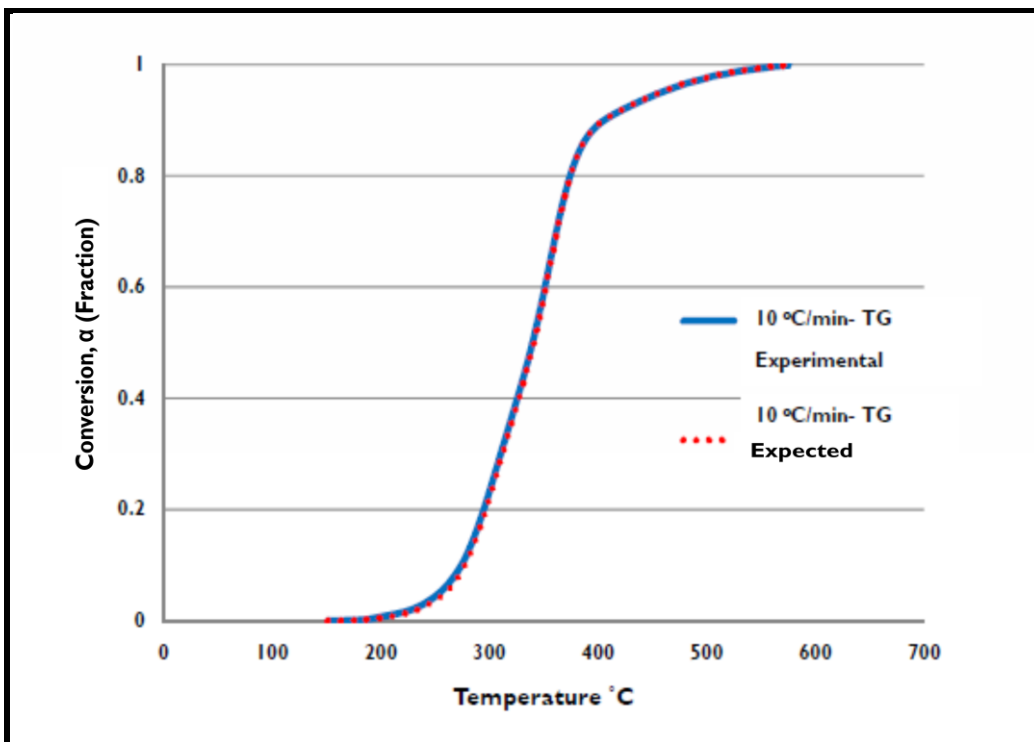


Figure J6: Expected and experimental curves for CS at 10 °C/min

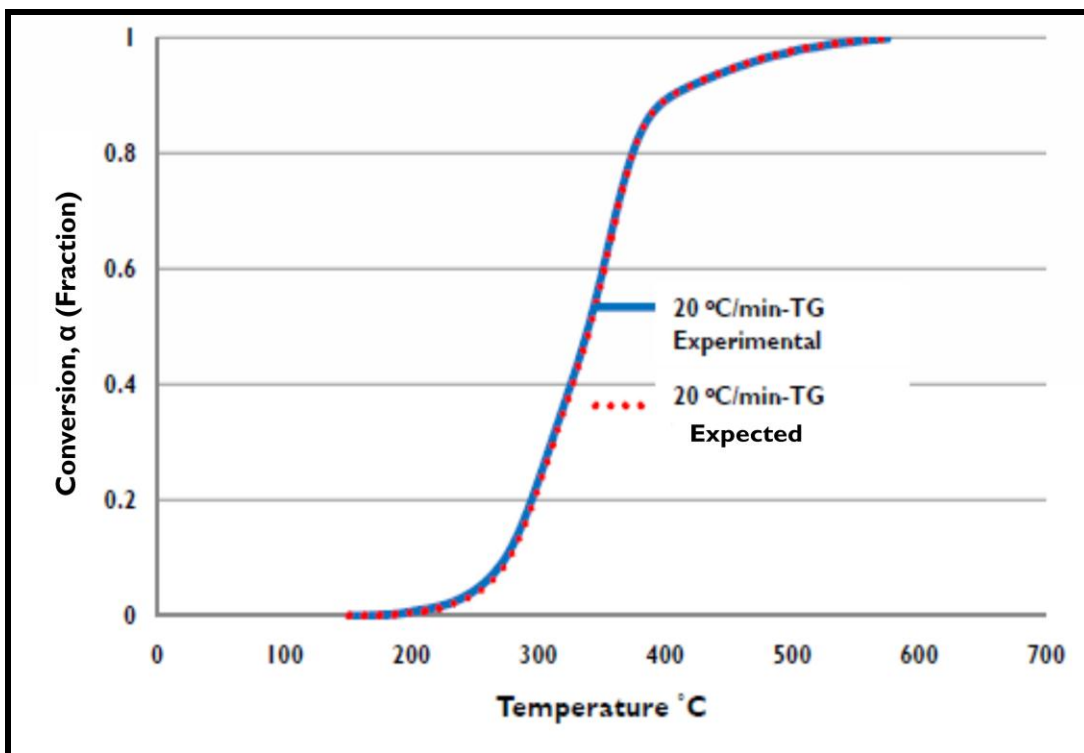


Figure J7: Expected and experimental curves for CS at 20 °C/min

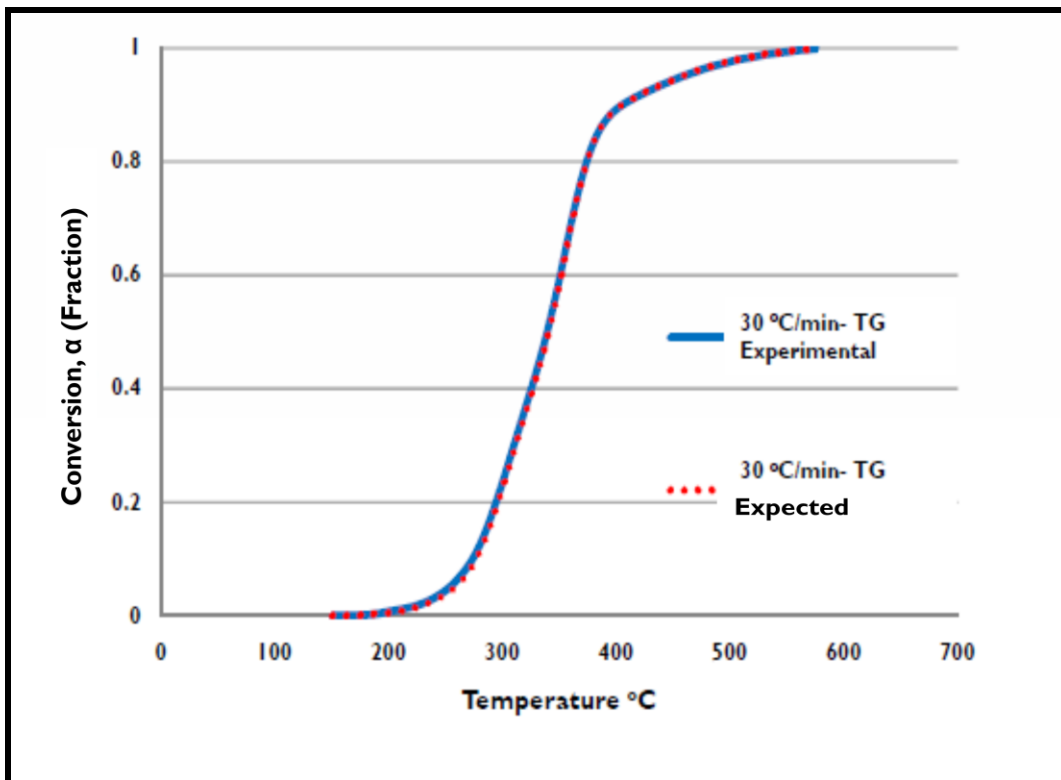


Figure J8: Expected and experimental curves for CS at 30 $^{\circ}\text{C}/\text{min}$

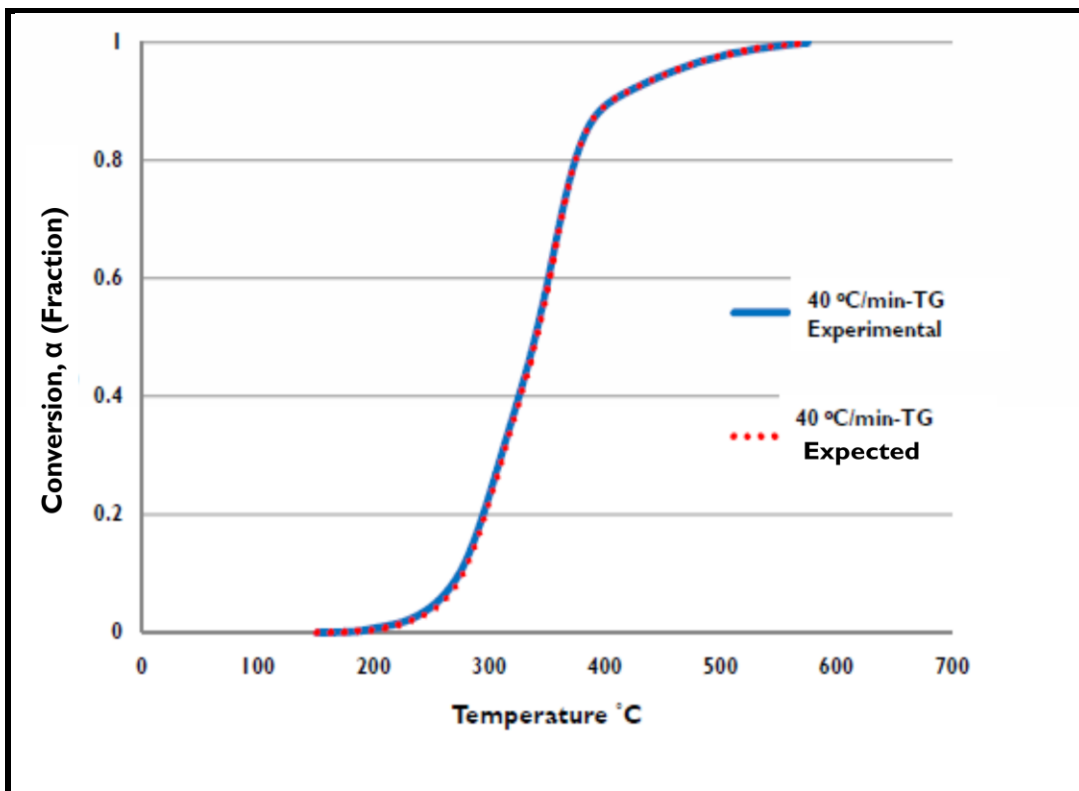


Figure J9: Expected and experimental curves for CS at 40 $^{\circ}\text{C}/\text{min}$

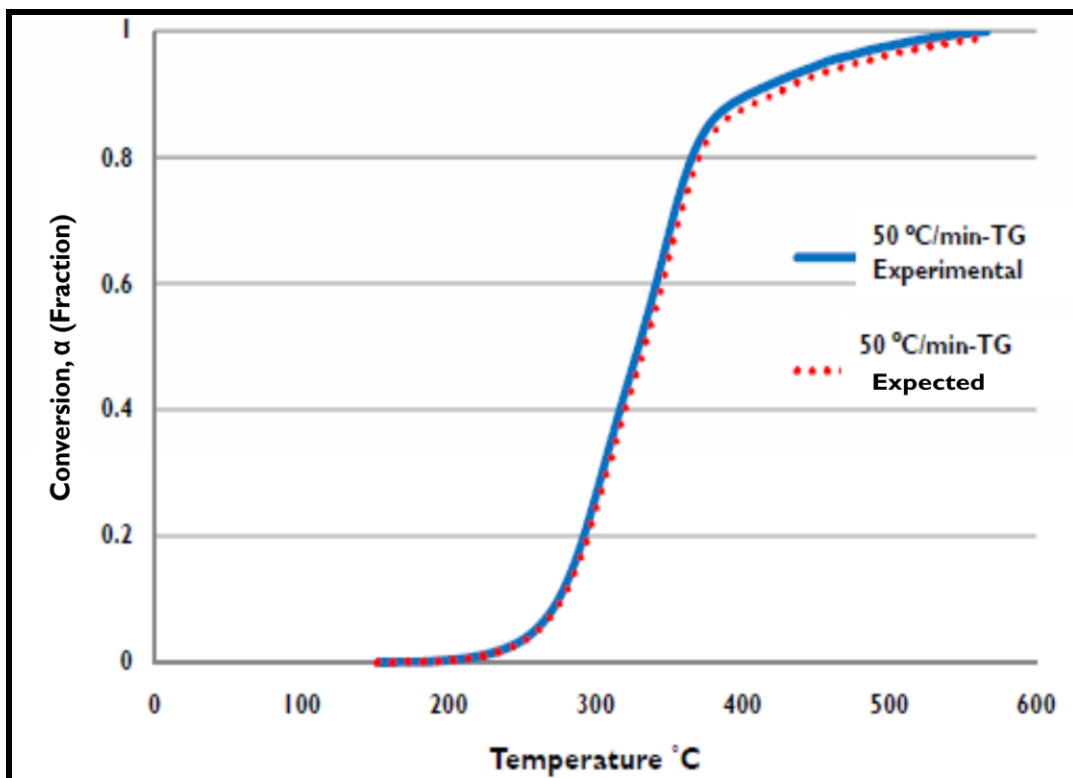


Figure J10: Expected and experimental curves for CS at 50 $^{\circ}\text{C}/\text{min}$

Appendix L: Sand particle size distribution

(U.S.) Mesh	Aperture in Microns (μm)	% Retained
25	710	0.2
30	600	-
35	500	6.7
40	425	-
45	355	34.3
50	300	-
60	250	37.7
70	212	10.2
80	180	-
100	150	8.7
120	125	-
140	106	2.0
200	75	0.2
-200	-75	0

Appendix M: Acetone evaporation graph

